Alma Mater Studiorum - Università di Bologna

DOTTORATO DI RICERCA IN

ONCOLOGIA, EMATOLOGIA E PATOLOGIA

Ciclo 34

Settore Concorsuale: 06/A2 - PATOLOGIA GENERALE E PATOLOGIA CLINICA

Settore Scientifico Disciplinare: MED/04 - PATOLOGIA GENERALE

ROLE OF NON-CODING RNA ALTERATIONS IN MELANOMA

Presentata da: Elisabetta Broseghini

Coordinatore Dottorato

Prof.ssa
Manuela Ferracin

Supervisore

Prof.ssa
Manuela Ferracin

Esame finale anno 2022

INDEX

1. ABSTRACT 1

2. ABBREVIATIONS 3

3. INTRODUCTION 7

3.1. Cutaneous Melanoma 7

3.1.1. Incidence and Epidemiology 7

3.1.2. Melanoma etiology 7

3.1.2.1. Environmental risk factors 8

3.1.2.2. Phenotypic risk factors 8

3.1.2.3. Familial melanoma history 9

3.1.2.4. Multiple Primary Melanoma 13

3.1.3. Melanoma onset and progression 13

3.1.3.1. Somatic genetic alterations in melanoma 14

3.1.3.2. Melanoma onset and progression models 16

3.1.4. Melanoma classification 18

3.1.4.1. Genomic classification 21

3.1.5. Pathological staging 21

3.1.5.1. T category 21

3.1.5.2. N Category 22

3.1.5.3. M category 23

3.1.5.4. Stage groups 24

3.1.5.5. Other histologic features 24

3.1.6. Diagnosis and prognosis 25

3.1.7. Treatment 27

3.1.7.1. Surgery and radiotherapy 27

3.1.7.2. Chemotherapy 27

3.1.7.3. Targeted Therapy 27

3.1.7.4. Immunotherapy 28

3.2. MICRORNA 30

3.2.1. miRNA biogenesis 30

3.2.1.1. The canonical pathway of miRNA biogenesis 31

3.2.1.2. Non-canonical miRNA biogenesis pathways 32

3.2.2. Mechanisms of miRNA-mediated gene regulation 33
3.2.2.1. MiRNA-mediated gene silencing via miRISC 33
3.2.2.2. MiRNA-mediated translational activation 34
3.2.2.3. MiRNA-mediated transcriptional and post-transcriptional gene regulation within the nucleus 34
3.2.3. Role of miRNAs in human tumors 35
3.2.3.1. Mechanisms of miRNA dysregulation in cancer 35
3.2.3.2. Significance of the altered miRNA expression in tumors 38
3.2.4. miRNAs in melanoma 40
3.2.4.1. miRNAs in melanogenesis and melanoma genesis 41
3.2.4.2. miRNAs in proliferation and cell cycle regulation 42
3.2.4.3. miRNAs in apoptosis, autophagy and ferroptosis 44
3.2.4.4. miRNAs in EMT and angiogenesis 45
3.2.4.5. miRNAs and melanoma microenvironment 47
3.2.4.6. miRNAs in hypoxia and metabolism 47
3.2.4.7. miRNAs as modulators of therapeutic response in melanoma 48
3.2.4.8. Circulating miRNAs as melanoma biomarkers 50
3.2.5. miRNA isoforms (isomiRs) 52
3.2.5.1. From the Canonical miRNAs to the discovery of isomiRs 53
3.2.5.2. Classification and nomenclature of isomiRs 53
3.2.5.3. Biogenesis of isomiRs 55
3.2.5.4. Significance of isomiR Functions 57
3.2.5.5. IsomiRs in Cancer 58
4. AIMS 60
5. MATERIALS AND METHODS 61
5.1. Samples 61
5.1.1. Clinical samples 61
5.1.2. Melanoma cell line 63
5.1.3. TCGA datasets 64
5.2 RNA extraction 64
5.2.1. FFPE samples 64
5.2.2. Melanoma cells 65
5.3. Small-RNA sequencing 65
5.3.1. Small-RNA sequencing 65
5.4 RNA quantification 67
5.4.1. miRNA quantification 67
5.4.2. isomiR quantification 68
5.4.3. mRNA quantification 70

5.5. Target analysis and validation 70
5.5.1. Transfection 70
5.5.2. Protein quantification 71
5.6. Statistical Analysis 72
5.6.1. small-RNA sequencing 72
5.6.2. miRNA association with clinicopathologic characteristics 72
5.6.3. mRNA association with survival 73
5.6.4. Graphpad Prism 6 73
5.6.5. MetaCalc software 73
5.7. Pathway analysis 74
5.7.1. Enrichment analysis 74
5.7.2. Target prediction 74
6. RESULTS 75
6.0. Pilot study: small RNA sequencing of benign nevi and melanoma 75
6.1. Defining the prognostic role of miRNAs in Cutaneous Melanoma 76
6.1.1.Comparison of global miRNA profile in thin and thick melanomas identified candidate prognostic miRNAs 76
6.1.2.Validation of miR-146a-5p and miR-21-5p as prognostic biomarkers in superficially spreading melanoma 78
6.1.3.miR-146a-5p and miR-21-5p expression is associated with outcome and prognostic features in superficially spreading melanoma 79
6.1.4.miR-146a-5p and miR-21-5p combined expression can complement BT in patient prognostication 81
6.2. Unraveling the role of miRNA network in multiple primary melanoma pathogenesis 83
6.2.1. The miRNA profile of multiple primary melanoma 83
6.2.2.Validation of miRNA differential expression in single melanomas, multiple primary melanomas, and in benign nevi 86
6.2.3. Functional annotation of multiple primary melanoma miRNA signature 88
6.3. Exploring the role of a miRNA variant of miR-125a-5p 92
6.3.1. IsomiR analysis revealed that a miR-125a-5p isoform is dysregulated in multiple primary melanoma 92
6.3.2. miR-125a-5p|0|–2 isomiR is highly expressed in many different tumors 95

6.3.3. Optimized Dumbbell- based ddPCR based assay allowed to quantify isomiR in melanoma cell lines and FFPE samples 96

6.3.4. Functional analysis of a specific isomiR of miR-125a-5p in melanoma..... 97

6.3.4.1. miR-125a-5p miRNA and isomiR regulated different target genes 97

6.3.4.2. SMARCE1 is specifically targeted by the isomiR form of miR-125a-5p 100

6.4. MiRNA isoforms contribution to melanoma pathogenesis 101

6.4.1.Mature miRNA profile and miRNA variants characterization in early-stage melanoma samples .. 101

6.4.2. End-site isomiRs are the most abundant and expressed isomiRs in FFPE Samples 103

6.4.3. Enrichment of isomiRs belonging the cancer-related miRNA family in BN and CM samples..... 103

6.4.4. Identification of isomiRs more expressed than the canonical form in early-stage melanoma 107

6.4.5. Benign nevi and early-stage melanoma present a different mature miRNA expression profile 108

6.4.6. Classification of isomiRs with a potentially relevant role in early-stage melanoma 110

6.4.6.1. IsomiRs with a similar trend in early-stage CM vs. BN and similar relative abundance 111

6.4.6.2. IsomiRs with a similar trend in CM vs. BN and different relative abundance..... 113

6.4.6.3. IsomiRs with opposite trend in CM vs. BN and similar relative abundance..... 114

6.4.6.4. IsomiRs with opposite trend in CM vs. BN and different relative abundance 114

6.4.7. IsomiR classification in fresh-frozen primary melanoma and metastasis from TCGA database.... 115

6.4.8. Identification of the isomiRs more expressed than the canonical form in fresh primary melanoma samples from TCGA 117

6.4.9. IsomiR expression contributes to distinguish primary melanoma and metastasis 118

6.4.10 Identification of isomiRs associated with driver gene mutations in TCGA samples..... 119

6.4.10.1. Identification of mature miRNAs associated with mutated NF1..... 119

6.4.10.2. Identification of mature miRNAs associated with mutated BRAF 120

6.4.10.3. Identification of mature miRNAs associated with mutated NRAS 124

7. DISCUSSION..... 125

7.1. Combined assessment of miR-21-5p and miR-146a-5p expression can be associated with BT measurement for SSM staging 125

7.2. Comprehensive characterization of miRNA expression and regulatory network highlights mechanisms of tumor development and molecular features differentiating MPMs from single CMs. 128

7.3 A specific 3'isomiRs of miR-125a-5p is more expressed and presents different target genes compared to the canonical miRNAs 130

7.4. Non-random dysregulation of specific isomiRs contributes to the understanding of the complex melanoma pathogenesis 132

8. CONCLUSION..... 138

9. BIBLIOGRAPHY..... 139

1. ABSTRACT

Cutaneous melanoma (CM) is a potentially lethal form of skin cancer whose worldwide incidence has been constantly increasing over the past decades. The most important histopathologic factor for CM staging is Breslow thickness (BT). Its correct determination is fundamental for pathologists because discrepancies lead to a change in stage with significant clinical implications, including incorrect and/or inappropriate prognostic information, investigation, management, and follow-up. A deeper understanding of the molecular processes guiding CM pathogenesis could improve diagnosis, treatment and prognosis. MicroRNAs (miRNAs) play a key role in CM biology.

The firs aim was to investigate miRNA expression in reference to BT assessment. We found that in superficially spreading melanomas (SSM), the combined miRNA expression of miR-21-5p and miR-146a-5p above or below 1.5 was significantly associated with overall survival and successfully identified all patients with relapsing SSM, suggesting that the combined assessment of these miRNAs expression in SSM in association with BT measurement, could aid in SSM staging.

Secondly, we decided to focus on multiple primary melanomas (MPMs). MPM patients are CM patients that develop multiple primary melanoma in their lifetime, and represent a model of high-risk CM occurrence. With the aim of improving our knowledge on MPM pathogenesis, we explored the miRNome of single CM and MPM through small RNA sequencing. Single CM and MPM present several dysregulated miRNAs, including key miRNAs involved in epithelial-mesenchymal transition. A different miRNA profile was observed between 1st and 2nd melanoma from the same patient. Ten miRNAs were further validated in a larger cohort. Pathway enrichment analysis of miRNA target genes revealed a more differentiated and less invasive status of MPMs compared to CMs. This putative and comprehensive characterization of the miRNA regulatory network of MPMs highlights mechanisms of tumor development and molecular features differentiating this subtype from single melanomas.

Recently, next generation sequencing (NGS) experiments revealed the existence of miRNA variants (isomiRs) with different length and sequence that provides an additional layer to the complex non-coding RNA world. We identified a shorter 3'isoform (hsa-miR-125a-5p|0|−2) as tenfold over-represented compared to the canonical form of miR-125a-5p. Target prediction analysis revealed that the miRNA shortening could change the pattern of target gene regulation, specifically in genes implicated in cell adhesion and neuronal differentiation. Bioinformatic analysis predicts a specific target of this isomiR, namely SMARCE1, that was confirmed by preliminary data.

1. ABSTRACT

Finally, we provide a comprehensive characterization of miRNA and isomiR dysregulation in benign nevi (BN) and early-stage melanomas. CM and BN express different and specific isomiRs and have a different isomiR abundance distribution. Moreover, isomiRs from the same miRNA can have opposite expression trends between groups. IsomiR expression was analyzed in primary melanoma and melanoma metastasis obtained from The Cancer Genome Atlas (TCGA) dataset of skin, and was tested is association with *NF1, BRAF* and *NRAS* mutations. The reported non-random dysregulation of specific isomiRs contributes to the understanding of the complex melanoma pathogenesis and serves as the basis for further functional studies.

2. ABBREVIATIONS

ACD	Adrenocortical Dysplasia Protein Homolog
AGO	Argonaute
AJCC	American Joint Committee on Cancer
Akt (PKB)	Protein Kinase B
Akt3	RAC-Gamma Serine/Threonine-Protein Kinase
AM	Acral Melanoma
ANK3	Ankyrin 3
Apaf1	Apoptotic Protease-Activating Factor 1
ARE	AU-Rich Element
ASIP	Agouti Signaling Protein
BAP1	BRCA1-Associated Protein-1
BAX	BCL2-Associated X Protein
Bcl-2	B-Cell Lymphoma 2
BCL6	B-Cell Lymphoma 6 Protein
Bcl-xL	B-Cell Lymphoma Extra-Large
Bim (BCL2L11)	Bcl-2-Like Protein 11
BN	Benign Nevi
BRAF	B-Raf Proto-Oncogene
BRAFi	BRAF Inhibitors
BSA	Bovine Serum Albumin
BT	Breslow Thickness
BTG2	Btg Anti-Proliferation Factor 2
CCND1	Cyclin D1
CCR4-NOT	Carbon Catabolite Repression—Negative On TATA-Less
CDC2	Cell Division Control Protein
CDCA8	Cell Division Cycle Associated 8
Cdk	Cyclin-Dependent Kinases
CDK4	Cyclin Dependent Kinase 4
CDKN2A	Cyclin Dependent Kinase Inhibitor 2a
CLDN2	Claudin 2
CM	Malignant Cutaneous Melanoma
c-Myc	C-Myc Protein
CNV	Copy Number Variants
CTLA-4	Cytotoxic T-Lymphocyte Protein 4
CXC	Chemokine Receptors
CXCL1	Melanoma Growth-Stimulating Activity A
CYP2D6	Cytochrome P450 Family 2
CYP2E1	Cytochrome P450 Family 2 Subfamily E Member 1
Db-ddPCR	Dumbbell Based Droplet Digital PCR Assay
ddPCR	Droplet Digital PCR Assay
DGCR8	DiGeorge Syndrome Critical Region 8
DN	Dysplastic Nevi
DTIC	Dacarbazine
E2F	Transcription Factor E2F
eiF4F	Eukaryotic Initiation Factor 4F

2. ABBREVIATIONS

EMT	Epithelial-Mesenchymal Transition
ETV1	Ets Variant Transcription Factor 1
EV	Extracellular Vesicle
EZH2	Enhancer Of Zeste Homolog 2
FC	Fold change
FFPE	Formalin-Fixed, Paraffin-Embedded
FOXD3	Forkhead Box D3
FOXM1	Forkhead Box M1
FTO	Fat Mass and Obesity Associated Gene
FXR1	Fragile-X-Mental Retardation Related Protein 1
GLYATL1	Glycine-N-Acyltransferase Like 1
gp100	Glycoprotein 100
GSTM1	Glutathione S-Transferase Mu 1
GSTP1	Glutathione S-Transferase Pi 1
GSTT1	Glutathione S-Transferase Theta 1
HIF	Hypoxia-Inducible Factor
HLA	Human Leukocyte Antigen
IHC	Immunohistochemistry
IL-8	Interleukin 8
IRF4	Interferon Regulatory Factor 4
isomiRs	Mirna Variants/Isoforms
ITGA6 (CD49f)	Integrin Alpha-6
KIT	Proto-Oncogene Receptor Tyrosine Kinase
LDH	Lactate Dehydrogenase
LFNG	Lunatic Fringe
LLM	Lentigo Maligna Melanoma
m7G	7-Methylguanosine M7g
MAPK (ERK)	Mitogen-Activated Protein Kinases
MBAIT	Melanocytic BAP1-Mutated Atypical Intradermal Tumors
MC1R	Melanocortin 1 Receptor1
MDSC	Myeloid-Derived Suppressor Cell
MEK, MAP2K7	Mitogen-Activated Protein Kinase Kinase 7
MET	Hepatocyte Growth Factor Receptor
microRNP	Mirna-Protein Complex
miRISC	Mirna-Induced Silencing Complex
miRNA	MicroRNA
MITF	Microphthalmia-Associated Transcription Factor
MLANA	Melanoma Antigen Recognized By T-Cells 1
MM	Melanoma Metastasis
MOMP	Mitochondrial Outer Membrane Permeabilization
MPM	Multiple Primary Melanoma
MRE	Mirna Response Element
mRNA	Messenger RNA
MTAP	Methylthioadenosine Phosphorylase
mTOR	Serine/Threonine-Protein Kinase mTOR
NF1	Neurofibromin 1
NGS	Next Generation Sequencing

2. ABBREVIATIONS

NK	Natural Killer Cell
NM	Nodular Melanoma
NOTCH4	Notch Receptor 4
NRAS	Neuroblastoma RAS Viral Oncogene Homolog
nt(s)	Nucleotide(s)
NUMB	Protein Numb Homolog
OB	Oligonucleotide/Oligosaccharide-Binding
OCA2	Oculocutaneous Albinism II
OCR	Oxygen Consumption Rate
OS	Overall Survival
OS	Overall Survival
p14/ $p14^{ARF}$	P14 Alternate Reading Frame
p16/ $p16^{INK4A}$	P16 Inhibitor of Cyclin-Dependent Kinase 4
p53	Cellular Tumor Antigen P53
PARP1	Poly ADP-Ribose Polymerase 1
PAX3	Paired Box 3
PCA	Principal Component Analysis
PD-1	Programmed Cell Death 1
PDCD4	Programmed Cell Death 4
PI3K	Phosphoinositol-3-Kinase
PIK3C2B	Phosphatidylinositol-4-Phosphate 3-Kinase Catalytic Subunit Type 2 Beta
Pol II	RNA Polymerase II
POT1	Protection Of Telomeres 1
pre-miRNA	Precursor miRNA
pri-miRNA	Primary miRNA
PTEN	Phosphatase And Tensin Homolog
PUMA	P53 Upregulated Modulator of Apoptosis
qPCR	Quantitative PCR
Rb	Retinoblastoma
RGP	Radial Growth Phase
RHC	Red Hair Color Phenotype
RNAi	RNA Interference
ROS	Reactive Oxygen Species
RPM	Read Per Million
RT	Reverse Transcription
SEER	Surveillance, Epidemiology, And End Results
shRNA	Short Hairpin RNA
siRNA	Small Interfering RNA
SIRT1	NAD-Dependent Protein Deacetylase Sirtuin-1
SLN	Sentinel Lymph Node
SMAD4	Smad Family Member 4
small RNA-seq	Small RNA-Sequencing
SMARCE1 (BAF57)	Swi/Snf Related, Matrix Associated, Actin Dependent Regulator of Chromatin, Subfamily E, Member 1
SNP(s)	Single Nucleotide Polymorphism(s)
SOX10	Sry-Box Transcription Factor 10
SSM	Superficially Spreading Melanoma
TCGA	The Cancer Genome Atlas

2. ABBREVIATIONS

TERF21P	Telomeric Repeat-Binding Factor 2-Interacting Protein 1
TERT	Telomerase Reverse Transcriptase
Tfdp2	Transcription Factor Dp-2
TIL	Tumor-Infiltrating Lymphocytes
TIMP3	Tissue Inhibitor of Metalloproteinase-3
TLR4	Toll-Like Receptor 4
TLR4	Toll-Like Receptor 4
TLX1 (HOX11)	T Cell Leukemia Homeobox 1
TLX3	T Cell Leukemia Homeobox 3
TMLHE	Trimethyllysine Hydroxylase, Epsilon
TMZ	Temozolomide
TNF- α	Tumor Necrosis Factor Alpha
TRAIL	TNF-Related Apoptosis-Inducing Ligand
TRIM44	Tripartite Motif Containing 44
TRPM1	Transient Receptor Potential Cation Channel Subfamily M Member 1
TTR	Time-To-Relapse
TYR	Tyrosinase
TYRP1	Tyrosinase-Related Protein 1
USP28	Ubiquitin-Specific Protease 28
UTR	Untranslated Region
UV	Ultraviolet
VDR	Vitamin D Receptor
VEGF	Vascular Endothelial Growth Factor
VGP	Vertical Growth Phase
WHO	World Health Organization
XPO5	Exportin 5
ZEB1	Zinc Finger E-Box Binding Homeobox 1
ZEB2	Zinc Finger E-Box Binding Homeobox 2
ZNF560	Zinc Finger Protein 560

3. INTRODUCTION

3.1. Cutaneous Melanoma

3.1.1. Incidence and Epidemiology

Cutaneous Melanoma (CM) is a malignant tumor that results from the transformation of pigment-producing cells known as melanocytes, which are predominantly located in the skin. CM accounts for 3-5% of all cutaneous cancers but it is the most lethal tumor among them, in fact it determines approximately 65% of all skin cancer deaths [1].

Worldwide incidence of CM has been increasing more rapidly than any other cancer type in the past decades, reaching an age-standardized rate of 3.4 per 100,000. However, this tumor affects principally fair-skinned populations, with variable incidence attributable to latitude and differences in sun exposure. In details, in fair-skinned population regions, such as Australia-New Zealand, Northern Europe and Northern America, this rate is higher and it exceeds 15 per 100,000 (35.8, 17.8 and 16.1, respectively) (source IARC 2020).

The most principally affected group is the geriatric population and the median age at diagnosis is 65 years. However, CM is also frequently diagnosed in adolescent and young adult populations [2]. The incidence increases linearly starting from the age of 25 years until the age of 50 years [3,4]. Men are generally more affected: the word incidence is 3.5% for men and 2.9% for women [5]. However, when age is considered, adolescent and young adult women are more susceptible to melanoma than men. On the other hand, after the age of 40, rates reverse, and the incidence among men is greater than in women [6].

The 5-year survival is about 95-98%, but it decreases dramatically when regional or distant metastases are present, in fact, this rate reduces to 63% and 20%, respectively [3].

3.1.2. Melanoma etiology

The pathogenesis of melanoma is complex and poorly understood. In fact, CM is considered a multi-factorial disease, which results from the combination of different factors, including environmental, phenotypic and genetic factors such as ultraviolet (UV) exposure, fair phototypes, multiple dysplastic nevi and a positive family/personal history of CM [7]. A family history of CM poses the highest risk for the development of melanoma [8,9].

3.1.2.1. Environmental risk factors

The most common environmental risk factor is UV radiation deriving from excessive sun exposure or use of tanning beds. The sun is major source of UV radiation and the direct association between sun exposure and increasing risk of melanoma have been highlighted by several studies [10,11].

Melanocytes are generally resistant to UV-induced apoptosis. However, the UV radiation, especially UV-B, leads to severe damage in DNA and melanocyte functions, by inducing direct and indirect DNA alterations. Among the direct damage due to UV exposure, there is the generation of thymine dimers, pyrimidine dimers, cyclobutane pyrimidine dimers and UV-endonuclease-sensitive-sites in double strand DNA. DNA alterations are generated also indirectly as a consequence of reactive oxygen species (ROS) generation [12]. The growth and the accumulation of genetic mutations lead to malignant transformation of melanocytes in CM [13].

Other factors include the level and type of sun protections, chronic or intermittent UV exposure, and history of sunburn in childhood. They are all related to the amount of UV radiations necessary to increase melanoma risk. The intense and intermittent sun exposure appears to be especially associated to developing CM, while the chronical pattern of exposure is related with non-melanoma skin cancer or actinic keratosis disease [14,15].

Since tanning sunbeds are an artificial source of UV radiation, they can increase the risk to develop CM. Indeed, people who frequently use tanning sunbeds expose themselves to a higher amount of UVA in comparison to sunbathing or outdoor activity related exposure [16].

Finally, sunburn is considered an acute sun exposure, and episodes of sunburn were positively associated to melanoma. Specifically, recurring episodes of sunburn in childhood (under 15 years) have been correlated with a higher risk of develop CM [11,15,17].

3.1.2.2. Phenotypic risk factors

Also phenotypic risk factors can contribute to the development of CM. A skin pigmentation phenotype (fair or light skin) and the presence of atypical and multiple nevi are considered important risk factor for CM.

Fair-skinned individuals showed reduced pigmentation and they are more likely to develop CM than more darkly pigmented individuals. A two-fold increased risk is conferred by red hair compared to black or dark grown hair. The presence of extensive freckling increases to a three-fold the risk of CM in people under age 40 [18]. A specific phototype which includes red hair, freckles, fair skin, light eyes and sun sensitivity increases the risk of CM [14,19].

The number and the size of melanocytic nevi are important risk factors of CM. Nevi can be congenital or acquired. People with >100 nevi have a significantly higher risk of CM [20]. Sometimes nevi have a suspicious dysplastic morphology and they are clinically called “atypical” or “dysplastic”, which are characterized by disproportional dimension (large nevi have a diameter >5mm, giant nevi have a diameter >20 cm), indistinct and irregular borders, and variable pigmentation. Several studies have found that approximatively 36% of melanomas origin in patients with pre-existing dysplastic nevus [17,21,22]. Patients that develop nevus-associated melanomas show a distinct risk profile that differs from that of patients with *de novo* melanomas [20]. In nevus-associated melanoma patients, melanomas are generally located on the trunk and belong to the superficial spreading subtype [21].

3.1.2.3. Familial melanoma history

Family history of melanoma has been widely correlated with an increased melanoma risk [8]. We defined a familial melanoma when in a family there are 2 first-degree relatives or 3 or more melanoma patients on the same side of the family (irrespective of degree of relationship) that are diagnosed with melanoma. In these families, the susceptibility to develop melanoma is inherited following an autosomal dominant inheritance pattern with incomplete penetrance [23]. The presence of germline mutation constitutes a risk factor for the hereditary form of the disease [8,24-26].

Melanoma susceptibility genes can be classified in high-risk genes and low to moderate risk genes. The first group includes genes that confer a high risk of developing melanoma when mutated in an individual and are usually associated with the presence of multiple melanomas within the family. The second group indicates genes that have a weak impact on melanoma susceptibility. Families with these variants usually have one or occasionally two melanoma cases [27]. However, more melanoma cases could be present in the family with a combination of low to moderate inherited variants. Moreover, families with low to moderate risk variants could have more melanoma cases if they live in areas with an increased UV radiation [28].

One of the principal high-risk germline mutations was found in Cyclin Dependent Kinase Inhibitor 2A (*CDKN2A*) [29,30]. The other high-risk melanoma susceptibly genes are Cyclin Dependent Kinase 4 (*CDK4*), BRCA1-associated protein-1 (*BAP1*), chemokine receptors (CXC) genes and four genes involved in the telomere maintenance: Telomerase Reverse Transcriptase (*TERT*), Protection of telomeres 1 (*POT1*), Adrenocortical dysplasia protein homolog (*ACD*) and Telomeric repeat-binding factor 2-interacting protein 1 (*TERF2IP).* In addition, there are variants in melanocortin 1 receptor (*MC1R*) and microphthalmia-associated transcription factor (*MITF*) that give a moderately increased risk to develop melanoma [27,31,32].

- High-risk genes

CDKN2A gene (Chr9p21.3) is the first gene described as associated with melanoma susceptibility and to date, it is the main high-risk gene involved in melanoma susceptibility [33]. Approximately 20-40% of familial melanomas present an autosomal dominant inheritance of germline *CDKN2A* mutations [27,29,34]. Two unrelated proteins are encoded by *CDKN2A* gene due to alternatively spliced transcripts: p16 inhibitor of cyclin-dependent kinase 4 ($p16^{INK4A}$, p16) and p14 alternate reading frame ($p14^{ARF}$, p14). Depending which exon is interested by the mutation, the mutation in *CDKN2A* can affect either only one of the two proteins or both. The role of $p16^{INK4A}$ is to prevent that cell enters in S-phase of the cell cycle by inhibiting CDK4. $p14^{ARF}$ is a positive regulator of Cellular tumor antigen p53 (p53) and therefore its loss is associated with accumulation of DNA damage [35]. Individuals carrying *CDKN2A* germline mutations have an inherited risk to develop other cancer types beyond melanoma, such as pancreatic cancer, breast, lung and other tobacco-related cancers [27]. Although *CDKN2A* mutations increase the risk to have melanoma, not all carriers of a *CDKN2A* mutation develop this cancer, suggesting that it needs the contribution of other environmental, clinical, and genetic factors to increase the risk of melanoma development [36-38].

CDK4 (Chr12q14.1) is the second high-risk melanoma susceptibility gene identified. *CDK4* is an oncogene and encodes for a member of the Ser/Thr kinase family. It is active during cell cycle G1 phase and, physiologically, is negatively regulated $p16^{INK4A}$. Both *CDKN2A* and *CDK4* mutations affect the same cellular pathway. *CDK4* was found mutated in several melanoma-prone families and, in all of them, the mutation interested the same amino acid, namely Arginine 24, which is localized in its $p16^{INK4A}$ binding domain. This mutation leads to escape from $p16^{INK4A}$ inhibition and to promote the progression of the cell cycle. In families carrying *CDKN2A* or *CDK4* mutations, there are no particular differences in phenotypic characteristics, such as age at diagnosis and number of melanomas [39,40].

TERT (Chr5p15.33) encodes for an enzyme that plays an important role in cellular senescence. This enzyme has a reverse transcriptase activity that maintains the telomere ends by addition of the telomere repeat TTAGGG. The principal mutation is a transversion T to G in the gene promoter, which was first identified in familial melanomas using high-throughput sequencing [41]. Interestingly, this specific mutation appears to be associated to a high-risk to develop early onset melanoma and other cancers.

BAP1 (Chr3p21) is considered a tumor suppressor gene and it is a deubiquitylase that participates in regulation of cell cycle, cell differentiation, cell death, gluconeogenesis and in DNA damage response [42]. *BAP1* germline mutations seem be associated with tumor predisposition syndrome, which is

associated with various cancers, including CM, uveal melanoma, mesothelioma, renal cell carcinoma, atypical spitz tumors, atypical intradermal tumors and multiple basal cell carcinomas [43,44]. In melanoma, *BAP1* germline mutations appear to be related with the presence of little pink or tan papules and nodules termed melanocytic BAP1-mutated atypical intradermal tumors (MBAITs) [44,45]. The inactivation of *BAP1* contributes to a small proportion of cutaneous melanoma, about 5% [46].

Copy number variants (CNV) analysis has allowed to identify a duplicated region on 4q13 that segregates with melanoma in one melanoma-prone family. There are 10 genes in this duplicated region, and most of them belong to a family of CXC chemokines, such as melanoma growth-stimulating activity α (*CXCL1*) and interleukin 8 (*IL-8*). CXCL1 and IL-8 promote melanoma growth *in vitro* and *in vivo* [47].

Some melanoma susceptibility genes play a role in telomere maintenance. Telomeres consist of tandem nucleotide repeats, namely TTAGGG, and are located at the ends of chromosomes. Telomeres shorten both with age and exposures associated with cancer risk, such as smoking and UV irradiation [48]. Cancer cells tend to implement processes to maintain telomere [49].

A germline mutation in the promoter of *TERT* was identified in a melanoma-prone family. *TERT* (Chr5p15) encodes for the catalytic subunit of the telomerase, which is the ribonucleoprotein complex that maintains telomere length [41].

POT1 (Chr7q31.33) belongs to the complex of Shelterin (also known as Telosome) that controls telomeres length and protects chromosome extremities from illegitimate recombination and abnormal chromosome segregation [50]. The majority of mutations are in the oligonucleotide/oligosaccharide-binding (OB) fold domains, which are crucial for its binding to telomeric single-strand DNA [51]. One of them is a Tyr89Cys variant of the N-terminal OB domain. 4% of melanoma families negative for *CDKN2A* and *CDK4* mutations present alterations in *POT1* [52].

Other germline mutations in two genes of the shelterin complex, namely *ACD* and *TERF2IP,* have been described in melanoma-prone families. The principal germline mutations of *ACD* and *TERF2IP* are associated with an earlier age of melanoma diagnosis, specifically, with a peak in the second decade [53]. Overall, the germline mutations in these four telomere maintenance genes may explain around 1% of familial melanomas [27].

- Moderate-risk genes

The role of the moderate-risk *MC1R* in melanoma susceptibility has been widely studied. *MC1R* (Chr16q24) encodes for the receptor for the α melanocyte-stimulating hormone and is one of the

master regulator genes in human pigmentation. *MC1R* is a highly polymorphic gene in the Caucasian population, and some variants have been associated with an increased risk of developing melanoma [54]. When the function of this gene is highly compromised, the red hair color phenotype (RHC) is usually observed. The most common *MC1R* variants are classified based on their association with RHC in r variants (p.V60L, p.V92M, p.R163Q) and in R variants (p.D84E, p.R142H, p.R151C, p.I155T, p.R160W, p.D294H). The r variants are slightly associated, while R variants are highly associated to RHC phenotype [55,56]. R variants are the most implicated variants in melanoma susceptibility: melanoma risk given by R variants is 2 times higher in the general population, and is increased to 3 times in familial melanoma. However, also a r variant, namely p.R163Q, has been associated with a higher risk of melanoma in geographic areas with high sun exposure [57]. Moreover, this r variant has been associated to a specific melanoma subtype linked to chronic sun damage, namely the lentigo maligna melanoma [58]. The presence of *MC1R* variants increases the melanoma penetrance in *CDKN2A* carriers [59].

MITF (Chr3p13) is considered a moderate-risk gene and it encodes for a basic-helix-loop-helix-leucine zipper transcription factor. MITF is a major regulator of melanocytes development and it has a crucial role in melanoma oncogenesis [60]. In melanoma, there is a recurrent germline mutation in *MITF*, namely the substitution of glutamic acid at position 318 with lysine, called MITF E318K. This mutation is a gain of function mutation and increases melanoma risk. *MITF* E318K mutation has been associated with a particular phenotype, which includes non-blue eye color, increased number of nevi and multiple primary melanomas [61,62].

- Low-risk genes

There are also gene variants that slightly increase melanoma risk, but no variant alone can reach a two-fold melanoma risk [63]. Low-risk genes can be classified based on their role: genes involved in the nevi count and pigmentation (agouti signaling protein (*ASIP*), Tyrosinase (*TYR*), Tyrosinase-related protein 1 (*TYRP1*), Oculocutaneous albinism II (*OCA2*), Methylthioadenosine phosphorylase (*MTAP*), and paired box 3 (*PAX3*)) [64,65]; genes involved in the immunologic system (interleukins such as IL-10, IL-1β, tumor necrosis factor alpha (*TNF-α*), human leukocyte antigen (*HLA*) class II genes, and interferon regulatory factor 4 (*IRF4*)) [66,67]; genes involved in metabolism (cytochrome P450 family 2 (*CYP2D6*), Glutathione S-Transferase Mu 1 (*GSTM1),* Glutathione S-Transferase Theta 1 *(GSTT1),* Glutathione S-Transferase Pi 1 (*GSTP1*), fat mass and obesity associated (*FTO*) gene, and Vitamin D receptor (*VDR*)) [68]-[69], and gene associated to chromatin (Poly ADP-ribose polymerase 1 (*PARP1*)) [67].

Familial melanoma has been associated to the presence of multiple cases of melanoma in different generations on one side of the family, to an early onset the disease, to the predominance of specific mutations, and often to the presence of multiple primary melanomas in the same person [70].

3.1.2.4. Multiple Primary Melanoma

A personal history of melanoma increases the risk of developing other tumors, and particularly other melanomas and non-melanoma skin cancers. Specifically, the frequency to develop at least one more primary melanoma is range between 0.2 and 10% of all diagnosed melanomas [29,71-74]. Multiple Primary Melanoma (MPM) refers to a patient that has developed at least two primary cutaneous melanomas in its lifetime. The highest risk is in the first year following the diagnosis of the primary melanoma; but the risk remains increased for at least 20 years [75].

The occurrence of MPM seems to be related to a genetic susceptibility and also to environmental factors, such as UV radiation exposure across geographical regions. The risk to develop the second melanoma is increased to 19% for melanoma patients with a positive family history. However, in MPM patients, the presence of the germline mutations associated to familial melanoma is lower than expected [29,76-79].

The germline mutations in *CDKN2A* are present in 8-15% of patients diagnosed with MPM without familial history and up to 40% in patients with familial melanoma [29,77,79-82]. Interestingly, the probability to found *CDKN2A* mutations is about 1% in sporadic melanoma patients without personal and/or familial history of melanoma [83]. An increased risk of MPM is also associated with nonsense germline mutations in *ACD* and *TERF2IP* genes [53]. In addition, the presence of dysplastic nevi (DN) increases up to 3 times the risk to have a second melanoma compared to melanoma patients without DN [84].

MPM patients represent a model of high-risk CM occurrence. However, there is a debate about the prognosis of MPM [85,86].

3.1.3. Melanoma onset and progression

Melanoma derives from the malignant proliferation of melanocytes. Melanocytes cells embryologically derive from neural crest cells that differentiate into melanocytes with the cooperation of several transcription factors, including Forkhead Box D3 (FOXD3), SRY-Box Transcription Factor 10 (SOX10), PAX3 and MITF. Melanocytes produce the brown-black skin pigment, know as melanin, and provide this pigment to keratinocytes. They are characterized by a low proliferative rate. UV radiation promotes both proliferation and melanin production of the melanocytes. However, the

acquisition of somatic mutations and alteration in specific pathways is associated with malignant transformation of melanocyte, namely melanoma [87].

3.1.3.1. Somatic genetic alterations in melanoma

The majority melanoma cases are attributable to randomly acquired genetic mutations, which can contribute to cancer development and metastasis progression. Somatic mutations often occur in genes implicated in the activation of the mitogen-activated protein kinases (MAPK) pathway, affecting cell proliferation, differentiation and survival [88], and in phosphoinositol-3-kinase/ protein kinase B (PI3K/Akt) pathway, affecting metabolism, proliferation, cell survival, growth and angiogenesis [89]. Both MAPK and PI3K/Akt pathways are frequently influenced by aberrations that are pivotal players in biology of different types of cancer, including melanoma [90]. In melanoma, somatic mutations are often located in the following genes: B-Raf Proto-Oncogene (also known as v-Raf murine sarcoma viral oncogene homolog B, *BRAF*), neuroblastoma RAS viral oncogene homolog (*NRAS*), Neurofibromin 1 (*NF1*), proto-oncogene receptor tyrosine kinase (*KIT*) and Phosphatase and Tensin homolog (*PTEN*). Somatic alterations are also found in genes already described, such as *MITF* gene.

BRAF (Chr7q34) encodes for a serine/threonine-protein kinase. Up to 50% of the UV-induced somatic mutations are present on *BRAF* gene, and 71-75% of melanomas showed at least a mutation in this gene [91]. *BRAF* mutations are usually gain-of-function. The most frequent is a missense mutation, namely an amino acid substitution at position 600: a hydrophobic valine is replaced by hydrophilic glutamic acid. This mutation is named BRAF V600E and it covers up to 90% of all BRAF mutations [92]. With BRAF V600E mutation, the kinase becomes constitutively active and insensitive to negative feedback mechanisms, inducing angiogenesis, evading apoptosis and promoting invasion and metastasis [93,94]. BRAF V600E mutation is also present is common nevi and atypical nevi [95-97]. Its rate is even higher in benign nevi compared to melanoma [98]. These findings shed light on the probable role of BRAF V600E as an early step in melanocytic transformation. However, in precursor benign lesion, this mutation alone is not relevant in promoting tumor progression [99].

In addition, there are other point mutations in the same position, such as V600K, V600D, V600R, which increase BRAF kinase activity. Mutations in other sites are less than 1% [92]. Patients with BRAF-mutated melanoma are often younger than other melanoma patients in term of diagnosis of primary melanoma and metastasis, and they frequently develop tumors with superficial spreading or nodular histology [100].

NRAS (Chr1p13.2) encodes for a small GTP binging protein of the RAS family that is involved in the MPAK pathway. *NRAS* mutations are associated with chronical sun exposure [101]. *NRAS* mutations

are found in about 15-30% of melanomas [102] and are often missense mutations, especially in exon 2 at codon 61, known as Q61-. These mutations account 80% of the *NRAS* mutations in melanoma and consist in substitution of the glutamine with a lysine (Q61K) or an arginine (named Q61R) or a leucine (Q61L). Q61- mutations impair GTP hydrolysis [103,104]. The constitutive activation of NRAS drives MAPK and PIK3/Akt pathways promoting cell-cycle dysregulation, pro-survival mechanisms, and cellular proliferation [105].

NRAS mutated melanoma are frequently lesions located at the extremities, and with lower rate of ulceration, thicker Breslow thickness and higher rate of mitosis compared to *BRAF* mutated melanoma [106]. Generally, *NRAS* and *BRAF* mutations are mutually exclusive in melanoma [107]. Patients with *NRAS* Q61- mutations tend to be older (>55 years) than patients with *BRAF* V600E mutation [106]. *NRAS* mutations are an independent adverse prognostic factor that leads to a shorter overall survival (OS) in comparison to *BRAF* mutated melanoma when the diagnosis occurs in advanced stage of disease [102,108]. On the other hand, in early stage of disease, *NRAS* mutations have no impact on OS [109].

NF1 (Chr17q11.2) is a tumor suppressor gene that encodes for a protein that inactivates the RAS/MAPK pathway by catalyzing the hydrolysis of active RAS-GTP to inactive RAS-GDP. The loss of function of NF1 induces a hyperactivation of RAS proteins and a promotion of both MAPK and PIK3/Akt pathways [110]. *NF1* mutations are the 3rd most common driver mutations in CM and they are reported in about 14% of melanomas [111]. *NF1*-mutated melanomas present higher tumor mutational burden (the amount of gene mutation that occurs in the genome of a cancer cell) that other subtypes and a robust UV-derived mutational signature. *NF1* mutations can co-occur with *BRAF* or *NRAS* mutations in melanoma [112].

KIT (Chr4q12) encodes for a transmembrane receptor with tyrosine kinase activity [113]. Frequent mutations are L576P (lysine to proline substitution on 576 codon) localized to exon 11 and K642E (methionine to glutamic acid substitution on 642 codon) localized to exon 13 [114]. These mutations induce gain of function of the protein, leading to a constitutive activation of kinase activity and a promotion of both MAPK and PI3K/Akt pathways [113]. Mutations in *KIT* gene occur in 1-3% of all melanomas, and are mutually exclusive with *BRAF* and *NRAS* mutations [115]. Mutated-*KIT* is especially found in 15% of acral and mucosal subtypes of melanoma [114,116].

PTEN (Chr10q23.31) is a tumor-suppressor gene that encodes for a key regulator of the PI3K signaling pathway. The partial or complete loss of gene function in tumoral cells promotes melanoma development by increasing Akt activity, stimulating mitogen signaling and decreasing apoptosis [117]. *PTEN* mutations are often frameshift or chromosomal deletion and they occur in up to 30% of

cutaneous melanoma [118]. *PTEN* mutations seem to be more prevalent in invasive and metastatic melanomas than in primary tumors [119]. *PTEN* mutations often co-exist with *BRAF* mutations and contribute to activate PI3K/Akt pathway, but they are mutually exclusive with *NRAS* mutations, which independently activate the same pathway [119,120]. *PTEN* is also regulated by epigenetic mechanisms [121].

MITF gene is interested also by somatic mutations, which can generate different isoforms. M-MITF is the central isoform in melanocyte development and carcinogenesis: it is found in about 80% of melanomas and is present at different stages of tumor progression [122]. *MITF* is important for the progression of BRAF V600E mutated melanomas [123]. Finally, mutations in *MITF* gene have been detected in 20% of metastatic melanomas [113].

3.1.3.2. Melanoma onset and progression models

For melanoma progression, two principal models have been described: one linear and one nonlinear.

- Linear model

The linear model for melanoma progression is known as the Clark model and consists in 6 lesional steps [124] (**Figure 1**):

1. the acquisition of a melanocytic nevus
2. the evolution in melanocytic nevus with lentiginous melanocytic hyperplasia (aberrant differentiation)
3. the progression in melanocytic nevus with aberrant differentiation and melanocytic nuclear atypia (melanocytic dysplasia)
4. the onset a primary melanoma with radial growth phase (RGP)
5. the acquisition of vertical growth phase (VGP) of primary melanoma
6. the progression in metastatic melanoma.

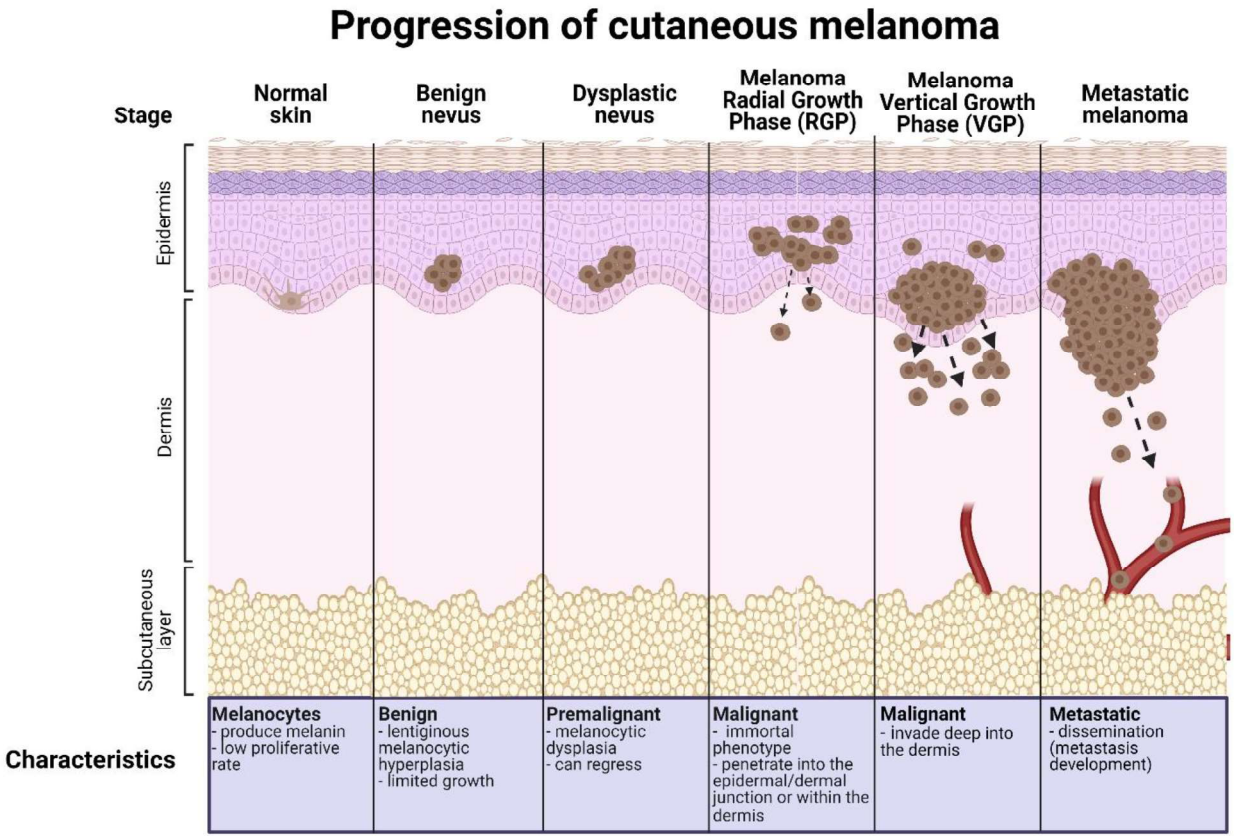

Figure 1. Progression of cutaneous melanoma. According to Clark model, melanoma progression starts from the transformation of normal melanocytes to benign nevi, which can proliferate to a pre-malignant lesion, namely dysplastic nevus. In the radial growth phase (RGP), melanoma cells proliferate toward the epidermis, followed by the invasion of the dermis in the vertical growth phase (VGP). The last stage consists in the formation of metastatic melanoma, which spreads in the bloodstream to invade other organs. Other models postulate that malignant cutaneous melanomas can arise directly as RGP/VGP tumors from a single transformed melanocyte (Figure from "Pathophysiology roles and translational opportunities of miRNAs in Cutaneous Melanoma", MicroRNA in Human Malignancies edited by Massimo Negrini, George Calin, Carlo Croce, *in press).*

The most recent discoveries have been significantly improved this model. The first stage is the formation of a benign nevus (BN), which results from the benign proliferation and aggregation of melanocytes. However, some of them are described as dysplastic nevi or atypical moles, because they present altered growth pattern. The transition from benign nevi to DN can be due to mutations in *BRAF* gene or to activation of Akt [7].

The over-proliferation of these cells causes their penetration into the epidermal/dermal junction. When the melanocytes proliferate remaining confined within the epidermal layer of the skin and do not invade the underlying dermis and deeper tissues, the neoplastic lesion is named melanoma *in situ*. This phase is characterized by altered apoptosis and cellular survival, which is may due to mutations

or epigenetic silencing with consequent inactivation of *CDKN2A* and impair of $p16^{INK4A}$-retinoblastoma (Rb) pathway [125], amplification of Cyclin D1 (CCND1), and inactivation of p53.

The next step consists in the invasion within the dermis by RGP that results in the formation of melanoma. It seems that melanocytes acquired an immortal phenotype with the activation of the TERT [126]. In the last stages of melanoma progression, there is a VGP, which allows to invade deep into the dermis to develop metastasis as final phase. The loss of epithelial (E)-cadherin and the aberrant expression of neural (N)-cadherin and αVβ3 integrin have been involved in the progression from RGP to VGP [127]. The last step of the linear model requires alterations that could repress apoptosis, allowing the survival far from the keratinocytes, such as mutations in *NRAS, KIT, PTEN, CDKN2A, MITF* [7].

- Nonlinear model

This model supposed that malignant melanoma, namely melanoma that develop metastases, can originate from each of the step described in the linear model, without necessary passing through all of them. This model is supported by the fact that melanoma stem cells are involved in melanoma origin, progression and metastasis [128]. Specifically, it seems that alterations in melanoma stem cells can promote the transformation in melanoma cells with RGP or VGP, or directly in metastatic cells [7].

The increasing knowledge and the discoveries of epigenetic, genetic and transcriptomic mechanisms that affect cancer development, suggest a more complex picture of melanoma onset, progression and metastasis.

3.1.4. Melanoma classification

Similarly to the majority of tumors, cutaneous melanoma is traditionally divided into primary and metastatic. Primary melanoma is further classified in melanoma *in situ*, namely when tumor cells are limited to the epidermis, and invasive melanoma, when tumor cells invade into the dermis.

According to the clinical and histopathological characteristics, invasive melanoma has been classified into four major histological subtypes: superficial spreading melanoma (SSM), nodular melanoma (NM), lentigo maligna melanoma (LMM) and acral melanoma (AM) [129] (**Figure 2**).

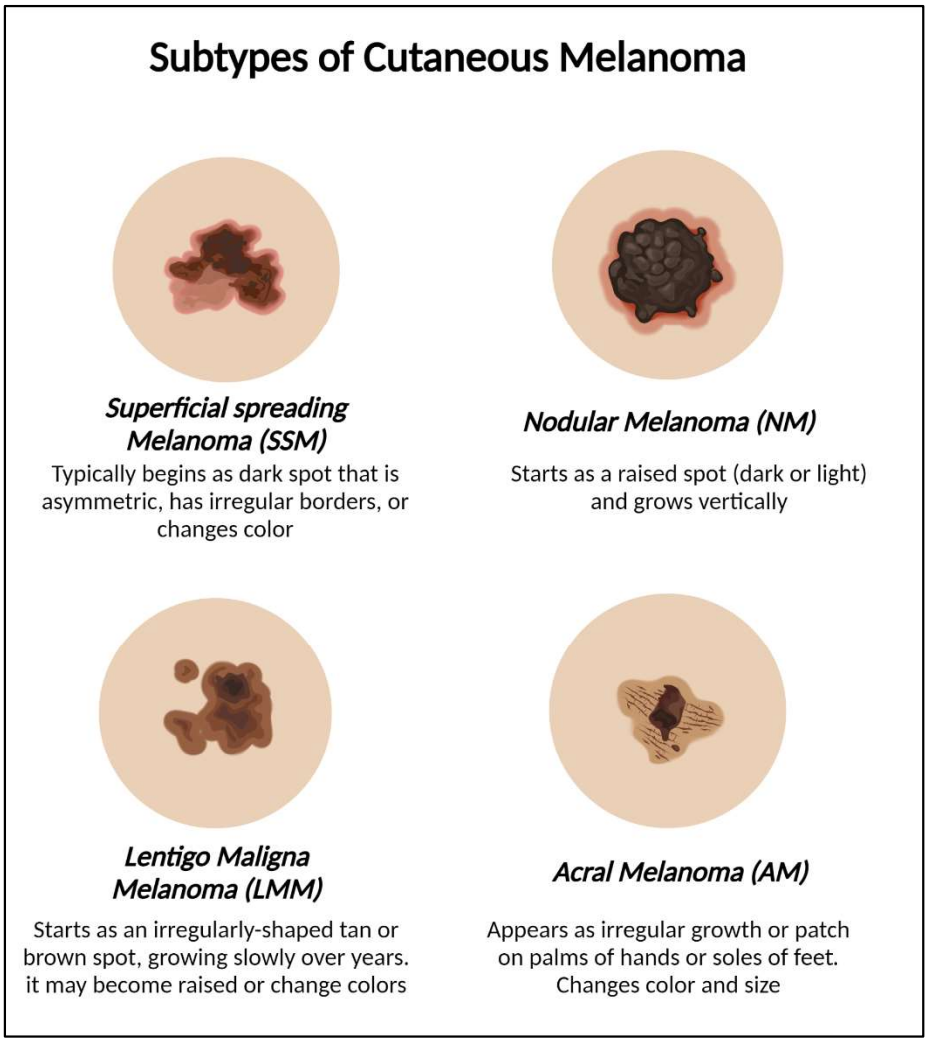

Figure 2. The four major histological subtypes of cutaneous melanoma: Superficial spreading melanoma (SSM), Nodular melanoma (NM), Lentigo maligna melanoma (LMM) and Acral melanoma (AM). Figure created with *Biorender.com*

- Superficial spreading melanoma

SSM is the more frequent subtype, and accounts for 41% of melanomas. Both melanoma *in situ* and SSM consist in a pigmented macule with irregular borders that can evolve into a papule or plaque. Differently from melanoma *in situ*, SSM is an invasive melanoma that penetrates into the superficial dermis. In fact, SSM presents first an RGP, where SSM growth in the epidermis or in the papillary dermis, and then a VGP, where SSM invades the deeper dermis [130].

SSM may arise *de novo* or in association with a nevus [131]. The major histologic property of SSM is the presence of tumor cells scattered throughout the epidermis in a reminiscent pattern of pigmented mammary Paget disease. The major clinical property of SSM is a spreading lesion that changes over time [132]. SSM localized often in sites prone to intense, sporadic sun-exposure, such as the trunk and extremities. SSM usually shows an irregularly shaped cutaneous macule > 6mm in size with variegation of colors [133].

- Nodular melanoma

NM accounts 16% of melanomas and it is characterized by an exophytic/nodular, brown-to-black, often eroded tumor. NM is often symmetric, elevated, small in diameter, and amelanotic and has a single color. NM localized mostly on the head and neck, and is commonly observed in men older than 50 years. Nodular subtype constitutes nearly half of the melanomas ticker than 2mm. Compared to the other subtypes, nodular melanoma possesses a more rapid growth rate, more biologically aggressive behavior, and an increased number of mitoses. NM seems to lack an initial RGP and rather begins with VGP [134].

- Lentigo maligna melanoma

In the elderly, lentigo maligna is defined as melanoma *in situ* localized on chronically sun-damaged skin, confined to the epidermis. On the other hand, if the lesion becomes invasive, the tumor is known as LMM. LMM ranges from 2.7 to 15% of melanomas. LMM consists in an irregular brown macule on chronically sun-damaged skin, such as the head and neck. UV radiation, particularly cumulative lifetime UV exposure, is the major risk factor for developing LM/LMM. Differently from SMM and NM that are associated with intense intermittent UV exposure, LM and LMM are associated with chronic UV exposure. The chronic UV exposure leads to a high mutation rate in this subtype. The prognosis for LM and LMM is excellent, in fact, the 5-year and 10-year disease-specific survival are 100% and 97.1%, respectively [135].

- Acral melanoma

AM is less frequent compared to the other subtypes; it is about 1-5% of melanomas. Despite its rarity, AM is the most common type of melanoma diagnosed in darker skin color people. Its most common subtype is the acral lentiginous melanoma (ALM). AM can be a macule/plaque or a nodule that grows slowly and localizes on the extremities with poorly circumscribed pigmentation. The typical CM risk factors, such as sun exposure, fair skin type, family or personal history of melanoma, and pre-existing melanocytic nevi, are not applicable to AM. The mechanical stress has been suggested as a risk factor for the development of AM [136]. AM has a poor prognosis that can be due to advanced stage at presentation. In fact, it seems that the reduced survival is primarily attributable to a delay in diagnosis and to a biologically aggressive behavior [137].

3.1.4.1. Genomic classification

Melanomas can be classified into four genomic subtypes based on the pattern of the most prevalent significantly mutated genes: mutant *BRAF*, mutant *RAS (N,H,K)*, mutant *NF1*, and Triple-wild type (Triple-WT). The first subgroup presents mutated-*BRAF* and *MITF* amplification. Patients are generally younger compared to the other subgroups. The mutated-RAS subgroup is characterized by MAPK activation and RAC-gamma serine/threonine-protein kinase (Akt3) overexpression. Patients from mutant *NF1* subgroup are older and with higher mutation burden. Finally, the triple wild-type subgroup is enriched of *KIT* mutations, focal amplifications and complex structural rearrangements. In addition, it lacks UV signature and manifests more copy number changes [138] (**Figure 3** from [138]).

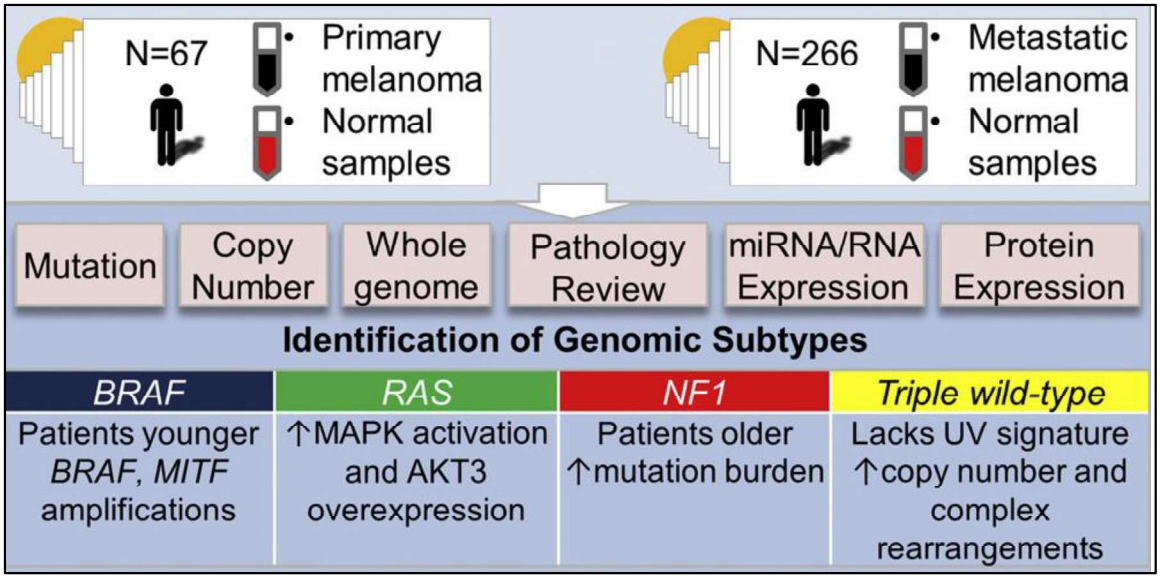

Figure 3. Identification of genomic subtypes of cutaneous Melanoma. The study represents the largest integrative analysis of cutaneous melanoma (331 patients) and establishes a framework for melanoma genomic classification: BRAF, RAS, NF1, and Triple-WT. Figure from graphical abstract of [138].

3.1.5. Pathological staging

The American Joint Committee on Cancer (AJCC) developed the TNM classification system for CM in according to the last World Health Organization (WHO) classification of melanoma [139]. It takes into consideration some relevant elements related to the different clinical staging of the tumor, including Breslow thickness, ulceration, metastases [140]. Clinical stage of tumor is defined after biopsy and/or clinical assessment of regional lymph nodes.

3.1.5.1. T category

T category refers to the measure of the thickness of the melanoma as defined by Dr. Alexander Breslow (from T1 to T4), and the definition of the ulceration status (a or b). Tumor thickness, known

also as Breslow thickness (BT), is measured from the top of the granular layer to the deepest invasive cell across broad base of the tumor (in the dermis or subcutis) [140]. Frequently, higher values of BT corresponds to poorer prognosis [141,142]. Ulceration status is defined by the total absence of an intact epidermis, in particular of the stratum corneum and basement membrane of dermo-epidermal junction and the presence of an associated host reaction (with fibrin deposition, neutrophils) above the primary melanoma [140,143].

Classification based on T category is reported in **Table 1** [1]. A cut-off of 0.8mm has been introduced to separate T1 melanomas with ulceration (T1a and T1b), because it was observed that patients with a thickness ≤ 0.8mm have a different prognosis compared to patients with a melanoma ≥ 0.8 or > 1.0mm, specifically a better prognosis [144].

Table 1. T classification in melanoma

T Category	Thickness	Ulceration status	Note
TX	-	-	Primary tumor thickness cannot be assessed
T0	-	-	No evidence of primary tumor (unknown primary tumor or completely regressed melanoma)
Tis (Melanoma *in situ*)	-	-	Transformed melanocytes proliferate remaining confined within the epidermal layer of the skin and do not invade the underlying dermis and deeper tissues
T1	≤ 1.0mm	unknown or unspecified	
T1a	< 0.8mm	without ulceration	
T1b	< 0.8mm	with ulceration	
	0.8-1.0mm	with or without ulceration	
T2	> 1.0-2.0mm	unknown or unspecified	
T2a	> 1.0-2.0mm	without ulceration	
T2b	> 1.0-2.0mm	with ulceration	
T3	> 2.0-4.0mm	unknown or unspecified	
T3a	> 2.0-4.0mm	without ulceration	
T3b	> 2.0-4.0mm	with ulceration	
T4	> 4.0mm	unknown or unspecified	
T4a	> 4.0mm	without ulceration	
T4b	> 4.0mm	with ulceration	

3.1.5.2. N Category

The N category indicates the number of tumor-involved regional lymph nodes (N1-3). In addition, there is a sub-classification (a-c) that reflects the presence or absence of in-transit, satellite, and/or microsatellite metastases. To investigate the presence of tumor cells, the sentinel lymph node (SLN) biopsy is performed. N classification is reported in **Table 2** [1].

Table 2. N classification

N category	Number of tumor-involved regional lymph node	Presence of in-transit, satellite, and/or microsatellite metastases
NX	Regional nodes not assessed (e.g., SLN biopsy not performed, regional nodes previously removed for another reason). Exception: pathological N category is not required for T1 melanomas, use Cn.	no
N0	No regional metastasis detected	no
N1	One tumor-involved node or in-transit, satellite, and/or microsatellite metastases with no tumor-involved nodes	
N1a	One clinical occult (e.g., detected by SLN biopsy)	no
N1b	One clinical detected	no
N1c	No regional lymph node disease	yes
N2	Two or Three tumor-involved node or in-transit, satellite, and/or microsatellite metastases with one tumor-involved nodes	
N2a	Two or three clinical occult (e.g., detected by SLN biopsy)	no
N2b	Two or three, at least one of which was clinically detected	no
N2c	One clinically occult or clinically detected	yes
N3	Four or more tumors-involved node or in-transit, satellite, and/or microsatellite metastases with two or more tumors-involved nodes, or any number of matted nodes without or with in-transit, satellite, and/or microsatellite metastases	
N3a	Four or more clinical occult (e.g., detected by SLN biopsy)	no
N3b	Four or more, at least one of which was clinically detected, or presence of any number of matted nodes	no
N3c	Two or more clinically occult or clinically detected and/or presence of any number of matted nodes	yes

3.1.5.3. M category

M category shows the absence or presence of distant metastasis (0-1), and the site(s) of development of metastasis (a-d). The latest melanoma classification has also maintained the analysis of serum Lactate dehydrogenase (LDH) levels as a classification feature, and it reported using the following suffix for M category: (0) LDH not elevated, (1) LDH elevated. M classification is described in **Table 3** [1].

Table 3. M classification

M category	Anatomic site	LDH level
M0	No evidence of distant metastasis	Not applicable
M1	Evidence of distant metastasis	
M1a	Distant metastasis to skin, soft tissue including muscle and/or nonregional lymph node	Not recorded or unspecified
M1a (0)		Not elevated
M1a (1)		Elevated
M1b	Distant metastasis to lung with or without M1a sites of disease	Not recorded or unspecified
M1b (0)		Not elevated
M1b (1)		Elevated
M1c	Distant metastasis to non-CNS visceral sites with or without M1a or M1b sites of disease	Not recorded or unspecified
M1c (0)		Not elevated
M1c (1)		Elevated

M1d	Distant metastasis to CNS with or without M1a, M1b or M1c sites of disease	Not recorded or unspecified
M1d (0)		Normal
M1d (1)		Elevated

Suffix for M category: (0) LDH not elevated, (1) LDH elevated. No suffix is used if LDH is not recorded or unspecified

3.1.5.4. Stage groups

Melanoma staging is based on the degree of disease spread: localized (stage I and II), regional (stage III) and distant (stage IV). Stage 0 corresponds to melanoma *in situ*, namely Tis. All Stage I and II are N0 and M0. Therefore, their stage changes depending on the T value. In addition, all Stages III have no metastasis (M0). Finally, stage IV includes any T, any N and distant metastasis (M1). The correspondence between stage and TNM classification can be found in **Table 4** [1].

Table 4. TNM Pathological Staging Overview

Stage	Tumor	Node	Metastasis
0	Tis	N0	M0
IA	T1a or T1b	N0	M0
IB	T2a	N0	M0
IIA	T2b or T3a	N0	M0
IIB	T3b or T4a	N0	M0
IIC	T4b	N0	M0
IIIA	T1a/b or T2a	N1a or N2a	M0
IIIB	T0 T1a/b or T2a T2b or T3a	N1b or N1c N1b/c or N2b N1a/b/c or N2a/b	M0
IIIC	T0 T1a/b or T2a/b or T3a T3b or T4a T4b	N2b/c or N3b/c N2c or N3a/b/c Any N≥N1 N1a/b/c or N2a/b/c	M0
IIID	T4b	N3a/b/c	M0
IV	Aby T, Tis	Any N	M1

3.1.5.5. Other histologic features

There are two other important histologic features in tumor prognosis, namely regression and the presence of Tumor-Infiltrating Lymphocytes (TILs).

Regression indicates the loss of the thickness of the lesions with scarring fibrosis and the presence of inflammation between an apparently separate nodule and the primary tumor (rather than normal stroma). When these findings are present, the nodule is considered to be an extension of the primary tumor and not a micro-metastasis. Relationship between regression and prognosis is controversial [145,146]. Finally, the histopathologic classification of TILs divided melanoma in three groups:

- absent TIL infiltrate: no lymphocytes are present or, if present, they do not interact with the tumor cells;
- non-brisk TIL infiltrate: focal areas of lymphocytic infiltration in the tumor (isolated, multifocal or segmental);
- brisk TIL infiltrate: TIL infiltration covers the entire base of the tumor.

3.1.6. Diagnosis and prognosis

The early detection of melanoma can considerably increase the chance of survival. Therefore, the recognition, detection and treatment are crucial. The cutaneous localization of melanoma is a great advantage, in fact, it allows a non-invasive skin exam for the early diagnosis [147].

Before the '80s, the diagnosis was performed with the identification of clinically macroscopic features. Successively, ABCDE criteria were introduced: ABCDE is acronym for Asymmetry, Border irregularity, Color variegation, Diameter, Evolving. These criteria are a simply, objective and adequate tool for morphological diagnosis, which allows to evaluate and differentiate common nevi from cutaneous lesions most suspected to develop in melanoma. The increment of the sensitivity of skin examination from 57% to 90% is due to the use of ABCDE criteria [148].

In the last years, the use of Dermoscopes (or Dermatoscopes, epiluminescent microscope) has been introduced, which are high resolution devices that allow increasing accuracy in melanoma detection. Dermoscope is a non-invasive technique, a handheld optical device that is enabled to show structures that are not visible to naked eye [149].

Also 3D technologies can be used to perform a correct screening, because it is possible to obtain total-body images through a system of many cameras that take photos of the entire body and to retrieve images in a digital 3D model. The advantage of this technique is to show every nevus or spot on the body, and to monitor every minimal change in the early stage of melanoma. It is particular useful for patients with high-risk to develop melanoma due to their personal or family history or those with multiple dysplastic nevi [150].

The development of many non-invasive *in vivo* techniques, such as Ultrasound, Confocal Scanning Laser Microscopy, Magnetic Resonance Imaging and Optical Coherence Tomography, has improved the diagnostic accuracy and sensitivity for skin tumors [151].

The gold standard for diagnosis remains the histological examination. An expert pathologist analyzed the biopsy and evaluated architectural and cytologic aspects of the melanoma to define diagnosis, staging and prognosis [152].

Molecular biomarkers can be used to the detection of melanoma. The immunohistochemistry (IHC) is especially useful for the interpretation of difficult cases. IHC detected biomarkers expressed in or on the surface of tumor cells [153].

For melanoma diagnosis, the most used biomarkers are melanocytic markers, which are used to determine if an ambiguous lesion has a melanocytic origin and if the lesion expresses proteins involved in melanosomes biogenesis, melanin synthesis or melanocyte differentiation. Common melanocytic markers used for melanoma diagnosis include Melanoma antigen recognized by T-cells 1 (MLANA), Glycoprotein 100 (gp100), S100 protein, MITF, Tyr and SOX10 [154]. Melanocytic markers are useful, but they stain all melanocytes and thus they do not discriminate between melanoma and benign melanocytes [154].

Other molecular biomarkers are proliferative markers that are used for diagnosis and prognosis of melanoma. Proliferative markers evaluate the cell cycle activity in a lesion, specifically, they determine the number of proliferating cell in the cell cycle: benign melanocytic lesion has a less proliferative rate, while malignant melanoma has a high proliferative index. The most common proliferative biomarkers are Ki-67 and phosphohistone H3 (PHH3). The limitation of these biomarkers is their lack of specificity for melanocytes [154].

As prognostic biomarkers, there are also some biomarkers detected in patient blood, plasma or serum. Among them, there is LDH, an independent prognostic indicator for malignant melanoma, used in the AJCC melanoma staging system. Elevated LDH is recognized as an adverse prognostic indicator for patients with stage IV melanoma [155].

Other factors that correlated with the prognosis are BT, ulceration, presence of metastases in regional lymph node or distant sites metastases [156-158]. BT usually increases with tumor progression [159]. Ulceration on microscopic melanoma sections is an adverse prognostic finding, in fact, the presence of ulceration has been associated with a reduction of the 5-year survival rate. In addition, ulcerated melanomas are thicker and more likely to have a nodular growth pattern [160]. On the other hand, the presence of TILs is an index of a favorable prognosis [120,161,162]. Beyond the classic evaluation of the biopsy, the sentinel lymph node biopsy is associated with tumor prognosis [163]. In fact, regional lymph nodes are the most common site of initial metastasis in CM patient. The process of mapping SLN is minimally invasive but it allows to find metastases also in patient with clinically occult disease. The presence of metastases or micro metastases in sentinel lymph node provides prognostic information needed by clinicians to decide the treatment plan [164].

3.1.7. Treatment

The treatments for melanoma include surgical resection, chemotherapy, targeted therapy and immunotherapy. Single agents or combined therapy can be used based on health of the patient, and stage and location of the tumor. Early-stage melanomas, namely stage I and II, are treated by surgery. Treating metastatic melanoma still remains an important challenge. The efficiency of the treatment can be impaired by the onset of drug resistance [165].

3.1.7.1. Surgery and radiotherapy

After the complete excision of an early-stage melanoma, radiotherapy can be used as adjuvant therapy to reduce the risk of local recurrence in high-risk clinical situations. Radiotherapy led to good outcome in metastatic melanoma, however it does not affect survival [166].

Stage III melanomas can be treated surgically in combination with adjuvant treatment, such as targeted therapy and immunotherapy, to obtain a better response to the treatment. In fact, BRAF-mutated (V600E and V600K) melanomas have improved survival outcomes thanks to adjuvant-targeted therapy with BRAF inhibitors (BRAFi), such as dabrafenib and trametinib. Adjuvant immunotherapy with Programmed cell death 1 (PD-1) inhibitors, such as nivolumab and pembrolizumab, increases relapse-free survival. Immunotherapy with high-dose of Cytotoxic T-lymphocyte protein 4 (CTLA-4) inhibitor, named ipilimumab, improves overall survival [167]. Due to high number of metastases or to low accessibility and difficult of detecting small metastatic lesions, it is unlikely that surgery completely cures metastatic melanoma [154].

3.1.7.2. Chemotherapy

Surgical treatment alone is not curative for melanoma patients with progressive, refractory, or relapsed diseases, and so drug therapies need to be used. Until recently, the chemotherapy was the only available treatment for patients with metastatic melanoma. Chemotherapeutic agents commonly used are temozolomide (TMZ) and dacarbazine (DTIC), alkylating agents, which block or slow cell proliferation by inhibiting DNA synthesis. These agents have been used alone or in combination [168]. The prognosis for patients with metastatic melanoma has been greatly improved by the discovery of new drugs. Nowadays, chemotherapy is only used after and when more effective treatments, such as target therapy and immunotherapy, fail [169].

3.1.7.3. Targeted Therapy

MAPK pathway is often altered and constitutively activated in melanoma, and its components are frequently mutated in melanoma cells. This provided the base for targeted therapies in melanoma.

Targeted therapy includes the use of BRAFi and mitogen-activated protein kinase kinase 7 (MEK, also known as MAP2K7) inhibitors (MEKi). Among the most effective BRAFi, there are vemurafenib and dabrafenib, which were approved for the treatment of metastatic and unresectable *BRAF*-mutated melanomas in 2011 and 2013, respectively [154]. In addition to BRAF, targeted therapy can be addressed against another component of the MAPK pathway, namely MEK. It was observed that MEKi act by inhibiting the growth and inducing apoptosis in *BRAF*- and *NRAS*-mutant melanoma cell lines. MEKi therapy is used in combination with BRAFi. Moreover, the combination of BRAFi and MEKi is more effective and less toxic than treatment with BRAFi alone, and it is the standard-of-care for patients with *BRAF*-mutated melanoma. Specifically, the MEKi trametinib has been approved in combination with the BRAFi dabrafenib, while the MEKi cobimetinib has been approved in combination with BRAFi vemurafenib [170].

The continuous use of BRAFi and MEKi agents has been associated with drug resistance [171]. There is a novel treatment option available for patients with *BRAF*-mutant melanomas, namely the combination of a new generation of BRAFi (Encorafenib) and MEKi (Binimetinib). The new combined treatment has similar response rate but a longer duration of response compared to dabrafenib and trametinib combination [172].

3.1.7.4. Immunotherapy

At the beginning of the ‘90s, the first immune therapy for metastatic melanoma based on interleukein-2 (IL-2) treatment was approved. This interleukin is a T-cell growth factor, which promotes expansion of anti-melanoma CD8+ T-cells but is also highly toxic [154].

To date, immune checkpoint inhibitors, namely antibodies against PD1, programmed death-ligand 1/2 (PD-L1/2) and CTLA-4, are the most effective immunotherapy in metastatic melanoma. The most immune checkpoint inhibitors used for melanoma treatment are ipilimumab (anti-CTLA-4 antibody), nivolumab and pembrolizumab (anti-PD-1 antibodies) [173], and atezolizumab (anti-PD-L1 antibodies). The combination of ipilimumab and nivolumab is preferred than the treatment with only one immune checkpoint inhibitor, but it leads to an increase of drug-related toxicity [174]. The side effects are usually immune-related inflammatory conditions of the skin, gastrointestinal system, and endocrine organs, that lead to the end of the treatment [175]. Moreover, many patients develop drug resistance.

Comparing immunotherapy with targeted therapy, the immunotherapy with anti-PD-1 drugs leads to lower response rates but longer response duration if compared to BRAFi/MEKi. For patients with stage IV melanoma, the combination of targeted therapy and immunotherapy is suggested: BRAFi

and MEKi combined with anti-PD-1 agents can improve the antitumor activity [176,177]. Results showed that the use of both targeted and immunotherapy therapies has improved the survival for most patients, and these therapies are now preferred for patients with metastatic melanoma.

3.2. MICRORNA

MicroRNAs (miRNAs) are small non-coding RNAs and are about 22 nucleotides (nts) in length. MiRNA are transcribed from DNA into primary miRNAs (pri-miRNAs) and processed into precursor miRNAs (pre-miRNAs) and mature miRNAs.

MiRNAs function as guide molecules in RNA silencing. Specifically, miRNAs can interact with different portions of target messenger RNAs (mRNAs), including 3′ untranslated region (UTR), 5′ UTR, coding sequence, and gene promoters, to repress mRNA translation into protein and/or to induce mRNA degradation by cleavage [178,179]. Moreover, under certain conditions, miRNAs have been shown to activate gene expression [180]. Finally, it has been suggested that miRNAs can be transferred between different subcellular compartments to control the rate of translation and transcription [181].

MiRNAs are fundamental in all development and biological processes [182]. Many human diseases, including tumors, have been associated with aberrant expression of miRNAs [183-185].

It was observed that miRNAs can be secreted into extracellular fluids, and extracellular miRNAs serve as signaling molecules to mediate cell-cell communications and can be used as potential biomarkers [186-188].

3.2.1. miRNA biogenesis

miRNA biogenesis is under tight temporal and spatial control. miRNA genes are transcribed by RNA polymerase II (Pol II) in long primary transcripts, which have a local hairpin structure where miRNA sequences are embedded [178]. About half of all currently identified miRNAs are intergenic, namely they are transcribed independently of a host gene and regulated by their own promoters. The other half of miRNAs are intragenic and processed mostly from introns and relatively few exons of protein coding genes [189,190]. Some miRNAs can be transcribed as one long transcript called clusters. For this reason, these miRNA can show similar seed regions, and in this case, they are considered a family [191]. The biogenesis of miRNA has been classified into canonical and non-canonical pathways [192] (**Figure 4** from O'Brein et al. [192]).

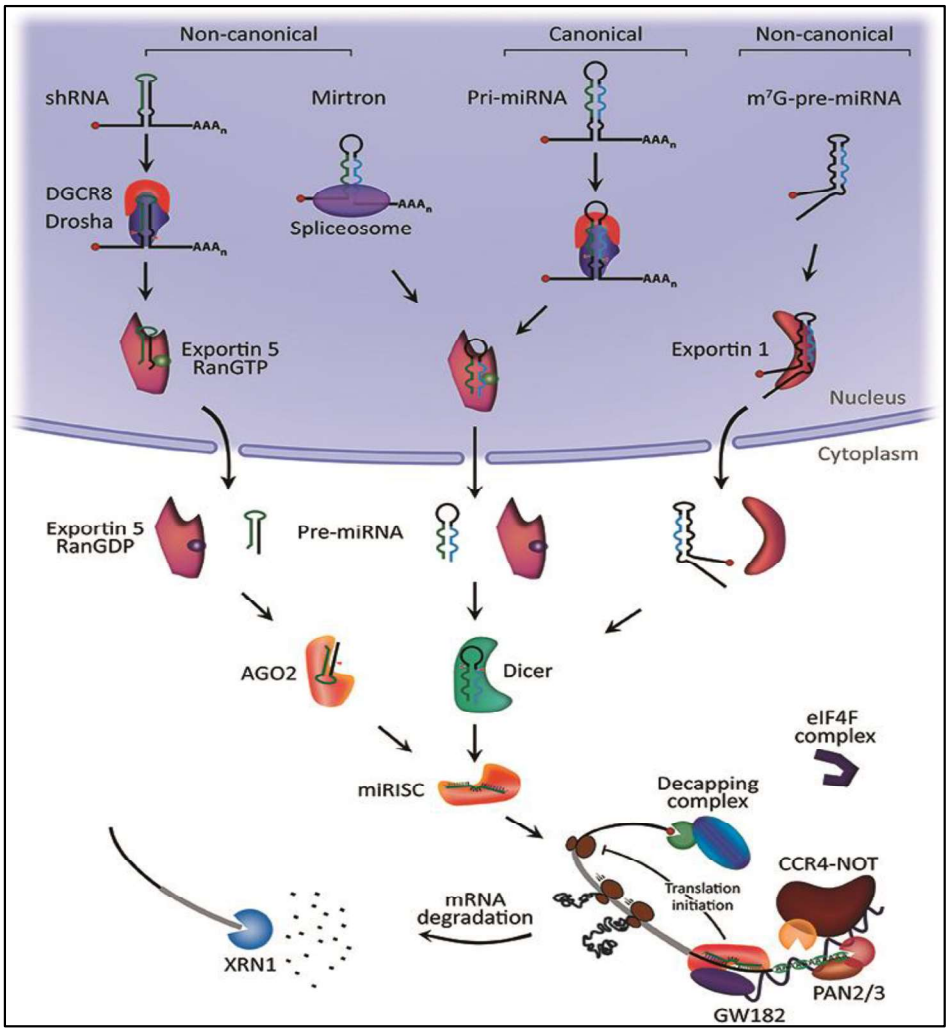

Figure 4. **MiRNA biogenesis and mechanism of action**. Canonical miRNA biogenesis begins with the generation of the pri-miRNA transcript. The microprocessor complex, comprised of Drosha and DGCR8, cleaves the pri-miRNA to produce the pre-miRNA. The pre-miRNA is exported to the cytoplasm in an Exportin5/RanGTP-dependent manner and processed to produce the mature miRNA duplex. Finally, either the 5p or 3p strands of the mature miRNA duplex is loaded into the Argonaute (AGO) family of proteins to form a miRNA-induced silencing complex (miRISC). In the non-canonical pathways, small hairpin RNA (shRNA) are initially cleaved by the microprocessor complex and exported to the cytoplasm via Exportin5/RanGTP. They are further processed via AGO2-dependent, but Dicer-independent, cleavage. Mirtrons and 7-methylguanine capped (m7G)-pre-miRNA are dependent on Dicer to complete their cytoplasmic maturation, but they differ in their nucleocytoplasmic shuttling. Mirtrons are exported via Exportin5/RanGTP while m7G-pre-miRNA are exported via Exportin1. All pathways ultimately lead to a functional miRISC complex. In most cases, miRISC binds to target mRNAs to induce translational inhibition, most likely by interfering with the eIF4F complex. Next, GW182 family proteins bound to Argonaute recruit the poly(A)-deadenylases PAN2/3 and CCR4-NOT. PAN2/3 initiates deadenylation while the CCR4-NOT complex completes the process, leading to removal of the m7G cap on target mRNA by the decapping complex. Decapped mRNA may then undergo 5′−3′ degradation via the exoribonuclease XRN1 [192].

3.2.1.1. The canonical pathway of miRNA biogenesis

The dominant pathway by which miRNAs are processed is known as the canonical biogenesis pathway. Pol II transcribes the pri-miRNA from its genes Then, pri-miRNA is processed and cleaved into pre-miRNA by the microprocessor complex, consisting of an RNA binding protein DiGeorge

Syndrome Critical Region 8 (DGCR8) and a ribonuclease III enzyme, named Drosha [193]. Specifically, the role of DGCR8 is to recognize some motifs within the pri-miRNA, including an N6-methyladenylated GGAC sequence [194], while Drosha acts by cleaving the pri-miRNA duplex at the base of the characteristic hairpin structure of pri-miRNA. This leads to the formation of a 2nt 3′ overhang on pre-miRNA [195]. After the formation of the pre-miRNA, this precursor is exported to the cytoplasm by exportin 5 (XPO5)/RanGTP complex. In the cytoplasm, pre-miRNA is processed by the RNase III endonuclease known as Dicer [193,196], which removes the terminal loop resulting in the generation of a mature miRNA duplex [197]. The name of the mature miRNA form is determined according to the directionality of the miRNA strand: the 5p strand derives from the 5′ end of the pre-miRNA hairpin while the 3p strand arises from the 3′ end. In an ATP-dependent manner, 5p and 3p strands of the mature miRNA duplex are loaded into the Argonaute (AGO) family of proteins (AGO1-4 in humans) to form a miRNA-induced silencing complex (miRISC) [198]. Depending on the cell type or cellular environment, the proportion of AGO loaded 5p or 3p strand varies greatly ranging from near equal proportions to predominantly one or the other [199].

In most of the cases, the strand with lower 5′ stability or 5′ uracil is preferentially loaded into AGO, and is named the guide strand, while the unloaded strand is called the passenger strand. The passenger strand of miRNA that contains no mismatches compared to the guide strand is cleaved by AGO2 and degraded by cellular machinery resulting in a strong strand bias. If miRNA duplexes have central mismatches or if they are not loaded into AGO2, they are passively unwound and degraded [178].

After the formation of a functional miRISC complex, miRISC binds to target mRNAs to induce translational inhibition, most likely by interfering with the eukaryotic initiation factor 4F (eIF4F) complex [192].

3.2.1.2. Non-canonical miRNA biogenesis pathways

Multiple non-canonical miRNA biogenesis pathways have been proposed. Generally, non-canonical miRNA biogenesis can be classified into Drosha/DGCR8-independent and Dicer-independent pathways.

The Drosha/DGCR8-independent pathway produces pre-miRNAs that look like Dicer substrates. In this group, there are mirtrons and 7-methylguanosine (m^7G)-capped pre-miRNA. Mirtrons are produced from the introns of mRNA during splicing and exported into the cytoplasm via XPO5/RanGTP [200,201]. m^7G-capped pre-miRNAs are directly exported to the cytoplasm through exportin 1 without the need for Drosha cleavage. In this case, there is a strong 3p strand bias most

likely due to the m7G cap preventing 5p strand loading into Argonaute [202]. However, both mirtrons and m^7G-capped pre-miRNA are dependent on Dicer to complete their cytoplasmic maturation.

The second group of non-canonical pathways includes miRNAs that did not need Dicer to become mature miRNAs. Dicer-independent miRNAs are processed by Drosha from endogenous short hairpin RNA (shRNA) transcripts and exported to the cytoplasm via XPO5/RanGTP. To complete their maturation within the cytoplasm, these pre-miRNAs require AGO2, because they are of insufficient length to be Dicer-substrates [203]. The entire pre-miRNA is loaded into AGO2, which cleaves 3p strand. The 3′-5′ trimming of the 5p strand completes their maturation [204].

Also in non-canonical miRNA biogenesis pathways, there is the formation of the miRISC complex.

3.2.2. Mechanisms of miRNA-mediated gene regulation

miRNAs can bind different sequences of their mRNA targets, and according to the portion they bind, the effects are different. Generally, the binding of miRNA to 3'UTR, 5′ UTR or coding regions leads to deadenylation and decapping of mRNA target resulting in silencing effects on gene expression [205-209]. On the other hand, when miRNA interacts with promoter region, an induction of the transcription is observed [210].

3.2.2.1.MiRNA-mediated gene silencing via miRISC

MiRISC consists of the guide strand and AGO protein [211]. The target specificity of miRISC is due to its interaction with complementary sequences on target mRNA, known as miRNA response elements (MREs). When the complementarity between miRISC and MRE is total, there is the induction of the AGO2 cleavages mRNA target [212]. This cleavage destabilizes the association between AGO and the 3′ end of the miRNA promoting its degradation [213,214].

However, generally, the interaction between miRISC and MRE is not fully complementary. In fact, most of MREs contain at least a central mismatch to their guide miRNA. Even though base pairing of miRNA and its target mRNA does not match perfect, the interaction occurs via the 5' seed region, namely the sequence of the residues 2-8 in the 5′ termini of the miRNA [207,215]. Moreover, additional paring at the 3′ end aids in the stability and specificity of the miRNA-target interaction [179]. A not fully complementary prevents the AGO2 endonuclease activity leading AGO2 to act as a mediator of RNA interference (RNAi). The formation of a silencing miRISC complex starts with the recruitment of the GW182 protein family, which binds to Argonaute to recruit the poly(A)-deadenylases PAN2/3, which initiates deadenylation, and Carbon Catabolite Repression—Negative On TATA-less (CCR4-NOT), which completes the process, leading to removal of the m^7G cap on target mRNA by the

decapping complex [216-218]. Finally, decapped mRNA undergoes to 5′−3′ degradation via the exoribonuclease XRN1 [219].

3.2.2.2.MiRNA-mediated translational activation

Some studies have reported upregulation of gene expression mediated by miRNAs. In serum starved cells, AGO2 and Fragile-x-mental retardation related protein 1 (FXR1), which is a protein related to the miRNA-protein complex (microRNP), were associated with AU-rich elements (AREs) at 3′ UTR to activate translation [220]. AGO2 and FXR1 are involved in the miRNA-mediated activation of translation [221].

Several miRNAs, such as let-7, were found to be associated with these two proteins with a role of activator of the translation during cell cycle arrest. However, these miRNAs inhibit translation in proliferating cells [220]. During amino acid starvation, it was observed gene activation promoted by miRNAs, which bind to the 5′ UTR of mRNAs of ribosomal proteins [222]. Also in quiescent cells, including oocytes, upregulation of gene expression by miRNAs was observed [221,223]. These results suggest that miRNAs can mediated the upregulation of gene expression under specific conditions.

3.2.2.3. MiRNA-mediated transcriptional and post-transcriptional gene regulation within the nucleus

The interaction of human AGO2 with TNRC6A (a GW182 family protein), which contains a nuclear localization and export signal, allowed AGO2 to be shuttle between the nucleus and cytoplasm through Importin-8 or Exportin-1 [224]. The nuclear localization of miRISC regulates both transcriptional rates and post-transcriptional levels of mRNA [224-226]. In addition, miRISC can associate with euchromatin at gene loci with active transcription [227]. When and how miRNAs exert their functions in the nucleus is still not understood.

Although the mechanism behind this is unclear, it seems that miRISC with low molecular weight can interact with mRNAs within the nucleus and induces nuclear mRNA degradation [224,226,228]. AGO and Drosha have been found involved in mRNA splicing [229,230]. In the nucleus of senescent fibroblasts, AGO2 interacted with miRISC and Rb to suppress the transcription of proliferation-promoting genes regulated by Rb/ transcription factor E2F (E2F). Moreover, let-7f binds to MREs localized in the promoters of two E2F target genes, Cell Division Cycle Associated 8 (*CDCA8)* and Cell division control protein (*CDC2)*, in an AGO2-dependent manner [225]. AGO2 was found to co-immunoprecipitate with euchromatin [225]. It was observed that nuclear miR-522 interacts with a DNA cruciform structure (a stem-loop on sense and antisense DNA strands) within the promoter of Cytochrome P450 Family 2 Subfamily E Member 1 (*CYP2E1*) and suppresses its transcription [231].

The role of miRISC in the regulation of chromatin state and structure and transcriptional control remain to be defined, however these data suggest a transcription factor-like role.

3.2.3. Role of miRNAs in human tumors

Several studies have demonstrated an important role of miRNAs in human cancer [232-234]. MiRNAs act as regulators, providing a direct interaction between the cancer cells and the surrender microenvironment [235]. Their deregulated (up and/or down) expression is fundamental for carcinogenesis [236]. Based on their targets, miRNAs can play different role in tumor onset and progression: they can act as oncogenes, named oncomiRs, when they repress tumor suppressor genes expression and sustain cancer development; or they act as tumor suppressor genes, namely they downregulate oncogenes or stimulate tumor suppressor factors, carrying out a protective role against tumor progression.

3.2.3.1.Mechanisms of miRNA dysregulation in cancer

miRNA expression is found dysregulated in human malignancies. The dysregulation can be due to chromosomal abnormalities, transcriptional control changes, epigenetic changes and defects in the miRNA biogenesis machinery [237].

- Amplification or deletion of miRNA genes

Alterations in genomic miRNA copy numbers and gene locations, including amplification, deletion or translocation, have been often associated with an abnormal miRNA expression in malignant cells compared to normal cells. The first discovery of miRNA gene location change was observed in B-cell chronic lymphocytic leukemia patients. These patients frequently present a deletion in chromosome 13q14, and this specific deletion was associated with downregulation of two miRNAs, namely miR-15a-5p and miR-16-5p. In fact, the *miR-15a/16-1* cluster gene localized in chromosome 13q14 [238]. Another example has been found in lung cancer, where the 5q33 region harboring miR-143-3p and miR-145-5p is often deleted, leading a decreased expression of both miRNAs [239].

On the other hand, the *miR-17-92* cluster gene, which locates in a region of 800bp in the non-protein-coding gene C13orf25 at 13q31.3 [240], was observed amplificated in B-cell lymphomas [241] and lung cancers [242], while the translocation of this cluster gene was observed in T-cell acute lymphoblastic leukemia [243]. Amplification and translocation result in overexpression of these miRNAs in these malignancies. High-resolution array-based comparative genomic hybridization in human ovarian cancer, breast cancer and melanoma has confirmed the high frequency of genomic alterations in miRNA loci [244].

Many miRNA genes located in cancer-associated genomic regions have been found in genome-wide investigations. These cancer-associated genomic regions could be a region of amplification, which might contain oncogenes; a region of loss of heterozygosity, which could harbor tumor suppressor gene; or fragile sites or common breakpoint regions [245]. These discoveries suggest that dysregulated expression of miRNAs in malignant cells could derive from the amplification or deletion of specific genomic regions containing miRNA genes.

- Transcriptional control of miRNAs

Several transcription factors control the expression of miRNAs, therefore, the dysregulation of some key transcription factors in cancer, such as c-Myc protein (c-Myc) and p53, can lead to abnormal expression of miRNAs.

c-Myc is frequently upregulated in many tumors and regulates cell proliferation and apoptosis. It was found that c-Myc can activates the transcription of the oncogenic *miR-17-92* cluster through its binding to E-box elements in miR-17-92 promoter [246], while it suppresses transcriptional activity of tumor suppressive miRNAs such as mir-15a, miR-26, miR-29, mir-30 and let-7 families [247].

In hepatocellular cancer, there are disruptions of the reciprocal regulation of c-Myc and some tumor suppressor miRNAs, such as miR-122-5p, miR-148a-5p and miR-363-3p. c-Myc blocks tumor suppressor miRNA expression by binding to their promoters, while miR-122 indirectly inhibits c-Myc transcription by targeting Transcription Factor Dp-2 (Tfdp2) and E2f1 [248], miR-148a-5p directly targets and inhibits c-Myc expression, and miR-363-3p destabilizes c-Myc by directly targeting ubiquitin-specific protease 28 (USP28) [249].

Another example of how transcriptional factor regulates miRNA expression to mediate tumor suppressive function is the p53-miR-34 regulatory axis [250]. Gene *TP53* is one of the most commonly mutated genes in human cancers and encodes for the tumor suppressor protein p53. p53 regulates the expression of many genes, including miRNA genes to regulate cell-cycle progression and apoptosis. miR-34 family (miR-34a/b/c) acts similarly to p53 in the same regulatory pathway. This miRNA family promotes cell-cycle arrest, cell senescence and apoptosis in cancer [251]. p53 promotes the expression of miR-34a to trigger apoptosis through direct binding to its promoter, while miR-34a induces p53 expression by targeting NAD-dependent protein deacetylase sirtuin-1 (SIRT1), a negative regulator of p53 via deacetylation [252-254]. p53 also regulates the expression of several miRNAs, including miR-605-5p [255], miR-1246 [256] and miR-107 [257].

- Dysregulated epigenetics change

Similar to protein-coding genes, also miRNA can be susceptible to epigenetic alteration, including DNA hypomethylation, aberrant DNA hypermethylation and disruption of the histone modification patterns [258,259].

AML1/ETO, a common AML-associated fusion protein, epigenetically silenced miR-223 expression through CpG methylation [260]. After simultaneous treatment with DNA methylation and histone acetylation inhibitors in T24 bladder cancer cells, several miRNAs have been found upregulated more than three folds. Among these miRNAs, there was miR-127-3p, which is embedded in a CpG island and is not expressed in cancer cells. Its upregulation due to the treatment was associated with the downregulation of proto-oncogene B-cell lymphoma 6 protein (BCL6), suggesting that DNA demethylation and histone deacetylase inhibition can activate the expression of miRNAs that may act as tumor suppressors [261].

The miRNA cluster of miR-148a and miR-34b/c undergoes to a specific hypermethylation-associated silencing in cancer cells, and the restoration of these miRNAs inhibits cancer cells motility, reduces tumor growth and inhibits metastasis formation *in vivo* [262]. Also miR-9-1, miR-124a and miR-145-5p are downregulated by DNA hypermethylation in breast, lung and colon carcinomas, respectively [263-265].

- Defects in miRNA biogenesis machinery

Mutation and aberrant expression of any components of the miRNA biogenesis machinery, such as Drosha, Dicer, DGCR8, AGO proteins and XPO5, could lead to an abnormal expression of miRNAs.

Drosha and Dicer are dysregulated in certain tumors. Drosha and DGCR8 present single-nucleotide substitution or deletion mutations in 15% of Wilms tumors, resulting to significantly downregulated expression of let-7a and miR-200 family [266]. In colorectal cancer cells, the impairment of Dicer1 promotes tumor initiation and metastasis [267]. In ovarian cancer, high mRNA levels of Dicer and Drosha have been correlated with increased median survival [268], while the decreased Dicer expression has been significantly associated with a reduction of patient survival [269,270]. In lung cancer patients, lower Dicer mRNA levels has been associated to reduced let-7 expression resulting in unfavorable postoperative survival [271].

Similarly to Dicer and Drosha, also human *EIF2C1/hAgo1* gene is often lost in Wilms tumors of the kidney [272]. In primary gastric cancer and corresponding lymph node metastases, AGO2 expression levels are significantly higher than that in healthy controls [273]. Lower AGO2 expression and

consequent reduction of RNAi efficiency has been found in melanoma compared with primary melanocytes [274].

XPO5 gene presents inactivating mutations in a subset of human tumors with microsatellite instability. In colorectal cancer cells, the insertion of an 'A' in exon 32 generates a truncated version of the protein, which loses the function to export pre-miRNAs. Pre-miRNAs localized therefore in the nucleus, leading in reduced miRNA processing. It was observed that the restoration of XPO5 reverses the impaired export of pre-miRNAs and has tumor suppressor action [275].

3.2.3.2.Significance of the altered miRNA expression in tumors

The hallmarks of human cancer consist of biological abilities acquired by the tumor cells during tumor development: sustainment of proliferative signaling and evasion from growth suppressors, resistance to cell death, activation of invasion and metastasis and induction of angiogenesis. Dysregulated miRNAs can affect the cancer hallmarks to promote tumor initiation and progression. Based on their target genes, miRNA could act as oncogene or tumor suppressor [276].

- Proliferation and cell cycle regulation

Cell proliferation is the most important hallmark of cancer and its alteration is the leading cause of carcinogenesis. Altered and uncontrolled proliferation can result from cell cycle dysregulation, in which there is an unbalance between promoting and suppressing cell proliferation signals. Some miRNAs take part into critical cell proliferation pathways, and their dysregulation is responsible for evading growth suppressors and sustaining proliferative signaling in cancer cells [237].

Several studies have found that miRNAs participate in regulation of E2F expression, which is a critical regulator of cell proliferation in a cell-cycle-dependent manner and induces target gene transcription during the G1 to S transition [277]. Among them, there are miRNAs of the *miR-17-92* cluster [246,278,279].

miRNAs can also affect cell-cycle progression, which is regulated by different cyclins, cyclin-dependent kinases (Cdks) and their inhibitors. Cyclin D1 and CDK4 expression is blocked by miRNA-545-3p in lung cancer cells, resulting in cell-cycle arrest [280]. In addition to affect the expression of Cdks and cyclins, miRNAs are also regulators of Cdk inhibitors expression. Among them, there is miR-221/222 that has been identified to directly target the Cdk inhibitor p27Kip1 in several cancer cell lines and primary tumor samples [281-284].

- Apoptosis

Uncontrolled cell growth is strongly connected with programmed cell death. Apoptosis can be activated by external signals (extrinsic pathway). Ligands bind death receptors that activate initiator caspases proteins, which activate effector caspases that induce apoptosis. On the other hand, there are also internal signals (intrinsic pathway), such as DNA damage, endoplasmic reticulum stress, hypoxia and metabolic stress. These signals stimulate proteins that induce mitochondrial outer membrane permeabilization (MOMP) resulting in the release of cytochrome c. Cytochrome c mediates apoptosome assembly, which activates caspase proteins to induce apoptosis [285].

The ways to evade apoptosis include mostly the loss of p53 tumor suppressor function, suppression of other proapoptotic factors, upregulation of anti-apoptotic regulators, and inhibition of death pathway induced by extrinsic ligands. miRNAs participate in the regulation of death pathways, including in the regulation of proapoptotic factors, such as BCL2-associated X protein (BAX), Bcl-2-like protein 11 (BCL2L11, also known as Bim) and p53 upregulated modulator of apoptosis (PUMA), and anti-apoptotic regulators, including B-cell lymphoma 2 (Bcl-2) and B-cell lymphoma extra-large (Bcl-xL)[237].

miR-192-5p, miR-194-5p and miR-215-5p are positive regulators of p53 in multiple myeloma [286]. MiR-221/222 block cell death by targeting the proapoptotic gene PUMA in human glioma cells [287]. Bcl-2 has been found regulated by miR-15a-5p, miR-16-5p [288], miR-204-5p [289], miR-148a-3p [290] and miR-365-3p [291]. miR-491-5p promotes apoptosis in ovarian cancer cells by directly inhibiting Bcl-xL expression and by inducing Bim accumulation [292]. MiR-21-5p represses the expression of Apoptotic protease-activating factor 1 (Apaf-1), which is an important component of the intrinsic mitochondrial apoptotic pathway, and it decreases protein levels of Fas ligand that is a key initiator of the extrinsic apoptotic pathway [293].

- Invasion and metastasis

Metastasis development is a multistep and dynamic biological event. During tumor progression, cells acquire new abilities, including the capacity to migrate and go through a de-differentiation program called epithelial-mesenchymal transition (EMT), which is considered an early and key step in the metastatic cascade. EMT is characterized by loss of cell adhesion through repression of E-cadherin and activation of genes associated with motility and invasion [294].

miR-155-5p promotes EMT by targeting an important regulator of cellular polarity tight junction formation and stability, namely RhoA GTPase [295]. Also miR-10b positively regulates cell migration

and invasion [296]. miR-9-5p promotes EMT by reducing the expression of E-cadherin in breast cancer cells via directly binding to its 3′-untranslate region [297].

In the mesenchymal cells, miR-200c-3p increases expression of E-cadherin and promotes an epithelial phenotype by inducing Hepatocyte growth factor receptor (MET) [298,299]. miR-203a-3p represses tumor cell invasion *in vitro* and lung metastatic colonization *in vivo* [300,301], while miR-212-3p inhibits colorectal cancer cell migration and invasion *in vitro* and pulmonary metastasis *in vivo* [302].

- Angiogenesis

Angiogenesis is a process to develop new blood vessels from pre-existing ones in response to starvation and hypoxia, which often occur in tumor tissues due to the significantly lower food and oxygen concentration compared to the surrounding normal tissues.

Vascular endothelial growth factor (VEGF) is an important angiogenic factor, which directs endothelial cells to build new vessels upon binding to its receptor. In addition, Hypoxia-inducible factor (HIF) is a key transcription factor that functions in response to hypoxia [303]. miRNAs can affect angiogenesis by targeting VEGF and HIF.

The most consistently and significantly induced miRNA during hypoxia is miR-210-3p [304-307]. MiR-424-5p is induced by hypoxia in endothelial cells to promote angiogenesis *in vitro* and *in vivo* [308]. miR-21-5p promotes angiogenesis by activating MAPK/Akt signaling pathways, resulting in high expression of HIF1α and VEGF [309].

On the other hand, there are miRNAs that inhibit angiogenesis, including miR-20b-5p, miR-509c-3p and miR-107. miR-20b-5p and miR-519c-3p negatively regulate angiogenesis by targeting VEGF and/or HIF1α [310,311]. miR-107 represses the expression of HIF1β, so low levels of miR-107 promotes tumor angiogenesis under hypoxic conditions [257].

3.2.4. miRNAs in melanoma

In melanoma, miRNAs are involved in several biological processes, including melanoma genesis, proliferation and cell cycle, apoptosis, invasion and metastasis, immune response [312], hypoxia and metabolism, and drug resistance. All these mechanisms are associated with the unbalance of an extensive pool of up and/or downregulated miRNAs [185,236]. In addition, miRNAs can be release in the bloodstream, known as circulating miRNAs. and they can be used as melanoma biomarkers.

3.2.4.1.miRNAs in melanogenesis and melanoma genesis

The pigment melanin is produced in melanosomes by melanocytes through a process named melanogenesis. MITF is a master regulator of melanogenesis and melanocyte development [313]. It regulates many genes, including pigmentation genes, anti-apoptotic genes, cell cycle promoting genes, genes involved in cell cycle arrest, motility and invasion genes and genes associated to melanocyte metabolism [314,315]. MITF has been found amplificated or mutated in both familial and sporadic melanomas [314]. Depending on the fine balance between proapoptotic and proliferative effects, MITF acts in a cancer-promoting or cancer-suppressing manner [316]. MITF regulates the expression of some miRNAs and many miRNAs have been found to target MITF [312] (**Figure 5**).

miR-211-5p is one of the most important melanocytic lineage-specific miRNA regulated by MITF. miR-211-5p represses MITF expression by inhibiting the MAPK pathway [317]. In melanocytes, MITF controls the transcription of miR-211-5p and its host gene, namely transient receptor potential cation channel subfamily M member 1 (*TRPM1*) gene. miR-211-5p is one of the most differentially expressed miRNAs between normal human melanocytes and melanoma cell lines and tumors [318-320].

Several miRNAs have been found as involved in MITF regulation including miR-101-3p [321], miR-137-3p [322-324], miR-148a-3p [323], miR-148b-3p [325], miR-155-5p [326], miR-182-5p [327], miR-218-5p [328], miR-26a-5p [329], and miR-340-5p [330].

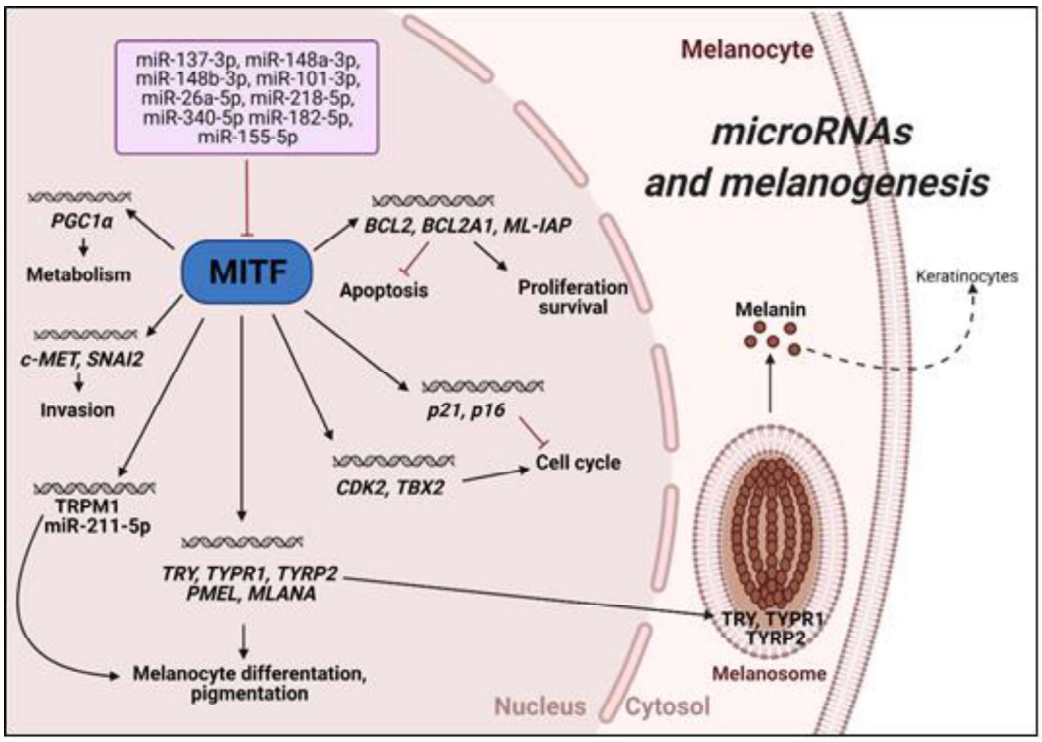

Figure 5. MicroRNAs in melanogenesis. MITF is a master regulator of melanocyte development and melanogenesis, and regulates genes involved in melanocyte differentiation, pigmentation, cell cycle, apoptosis, proliferation and survival, metabolism and invasion. The expression of MITF is regulated by several

microRNAs (violet box) (Figure from "Pathophysiology roles and translational opportunities of miRNAs in Cutaneous Melanoma", MicroRNA in Human Malignancies edited by Massimo Negrini, George Calin, Carlo Croce, *in press)*.

3.2.4.2.miRNAs in proliferation and cell cycle regulation

Melanomas with high growth rate are considered high-risk tumors [331]. miRNAs can regulate melanoma proliferation by inducing proliferative signals or by repressing growth-suppressive targets. Moreover, there are several miRNAs that modulate the cell cycle regulators thus affecting the proliferation [312,332] (**Figure 6**).

Among the miRNAs that promote the proliferation, there are: miR-10b-5p [333], miR-106b-5p [334,335], miR-135a-5p [336], miR-146a-5p [337], miR-19b-3p [338], miR-20a-5p [339], miR-21-5p [340], miR-221 family (miR-221-3p and miR-222-3p) [341], miR-25-3p [342,343], miR-4286 [344], miR-519-3p [345], miR-532-5p [346] and miR-675-3p [347].

On the other hand, there are several miRNAs that can inhibit proliferation and/or induce cell cycle arrest by downregulating multiple components of the cell cycle machinery [332], including let-7 family (let-7a-5p and let-7b-5p) [329,348], miR-101-3p [321], miR-124-3p [349,350], miR-125a-5p [351], miR-125b-5p [352], miR-126-3p/126-5p [353], miR-136-5p [354], miR-137-3p [324,355,356], miR-138-5p [357],[358], miR-145-5p [359,360], miR-155-5p [361,362], miR-193b-3p [363,364], miR-194-5p [365], miR-199a 5p [366], miR-200 family (miR-200a-3p, miR-200b-3p, miR-200c-3p, miR-429) [367-371], miR-203a-3p [372,373], miR-205-5p [374-376], miR-206 [377], miR-218-5p [378], miR-22-3p [379], miR-26a-5p [329,380], miR-29a-3p [381,382], miR-30a 5p [383], miR-31-5p [384], miR-33a-5p [385,386], miR-338-3p [387], miR-34 family [388], miR-340-5p [389], miR-342-3p [390], miR-365a-5p [391], miR-485-5p [392], miR-524-5p [393], miR-605-5p [394], miR-675-5p [395] and miR-9-5p [396].

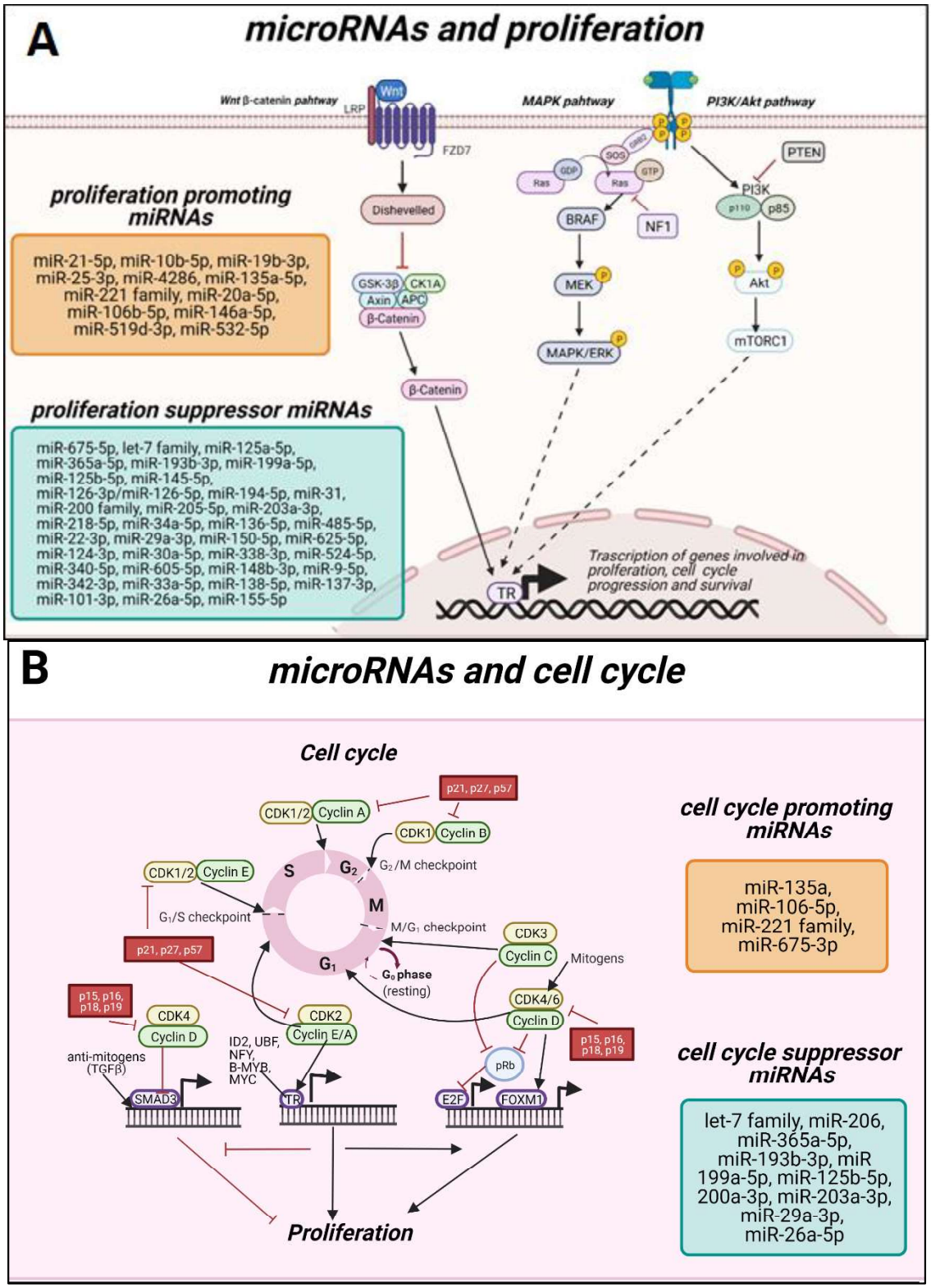

Figure 6. MicroRNAs in proliferation and cell cycle. A) Proliferation is induced by several cellular pathways, including Wnt-β-catenin, MAPK and PI3K/Akt pathways. microRNAs can promote or repress the expression of proteins involved in cell proliferation, by acting as oncomiRs (orange box) or tumor suppressor miRNAs (green box). B) Cell cycle phases: S-phase (S), mitosis (M); transition phases (G1 and G2), whereas G0 indicate quiescent cells. Several microRNAs regulate cell cycle progression by targeting proteins involved in the promotion of cell cycle, such as cyclins and cyclin dependent kinases (CDKs), or involved in the arrest of cell cycle, including p15, p16, p18, p18, p21, p27 and p57 (Figure from "Pathophysiology roles and translational opportunities of miRNAs in Cutaneous Melanoma", MicroRNA in Human Malignancies edited by Massimo Negrini, George Calin, Carlo Croce, *in press*).

3.2.4.3.miRNAs in apoptosis, autophagy and ferroptosis

miRNAs play an important role in the regulation of the apoptosis by targeting anti-apoptotic proteins, including BCL2 and BCL2-like 1, or by regulating positively or negatively p53 [397,398]. miRNAs that act as anti-apoptotic agents include miR-15b-5p [399], miR-182-5p [327], miR-21-5p [340,400] and miR-4286 [344]. On the other hand, miRNAs with a pro-apoptotic action include miR-124-3p [349], miR-125b-5p [352], miR-137-3p [324], miR-155 [361,362], miR-18b-5p [401], miR-205-5p [376], miR-26a-5p [329,380,402], miR-29a-3p [382], miR-365a-5p [391] and miR-485-5p [403] (**Figure 7**).

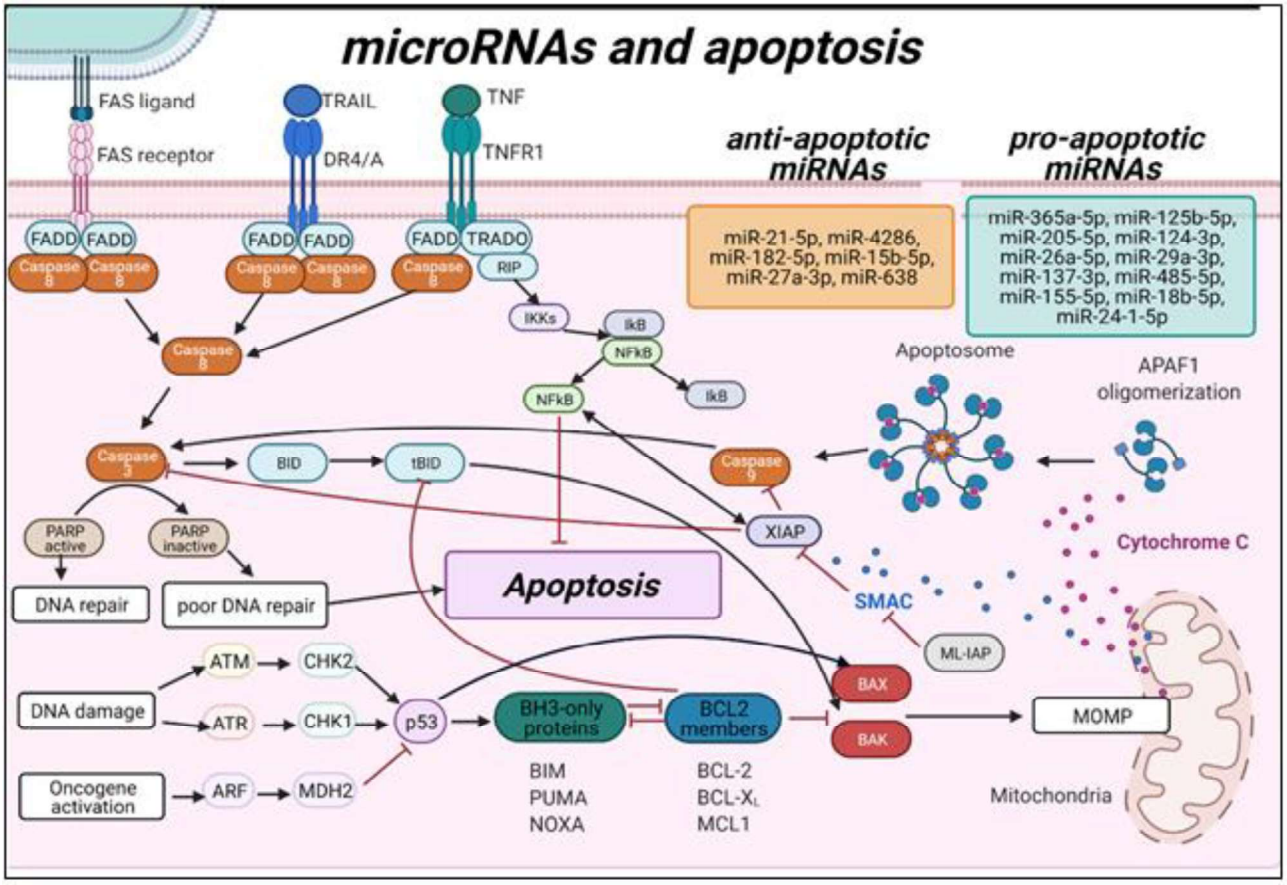

Figure 7. MicroRNAs in programmed cell death. Apoptosis can be activated by extrinsic or intrinsic signals. The extrinsic pathway is induced when death ligands bind death receptors, which lead to the activation of initiator caspases, such as caspase 8, and consequent activation of effectors caspases, such as caspase 3,9, thus promoting apoptotic cell death. The intrinsic pathway induces mitochondrial outer membrane permeabilization (MOMP) resulting in the release of cytochrome c from mitochondria. The formation of the apoptosome promotes caspase 9 activation, which actives caspase 3 to induce cell death. microRNAs can act as oncomiRs, i.e. protecting from apoptosis (orange box), or tumor suppressor, i.e. stimulating the apoptosis (green box). (Figure from "Pathophysiology roles and translational opportunities of miRNAs in Cutaneous Melanoma", MicroRNA in Human Malignancies edited by Massimo Negrini, George Calin, Carlo Croce, *in press*).

In response to stressful condition as hypoxia or starvation for the maintenance of metabolic homeostasis and viability, tumor cells activate a survival program known as autophagy [404]. A dysregulation in autophagy process can lead to programmed cell death. In cancer, autophagy can be pro- or anti-tumorigenic. Currently, it believed that autophagy has a tumor suppressive role in the

early stages of cancer, while a tumor-promoting action in established tumors [405]. So, miRNAs are divided in pro-autophagic, such as miR-216b-5p [406], and anti-autophagic, including miR-290-295 cluster [407].

Some miRNAs affect both apoptosis and autophagy, specifically miR-27a-3p [408] and miR-638 [409] that inhibit apoptosis and autophagy, while miR-24-1-5p promotes apoptosis and autophagy [410].

Erastin-induced ferroptosis, which is an iron-dependent cell death driven by small molecules or conditions that promote lipid-based ROS accumulation, is promoted by the downregulation of miR-137-3p [411]. In addition, ferroptosis is regulated by miR-9-5p in melanoma [412].

3.2.4.4.miRNAs in EMT and angiogenesis

During melanoma progression, tumor cells acquire the capacity to migrate and go through the de-differentiation program known as EMT. For the development of metastasis, EMT process is fundamental: EMT has been reported to occur in melanoma cells, where it promotes the metastatic phenotype of malignant melanocytes [413]. In melanoma, several miRNAs have been associated to EMT (**Figure 8A**) with a promoting action, such as miR-10b-5p [333], miR-106b-5p [414], miR-1246 [415], miR-1908-5p[416], miR-17-5p [417], miR-182-5p [327,418], miR-199a-5p[416], miR-199a-3p [416], miR-214-3p [418,419], miR-21-5p upregulation [340,418,420], miR-221/222 family [341], miR-224/miR-452 cluster (miR-224-5p and miR-452-5p[421], miR-25-3p [342,343], miR-30b-5p [422], miR-30d-5p [422], miR-373-3p [423], miR-519-3p [345], miR-576-5p [418,424], and miR-638 [409].

Several miRNAs that inhibit EMT, invasion and metastasis have been identified, including let-7a-5p [425], miR-101-3p [321,418], miR-124-3p [349,350], miR-126-3p/5p [418,426], miR-137-3p [324,427], miR-138-5p [357,428], miR-145-5p [429], miR-148b-3p [419,430], miR-150-5p [431],[432], miR-153-3p [433], miR-193b-3p [424]. miR-194-5p [434], miR-200 family (miR-200a-3p, miR-200b-3p, miR-200c-3p and miR-429) [367,369-371], miR-205-5p [375], miR-203a-3p [372,435], miR-211-5p [318,320,436,437], miR-218-5p [378]. miR-30c-1-3p [424], miR-22-3p [379,438,439], miR-29a-3p [382], miR-30a-5p [383,440], miR-30c-1-3p [424], miR-338-3p [387], miR-339-3p [418], miR-34 family (miR-34a-5p, miR-34b-3p, miR-34c-5p) [441,442], miR-340-5p, [389], miR-342-3p [390], miR-376a-3p [443], miR-378a-3p (upon adenosine-to-inosine (A-I) editing) [444], miR-455-5p (upon A-I editing) [445], miR-485-5p [392],[403], miR-524-5p [393], miR-542-3p [446], miR-625-5p [447], miR-675-5p [395], miR-7-5p [448], and miR-9-5p [396,449].

Angiogenesis plays an important role in many tumors, including melanoma where it leads to melanoma growth and metastasis dissemination [450]. Malignant melanoma cells and endothelial cells present on their surface several growth factors receptors that lead to the promotion of angiogenesis

[451]. Also for this biological process, some miRNAs have been identified. In details, there are some pro-angiogenesis miRNAs, including miR-1908-5p [416], miR-199a-5p [416] and miR-378a-5p [452], while miR-23b-3p is an anti-angiogenic miRNA [453] (**Figure 8B**).

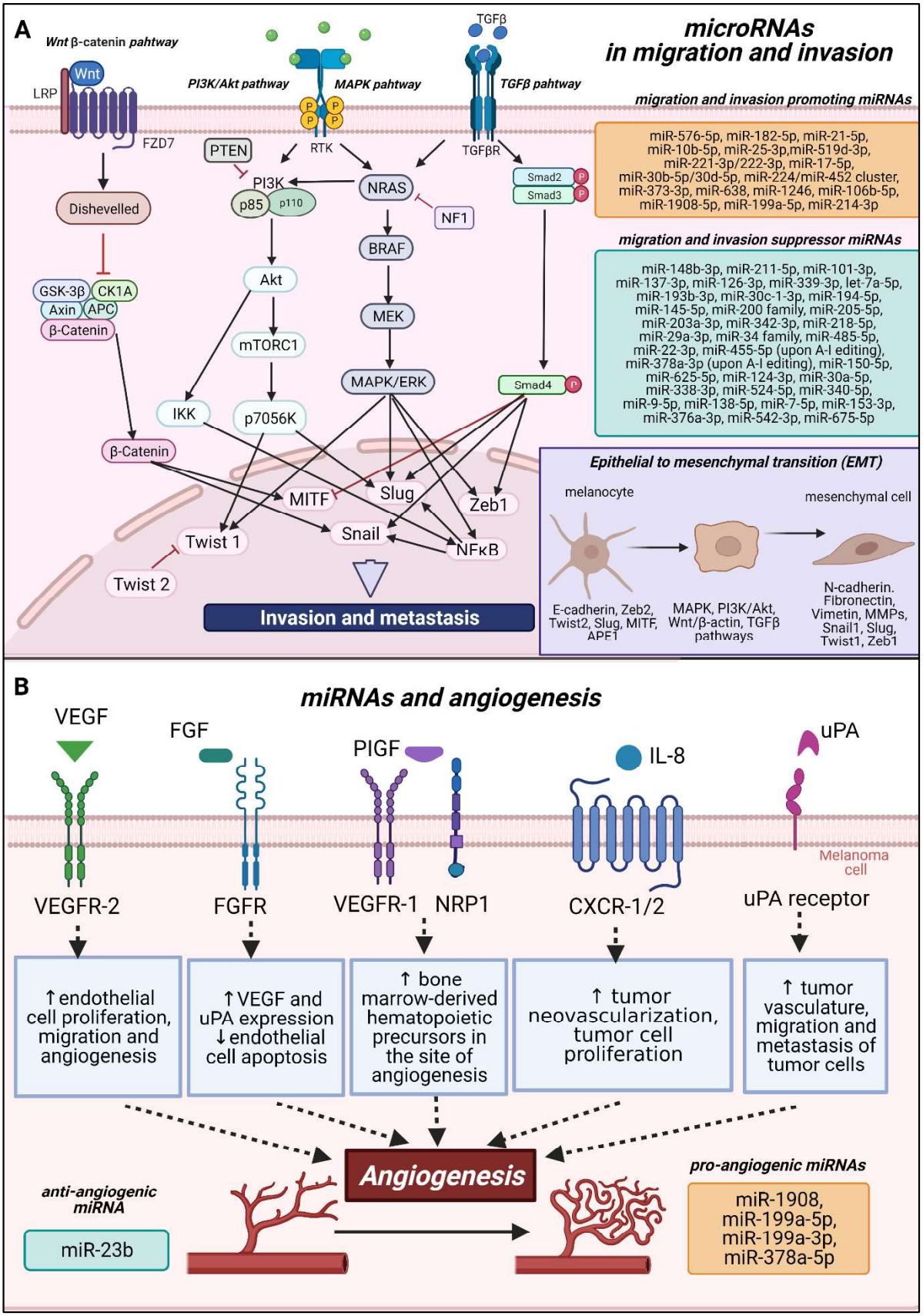

Figure 8. microRNAs in melanoma migration, invasion and angiogenesis. A) Melanoma cells activate the epithelial to mesenchymal transition (EMT) pathway to promoted migration, invasion and metastasis. Several proteins, including Wnt β-catenin, PI3K/Akt, MAPK and TGFβ, regulate EMT. By targeting proteins from these pathways, miRNAs promote (orange box) or suppress (green box) migration and invasion of melanoma cells, acting as oncomiRs and tumor suppressors miRNAs, respectively. B) Angiogenesis is a fundamental hallmark for melanoma progression and dissemination. Malignant melanoma cells and endothelial cells presents on their surface growth factors receptors that promote angiogenesis and are regulated by miRNAs. Some miRNAs are implicated in angiogenesis with a promoting (orange box) or suppressor role (green box). (Figure from "Pathophysiology roles and translational opportunities of miRNAs in Cutaneous Melanoma", MicroRNA in Human Malignancies edited by Massimo Negrini, George Calin, Carlo Croce, *in press*).

3.2.4.5.miRNAs and melanoma microenvironment

The role of the immune system in melanoma has been intensely studied. The immune surveillance, especially T-cell activity, acts against melanoma. miRNAs can regulate immune system members by affecting the activity of key elements of both innate and adaptative immunity [454].

Melanoma cells escape from immune surveillance with mechanisms, which were recently targeted by immune checkpoint inhibitors, such as anti-CTLA4 and anti-PD1 [455]. miRNAs can regulate the expression of immune checkpoints, including miR-146-5p, miR-17-5p [456] and miR-28-3p [457].

miRNAs can regulate immune responses mediated by natural killer (NK) cells, macrophage, and myeloid-derived suppressor cell (MDSC), and they can present an immune evasive or suppressive activity [458], such as miR-21-5p, miR-29a-3p, miR-142-3p, miR-223-3p [459], miR-376a-3p [460], miR-34a-5p/34c-5p, miR-499a/c [461], miR-155-5p [326,462] and miR-494-3p [463].

miRNAs can affect adaptive immunity network by regulating T cell activity, thus acting as immunosuppressive miRNAs, such as miR-30b-5p and miR-30d-5p [422]. Melanoma can impair T cell functionality by upregulated miR-101-3p and miR-26a-5p in effector T cells [464].

Immune escape can be promoted also by hypoxic microenvironment [465]. HIF-induced miR-210-3p expression results in escape from cell lysis by antigen-specific cytotoxic T lymphocytes (CTL or CD8+ T cells) [466].

UVR-induced inflammation can promote immune-evasion [105] and leads to a downregulation of miR-193b-3p, miR-342-3p, miR-186-5p, miR-130a-3p and miR-146a-5p [467].

3.2.4.6.miRNAs in hypoxia and metabolism

In order to survive, tumor cells need to acquire the ability to adapt and survive in a hostile microenvironment, such as in hypoxia condition and starvation. Hypoxia affects cell metabolism: it mediates metabolic switch from an oxidative to a glycolytic metabolism, known as Walburg effect

[468]. An important miRNA involved in the hypoxia is miR-210-3p that promotes cell cycle and tumor growth in absence of oxygen [469].

There are several other miRNAs involved in the regulation of hypoxia and metabolism. High expression of HIF1α leads to the downregulation of tumor suppressor miRNAs, such as miR-138-5p [428], miR-340-5p [470], miR-33a-5p and miR-18b-5p [386,471]. 138-5p also reduces glucose consumption and lactic acid production inhibiting glycolysis [357]. Let-7a-5p favors oxidative phosphorylation and induces oxidative stress [472]. miR-150-5p reduces glycolysis and increasing oxygen consumption rate (OCR) [432]. Also miR-625-5p inhibits glycolysis [473]. miR-211-5p increases oxygen consumption [474] and promotes the switch from glycolysis to oxidative phosphorylation through PGC1α and mitochondrial biogenesis [317].

Targeting glutamine metabolism sensitizes melanoma cells to TNF-related apoptosis-inducing ligand (TRAIL)-induced death [475]. Glutamine catabolism is inhibited by miR-137-3p [411,476] and miR-605-5p [477].

3.2.4.7.miRNAs as modulators of therapeutic response in melanoma

The expression of specific miRNAs in melanoma cells could affect the response to targeted therapy: some of them are able to induce drug resistance, while others are able to restore drug sensitivity (**Figure 9**).

Some miRNAs are associated with drug resistance or sensitivity in the contest of BRAFi and BRAFi/MEKi. MiR-34a-5p, miR-100-5p and miR-125b-5p block apoptosis and promote drug resistance [478]. miR-514a-3p affects the sensitivity of BRAFi conferring resistance to these inhibitors [479]. miR-1246 significantly reduces the antiproliferative effects of the BRAFi [480].

On the other hand, miR-126 3p [426], miR-199b-5p [481], miR-200c-3p [482], miR-524-5p [483], miR-550a-3-5p [484], miR-579-3p [485] and miR-7-5p [486] confer sensitivity to BRAFi. It was observed that the combination of miR-32-5p and vemurafenib is more effective than either vemurafenib or miR-32-5p treatment alone [487]. miR-216b-5p promotes the antitumor activity of vemurafenib in BRAF(V600E) melanoma cells [406].

Metastatic melanoma can be treated with immunotherapies, and miRNAs can regulate directly or indirectly the expression of immune checkpoints, acting on tumor cells or immune cells, respectively [488]. Some miRNAs have been found associated with immunotherapy. The expression of miR-222-3p in melanoma was significantly lower in responsive patients to ipilimumab than patients that have no clinical benefit from treatment [489]. Anti-PD-1 treatment increases miR-155-5p expression in CD8+ T-cells [490]. A set of miRNAs (miR-146a-5p, miR-155-5p, miR-125b-5p, miR-100-5p, let-

7e-5p, miR-125a-5p, miR-146b-5p, miR-99b-5p) has been associated with MDSCs and resistance to treatment with immune checkpoint inhibitors in melanoma patients [491].

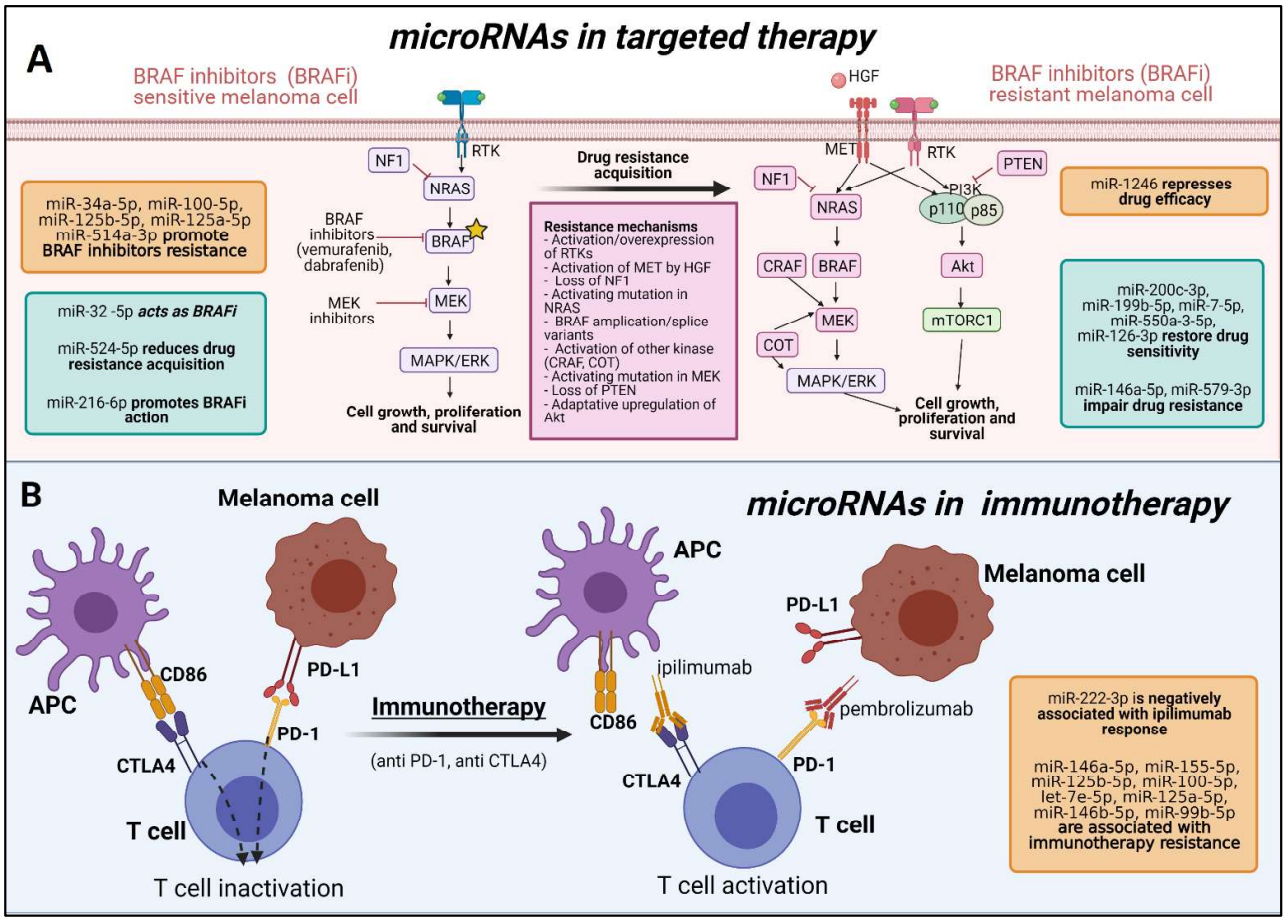

Figure 9. MicroRNAs in targeted therapy and immunotherapy. A) Melanoma with mutated and activated BRAF can be treated with targeted therapy, including BRAF and/or MEK inhibitors. Some miRNAs affect the inhibitors activity by promoting their efficacy (green box, in the left) or impairing efficacy and inducing drug resistance (orange box). However, drug sensitivity in drug resistant cells, can be restored by the action of specific miRNAs (green box, in the right). B) Immunotherapy is based in the blockage of T cell receptors, such as PD1 or CTLA4, resulting in the activation of CD8+ T cells against the tumor. The treatment with immune checkpoint inhibitors is effective in melanoma but leads to the acquisition of immunotherapy resistance. The response to treatment and acquisition of immunotherapy resistance in melanoma can be regulated by miRNAs. (Figure from "Pathophysiology roles and translational opportunities of miRNAs in Cutaneous Melanoma", MicroRNA in Human Malignancies edited by Massimo Negrini, George Calin, Carlo Croce, *in press*).

miRNAs affect also other types of treatment of melanoma, and miRNAs expression can be induced by the treatment. The miRNA expression has been analyzed in pre-treatment and post-treatment with the Serine/threonine-protein kinase mTOR (mTOR) inhibitor, namely Temsirolimus, and the anti-VEGF antibody, namely Bevacizumab, in human metastatic melanoma tissue samples. 15 miRNAs have been found upregulated in the post-treatment (miR-125b-5p, miR-320a-5p, miR-320b, miR-320c, miR-320d, miR-320e, let-7b-5p, let-7c-5p, miR-10b-5p, miR-29c-3p, miR-100-5p, miR-145-5p, miR-140-3p, miR-99a, miR-4328), and twelve of these fifteen are known tumor suppressor miRNAs [492].

In melanoma, miR-30a-5p enhances chemoresistance to cisplatin [493]. On the contrary, miR-31-5p functions as protective miRNA, in fact it increases chemosensitivity [384]. The overexpression of miR-211-5p can restore cisplatin susceptibility in cisplatin-resistant cells [494]. The overexpression of miR-203a-3p sensibilizes malignant melanoma cells to temozolomide chemotherapy [495]. In melanoma patients treated with carboplatin/paclitaxel, miR-659-3p has been found to be positively associated with progression-free survival [496].

3.2.4.8.Circulating miRNAs as melanoma biomarkers

The tumor can release cell free miRNAs in the bloodstream, where they remain stable and are resistant to RNAse activity. A fraction of cell-free miRNAs is bound to macromolecular complexes, such as cholesterol and lipoproteins, Argonaute 2 proteins and extracellular vesicles (EVs). EVs, can also carry miRNAs inside and are one of the main sources of miRNAs in the blood [497].

Liquid biopsy allowed to measured miRNA levels in a non-invasive way approach. Dysregulated miRNA levels have been observed in the serum and plasma of cancer patients compared to healthy controls, suggesting that circulating miRNAs could be used as diagnostic biomarkers [498], as well as markers of prognosis [499].

The management of melanoma depends greatly on early diagnosis: melanoma is almost 100% curable by surgical resection when it is detected at early, non-metastatic stages. Therefore, it is essential to identify diagnostic biomarkers, including miRNAs. Another promising application of circulating miRNAs is the early detection of recurrence. **Table 5** reports the main studies on diagnostic and prognostic cell-free miRNA biomarkers in melanoma (*Durante et al., manuscript submitted*).

Table 5. Circulating miRNA as biomarkers in melanoma

miRNA/miRNA signature	Type of biomarker	Expression	Sample	Reference
16 miRNA signature (miR-186-5p, let-7d-3p, miR-18a-3p, miR-145-5p, miR-99a-5p, miR-664a-3p, miR-501-5p, miR-378a-5p, miR-29c-5p, miR-1280*, miR-365a-3p, miR-1249-3p, miR-328-3p, miR-422a, miR-30d-5p, miR-17-3p)	diagnostic	dysregulated in metastatic melanoma patients (stages III and IV) *vs*. healthy control individuals	55 whole blood samples	[500]
miR-145-5p, miR-10b-5p, miR-155-5p	diagnostic	downregulated in melanoma patients vs. healthy controls	226 whole blood samples	[501]
miR-320a-5p	diagnostic	upregulated in melanoma *vs*. other tumors and healthy controls	207 plasma samples	[502]
miR-15b-5p, miR-149-3p, miR-150-5p	diagnostic	upregulated in melanoma patients *vs*. healthy controls	62 plasma samples	[503]

miR-193a-3p, miR-524-5p	diagnostic	downregulated in melanoma patients vs. healthy controls	62 plasma samples	[503]
miR-185-5p, miR-1246	diagnostic	dysregulated in metastatic patients vs. healthy controls	119 plasma samples	[504]
19 miRNAs of the MEL38 signature (miR-301a-3p, miR-424-5p, miR-27a-3p, miR-34a-5p, miR-497-5p, miR-299-3p, miR-152-3p, miR-1910-5p, miR-181b-5p, miR-548a-5p, miR-454-3p, miR-4532*, miR-1537-3p, miR-1258, miR-431-5p, miR-450a-5p, miR-2682-5p, miR-337-5p, miR-154-5p)	diagnostic	upregulated in melanoma patients *vs.* healthy controls	48 plasma samples	[505]
19 miRNAs of the MEL38 signature (miR-205-5p, miR-548l, miR-1269a, miR-624-3p, miR-138-5p, miR-1-5p, miR-3928-3p, miR-3131, miR-1973, miR-520d-3p, miR-548ad-3p, miR-553, miR-764, miR-1302, miR-522-3p, miR-1264, miR-1306-5p, miR-219a-2-3p, miR-4787-3p)	diagnostic	downregulated in melanoma patients vs. healthy controls	48 plasma samples	[505]
miR-29c-5p, miR-324-3p	diagnostic	downregulated in metastatic melanoma patients (stage IV) *vs.* healthy controls	48 serum samples	[506]
miR-122-5p, miR-3201	diagnostic	upregulated in melanoma patients vs. healthy controls	126 serum samples	[507]
miR-17-5p, miR-19a-3p, miR-21-5p, miR-126-3p, miR-149-5p	diagnostic	upregulated in metastatic sporadic melanoma patients vs. healthy controls	26 plasma-derived exosomes samples	[508]
miR-125b-5p	diagnostic	downregulated in advanced melanoma patients vs. healthy controls	46 serum-derived exosomes samples	[509]
miR-15b-5p, miR-33a-5p	prognostic	downregulated in melanoma patients with high-risk of recurrences	50 serum samples	[510]
MEL18 signature (miR-152-3p, miR-1537-3p, miR-154-5p, miR-27a-3p, miR-299-3p, miR-301a-3p, miR-337-5p, miR-4787-3p, miR-199b-5p, miR-660-5p, let-7e-5p, miR-652-3p, miR-331-3p, miR-105-5p, miR-127-5p, miR-521, miR-1180-3p, miR-3127-5p)	prognostic	dysregulated in non-metastatic (stage I/II) and metastatic (stage III/IV) melanoma patients	48 plasma samples	[505]
miR-150-5p, miR-199a-5p, miR-424-5p	prognostic	upregulated in melanoma patients with high-risk of recurrences	50 serum samples	[510]

miR-150-5p, miR-9-5p, miR-145-5p, miR-155-5p, miR-203a-3p, miR-205-5p	prognostic	dysregulated in metastatic melanoma patients vs. non-metastatic melanoma patients	27 serum samples	[511]
miR-150-5p, miR-30d-5p, miR-15b-5p, miR-425-5p	prognostic	associated with recurrence-free and overall survival	283 serum samples	[512]
miR-10b-5p	prognostic	positively correlated with lymph node metastasis, advanced clinical stage	115 serum samples	[513]
miR-21-5p	diagnostic / prognostic	upregulated in melanoma patients vs. healthy controls; associated with tumor burden	207 plasma samples (8), 56 plasma samples (79)	[502,514]
miR-210-3p	diagnostic / prognostic	upregulated in melanoma patients vs. healthy controls; high expression correlates with poor prognosis	264 plasma samples	[515]
miR-16-5p	diagnostic/prognostic	downregulated in melanoma patients *vs.* healthy controls; negatively correlated with ulceration, tumor thickness, AJCC stage; positively correlated with patient survival	240 serum samples	[516]
miR-206	diagnostic / prognostic	downregulated in melanoma patients *vs.* healthy controls; low expression correlates with poor prognosis	90 serum samples	[517]
miR-221-3p	diagnostic/prognostic	upregulated in melanoma patients vs. healthy controls, positively correlated with BT	114 serum samples [518], 126 serum samples [519]	[518] [519]
2 miRNAs of MELmiR-7 (miR-16-5p, miR-211-5p)	diagnostic/prognostic	negatively correlated with	385 serum samples	[520]
5 miRNAs of MELmiR-7 (miR-4487, miR-4706, miR-4731, miR-509-3p, miR-509-5p)	diagnostic/prognostic	downregulated in melanoma patients vs. healthy controls	385 serum samples	[520]
miR-532-5p, miR-106b	diagnostic/prognostic	upregulated in melanoma patients vs. healthy controls	60 serum-derived exosomes samples	[521]

* Later removed from miRBase

3.2.5. miRNA isoforms (isomiRs)

Next Generation Sequencing (NGS) technologies identified several miRNA variants of heterogeneous lengths and/or sequences. These variants, named miRNA isoforms (isomiRs), were initially ascribed as sequencing errors/artifacts, while now they are considered non-canonical variants

that originate from physiological processes. The discovery of isomiRs underlined the complexity of the small RNA transcriptional landscape in several diseases, including cancer. Although isomiRs abundance, biological activity, and function are not completely understood, their analysis and study are of great interest due to their high frequency in the human miRNome, to their presumed functions in cooperating with the canonical miRNAs, and to the potential for exhibiting novel functional roles [522].

3.2.5.1.From the Canonical miRNAs to the discovery of isomiRs

miRNAs are characterized by specific sequences. In fact, for each miRNA, miRBase, namely the database for miRNAs, reports a unique sequence, which is named canonical miRNA [523]. In 2007, a small RNA sequencing experiment performed in 26 different organ systems and cell types from humans and rodents identified miRNA variants in approximately 20% of clone sequences [524]. Also miRNAs from human embryonic stem cells showed sequence variations from their canonical form. The term isomiR was coined to refer to these miRNA isoforms/variants [525].

Initially, isomiRs were attributed to post-transcriptional modifications or PCR/sequencing technical errors. However, NGS technologies and sophisticated analysis algorithms demonstrated that these newly discovered variants cannot be considered as technical artifacts. In fact, isomiRs are considered molecules with *in vivo* functional and evolutionary importance [526,527].

3.2.5.2.Classification and nomenclature of isomiRs

IsomiRs are heterogeneous molecules characterized by different nucleotide sequences and/or lengths with respect to their canonical counterparts.

Depending on the modification, five classes of isomiRs have been described: (1) isomiRs with alterations at the 5′ end; (2) isomiRs with alterations at the 3′ end; (3) isomiRs with alteration at both 5’ end and 3’ end, (4) isomiRs with polymorphisms within the sequence, without any difference in length; (5) isomiRs with polymorphism and 5′ and/or 3′ changes.

IsomiRs with alterations at 5’ and 3’ ends can be extensive classify in isomiRs with addition or deletion of nts at 5’ and 3’ ends. Depending on the correspondence of the added nucleotides with the flanking precursor sequence, the addition of nts can be further defined as template or non-template [528].

Loher et al. developed an annotation system to label isomiRs with 5' end and/or 3' end alterations [529]. This nomenclature indicates the name of the canonical miRNA, 5' end (start site), 3'end (end-site) and the eventual insertion of uracil in the 3' end of the isomiR compared to the canonical miRNA. In details, to define the start-site and end-site, zero indicates the same terminus of the canonical miRNA, while positive sign (+) or negative sign (-) followed by the number indicates the isomiR nucleotide shift in the 3' or 5' direction, respectively, when compared with canonical miRNA (**Figure 10**).

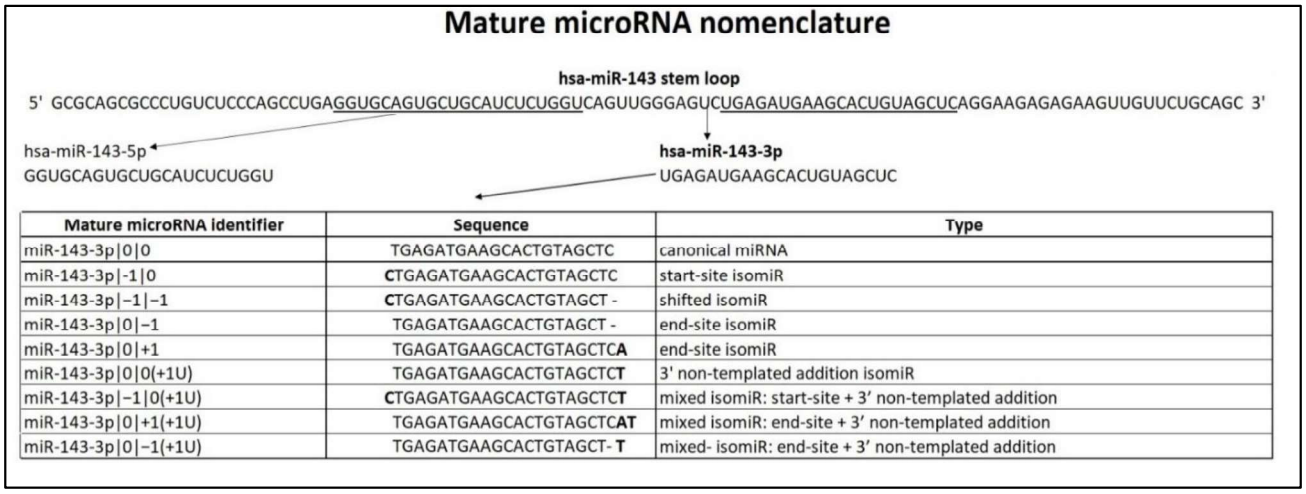

Mature microRNA identifier	Sequence	Type
miR-143-3p|0|0	TGAGATGAAGCACTGTAGCTC	canonical miRNA
miR-143-3p|-1|0	**C**TGAGATGAAGCACTGTAGCTC	start-site isomiR
miR-143-3p|−1|−1	**C**TGAGATGAAGCACTGTAGCT -	shifted isomiR
miR-143-3p|0|−1	TGAGATGAAGCACTGTAGCT -	end-site isomiR
miR-143-3p|0|+1	TGAGATGAAGCACTGTAGCTC**A**	end-site isomiR
miR-143-3p|0|0(+1U)	TGAGATGAAGCACTGTAGCTC**T**	3' non-templated addition isomiR
miR-143-3p|−1|0(+1U)	**C**TGAGATGAAGCACTGTAGCTC**T**	mixed isomiR: start-site + 3' non-templated addition
miR-143-3p|0|+1(+1U)	TGAGATGAAGCACTGTAGCTC**AT**	mixed isomiR: end-site + 3' non-templated addition
miR-143-3p|0|−1(+1U)	TGAGATGAAGCACTGTAGCT- **T**	mixed- isomiR: end-site + 3' non-templated addition

Figure 10. Example of mature microRNA nomenclature of miR-143-3p. miR-143 stem loop originates two canonical miRNAs, namely miR-143-5p and miR-143-3p. 9 mature microRNAs (canonical miRNA + isomiRs) of miR-143-3p were detected. The table reports nomenclature, sequence and type of mature microRNA. Nucleotides in bold correspond to additional nucleotides compared to the canonical sequence; "-" indicates the deletion of a nucleotide compared to the canonical sequence (Figure from Broseghini et al., [530]).

IsomiR were named depending on the change from the canonical miRNA:

- start-site isomiRs: isomiRs that change in the 5' end with deletion or addition of nts that match with stem loop;
- end-site isomiRs: isomiRs that change in the 3' end, with deletion or addition of nts that match with stem loop;
- 5' non-templated addition isomiRs: isomiRs with addition of nts at the 5'end, which do not match with stem loop sequence;
- 3' non-templated addition isomiRs: isomiRs with addition of nts at the 3' end that do not match with stem loop sequence. In the majority of cases, there is the addition of one or more uracils;
- shifted isomiRs: start-site and end-site are both shifted to 5' or to 3' direction, but the length of the isomiR is identical to the canonical miRNA;
- mixed isomiRs: isomiRs with more than one of the above variations.

3.2.5.3.Biogenesis of isomiRs

The isomiR biogenesis has not been completely clarified yet. It seems that isomiRs can arise from different and not completely understood mechanisms, such as alternative Drosha and/or Dicer cleavage of the precursor miRNAs [531], post-transcriptional modifications made by nucleotidyl transferase, which adds nucleotides to the pre-miRNA or mature miRNA ends [532-534], and editing of RNA and single nucleotide polymorphisms (SNPs) [522] (**Figure 11** from van der Kwast et al. [535].

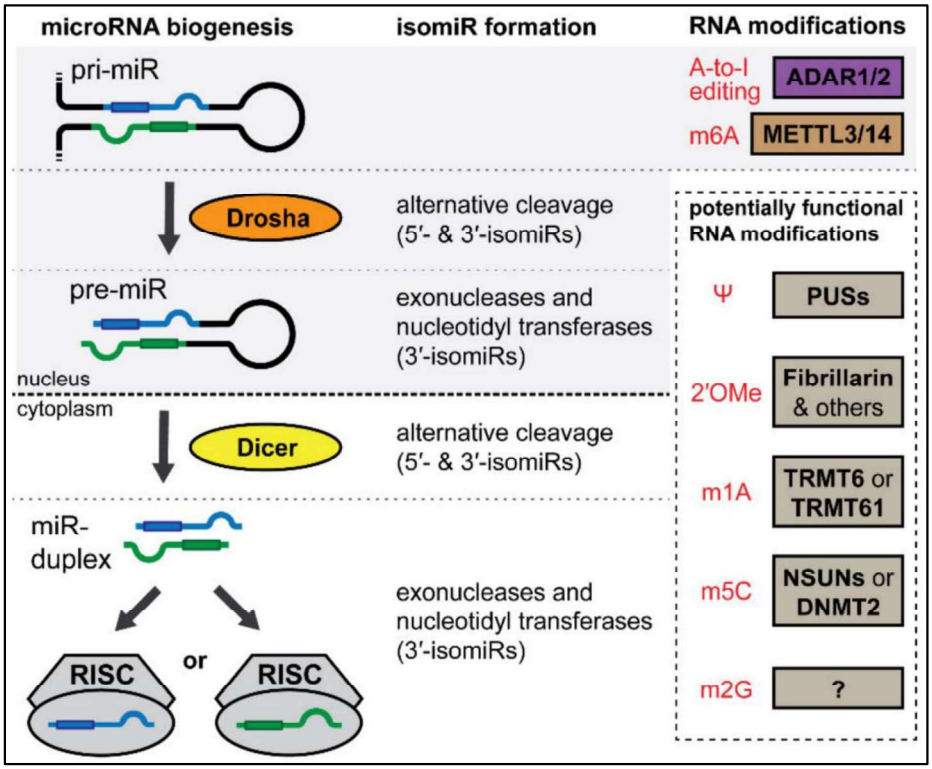

Figure 11. MiRNA biogenesis and alterations that induce isomiR formation or microRNA nucleotide modifications. Transcription of the miRNA containing gene forms the pri-miR. Drosha cleaves the pri-miR to generate the pre-miR. The pre-miR cleaved by Dicer in the cytoplasm yielding the miRNA duplex. Either side of the duplex can be incorporated into the RNA-induced silencing complex (RISC) to become a functional mature microRNA. IsomiRs can be formed during miRNA biogenesis when Drosha or Dicer cleave in alternative locations, or when exonucleases or nucleotidyl transferases remove or add nucleotides to the 3′-end of the pre-miR or the mature microRNA. RNA nucleotide modifications with known or potential functional implications on miRNA biogenesis or functioning are shown in red with their ‘writers’ next to them [535].

- Drosha/Dicer Non-Canonical Cleavage

In the canonical biogenesis pathway, Drosha and Dicer enzymes cleavage sequentially the primary transcript at 5′ and 3′ termini to generate miRNAs [531]. Drosha/DGCR8 complex performs a cleavage at the level of specific positions with respect to the basal (approximately 11 nts away) and the apical (approximately 22nts away) junctions of the pri-miRNA to generate pre-miRNA. Then, Dicer recognizes the pre-miRNA termini via the PAZ domain and cuts the short hairpin pre-miRNA in a site located approximately 22nts away from the 5′/3′ ends. Thus, the terminal loop is removed and

the duplex miRNAs is generated, which contains guide and passenger strands [178] (**Figure 12** from Zelli et. al [522]).

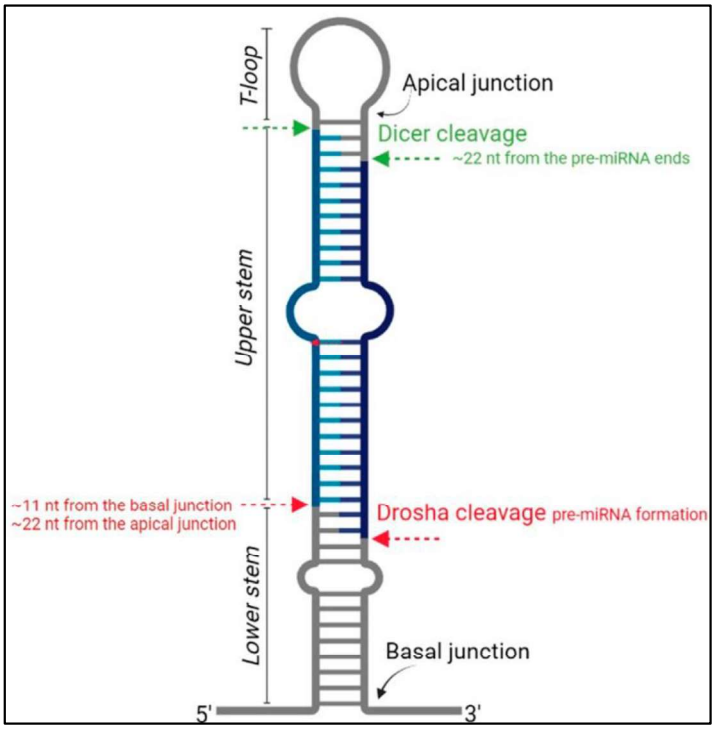

Figure 12. miRNAs and possible isomiRs biogenesis through sequential cleavages mediated by Drosha and Dicer enzymes [522].

Experimental models suggest that modification of the pri-miR loop size, or alterations of the stem length or the single-stranded sequences at its base, are all related to Drosha cleavage imprecision. Similarly, Dicer cleavage imprecision appears to be dependent on pre-miR structure and sequence [536]. These cleavage imprecisions can be responsible of the generation of new 5′ and 3′ variants [537-539]. Germline and somatic mutations in genes involved in miRNA biogenesis, such as *DROSHA*, *DGCR8*, *DICER1*, and *XPO5* genes can represent another mechanism responsible for the isomiRs generation and different expression levels in several diseases, including cancer [522]. By analyzing cancer somatic mutations in miRNA biogenesis genes, it was suggested that *DICER1* hotspot mutations could impact the expression levels of some isomiRs [540].

- Exoribonucleases and Nucleotidyl Transferases

In *Drosophila melanogaster*, it was found an exoribonuclease, named 3′-to-5′ Nibbler, that was able to induce 3′ end trimming in more than 25% of *Drosophila* miRNAs, after AGO1 loading. Trimming of miRNA 3′ ends can take place as a final step in miRISC assembly and is possible required to improve target mRNA repression. The depletion of Nibbler exoribonuclease leads to the formation of miRNAs intermediates longer than 22nts, resulting in developmental defects [541].

Uridyl or adenosyl-transferases are nucleotidyl transferases, namely template-independent polymerases able to add nucleotides at the 3′-terminus of RNAs. miRNA stability and performance can be affected by nucleotide additions, which are conserved in animals, occur at certain loci, and are catalyzed by enzymes involved also in the regulation of other RNAs [532,542,543].

- Editing of RNA and SNPs

Adenosine-Inosine (A-I) substitution is mediated by the adenosine deaminases ADARs [544,545] and can occur in the processing of pri-miRNA and pre-miRNA. If the A-I change is within the seed sequence, given the identification of I as G, RNA editing can affect the role of the miRNA, resulting for example in the regulation of new target genes [546,547].

SNPs occur at 1% frequency in the human genome and are involved in determining the inter-individual diversity and susceptibility to diseases. SNPs have been found also in miRNAs where they are responsible of defects in miRNAs maturation and of alterations in miRNA:mRNA interactions in cancer [522]. For example, the SNP rs2910164 in the pre-miRNA of miR-146a-5p has been linked to the risk of developing cervical cancer [548].

3.2.5.4.Significance of isomiR Functions

IsomiRs seem to play a role either in supporting [527] or competing [549] their canonical counterparts. The majority of isomiRs presents 3′ variations, leaving the 5′ end and the seed region unmodified [526]. Nevertheless, it has been observed that 3′ end is important because it can reinforce and maintain stability and specificity during miRNA-MRE interaction, especially when there are mismatches within the seed region [179,550,551]. Thus, also 3′ variations could have a functional impact. Both variations at the level of the 5′ end, namely addition and deletion, lead to a seed shifting with consequent functional effects [552], resulting in a possible gain or loss of function in terms of target recognition [553].

Many human miRNAs can associate with all AGO proteins, although several of them are preferably loaded into specific AGO proteins [554]. It was observed that also isomiRs can interact with AGO proteins [555,556] and some miRNA alterations seem to determine the preference to a different AGO protein loading [557], suggesting that isomiRs could affect miRISC function.

- isomiRs Detection and Quantification

To date, there are not available commercial kits able to detect isomiRs. However, some methods have been developed for the detection and quantification of isomiRs expression, including NGS and qRT-PCR approaches.

NGS is the methodology of choice for the detection and quantification of miRNAs and isomiRs, particularly for the discovery of new isoforms. A limitation of this approach is the lack of standardized data analysis protocols and normalization methods [528]. In addition, there is a possible overestimation of isomiRs detected [558].

The most common techniques for the analysis of small RNAs are based on poly(A) and stem-loop qRT-PCR. The advantages of these methods are their high level of specificity and the relatively low impact in terms of experimental times and costs [559]. On the other hand, limitations include the need to know the sequence and the limited precision in the discrimination of sequences that differ by only one/few nucleotides, especially if poorly represented in the sample, as often occurs for isomiRs. In addition, there is the impossibility of discovering new molecules [560,561].

For the analysis of isomiRs expression, some PCR-based methods were developed, such as Dumbbell-PCR [562,563], two-tailed RT-qPCR [564] and Multiplex Single Base Primer Extension Assay [565].

- Resources and Tools for isomiR Analysis

In 2016, a database was created with 308,919 isomiRs derived from 4706 mature miRNAs (https://mcg.ustc.edu.cn/bsc/isomir/) [566]. There are two database with the aim of describing the polymorphisms in miRNAs and their target sites, namely PolymiRTS database (https://compbio.uthsc.edu/miRSNP/) [567] and miRNASNP-v3 (http://bioinfo.life.hust.edu.cn/miRNASNP/) [568].

The Tumor Isomir Encyclopedia (TIE, https://isomir.ccr.cancer.gov/) database has been recently created to compare isomiR expression across more than 11,000 tumor samples from The Cancer Genome Atlas (TCGA) [569]. Other resources for the analysis of isomiRs can be further found at https://tools4mirs.org/software/isomirs_identification/.

3.2.5.5.IsomiRs in Cancer

IsomiRs can differ in abundance, stability, and role from canonical miRNAs, and they can be functionally redundant or discrepant compared to their canonical counterparts. Some isomiRs are ubiquitous in expression, while others present tissue-specific expression and abundance [570]. IsomiRs seem to play an important role in the pathogenesis and progression of several cancers and they could also contribute to cancer molecular heterogeneity. IsomiRs can also be promising cancer diagnostic and prognostic biomarkers. In fact, a panel of 50 5′ end isomiRs was able to effectively classify more than thirty different tumor types [571]. Compared to miRNAs expression, isomiRs expression was proven to be superior in the classification of these different cancer types [570,572].

There are two studies that analyzed isomiRs in melanoma. Kozubek et al identified a specific isomiR arising from *miR-144/451a* cluster, namely miR-451a.1, which is the most abundant isomiR of miR-451a [573]. The same isomiR (miR-451a.1) expression was found upregulated in normal skin, with a progressive decrease in melanoma and dysplastic nevi compared to common nevi. In addition high levels of mature miR-451a.1 has been associated with a significant reduction of cell migration and inhibition of invasion [574].

4. AIMS

The main aim of this study is to analyze the role of non-coding RNA alterations in melanoma, specifically the contribution of miRNAs to melanoma pathogenesis and their use as disease biomarkers.

Specific objectives are:

- The investigation of the association between specific miRNAs and clinical and histopathological features of melanoma, to study miRNA expression in reference to BT assessment defining the prognostic role of specific miRNAs in melanoma;
- The identification and validation of a miRNA panel able to discriminate between single and multiple primary melanoma, and between the first and subsequent melanomas from the same patient to unravel the role of miRNA network in multiple primary melanoma pathogenesis;
- The identification and functional characterization of miRNA isoforms that could explain the heterogeneity of melanoma and contribute to understand melanoma pathogenesis.

5. MATERIALS AND METHODS

5.1. Samples

5.1.1. Clinical samples

Clinical samples were provided by the Melanoma center of the Dermatology Unit at Bologna University Hospital. The study was approved by Comitato Etico Indipendente di Area Vasta Emilia Centro—CE-AVEC, Emilia-Romagna Region (number 417/2018/Sper/AOUBo). Tumor and nevi samples were formalin-fixed, paraffin-embedded (FFPE) samples. For each sample, five to six tissue sections on glass slides were obtained. One section was stained with hematoxylin-eosin and was examined by an expert pathologist to select the tumor/nevus area, which was macrodissected before RNA extraction.

- Pilot group for Small RNA Sequencing

The 24 histopathologic specimens were evaluated by two dermato-pathologists and classified into benign nevi (n=3) and melanomas (n=21). BN includes patients with no prior diagnosis of CM or non-melanoma skin cancer and a follow-up of at least 10 years. CM includes 11 patients with SSM (stage I, Breslow range = 0.3-0.8mm), and one patient with NM (stage II, Breslow = 2.5mm). The group of melanomas was further classified in single primary CM (n=4) and multiple primary melanoma (n=17). Single primary CM derived from CM patients with no history of prior CMs and a follow-up of at least 10 years. MPM samples are from 8 patients with prior diagnosis of ≥2 CMs and consist of eight 1st MPM, eight 2nd MPM and one 3rd MPM. Three of 8 patients had a family history of melanoma.

- Samples for miRNA-associated Breslow analysis

For miRNA-associated Breslow analysis, we start from small-RNA sequencing data from 3 BN and 20 CM. For the validation analysis, we collect 115 samples obtained from the Dermatopathology unit of the University of Bologna, Bologna, Italy (78 cases) and Pathology Unit at the University of Turin, Torino, Italy (37 cases). Confirmed primary cutaneous SSMs and NMs were included in this study. Clinical data are reported in **Table 6** [575]. Histopathologic subtype other than SSM or NM (acral lentiginous melanoma, lentigo maligna melanoma), melanoma *in situ*, regressed melanoma were exclusion criteria.

Table 6. Clinical and tumor features of patients with cutaneous SSM and NM

	SSM (n=90)	NM (n=45)
Gender		
Male	60 (66.7%)	20 (80%)
Female	30 (33.3%)	5 (20%)
Age of diagnosis		
Mean (y)	56.03 (24-85)	56.53 (18-81)
Location of the primary tumor		
Head and neck	5 (5.6%)	1 (4%)
Trunk	56 (62.2%)	12 (48%)
Limbs	29 (32-2%)	12 (48%)
Breslow tumor thickness (mm)		
<0.8	53 (57.4%)	
0.8-1	15 (16.7%)	3 (12%)
>1-2	13 (14.4%)	10 (40%)
>2-4	8 (8.9%)	11 (44%)
>4	1 (1.1%)	1 (4%)
Mean (BT)	0.897 mm (0.2-4.8)	2.29mm (0.8-4.3)
Mitosis		
≥1/mm^2	27 (30%)	23 (92%)
<1/mm^2	63 (70%)	2 (8%)
TIL		
Brisk	19 (21.2%)	2 (8%)
Not brisk	36 (40.0%)	3 (12%)
No	35 (38.9%)	
Not evaluated		20 (80%)
Regression		
Yes	44 (48.9%)	7 (28%)
No	25 (27.8%)	5 (20%)
Not identified	21 (23.3%)	13 (52%)
Metastases		
Absent	80 (88.9%)	9 (36%)
Present	10 (11.1%)	16 (64&)
- sentinel lymph node	1 (1.1%)	8 (32%)
- visceral	9 (10%)	8 (32%)
Outcome		
Mean follow-up	41	40
Death	5 (5.6%)	12 (48%)

Abbreviations: BT, Breslow thickness; NM, nodular melanoma; TIL, tumor-infiltrating lymphocytes; SSM, superficially spreading melanoma

- Samples for MPM study

For MPM study, we use small-RNA sequencing data from 3 BN, 4 single primary CM and 17 MPM. For the validation analysis, retrospective case series of 47 samples from 29 patients was collected and was classified into three groups: 3 BN, 9 single primary CM, and 35 MPM (17 patients). Clinical characteristics are reported in **Table 7** [576].

Table 7. Patient characteristics of MPM study

	Benign Nevi (BN)	Cutaneous Melanoma (CM)	Multiple Primary Melanoma (MPM)		
			MPM 1st	MPM 2nd	MPM 3rd
Gender (n;%)					
Male	0 (0%)	3 (33.3%)	13 (76.5%)		
Female	3 (100%)	6 (66.7%)	4 (23.5%)		
Total	3	9	17		
Histology (n;%)					
Compound melanocytic nevus	2 (66.7%)	-	-	-	-
Dermal nevus	1 (33.3%)	-	-	-	-
Superficial spreading melanoma	-	4 (44.5%)	15 (88.2%)	16 (94.1%)	1 (100%)
Superficial spreading melanoma with vertical growth phase	-	3 (33.3%)	1 (5.9%)	-	-
Nodular melanoma	-	2 (22.2%)	1 (5.9%)	-	-
Nevus-associated melanoma	-	0	-	1 (5.9%)	-
Age at diagnosis (n;%)					
< 50	3 (100%)	7 (77.8%)	8 (47%)	7 (41.2%)	1 (100%)
≥ 50	0 (0%)	2 (22.2%)	9 (53%)	10 (58.8%)	-
Mean (range)	31 (27-39)	59 (29-85)	53 (30-80)	55 (31-83)	36
Localization (n; %)					
Trunk	3 (100%)	6 (66.7%)	13 (76.5%)	14 (82.4%)	1 (100%)
Limbs	-	2 (22.2%)	3 (17.6%)	3 (17.6%)	-
Head and neck	-	1 (11.1%)	1 (5.9%)	-	-
Breslow thickness (n;%)					
< 0.8 mm	-	1 (11.1%)	12 (70.6%)	17 (100%)	1 (100%)
≥ 0.8 mm	-	8 (88.9%)	5 (29.4%)	0 (0%)	-
Family history of melanoma (n;%)					
Yes	-	-	3 (17.6%)		
No	-	-	14 (82.4%)		

- Samples for isomiR study

For isomiR analysis, we start from small-RNA sequencing data from 3 BN and 20 CM. For the validation analysis, 11 SSM melanoma samples from the MPM study cohort were used.

5.1.2. Melanoma cell line

SK-Mel-28 melanoma cells were obtained from the ATCC. SK-Mel-28 were cultured in RPMI medium with 10% fetal bovine serum, 1% L-Glutamine and 1% Penicillin-Streptomycin (10,000 U/mL).

5.1.3. TCGA datasets

- TCGA 32 cancers

For TCGA analysis regarding miR-125a-5p and its isomiR, short RNA-seq aligned BAM files were downloaded from the Genomic Data Commons Data Portal (https://portal.gdc.cancer.gov/) for all 32 cancer types.

- TCGA SKCM Cohort

Mutation status of *BRAF*, *NRAS* and *NF1* and small-RNA sequencing data were collected from 323 melanoma fresh-frozen samples from TCGA, including 63 primary CM and 260 melanoma metastases.

In TCGA database, ”metastatic melanoma” refers to the metastatic tissue and not to the primary melanoma that have metastasized. To avoid misunderstanding, we preferred to refer to this group as melanoma metastasis (MM), instead of metastatic melanoma.

Most of CM are II or III stage (37 samples are stage II, 19 are stage III, 3 are stage IV, and for four of them the stage was not reported). The biopsy site includes: 58% lymph nodes, 21% connective, subcutaneous and other soft tissues, 17% Skin and 4% other.

For 66 melanomas, the *NF1* mutation gene status was available, in details, 51 samples have at least one mutation, and 15 are the wild type. *BRAF* mutation gene status was available for 187 melanomas, namely 168 have at least one mutation, 19 are wild type. Finally, *NRAS* mutation gene status was available for 111 melanomas, including 85 with at least one mutation and 26 wild type.

All detailed data of this melanoma dataset are available on National Cancer Institute GDC Data Portal site (https://portal.gdc.cancer.gov, accessed on 1 June 2021).

5.2 RNA extraction

5.2.1. FFPE samples

RNA was isolated from five 10μm-thick FFPE sections using miRNeasy FFPE kit (Qiagen) according to the manufacturer’s instructions. Deparaffinization was performed with xylene, followed by an ethanol wash. RNA was eluted in 30μl of RNAse-free water. RNA yield and quality were assessed with NanoGenius Spectrophotometer (ONDA Spectrophotometer). No samples were excluded owing to insufficient RNA quantity. RNA samples were stored at −80 °C.

5.2.2. Melanoma cells

RNA was isolated from 10^6 melanoma cells (SK-Mel-28) using miRNeasy Mini Kit (Qiagen) according to the manufacturer's instructions. RNA was eluted in 30µl of RNAse-free water. RNA yield and quality were assessed with NanoDrop 2000/2000c Spectrophotometers (Thermofisher). RNA samples were stored at −80 °C.

5.3. Small-RNA sequencing

5.3.1. Small-RNA sequencing

We analyzed 3 BN and 21 melanomas, which include 4 single CM and 17 MPMs from 8 different patients. Libraries were generated using TruSeq Small RNA Library PrepKit v2 (Illumina, RS-200-0012/24/36/ 48), according to manufacturer's indications. Briefly, 35ng of purified RNA was ligated to RNA 3' and 5' adapters, converted to cDNA and amplified using Illumina primers containing unique indexes for each sample. High Sensitivity DNA (HS-DNA) kit (Agilent Technologies, USA5067-4626) was adopted for library quantifications using Agilent Bioanalyzer (Agilent Technologies) and the 24 DNA libraries were combined in equal amount to generate a libraries pool. Pooled libraries underwent to size selection employing magnetic beads (Agencourt, Beckman Coulter) and amplicons with a length in the 130-160bp range were recovered. 20pM of pooled libraries were quantified using the HS-DNA Kit, and were denatured, neutralized, and combined with a Phix control library (standard library normalizator). A final concentration of 1.8pM of the pooled libraries (obtained by dilution with a dedicated buffer as described in Illumina protocol guidelines) was obtained and sequenced using Next-Seq500/550 High Output Kit v2 (75 cycles) (Illumina, FC-404-2005) on the Illumina NextSeq500 platform. Raw base-call data were demultiplexed using Illumina BaseSpace Sequence Hub and converted to FASTQ format.

- miRNA identification

After a quality check with FastQC tool [577], the adapter sequences were trimmed using Cutadapt [578], which was also used to remove sequences shorter than 16 nucleotides and longer than 30 nucleotides. Reads were mapped using the STAR algorithm [579]. Only reads that mapped unambiguously to the reference genome retrieved from miRBase 21 database (at least 16 nucleotides aligned, with 10% mismatch allowed) were used for the downstream analyses. Raw counts from mapped reads were obtained using the HTseq-count script from the HTSeq tools [580]. Counts were normalized using DESeq2 Bioconductor package [581]. The small-RNA sequencing raw data (FASTQ format) are available through European Nucleotide Archive (ENA) with the following accession number: PRJEB35819.

- IsomiR identification and labelling
  - isomiR identification

IsoMiRmap tool was used for mapping of sequence reads and isomiR quantification [582]. isoMiRmap pipeline identifies and quantifies all isomiRs through the direct processing of short RNA-sequencing dataset. Briefly, for each short RNA-sequence dataset, the sequence reads were quality trimmed using the Cutadapt tool [578], keeping only those reads between 18 and 26 nts in length. Each resulting read is subsequently compared to a "lookup" table containing all possible isomiRs from miRbase release 22 hairpin sequences. All sequences are required to have exact matches to the isomiR lookup table, after which they are then counted and quantified in read per million (RPM). Only reads that passed quality trimming and filtering, and could be aligned exactly to miRNA arms were used in the denominator of this calculation. This approach identifies 5'-isomiRs, 3'-isomiRs, 5'-and-3' mixed isomiRs, as well as 3' and 5' non templated post-transcriptional additions. This approach was used for all datasets, the one generated here and those samples represented in TCGA.

  - IsomiR labelling and classification

To simplify the labeling of the isomiRs, we used the annotation system developed by Loher et al [529]. Nomenclature specifies the name of the canonical miRNA, 5' end (start-site), 3'end (end-site) and the eventual insertion of uracil of the isomiR compared to the canonical miRNA sequence found in miRBase database. In details, to define the start-site and end-site, zero indicates the same terminus of the canonical miRNA, while positive sign (+) or negative sign (-) followed by the number indicates the isomiR nt shift in the 3' or 5' direction, respectively, when compared with miRBase miRNA sequence.

Depending on the change from the canonical miRNA, isomiRs have been classified in six different group: start-site isomiRs (those isomiRs that vary in the start-site with deletion or addition of nts that match with stem loop), end site isomiRs (those isomiRs that vary in the end-site, with deletion or addition of nts that match with stem loop), 5' non-templated addition isomiRs (isomiRs with addition of nts at the 5' end, which do not match with stem loop), 3' non-templated addition isomiRs (isomiRs with addition of nts at the 3'that do not match with stem loop sequence), shifted isomiRs (start-site and end-site are both shifted to 5' or to 3' direction, but the length of the isomiR is identical to the canonical miRNA), and mixed isomiRs (isomiRs with more than one variation).

5.4 RNA quantification

5.4.1. miRNA quantification

- miRCURY assay

miRCURY assay allows the quantification of the sum of canonical miRNA and 5- isoforms. RNA extracted from FFPE samples was converted to cDNA using miRCURY LNA RT kit (Qiagen, catalog number 339340). Reverse-transcription (RT) reaction was performed as follows: 2µl miRCURY RT Reaction Buffer, 4.5µl RNase-free water, 1µl miRCURY RT Enzyme Mix, 0.5µl UniSp6 spike-in, and 2µl template RNA (5ng/µl). RT cycling protocol consisted in 60min at 42°C, 5min at 95°C, and cooling at 4°C. cDNA samples were stored at−20°C.

RT-quantitative PCR (qPCR) was performed using miRCURY LNA SYBER Green PCR kit (Qiagen, catalog number 339346) and primers from miRCURY LNA miRNA PCR Assays (Qiagen, catalog number 339306): hsa-miR-146a-5p (catalog number YP00204688), hsa-miR-21-5p (catalog number YP00204230), hsa-miR-125a-5p (catalog number YP00204339), hsa-miR-125b-5p (catalog number YP00205713), hsa-miR-149-5p (catalog number YP00204321), hsa-miR-200b-3p (catalog number YP00206071), hsa-miR-205-5p (catalog number YP00204487), hsa-miR-211-5p (catalog number YP00204009), hsa-miR-25-3p (catalog number YP00204361) and hsa-miR-92b-3p (catalog number YP00204384). For Breslow analysis, SNORD44 (catalog number YP00203902) and SNORD48 (catalog number YP00203903) were used as reference genes. For MPM analysis, hsa-miR-16-5p (catalog number YP00205702) was used as reference miRNA due to its stability across samples in NGS experiment.

For each miRNA target, cDNA was diluted at the ratio of 1:80 with the exception of miR-92b-3p, for which cDNA was diluted 1:4. Cycling program consisted in 10 min at 95 °C and 2-step cycling (40 cycles) of denaturation (10 s at 95 °C), and combined annealing/extension (60 s at 60 °C). Each assay was tested in triplicate. Raw Cq values were obtained from BioRad CFX software. Interplate calibrators were used to standardize miRNA Cq values across plates. The calculation of relative expression was performed using $2^{-\Delta Ct}$ methods.

- miSCRIPT assay

miSCRIPT assay allows the quantification of the sum of canonical miRNA, 5- and 3-isoforms. RNA from 39 samples, including 5 CMs and 34 MPMs, was reverse transcribed using miSCRIPT HiSpec Buffer from miSCRIPT II RT kit (Qiagen, catalog number 218161) according to the manufacturer's instructions. In details, RT reaction was prepared in a total reaction volume of 10µl with 2µl miScript

HiSpec Buffer, 1µl miScript Nucleics Mix, 4µl RNase-free water, 1µl miScript Reverse Transcriptase Mix, and 2µl template RNA (5ng/µl). RT cycling protocol consisted in 60min at 37°C, 5min at 95°C, and cooling at 4°C. cDNA samples were stored at −20°C.

RT-qPCR was performed using miSCRIPT SYBER Green PCR kit (Qiagen, cod. number 218073) and primers from miSCRIPT Primer Assays (Qiagen, catalog number 218300): hsa-miR-125a-5p (cod. number MS00003423) and RNA U6 (RNU6) (cod. number MS00033740). Reaction mix was prepared with 10µl QuantiTect SYBR Green PCR Master Mix, 2µl miSCRIPT Universal Primer, 2µl miScript target Primer, 3µl RNase-free water, and 3µl cDNA template (1:40). Cycling program consisted in 15min at 95°C and a 3-step cycling (40 cycles) of denaturation (15s at 94°C), annealing (30s at 55°C), and extension (30s at 70°C). Each assay was tested in triplicate. Raw Cq values were obtained from BioRad CFX software. Small nuclear RNU6 was used as reference gene. The calculation of relative expression was performed using $2^{-\Delta Ct}$ methods.

5.4.2. isomiR quantification

- Db-ddPCR

Dumbbell based droplet digital PCR assay (Db-ddPCR) is based on Dumbbell-PCR [563]. This method consists in three steps: adapter ligation, reverse transcription and quantification with droplet digital PCR (ddPCR). **Table 8** reports sequences of adapters (3'-Db-adapter), reverse transcription primer (RT primer), ddPCR primers (Forward and Reverse primers) and TaqMan MGB probes for the quantification of canonical miR-125a-5p and for its shorter 3'isoform, namely miR-125a-5p|0|−2. The 3'-Db-adapters, RT primer, Forward and Reverse primers were designed and then provided by Integrated DNA Technologies IDT. TaqMan MGB probes (cat number 4316034) were designed with 5'dye (FAM) and 3'quencer (MGBNFQ); and then ordered by Thermofisher. In addition, **Table 8** reported also synthetic oligonucleotides sequences of canonical and isomiR, which were used to test and optimize the protocol (ordered by IDT).

Table 8. Sequences of adapters, primers and probes for Db-ddPCR assay

Adapter/ primer/oligonucleotide	Sequence (5'->3', for detection of canonical miR-125a-5p)	Sequence (5'->3', for detection of isomiR 125a-5p)
3'-Db-adapter	/5Phos/CTCAGTGCAGGGTCCGAGGTA TTCGCACTGAGTCACAG/3InvdT/	/5Phos/CTCAGTGCAGGGTCCGAGGTA TTCGCACTGAGACAGG/3InvdT
RT primer	CTCAGTGCGAATACCTCGGACCCT	Same as left
Forward primer	GCAGTCCCTGAGACCCT	GCAGTCCCTGAGACCC
Reverse primer	CGAATACCTCGGACC	Same as left
TaqMan probe	6FAMCTGTGACTCAGMGBNFQ	6FAMACCTGTCTCAGMGBNFQ
Synthetic oligonucleotides	P-UCCCUGAGACCCUUUAACCUGUGA-	P-UCCCUGAGACCCUUUAACCUGU

- Adapter Ligation

Adapter ligation is the first step of Db-based ddPCR. For cell samples, we used 20ng of total RNA in 1ul, while for FFPE samples we used 10ng of total RNA in 1ul. Cellular total RNA (1µl) was mixed with 20pmol of the 3′-adapter (1µl) in a 1.5ml centrifuge tube that was incubated at 90°C for 3min, and immediately 0.5µl of 10X Annealing buffer (composed with 50mM TrisHCl pH8, 5mM EDTA, 100mM $MgCl_2$) was added. The mixture was incubated at 37°C for 20min to allow annealing and hybridization. Then, 1µl 10X Ligase buffer, 0.1µl T4 RNA Ligase 2, 0.5µl $MgCl_2$ 100mM, 2µl 50% PEG8000 and 3.9µl RNase-free water were added. Ligation cycling protocol consisted in 60min at 37°C, 5min at 80°C, and cooling at 4°C.

- Reverse Transcription

CDNA conversion was performed with Superscript III reverse transcriptase (cat number18080044, Thermofisher). 10µl of ligated RNA was mixed with 1µl RT Primer 5µM, 0.5µl dNTP Mix (10mM each, cat number R0192, Thermofisher) and 2.5µl RNase-free water. The reaction tube was incubated 2min at 90°C, 5min at 65°C, and placed for 1min in ice. Subsequently, 4µl 5X First strand Buffer, 1µl 100 mM DTT, 0.5µl RNasin Ribonuclease Inhibitor (cat number N2111, Promega) were added to the reaction. Reverse transcription cycling protocol consisted in 60min at 66°C, 15min at 70°C, and cooling at 4°C. cDNA were stored at -20°C.

- ddPCR

ddPCR was performed using ddPCR Supermix for Probes (no dUTP) assay (Biorad, cat number 1863024) for droplet generation in the QX200 Droplet Digital PCR Systems (Biorad), according to the manufacturer's instructions. Components for the preparation of the ddPCR reaction to be load in the QX200 Droplet Generator (Bio-Rad, cat number 1864002) include: 10µl 2X ddPCR Supermix for Probes (no dUTP), 0.3µl TaqMan MGB Probe 10µM, 0.3µl Forward primer 10µM , 0.3µl Reverse primer 10µM, 4.1µl RNase-free water and 5µl cDNA sample. cDNA was diluted according to the sample type: cDNA was diluted 1:500 for miRNA or isomiR transfected cells, 1:5 for untransfected cells, scramble transfected cells and FFPE sample.

Upon completion of droplet generation, the droplets were carefully transferred to a 96-well PCR plate (Eppendorf, H0030128605). The plate was heat-sealed with a pierceable aluminum foil and placed in a thermal cycler. Thermal cycling conditions are: Enzyme activation (10min at 95°C), 3-step cycling (40 cycles) of denaturation (30s at 94°C), annealing (15s at 45°C), and extension (45s at 60°C), enzyme deactivation (10min at 98°C) and cooling at 4°C. In every step, we used a ramping rate of 2°C/second.

When ddPCR was completed, plate was transferred into the plate holder of the QX200 Droplet Reader (Bio-Rad, cat. no. 1864003). At the end of the plate reading, the resulting data were analyzed with QuantaSoft software v1.7.

5.4.3. mRNA quantification

RNA was converted in cDNA with iScript Reverse Transcription Supermix for RT-qPCR (cat number 1708840, Biorad). RT reaction was performed as follows: 2µl iScript RT Supermix, 6µl RNase-free water and 2µl template RNA (10ng/µl). RT cycling protocol consisted in 5min at 25°C, 20min at 46°C, 1min at 95°C and cooling at 4°C. cDNA samples were stored at−20°C.

RT-qPCR was performed using SsoAdvanced Universal SYBR Green Supermix (cat number 1725271, Biorad) and primers PrimePCR SYBR Green Assay (cat number 10025716): SMARCE1 (human, cat number qHsaCED0042335) and beta-Actin (human, cat number qHsaCED0036269). Reaction mix was prepared with 10µl 2X SsoAdvanced Universal SYBR Green Supermix, 1µl 20X PrimePCR SYBR Green Assay, 8µl RNase-free water, and 1µl cDNA template (undiluted). Cycling program consisted in 10 min at 95 °C and 2-step cycling (40 cycles) of denaturation (10 s at 95 °C), and combined annealing/extension (60 s at 60 °C). Each assay was tested in triplicate. Raw Cq values were obtained from BioRad CFX software. Interplate calibrators were used to standardize miRNA Cq values across plates. The calculation of relative expression was performed using $2^{-\Delta Ct}$ methods.

5.5.Target analysis and validation

5.5.1. Transfection

Transfection was performed using Lipofectamine 2000 DNA Transfection Reagent (cat number 11668019, Thermofisher) according to manufacturer's instructions. There were the following conditions: cells transfected with canonical miR-125a-5p mirVana miRNA mimic (cat number MIMAT0006181, Thermofisher), cells transfected with isomiR miR-125a-5p|0|–2 mirVana miRNA mimic (cat number MIMAT0035923, Thermofisher), cell transfected with a scramble oligonucleotide (MISSION miRNA, Negative Control 2, Sigma-Aldrich) and untransfected cells.

Briefly, at day zero, in each well (6-well plate), 10^6 SK-Mel-28 cells were seeded in 2ml of medium. At day 1 (transfection day), we prepared two dilution mixes. The first mix consists in 150µl of OptiMEM medium and 9µl of Lipofectamine 2000 DNA Transfection Reagent. The second one includes 150µl of OptiMEM medium and 3µl of mimic. 150µl of each mix were put together (miRNA-lipid complex mix) and incubate for 5min. Then, in each well, we added 250µl of the miRNA-lipid complex mix. Cells were collected at 4 different time points: 24h, 48h, 72h and 96h after the transfection.

For each condition and time point, we used two wells of a 6-well plate: one well has been used for RNA extraction to calculate mRNA target expression, while one well has been used for protein extraction.

5.5.2. Protein quantification

- Cell lysis

In an Eppendorf tube, pellet of 10^6 SK-Mel-28 cells was resuspended with 100ul of RIPA buffer (10ml RIPA with 1 protease inhibitors tablet). After an incubation of 30 min in ice, the tube was centrifuged at 14000g for 15 min at 4°C. Supernatant phase was collected and stored at -80°C.

- Bradford protein assay

Bovine serum albumin (BSA) was diluted in water to generate the standard curve: 1000µg, 500µg, 250µg, 125µg, 62.5µg and 0µg. 5µl of protein samples were diluted in 35µl water (1:8 dilution). In each well of a 96 well clear plastic plate we add 5µl of diluted samples or standards and 250µl of Bio-Rad Protein Assay Dye Reagent (diluted 1:4 in water). After incubation of 5min, the absorbance (λ=595nm) was measured on plate reader with Gen5 software (Agilent Technologies). Standards absorbance values were used to calculate a standard curve. Absorbance values of unknown protein samples have been then interpolated onto the formula for the standard curve to determine their concentrations.

- Western blot

2-Mercaptoethanol was diluted 1:10 in 4x Laemmli Sample Buffer (cat number 1610747, Biorad) to obtain sample buffer. In an Eppendorf tube, we added 30µg of protein, 12.5µl of samples buffer and water to get a final volume of 50µl. Samples were heated at 100°C for 8 min and then placed in ice. Samples were loaded in 4-15% Mini-PROTEAN TGX Precast Protein Gel (Biorad) and run at 100V for 1h. Transfer was performed with nitrocellulose membrane at 100V for 1h. Membrane was blocked with blocking buffer (5% nonfat dry milk blocker, Biorad) for 1h. Primary Antibody staining was performed overnight at 4°C with: SMARCE1 1:1000 (rabbit, cat number ab70540, Abcam), Cyclophilin A 0.1ug/ml (goat, cat number AF3589, R&D system). Secondary antibodies, namely irDye800CW anti rabbit (LI-COR Biosciences) and in irDy800CW donkey anti goat (LI-COR Biosciences) were diluted 1:10 000 and incubated for 1h at room temperature. All antibodies were diluted in 5% nonfat dry milk blocker. Membrane acquisition was performed with the 800nm channel of Odyssey Imaging Systems (LI-COR Biosciences)

5.6.Statistical Analysis

5.6.1. small-RNA sequencing

Normalized sequencing data were imported and analyzed in GeneSpring GX software (Agilent Technologies). For the comparison of the global miRNA profile between thin *vs.* thick melanomas, we used a fold-change >1.5 filter and a moderate t-test (*p value* <0.05).

Differentially expressed miRNAs were identified using a fold-change >1.5 filter and moderated t-test (false discovery rate 5% with Benjamini-Hochberg correction) in CM *vs*. MPM comparison, and using fold-change >1.2 and paired t-test (*p value* < 0.05) in first *vs*. second MPM comparison. Cluster analysis was performed using Manhattan correlation as a similarity measure. Principal component analysis (PCA) was performed on 24 samples using all human miRNAs detected by NGS analysis (n = 1629).

Differentially expressed mature miRNAs (canonical miRNAs + isomiRs) were identified using a fold change (FC) > 2 filter and moderated t-test (FDR 5% with Benjamini-Hochberg correction) in benign nevi *vs*. melanoma comparison (small RNA-seq data). For TCGA SKCM data, we applied a fold-change > 1.5 and t-test unpaired (FDR 5% with Benjamini-Hochberg correction) in primary melanoma vs. melanoma metastasis comparison. To analyze the association between isomiR and the melanoma-linked mutations, we performed an unpaired t-test with unequal variance (Welch correction) (FDR 5% with Benjamini-Hochberg correction).

5.6.2. miRNA association with clinicopathologic characteristics

Continuous variables were reported through median and interquartile range, whereas categorical variables were described through frequency distribution. Time to relapse was defined as the time elapsed between diagnosis and relapse. OS was defined as the time elapsed between diagnosis and death from any cause or the last follow-up.

Individual and combined miRNA expression and BT were tested in univariate models by Cox regression with 95% CI. The survival curves were estimated by the Kaplan-Meier method, and the log-rank test was performed to test differences between the survival curves. The association between miRNA expression (normalized on two reference genes) and BT was investigated with Pearson's correlation (r) and linear regression analysis. A value of two-sided *p value* < 0.05 was considered significant.

5.6.3. mRNA association with survival

- MPM study

Association of gene expression with overall survival in TCGA SKCM cohort was obtained using Oncolnc website (http://www.oncolnc.org) and log rank test was used to calculate the *p value*.

- isomiR study

Association of gene expression with overall survival in TCGA SKCM cohort was obtained using Human Protein Atlas (https://www.proteinatlas.org).

Based on the FPKM (Fragments Per Kilobase of transcript per Million mapped reads) value of each gene, patients were classified into two expression groups, namely low" (under cut off) or "high" (over cut off), and the correlation between expression level and patient survival was examined. The prognosis of each group of patients was analyzed with Kaplan-Meier survival estimators, and the survival outcomes of the two groups were compared by log-rank tests. The best expression cut-off refers the FPKM value that yields maximal difference with regard to survival between the two groups at the lowest log-rank *p value*.

5.6.4. Graphpad Prism 6

Graphpad Prism 6 (GraphPad Software) was used for statistical analyses. The association between BT and miRNA categorical groups and relapse events was investigated with Fisher's exact test or Mann-Whitney U test.

Group comparison (BN, CM and MPM) was performed using unpaired t-test, when data had a normal distribution, with or without Welch's correction according to the significance of the variance test. Data that did not present a normal distribution were compared using Mann-Whitney non-parametric test. Paired t-test was used to compare miRNA expression level in the 1st and 2nd melanomas from the same patient. Two-tailed *p values* were used in text and figures.

Graphpad Prism 6 was also used to perform specific isomiR comparisons using the Mann-Whitney non-parametric test.

5.6.5. MetaCalc software

MetaCalc software was used for survival analyses, namely association of BT value and miRNA combined (average expression of miR-21-5p and miR-146a-5p) with overall survival and time to relapse.

5.7.Pathway analysis

5.7.1. Enrichment analysis

Pathway and network analyses of differentially expressed miRNAs, miR-125a-5p isomiR and canonical miRNA, and their targets were investigated using the web-based software MetaCore (Clarivate). A *p-value* of 0.05 was used as a cut-off to determine significant enrichment.

5.7.2. Target prediction

IsomiR targets were predicted using the RNA22 algorithm [583]. Targets were allowed to be present in the 5′-UTR, coding sequence, and 3′-UTR of the candidate mRNA. We selected only those targets that had a *p-value* < 0.01 and a predicted binding energy < −16 kcal/mol, while also allowing G : U wobbles and bulge's within the seed region.

6. RESULTS

6.0. Pilot study: small RNA sequencing of benign nevi and melanoma

We obtained the global miRNA expression profile of melanomas and normal tissues (benign nevi) to investigate the contribution of small non-coding RNA alterations in melanoma pathogenesis. In particular, we focused on a specific group of melanoma patients, namely those that in their lifetime have developed two or more primary melanomas, the so-called multiple primary melanomas [576].

For this purpose, we selected a pilot group to perform a small RNA seq with the Illumina platform. We collect RNA from 3 benign nevi, 4 single cutaneous melanomas, and 17 multiple primary melanomas (8 patients). All melanomas are classified as early-stage melanomas. The MPM group includes 3 patients with familial melanoma and 5 patients without melanoma familiarity. For 7 MPM patients, we collected RNA from the first and the second melanomas, while for one patient also the third melanoma was provided. A total of 24 samples were used for small RNA seq, and we identified 1629 miRNAs expressed in melanoma and nevus cells. The obtained small RNA seq data have been used as starting point for the following analysis:

- Study of the association between specific miRNAs and clinical and histopathological features of melanoma
- Identification and validation of a miRNA profile of multiple primary melanoma
- Identification and functional characterization of isomiRs.

6.1. Defining the prognostic role of miRNAs in Cutaneous Melanoma

Breslow thickness measures how far melanoma cells invaded the skin layer and it is the main prognostic feature in melanoma staging: a ticker BT is associated with a worst prognosis [140]. We investigated the role of miRNAs in melanoma prognosis, specifically, looking to the association of miRNA expression with BT, number of mitosis, regression, overall survival, and time to relapse [575]. For this specific analysis, single and multiple melanomas were included in the same group. However, to perform the association analysis, melanomas were classified based on their subtype: superficial spreading melanoma and nodular melanoma.

6.1.1. Comparison of global miRNA profile in thin and thick melanomas identified candidate prognostic miRNAs

We used small-RNA sequencing data of 20 melanomas (19 SSM and 1 NM), which were further classified in two groups according to their Breslow thickness (BT): 15 thin melanomas (BT <0.8mm) and 5 thick melanomas (BT ≥ 0.8mm). The comparison of the global miRNA profile of these two groups identified miRNAs that potentially correlating with BT. A list of 50 miRNA differentially expressed between the two groups (FC >2, *p value* <0.05) was obtained, and it included 22 downregulated miRNA and 28 upregulated miRNA in thick melanomas compared to thin melanomas (**Table 9**).

Table 9. List of microRNAs differentially expressed in thick and thin melanomas

microRNA	*p value* ([thick] Vs [thin])	Regulation ([thick] Vs [thin])	FC ([thick] Vs [thin])
hsa-miR-100-5p	0.0009	down	-2.05
hsa-miR-1247-5p	0.0128	down	-2.09
hsa-miR-125a-5p	0.0009	down	-2.13
hsa-miR-125b-5p	0.0003	down	-2.15
hsa-miR-144-3p	0.0070	down	-5.14
hsa-miR-149-5p	0.0001	down	-2.81
hsa-miR-193b-5p	0.0074	down	-2.57
hsa-miR-195-3p	0.0014	down	-2.16
hsa-miR-200b-3p	0.0016	down	-2.45
hsa-miR-200b-5p	0.0053	down	-2.93
hsa-miR-224-5p	0.0048	down	-2.01
hsa-miR-320b	0.0133	down	-2.57
hsa-miR-375	0.0054	down	-3.69
hsa-miR-4662a-5p	0.0095	down	-3.19
hsa-miR-485-5p	0.0044	down	-3.12
hsa-miR-486-5p	0.0129	down	-2.85
hsa-miR-6510-3p	0.0068	down	-2.85
hsa-miR-6511b-3p	0.0062	down	-2.94
hsa-miR-654-5p	0.0102	down	-2.48

hsa-miR-6821-5p	0.0153	down	-2.92
hsa-miR-885-5p	0.0141	down	-2.16
hsa-miR-96-5p	0.0431	down	-2.06
hsa-miR-1287-5p	0.0133	up	2.08
hsa-miR-1303	0.0380	up	2.00
hsa-miR-142-3p	0.0011	up	3.31
hsa-miR-142-5p	0.0086	up	2.38
hsa-miR-146a-5p	0.0347	up	2.27
hsa-miR-146b-5p	0.0036	up	2.29
hsa-miR-150-3p	0.0215	up	2.52
hsa-miR-150-5p	0.0264	up	2.20
hsa-miR-155-5p	0.0014	up	4.06
hsa-miR-181a-3p	0.0001	up	2.25
hsa-miR-185-5p	0.0314	up	2.14
hsa-miR-20b-5p	0.0190	up	2.15
hsa-miR-212-3p	0.0120	up	2.78
hsa-miR-21-3p	0.0003	up	3.06
hsa-miR-21-5p	0.0009	up	2.80
hsa-miR-223-5p	0.0484	up	2.08
hsa-miR-301b	0.0308	up	2.67
hsa-miR-31-5p	0.0231	up	3.90
hsa-miR-3614-5p	0.0000	up	2.71
hsa-miR-363-3p	0.0329	up	3.10
hsa-miR-424-3p	0.0463	up	2.35
hsa-miR-424-5p	0.0181	up	3.16
hsa-miR-4454	0.0437	up	2.20
hsa-miR-501-5p	0.0062	up	2.43
hsa-miR-510-5p	0.0044	up	3.26
hsa-miR-542-5p	0.0118	up	3.19
hsa-miR-584-5p	0.0357	up	2.52
hsa-miR-887-3p	0.0307	up	2.26

We focused on upregulated miRNAs and we performed a correlation analysis between normalized expression of miRNA (>5) and BT (mm). Person's r correlation index and two tailed *p value* of the five significant better correlated BT/miRNA pair were reported in **Table 10**. The correlation between the expression of the first two miRNAs, namely miR-21-5p and miR-146a-5p, with the BT was analyzed in a larger cohort.

Table 10. miRNAs significantly correlating with Breslow thickness in 20 primary melanomas

miRNA	Pearson r	95% confidence interval	R square	p value (two-tailed)
BT vs. hsa-miR-146a-5p	0.7424	0.4347 to 0.8949	0.5511	0.0003
BT vs. hsa-miR-21-5p	0.7369	0.4248 to 0.8924	0.543	0.0003
BT vs. hsa-miR-181a-3p	0.7287	0.4101 to 0.8888	0.5309	0.0004
BT vs. hsa-miR-21-3p	0.7254	0.4043 to 0.8873	0.5262	0.0004
BT vs. hsa-miR-155-5p	0.6165	0.2252 to 0.8365	0.38	0.0049

6.1.2. Validation of miR-146a-5p and miR-21-5p as prognostic biomarkers in superficially spreading melanoma

We measured the expression of miR-21-5p and miR-146a-5p in 90 archive FFPE SSM and 25 NM samples from two independent cohorts. Individual and combined miRNA expression of miR-21-5p and miR-146a-5p was correlated with BT and the strong positive correlation was confirmed only in SSM histologic subtype. Specifically, miR-21-5p and miR-146a-5p showed both a *p value* < 0.0001 and a Pearson's r of 0.79 and 0.62, respectively. However, the highest and most significant correlation index is provided by the combination of miR-21-5p and miR-146-5p normalized expression (Pearson's r = 0.8) (**Figure 13**). The correlation between individual and combined expression of these two specific miRNAs was linear and evident also when considering tumors with thickness < 2mm (**Figure 13**).

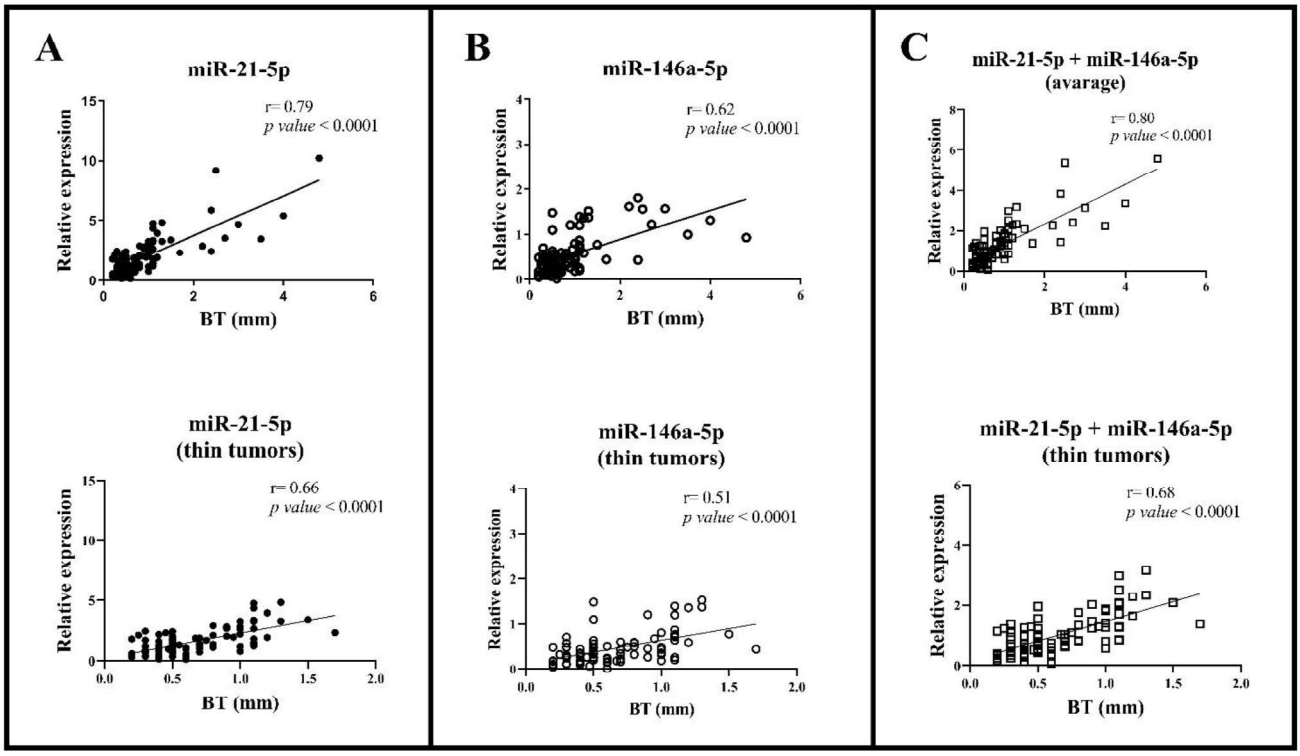

Figure 13. Correlation of miRNA expression with BT in SSMs. (a) Distribution of paired miR-21-5p and BT values in 90 SSMs (upper panel) and focus on <2-mm-thick tumors (lower panel). Simple linear regression is shown. (b) Distribution of paired miR-146a-5p and BT values in 90 SSMs (upper panel) and focus on <2mm thick tumors (lower panel). Simple linear regression is shown. (c) Distribution of miRNA average (miR-21-5p and miR-146a-5p) and BT values in 90 SSMs (upper panel) and focus on <2mm-thick tumors (lower panel). Simple linear regression is shown. BT, Breslow thickness; miRNA, microRNA; SSM, superficially spreading melanoma.

On the other hand, results showed no correlation between individual and combined expression of miR-21-5p and miR-146a-5p and BT in nodular melanomas (**Figure 14**).

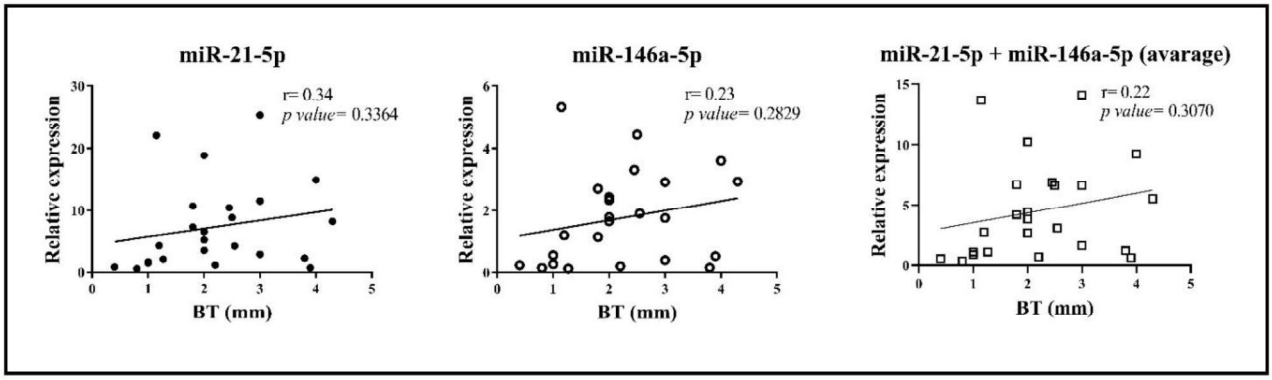

Figure 14 Correlation of miRNA expression with BT in NMs. Distribution of paired miR-21-5p, miR-146a-5p and miRNA average (miR-21-5p and miR-146a-5p) and BT values in 25 NMs. The correlation is not significant. BT, Breslow thickness; miRNA, microRNA; NM, nodular melanoma.

6.1.3. miR-146a-5p and miR-21-5p expression is associated with outcome and prognostic features in superficially spreading melanoma

On univariate analysis for OS, NM associated with worse outcomes when compared with SSM, including SSM with BT >0.8 mm (**Figure 15**). Overall, NM prognosis was poor (12 of 25 deceased patients).

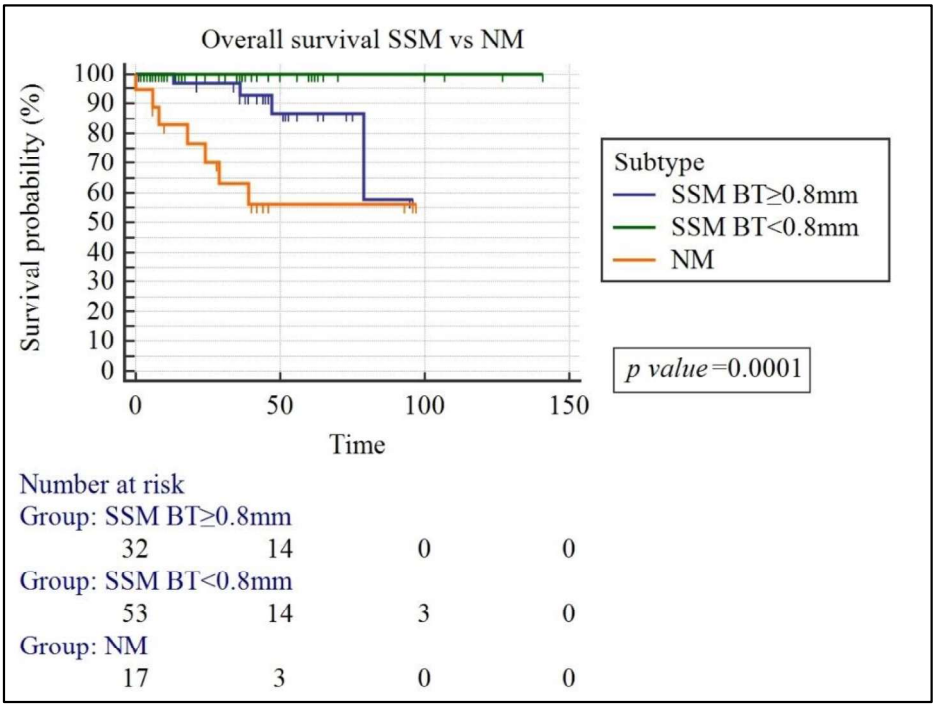

Figure 15 Kaplan-Meier plots for OS in SSM and NM. The plots show a significant difference in OS curves between patients with SSM with BT ≥ 0.8 mm versus BT < 0.8 mm and patients with NM melanomas. BT, Breslow thickness; NM, nodular melanomas; OS, overall survival; SSM, superficially spreading melanoma.

The combined expression of miR-21-5p and miR-146a-5p was used on univariate analysis for OS and for time-to-relapse (TTR). Significant differences were observed between group of patients with miRNA combined expression ≥1.5 and <1.5. Specifically, patients with combined miRNA expression

lower than 1.5 had a better outcome than those with miRNA expression ≥1.5 (*p value* = 0.0021 for OS and *p value* < 0.0001 for TTR). Moreover, the association of combined miRNA expression with outcomes was most significant than BT (*p value* = 0.0330 for OS and *p value*= 0.0030 for TTR) (**Figure 16**).

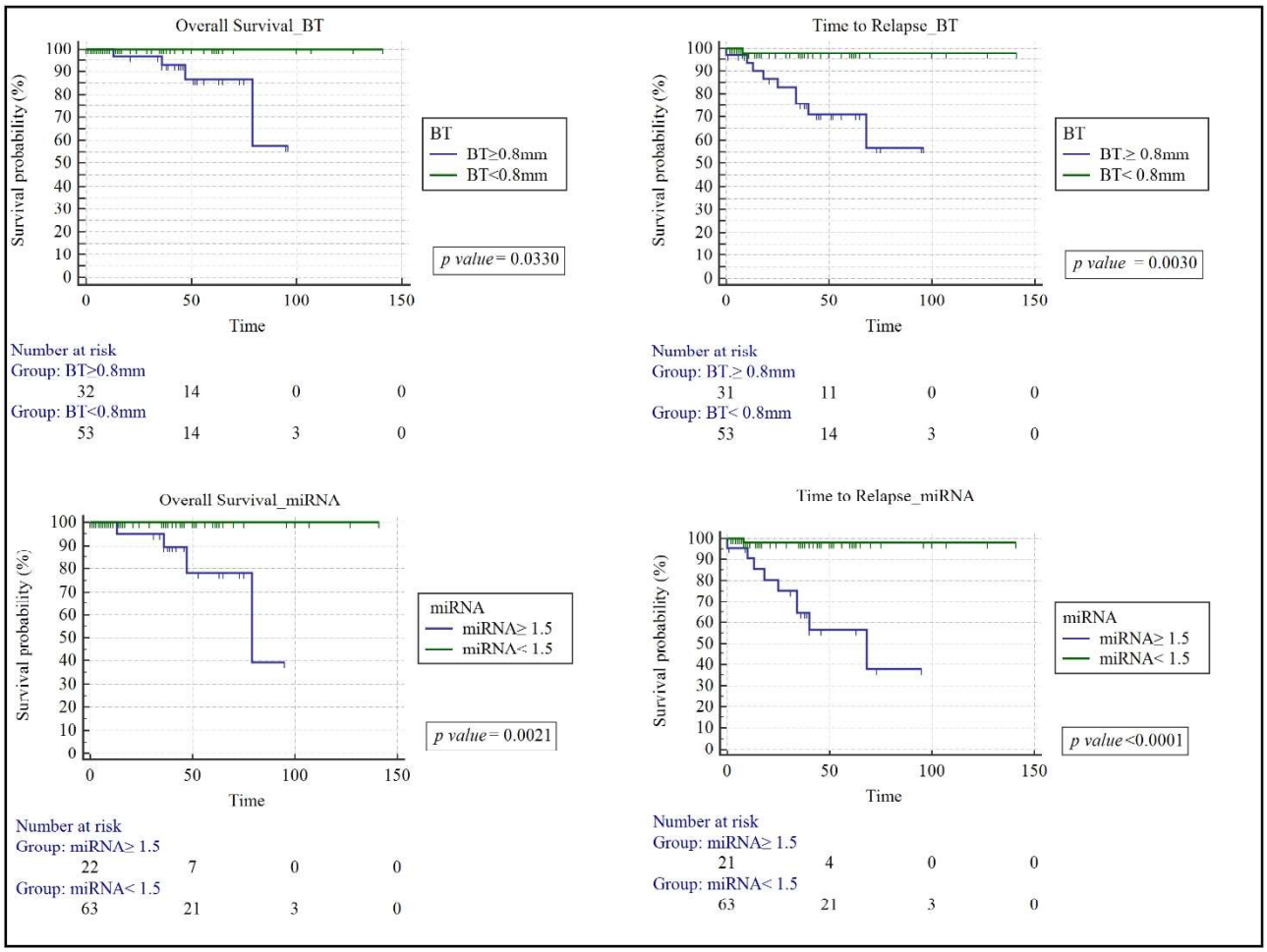

Figure 16. Kaplan-Meier plots for OS and TTR. The plots show significantly different OS and TTR curves in patients with BT≥ 0.8mm versus those with BT < 0.8 mm (upper panels) and patients with miRNA expression ≥1.5 versus those with miRNA < 1.5 (lower panels). BT, Breslow thickness; miRNA, microRNA; OS, overall survival; TTR, time-to-relapse.

We examined the association between miR-21-5p and miR-146a-5p combined expression and SSM prognostic molecular characteristics, namely regression, mitosis, and presence of TILs. The presence of regression did not impact miRNA expression. On the other hand, combined miRNA expression is associated with mitosis and with the presence of TILs. Specifically, the presence of higher mitotic rate (mitotic index > 1/mm^2) and TILs-positive tumors, independently from the type of lymphocyte

infiltration, are related to higher level of combined miRNA expression (*p value* <0.0001 and *p value* =0.049, respectively) (**Figure 17**).

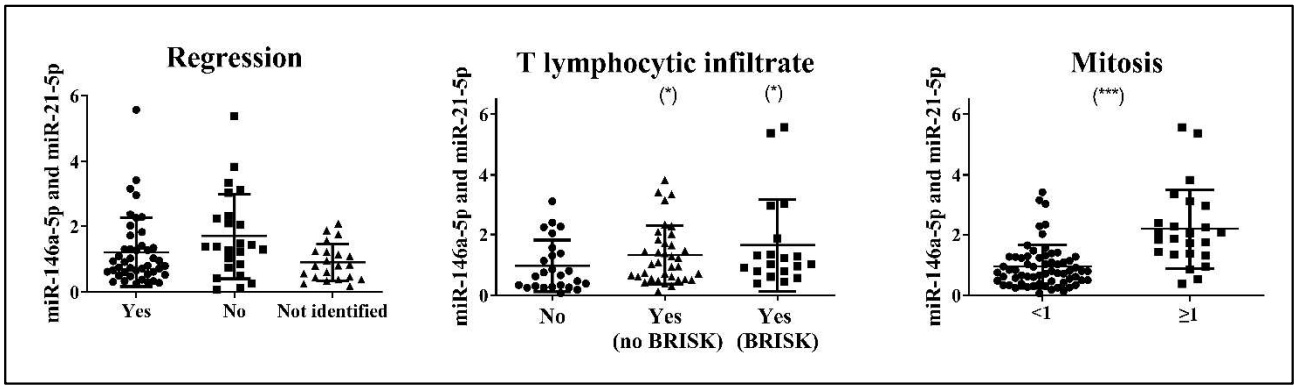

Figure 17. Scatter plot distribution of miRNA expression in melanoma prognostic groups. Association of the combined miR-21-5p and miR-146a-5p expression with melanoma prognostic molecular characteristics: regression, T-lymphocyte infiltrate that are further classified in brisk and not-brisk; and mitosis. **p value* < 0.05 at Mann-Whitney U test; ****p value* < 0.0001 at Mann-Whitney U test. miRNA, microRNA.

6.1.4. miR-146a-5p and miR-21-5p combined expression can complement BT in patient prognostication

We analyzed the use of BT and combined miRNA expression cut-off (0.8mm and 1.5, respectively) as prognostic marker to detect high risk patients, namely relapsing patients. In this analysis, we included 89 out of 90 patients, because one patient had a previous tumor in another site (lymphoma). Among the SSM patients, 79 patients were free from metastasis, while 9 patients have developed metastasis. In addition, there was a patient who presented a positive sentinel lymph node, so he had undergone to a total right axillary lymphadenectomy. This patient was included in the high-risk group, despite he did not relapse.

Relapsing and non-relapsing patients were categorized among group with BT above or below 0.8mm and relapsing and non-relapsing patients were grouped by with miRNAs combined expression ≥1.5 and <1.5. Evaluating these two parameters, we observed that both 0.8mm BT and 1.5 combined miRNA expression cut-offs successfully identified all the 9 relapsing patients. The patient who have undergone to lymphadenectomy but did not develop metastasis, was not identified in the high-risk group. When compared to BT, 1.5 miRNA expression value reduced the number of subjects in the high-risk group that did not have metastasized (24 vs 35). This result suggested that the combined expression of miR-21-5p and miR-146a-5p could effectively add to BT evaluation in patient prognosis (**Table 11**).

Table 11. Association Table of BT and miRNA expression with outcome

	BT		
	≥0.8	**<0.8**	**Total**
Relapse	9	1	10
No relapse	26	53	79
Total	35	54	89
	Two-miRNA combination		
	≥1.5	**<1.5**	**Total**
Relapse	9	1	10
No relapse	15	64	81
Total	24	65	89

Abbreviation: BT, Breslow thickness; miRNA, microRNA. [1]The two-tailed *p value* equals 0.0008 at Fisher's exact test. [2]The two-tailed *p value* is less than 0.0001 at Fisher's exact test.

6.2. Unraveling the role of miRNA network in multiple primary melanoma pathogenesis

During their lifetime about 8% of patients with single melanoma will develop multiple primary melanomas. This risk is higher in the first year after the first diagnosis and remained increased for several years. Patients affected by MPM could have a genetically determined susceptibility, though germline mutations in hereditary melanoma genes are rarely detected. Since data about the role of miRNAs in multiple primary melanoma are limited, we decided to analyze and compare miRNA expression in CM vs MPM, and in 1st vs 2nd melanomas in MPM patients [576].

6.2.1. The miRNA profile of multiple primary melanoma

From small RNA-seq data, we obtained the global miRNA profile of 17 MPM samples belonged to 8 MPM patients. For each patient, we analyzed the 1st and 2nd melanoma, in addition, for one patient, also the 3rd one. Among the MPM patients, three of them had a family history of melanoma.

Comparing the global miRNA profile between familial and nonfamilial MPM, we observed similarities and a great overlapping in miRNA profile (**Figure 18A**). Moreover, a statistical comparison between familial and nonfamilial MPMs did not show any significant difference. Therefore, familial and nonfamilial MPMs were considered as a unique group in all subsequent analyses.

The global miRNA profile of 17 MPMs was also compared to 4 single melanomas and 3 benign nevi. We performed an unsupervised PCA of all 1629 detected miRNAs, which revealed that the MPM miRNA profile is different form single melanomas and benign nevi (**Figure 18A**). Specifically, it seems that MPMs showed a miRNA profile intermediated between single CM and BN. Comparing the miRNA profile in MPM and CM, we obtained a list of 22 miRNAs differentially expressed (adjusted $p\ value < 0.05$), which confirmed the separation between MPM and CM in a cluster analysis (**Figure 18B,C**) (**Table 12**).

First and second melanomas of MPM patients showed some differences in miRNA profile, in fact, evaluating miRNA expression using paired statistical analysis, we obtained 37 miRNAs that are differentially expressed between the 1st and 2nd MPM (paired t-test, $p\ value < 0.05$), whose expression clearly separate the groups in the cluster analysis (**Figure 18B,D**) (**Table 13**).

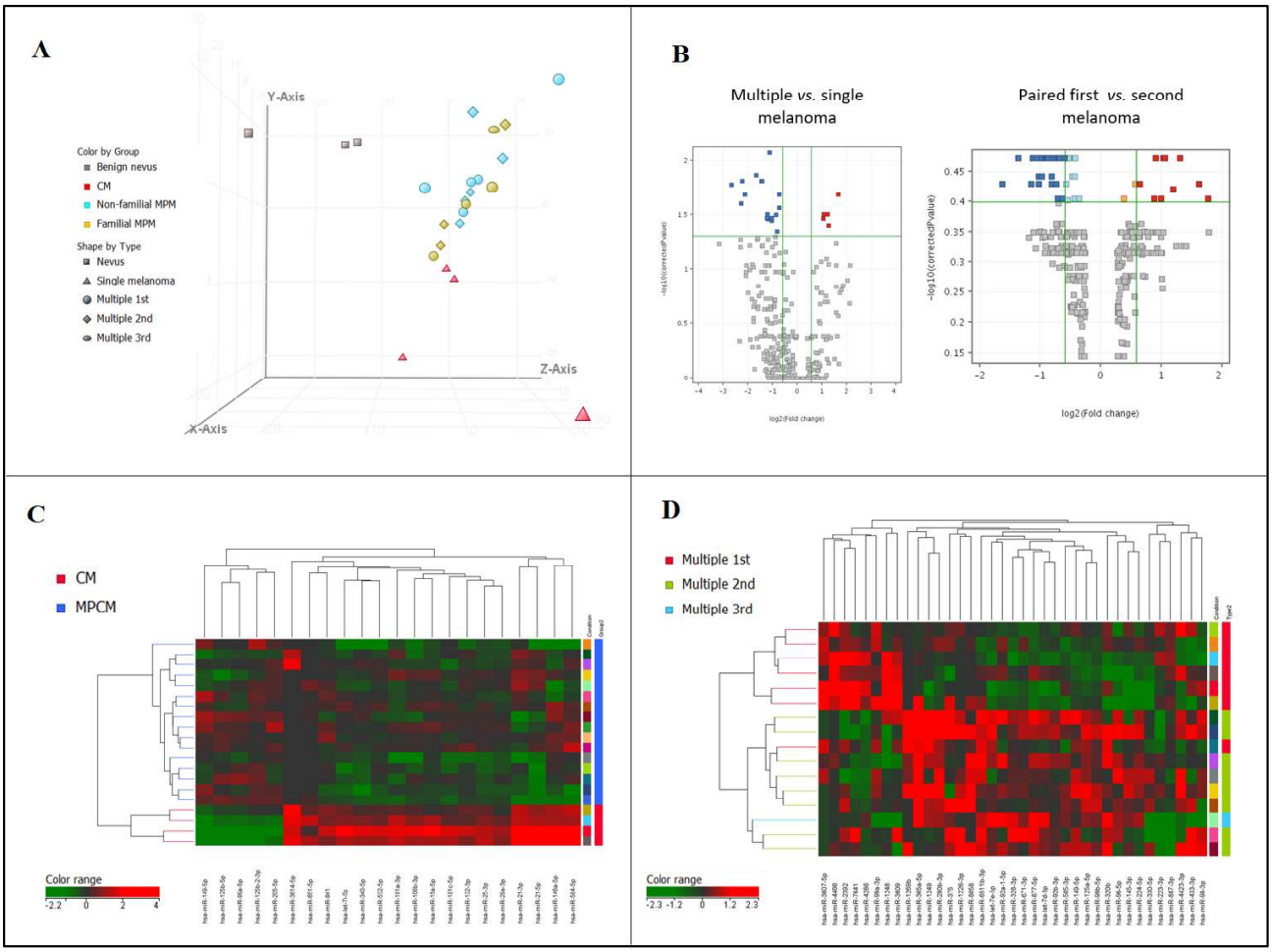

Figure 18. Single and multiple melanoma classification based on the miRNA profile. A) Unsupervised principal component analysis (PCA) of 24 samples based on the expression profile of all the miRNAs detected at NGS analysis. Familial (yellow) and non-familial (cyan) multiple primary melanomas display a similar microRNA profile, which is different from single cutaneous melanoma (red) and benign nevi (gray). B) Volcano plot showing the differentially expressed miRNAs at the selected *p value* and fold-change combinations. C) Cluster analysis and heatmap representation of multiple and single melanoma based on the expression of 22 differentially expressed miRNAs (moderated t-test, adjusted *p value* < 0.05). Red and green color represent the increased or reduced expression across samples. D) Cluster analysis and heatmap representation of the first and second melanomas from the same patient based on the expression of 37 differentially expressed miRNAs (paired t-test, *p value* < 0.05). Red and green color represent the increased or reduced expression across samples.

Table 12. List of microRNAs differentially expressed in multiple vs. primary melanoma

microRNA	adjusted *p-value*	Regulation MPM vs. CM	Fold change
hsa-let-7i-5p	0.0153	down	-2.7
hsa-miR-106b-3p	0.0347	down	-2.3
hsa-miR-132-3p	0.045	down	-1.8
hsa-miR-146a-5p	0.025	down	-4.8
hsa-miR-15a-5p	0.0314	down	-2.3
hsa-miR-181a-3p	0.0153	down	-2.7
hsa-miR-181c-5p	0.036	down	-2
hsa-miR-21-3p	0.0153	down	-4.7

hsa-miR-21-5p	0.0205	down	-4.3
hsa-miR-25-3p	0.0084	down	-2.2
hsa-miR-29a-3p	0.0205	down	-1.7
hsa-miR-340-5p	0.0341	down	-2.4
hsa-miR-3614-5p	0.0135	down	-3.2
hsa-miR-532-5p	0.0341	down	-2.1
hsa-miR-584-5p	0.0167	down	-6.3
hsa-miR-651-5p	0.0275	down	-1.7
hsa-miR-941	0.0318	down	-1.8
hsa-miR-125b-2-3p	0.0314	up	2.1
hsa-miR-125b-5p	0.0398	up	2.4
hsa-miR-149-5p	0.0205	up	3.2
hsa-miR-205-5p	0.0344	up	2.1
hsa-miR-99a-5p	0.0314	up	2.4

Table 13. List of microRNAs differentially expressed in paired multiple melanomas from the same patient

microRNA	p-value (paired)	Regulation 1st vs 2nd MPM	Fold change
hsa-let-7d-3p	0.0174	down	-1.8
hsa-let-7e-5p	0.0153	down	-2
hsa-miR-1226-3p	0.0345	down	-3.1
hsa-miR-1249	0.0338	down	-1.8
hsa-miR-125a-5p	0.0063	down	-1.9
hsa-miR-1269b	0.0254	down	-2
hsa-miR-145-3p	0.0313	down	-1.7
hsa-miR-149-5p	0.0157	down	-1.7
hsa-miR-200b-3p	0.0134	down	-1.8
hsa-miR-224-5p	0.0135	down	-1.8
hsa-miR-320b	0.0243	down	-2
hsa-miR-328-3p	0.0103	down	-1.9
hsa-miR-330-5p	0.006	down	-1.5
hsa-miR-365a-5p	0.0398	down	-1.6
hsa-miR-375	0.0166	down	-1.8
hsa-miR-433-3p	0.0019	down	-2.2
hsa-miR-4423-3p	0.009	down	-2
hsa-miR-505-3p	0.0194	down	-1.8
hsa-miR-6511b-3p	0.0299	down	-2
hsa-miR-671-3p	0.0431	down	-1.6
hsa-miR-8058	0.0334	down	-2.2
hsa-miR-877-5p	0.016	down	-2.1

hsa-miR-92a-1-5p	0.0464	down	-1.6
hsa-miR-92b-3p	0.01	down	-1.6
hsa-miR-96-5p	0.0062	down	-2.6
hsa-miR-98-3p	0.0246	down	-1.8
hsa-miR-99b-5p	0.0054	down	-1.6
hsa-miR-1248	0.0423	up	3.4
hsa-miR-223-3p	0.0458	up	1.8
hsa-miR-2392	0.0362	up	2.3
hsa-miR-3607-5p	0.0308	up	3.1
hsa-miR-3609	0.0028	up	2.5
hsa-miR-4286	0.0071	up	1.9
hsa-miR-4466	0.019	up	2
hsa-miR-7641	0.0129	up	2.1
hsa-miR-887-3p	0.0441	up	2
hsa-miR-99a-3p	0.0342	up	1.6

6.2.2. Validation of miRNA differential expression in single melanomas, multiple primary melanomas, and in benign nevi

We selected nine miRNAs for an independent validation in 47 samples including 3 benign nevi, 9 CM and 35 MPMs by using quantitative RT-PCR. We selected six miRNAs differentially expressed between CM and MPM, including 3 upregulated (miR-21-5p, miR-25-3p, and miR-146a-5p) and 3 downregulated (miR-125b-5p, miR-149-5p, and miR-205-5p) in CM compared to MPM. Among the downregulated miRNAs, there were two, namely miR-205-5p, miR-149-5p, that are differently expressed in the comparison between 1st and 2nd MPM, in particular they are upregulated in 2nd MPM compared to 1st MPM. In addition, we included other two miRNAs that are upregulated in the 2nd MPM compared to 1st MPM (miR-200b-3p, miR-92b-3p). Finally, we decided to analyze the expression of miR-211-5p whose genetic locus is located inside the melastatin-1/*TRPM1* gene and whose expression is particularly high in benign nevi, while, according to our small RNA-seq results, the expression has a borderline statistical significance when compared to CM or MPM. As reference gene, we used miR-16-5p since its expression is invariant among NGS samples.

Figure 19 showed the expression distribution of these 9 miRNAs in BN, CM and MPM samples. MiR-21-5p expression was confirmed to be significant upregulated in CM compared to MPM (*p value* = 0.0005). We observed a statistically significant miR-25-3p downregulation in CM and MPM compared to BN (*p values* =0.0357 and 0.0154 respectively), while miR-146a-5p was downregulated in MPM compared to BN and CM (*p value*= 0.0005 and *p value*< 0.0001, respectively). miR-125b-

5p show a similar expression level in CM and BN, and a trend toward increased expression in MPM. MiR-200b-3p, miR-205-5p, and miR-149-5p are significantly upregulated in MPM compared to CM (*p values* =0.0176, 0.0004 and 0.0003, respectively). miR-92b-3p is significantly downregulated in MPM compared to BN (*p value* < 0.0001). Finally, miR-211-5p is progressively downregulated in multiple and single melanomas (*p values* = 0.0009 and 0.0182, respectively) (**Figure 19**).

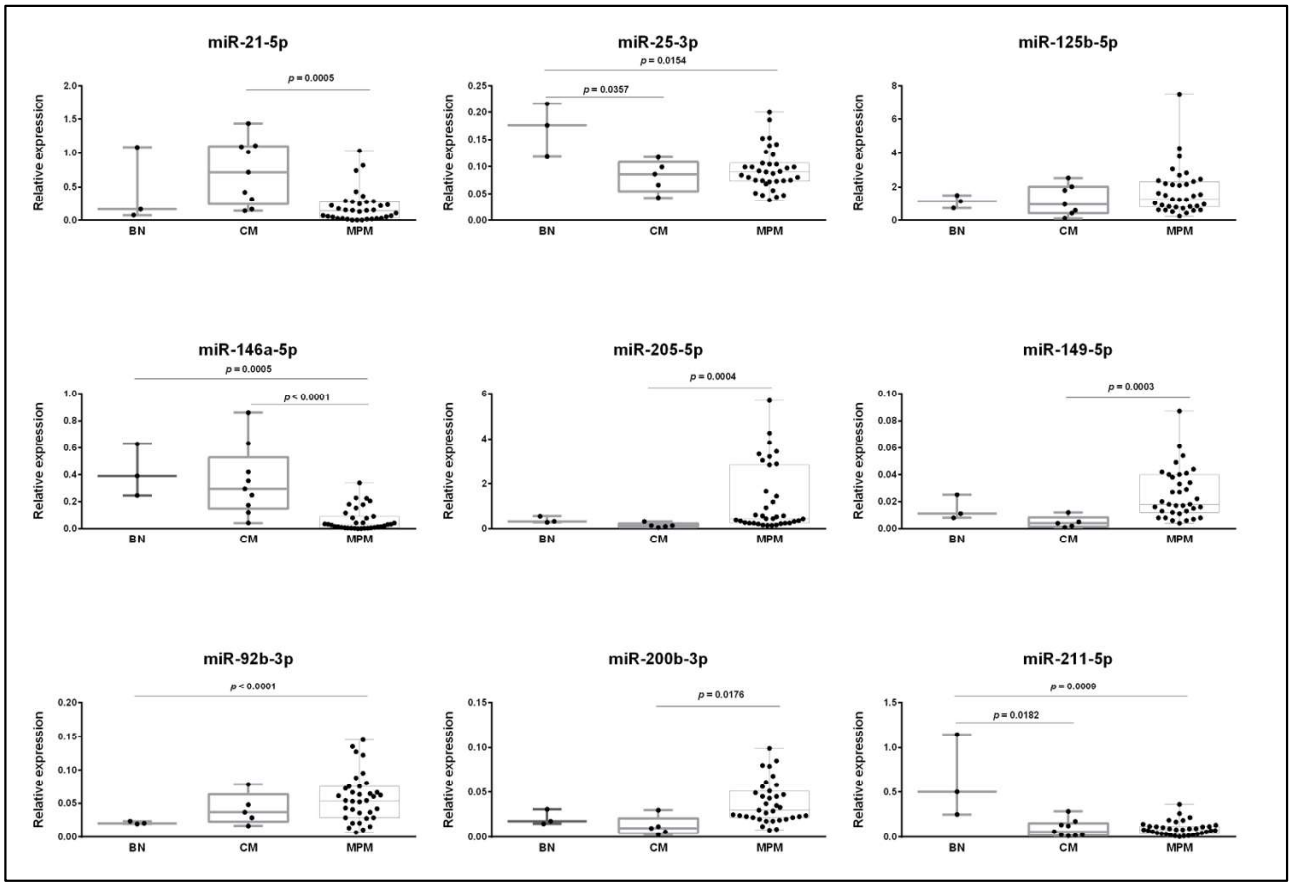

Figure 19. Differential microRNA expression in benign nevi (BN), cutaneous melanoma (CM), and in multiple primary melanoma (MPM). Box and whiskers graph representation of nine microRNAs differentially expressed in single and multiple primary melanomas *(p value* < 0.05). MPM shows higher expression levels of miR-205-5p, miR-200b-3p, and miR-149-5p compared to CM, and higher expression of miR-92b-3p compared to BN. MPM downregulates miR-21-5p compared to CM and miR-146a-5p compared to CM and BN. BN upregulates miR-25-3p and miR-211-5p compared to CM and MPM. Each miRNA was tested in triplicate by quantitative RT-PCR. Relative miRNA expression was normalized on invariant miR-16-5p. The bar shows minimum and maximum values; superimposed points represent all individual values.

The expression distribution of miR-149-5p, miR-92b-3p, miR-200b-3p, and miR-205-5p between paired 1st and 2nd melanomas from the same MPM patient is represented in **Figure 20**. The significant upregulation observed in NGS data for miR-149-5p, miR-92b-3p, miR-205-5p, and miR-200b-3p in 2nd MPM tumor was confirmed in this larger validation group of samples (*p values*= 0.0484, 0.0035, 0.0084 and 0.0029, respectively) (**Figure 20**).

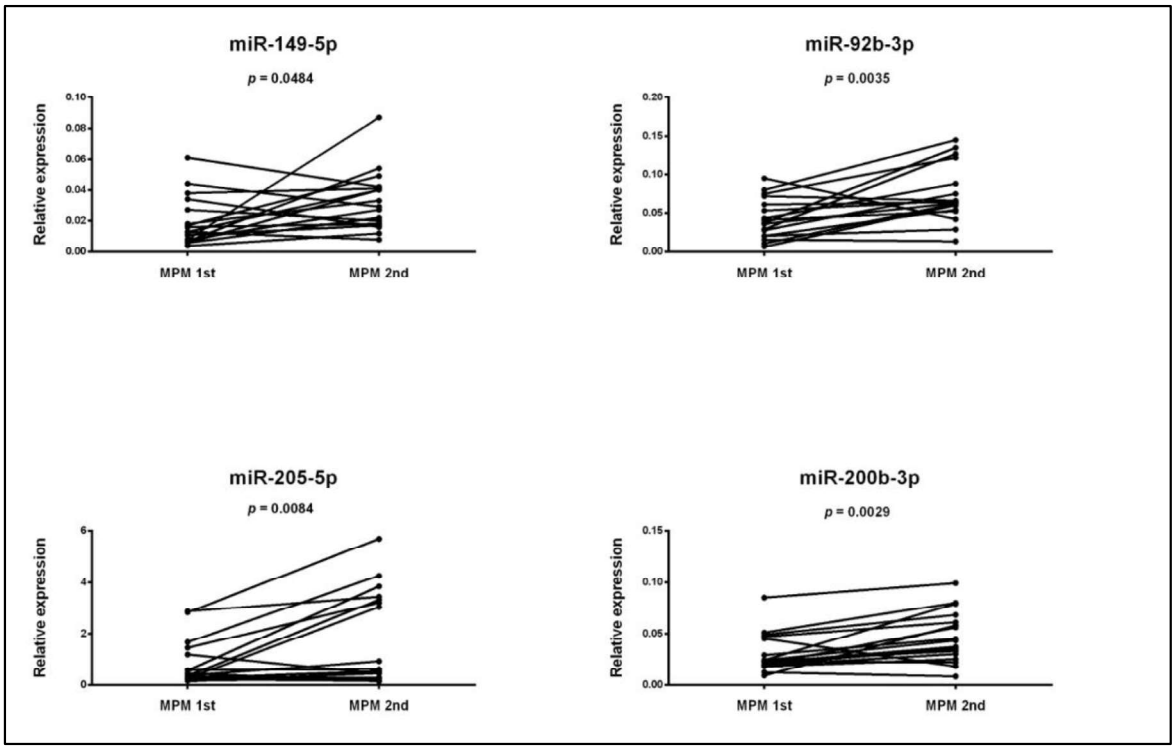

Figure 20. Differential microRNA expression in first vs. second melanoma from the same patient. Before-after plot showing the paired expression of 4 selected microRNAs in 17 multiple primary melanoma (MPM) patients. miR-92b-3p, miR-205-5p, miR-200b-5p, and miR-149-5p are significantly downregulated in the first melanoma compared to the second melanoma. Each miRNA was tested in triplicate by quantitative RT-PCR. Relative miRNA expression was normalized on invariant miR-16-5p. Paired t-test *p value* is reported.

6.2.3. Functional annotation of multiple primary melanoma miRNA signature

The list of 22 miRNAs obtained from the comparison between MPM vs CM from NGS data (**Table 12**) was upload in MetaCore software in order to identify the pathways that are significantly regulated by these miRNAs (**Table 14**) and the most significant miRNAs/targets networks (**Figure 21A**).

Table 14. Pathway enrichment analysis of 22 microRNAs differentially expressed in CM vs. MPM

Enrichment by Pathway Maps

Maps	*p value*	FDR	Total	In Data	Network Objects from Active Data
microRNA in Prostate Cancer	3.1729E-10	8.884E-09	51	6	microRNA 125b, microRNA 15a, microRNA 205, microRNA 106b, microRNA 21, microRNA 146a
Development_MicroRNA-dependent regulation of EMT	1.0715E-05	0.000144	24	3	miR-205-5p, miR-205-3p, microRNA 205
Brca1 in ovarian cancer	1.5429E-05	0.000144	27	3	miR-146a-3p, microRNA 146a, miR-146a-5p

NRSF-dependent transcription deregulation in Huntington's Disease	4.7521E-05	0.0003326	39	3	microRNA 29a, microRNA 132, miR-132-3p
Suppression of p53 signaling in multiple myeloma	0.00010059	0.0004694	50	3	miR-181a-5p, miR-25-3p, miR-106b-5p
TGF-beta signaling via microRNA in breast cancer	0.00010059	0.0004694	50	3	miR-181a-5p, microRNA 21, miR-21-5p
PR action in breast cancer: stimulation of metastasis	0.00060342	0.0024137	20	2	microRNA 29a, miR-29a-3p
Signal transduction_Angiotensin II/ AGTR1 signaling via TGF-beta 1 and SMADs	0.0026682	0.0093387	42	2	microRNA 21, miR-21-5p
Anti-apoptotic action of ErbB2 in breast cancer	0.00391176	0.0121699	51	2	miR-15a-5p, microRNA 15a
MicroRNAs in melanoma	0.00486402	0.0128091	57	2	miR-205-5p, miR-532-5p
Hyaluronic acid/ CD44 signaling in cancer	0.00503213	0.0128091	58	2	microRNA 21, miR-21-5p
Regulation of microRNAs in colorectal cancer	0.00573111	0.0133726	62	2	microRNA 21, miR-21-5p
ErbB2-induced breast cancer cell invasion	0.00666379	0.0143528	67	2	microRNA 21, miR-21-5p
Hypertrophy of asthmatic airway smooth muscle cells	0.0072544	0.0145088	70	2	miR-25-3p, microRNA 25
Stem cells_Hypothetical role of microRNAs in fibrosis development after myocardial infarction	0.04686304	0.0874777	26	1	miR-21-5p
Upregulation of MITF in melanoma	0.06432291	0.1125651	36	1	miR-340-5p
Development_Regulation of lung epithelial progenitor cell differentiation	0.07293794	0.1140681	41	1	miR-106b-5p
Transcription targets of Androgen receptor involved in Prostate Cancer	0.07465184	0.1140681	42	1	microRNA 125b
Signal transduction_Angiotensin II/ AGTR1 signaling via JAK/STAT	0.0797754	0.1140681	45	1	microRNA 21
K-RAS signaling in lung cancer	0.08147723	0.1140681	46	1	microRNA 21
EGFR signaling pathway in lung cancer	0.09330618	0.1244082	53	1	microRNA 21
Role of microRNAs in cell migration, survival and angiogenesis in colorectal cancer	0.11652929	0.1458437	67	1	miR-21-5p
Role of microRNAs in cell proliferation in colorectal cancer	0.11980016	0.1458437	69	1	miR-21-5p

Signal transduction_Angiotensin II/AGTR1 signaling via Notch, Beta-catenin and NF-kB pathways	0.13115743	0.1481678	76	1	microRNA 21
Signal transduction_Angiotensin II/ AGTR1 signaling via RhoA and JNK	0.13437658	0.1481678	78	1	microRNA 21
Main pathways of Schwann cells transformation in neurofibromatosis type 1	0.13758434	0.1481678	80	1	miR-106b-5p
Immune response_IFN-alpha/beta signaling via PI3K and NF-kB pathways	0.15972307	0.1656387	94	1	microRNA 21
Androgen receptor activation and downstream signaling in Prostate cancer	0.18436017	0.1843602	110	1	microRNA 125b

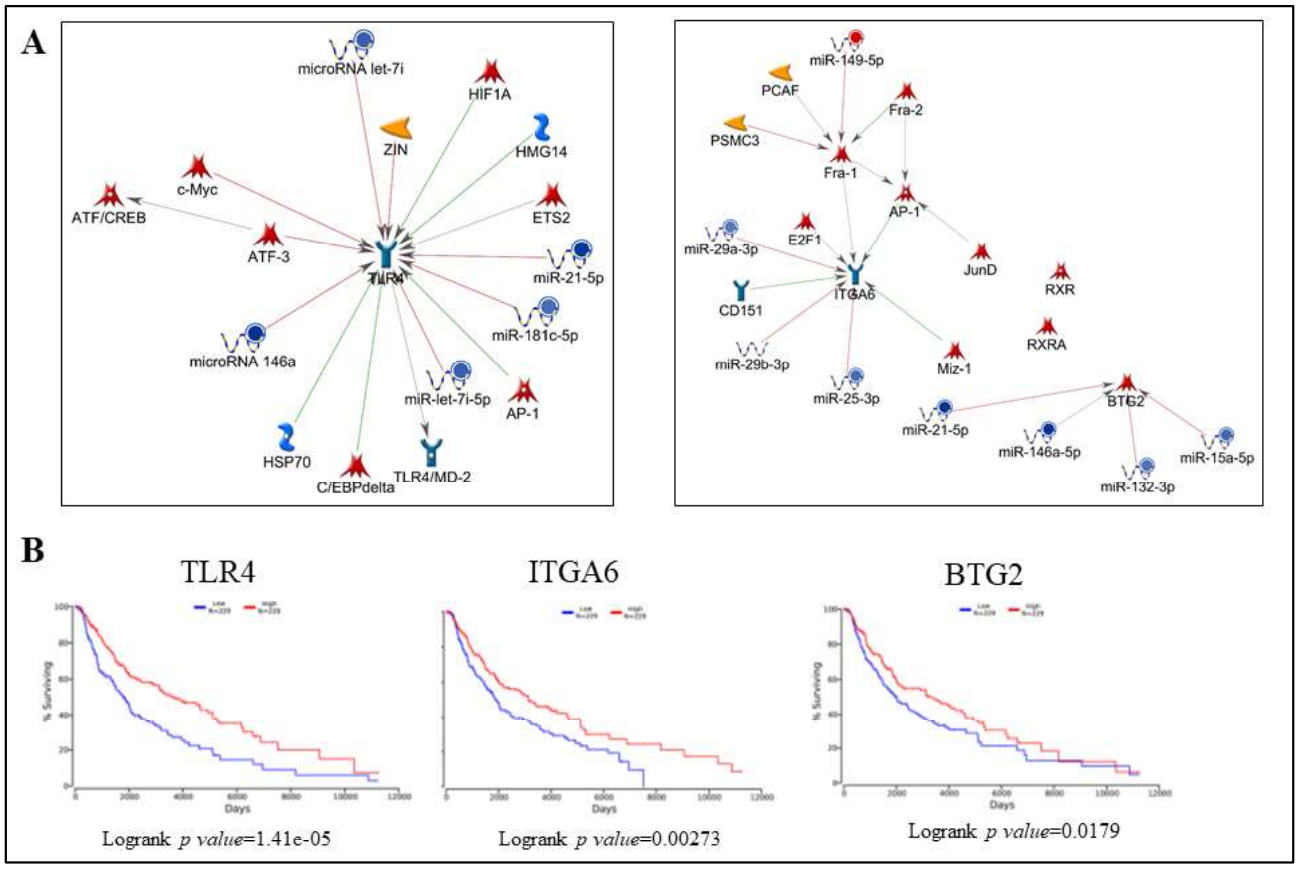

Figure 21. MetaCore miRNA/targets network analysis of 22 miRNAs differently expressed in multiple primary melanoma (MPM) compared to cutaneous melanoma (CM). A) The maps obtained using MetaCore network analysis illustrate the genes involved in MPM specific biology. miRNA downregulated in MPM vs. CM are shown as blue circles, upregulated as red circles. B) Differentially expressed miRNAs result in the dysregulation of three target hubs: TLR4, ITGA6 and BTG2, whose expression is associated with a better prognosis in TCGA SKCM cohort (low expression n=229, low expression n=229, total n=458).

EMT-associated miRNAs, such as miR-149-5p, miR-200 family, and miR-205-5p, were found upregulated in MPM compared to single CM and even nevi (**Figure 20**). Specifically, MPM has

higher expression of miRNA involved in the inhibition of EMT pathway, in fact, they targets EMT-promoted genes: miR-149-5p inhibits Forkhead Box M1 (*FOXM1*) [584], whereas miR-200 family and miR-205-5p target Zinc Finger E-Box Binding Homeobox 1 (*ZEB1*) and Zinc Finger E-Box Binding Homeobox 2 (*ZEB2*) genes [585,586]. Therefore, EMT pathway appears to be specifically activated in single melanomas (**Figure 22**).

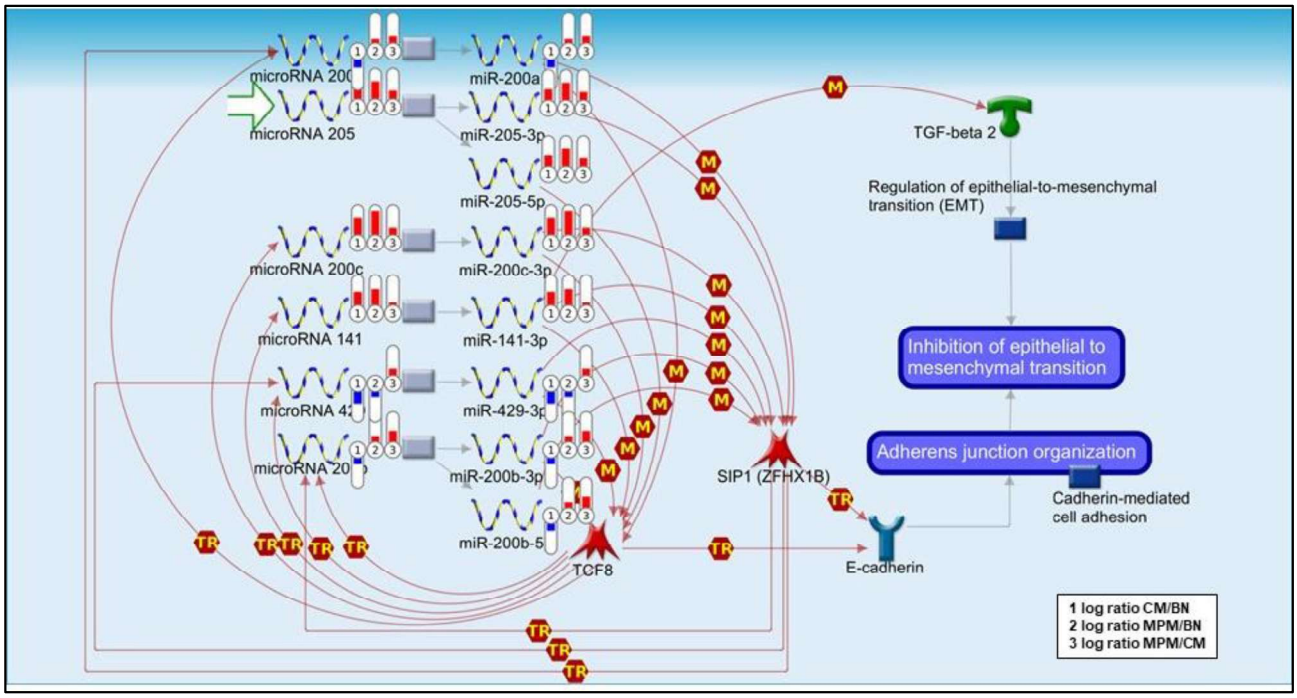

Figure 22. MetaCore pathway analysis showing the involvement of differently expressed miRNAs in epithelial-mesenchymal transition (EMT). EMT pathway representation with regulating miRNAs. Log ratio of miRNA expression level in CM/BN (1), MPM/BN (2), and MPM/CM (3) is visualized on the maps as a thermometer-like figure. Upward thermometers have a red color and indicate upregulated signals, and downward (blue) ones indicate downregulated expression level of specific microRNAs. "M" indicates microRNA binding (regulation of gene expression by binding of microRNA to target mRNA), whereas "TR" indicates Transcription regulation (physical binding of a transcription factor to target gene's promoter). MPM showed higher expression levels of microRNAs involved in the inhibition of epithelial-mesenchymal transition (EMT), including miR-205-5p and miR-200b-3p. (BN, benign nevi; CM, cutaneous melanoma; MPM multiple primary melanoma).

The MetaCore network analysis identified three hub genes (Toll-like receptor 4 (*TLR4*), Integrin alpha-6 (*ITGA6*), and BTG Anti-Proliferation Factor 2 (*BTG2*)) targeted by multiple miRNAs, either up- or downregulated in multiple melanomas. When we evaluated the association of TLR4, ITGA6, and BTG2 gene expression with melanoma prognosis, we found that their higher expression (median cut-off) was significantly associated with a worse overall survival in TCGA SKCM cohort of 458 samples (**Figure 21B**).

6.3. Exploring the role of a miRNA variant of miR-125a-5p

6.3.1. IsomiR analysis revealed that a miR-125a-5p isoform is dysregulated in multiple primary melanoma

NGS data showed that miR-125a-5p was upregulated in the 2nd melanoma compared to 1st melanoma in MPM patients. However, miR-125a-5p differential expression in MPM was not confirmed during validation by qPCR technology and we wondered about a possible explanation. We observed that the reads generated by the NGS experiment and attributed to mature miR-125a-5p following the standard matching pipelines were actually shorter by 1 (lack of A at the 3' end), or most frequently 2 nucleotides (lack of GA at the 3-end) in all samples (**Figure 23**).

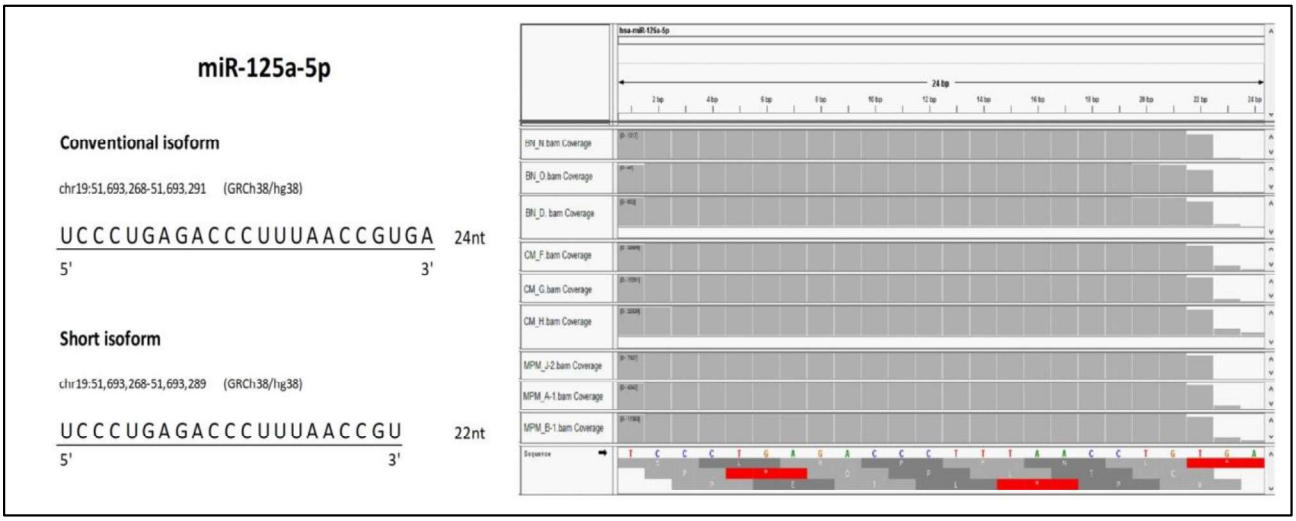

Figure 23. The -2nt shorter isoform of miR-125a-5p is more represented than the conventional form in our NGS data from benign nevi (BN), cutaneous melanoma (CM) and multiple primary melanoma (MPM). Sequence and chromosomal position of conventional and -2nt shorter isoform of miR-125a-5p. IGV representation of miR-125a-5p sequencing reads in exemplary BN, CM MPM samples shows that the reads for the conventional miR-125a-5p (24nt) are few or absent in comparison to the shorter isoforms (22-23nt).

We used the term "canonical" to refer to the sequence of a miRNA reported on miRBase, while all the miRNA variants were called isomiRs. We analyzed and classified all canonical miRNAs and isomiRs in our NGS data by using isoMiRmap tool. For the nomenclature of isomiRs, we used the one proposed by Loher et al. [529]. We calculated the average expression in all sequenced samples and the ratio between each miR-125a-5p isomiR and the canonical form. miR-125a-5p|0|–2, namely the isomiR of miR-125a-5p that lacks two nucleotides at the 3' end, is the most expressed isomiR of miR-125a-5p with a ratio isomiR/canonical miRNA of 13.56.

Looking at NGS data, quite peculiarly, canonical miR-125a-5p and miR-125a-5p|0|−2 isoform showed opposite expression trends in nevi, single primary melanomas, and MPMs (**Figure 24**).

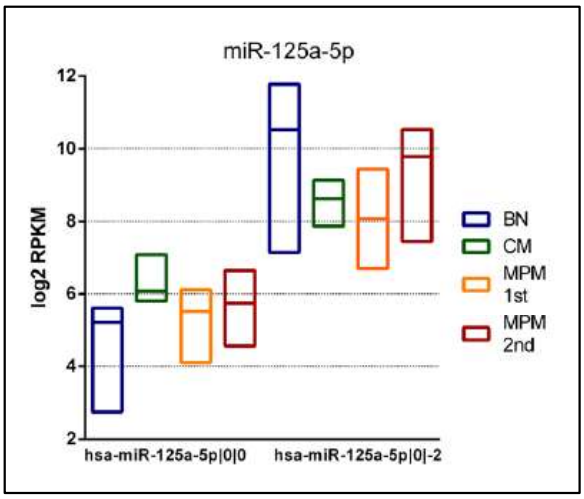

Figure 24 Comparison of miR-125a-5p isomiR expression in benign nevi (BN), cutaneous melanoma (CM), and multiple primary melanoma (MPM). Floating bar chart of miR-125a-5p isomiR expression. Canonical miR-125a-5p (hsa-miR-125a-5p|0|0) shows a lower expression level and opposite expression trend in BN, CM, and MPM if compared to its shorter isomiR (hsa-miR-125a-5p|0|−2). Bars represent min-max and median values.

We tested two different technical approaches in all samples for isomiR quantification based on commercial RT-qPCR kits, namely miRCURY LNA and miSCRIPT. Specifically, miRCURY LNA assay design was used to quantify the canonical form (including the 5' isoforms, which are not abundant/detected in our NGS data), while miSCRIPT assay was used to detect all the isoforms, as a consequence of the use of an universal reverse primer during miRNA amplification (**Figure 25**).

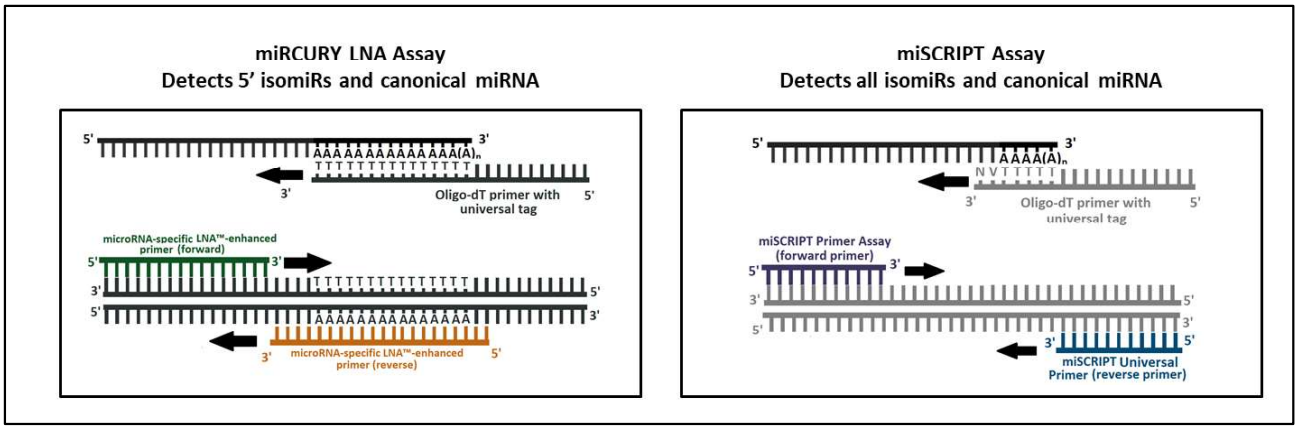

Figure 25. miRCURY LNA and miSCRIPT assay. Differences between miRCURY LNA and miSCRIPT assay designs (Qiagen) allowed the quantification of the miR-125a-5p canonical form (24nt) and 5' isoforms or the quantification of all miR-125a-5p isoforms, respectively. The presence of a miRNA-specific reverse primer in miRCURY LNA assay allows to amplify and quantify only the canonical form of the miRNA, while the presence of a universal reverse primer in miSCRIPT Assay allows to amplify and quantify all miRNA isoforms, with different sequences at the 3' end.

Since miRCURY did not quantify the predominant isomiR of miR-125a-5p, NGS data could not be validated, in fact, results revealed a lack of variation between single and multiple melanomas, and a higher expression in the 1st vs 2nd melanoma.

Since the predominance of miR-125a-5p|0|–2 compared to the canonical miRNA and the other isomiRs, we assumed that the miSCRIPT assay could provide a bona fide quantification of this specific isomiR. As expected, higher expression level of miR-125a-5p in MPMs vs. CMs and in the 2nd vs 1st tumor from the same patient was observed (**Figure 26**).

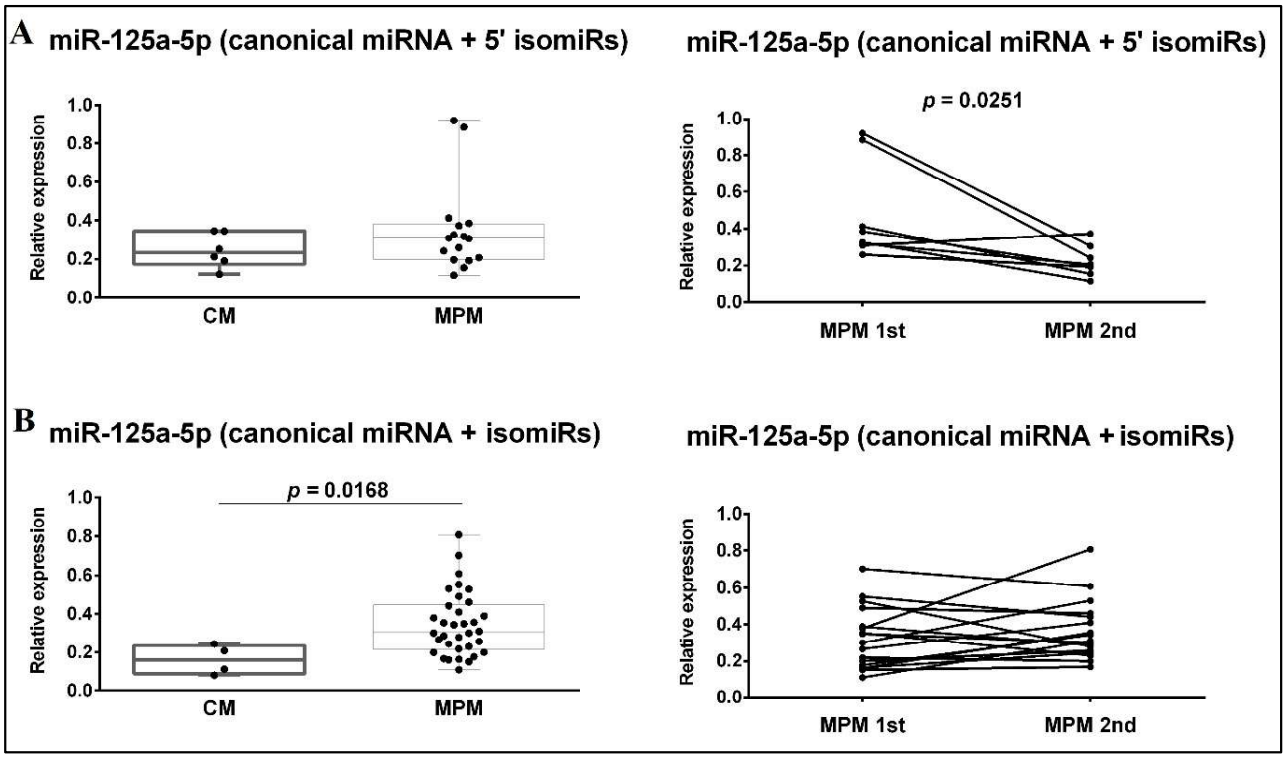

Figure 26 Comparison of miR-125a-5p isomiR expression in cutaneous melanoma (CM), and multiple primary melanoma (MPM) with two different assays. Box and whiskers graph representation of canonical miR-125a-5p expression assessed with miRCURY LNA assay and overall expression of all miR-125a-5p isoforms, detected using miSCRIPT assay. Results show that the combined expression of miR-125a-5p isoforms of levels is higher in MPM compared to CM. The bar shows minimum and maximum values; superimposed points represent all individual values. Before-after plot of canonical miR-125a-5p expression (miRCURY LNA assay) and all miR-125a-5p isoforms (miSCRIPT assay) show an opposite trend in the first and second melanoma from the same patient.

6.3.2. miR-125a-5p|0|−2 isomiR is highly expressed in many different tumors

As a further confirmation of our findings, we analyzed the expression of hsa-miR-125a-5p|0|−2 (isomiR, 22nt long) and 0|0 (canonical miRNA, 24nt long) isoforms across all TCGA tumor types. We discovered an overall higher expression of the isomiR in human cancers and a specifically altered isomiR/canonical miR-125a-5p ratio in SKCM (CM cohort), which shows the largest variation (**Figure 27**).

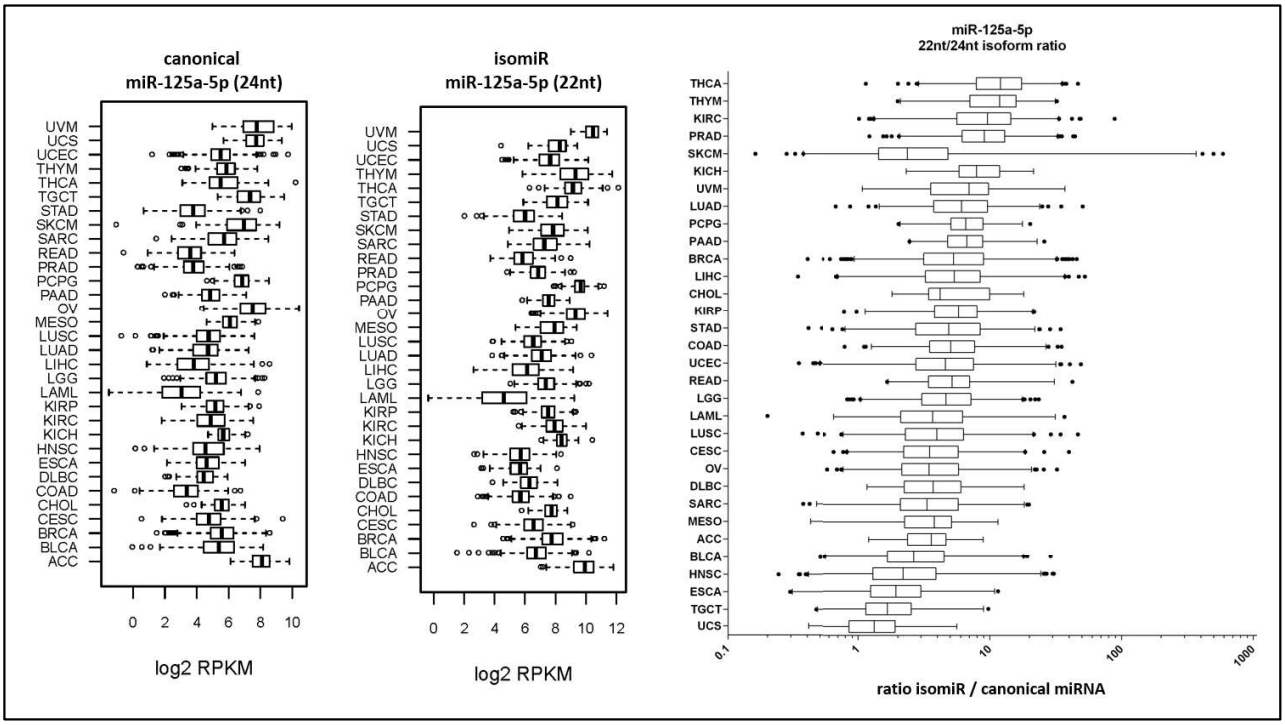

Figure 27. Canonical hsa-miR-125a-5p|0|0) and hsa-miR-125a-5p|0|−2 isomiR expression across 32 TCGA tumor types. miR-125a isomiR is most expressed in many cancer types. Box and whiskers graphs of canonical and shorter isoform of miR-125a-5p show variable expression levels, represented here as log2 RPKM data, across 32 different cancer type. miR-125a-5p isoform is most abundant in many cancer types and shows a specifically high canonical/isoform ratio in the melanoma (SKCM) group. The bar shows 1-99 percentile values. TCGA abbreviations: ACC, adrenocortical carcinoma; BLCA, bladder urothelial carcinoma; BRCA, breast invasive carcinoma; CESC, cervical squamous cell carcinoma and endocervical adenocarcinoma; CHOL, cholangiocarcinoma; COAD, colon adenocarcinoma; DLBC, lymphoid neoplasm diffuse large B-cell lymphoma; ESCA, esophageal carcinoma; HNSC, head and neck squamous cell carcinoma; KICH, kidney chromophobe; KIRC, kidney renal clear cell carcinoma; KIRP, kidney renal papillary cell carcinoma; LAML, acute myeloid leukemia; LGG, brain lower grade glioma; LIHC, liver hepatocellular carcinoma; LUAD, lung adenocarcinoma; LUSC, lung squamous cell carcinoma; MESO, mesothelioma; OV, ovarian serous cystadenocarcinoma; PAAD, pancreatic adenocarcinoma; PCPG, pheochromocytoma and paraganglioma; PRAD, prostate adenocarcinoma; READ, rectum adenocarcinoma; SARC, sarcoma; SKCM, skin cutaneous melanoma; STAD, stomach adenocarcinoma; TGCT, testicular germ cell tumors; THCA, thyroid carcinoma; THYM, thymoma; UCEC, uterine corpus endometrial carcinoma; UCS, uterine carcinosarcoma; UVM, uveal melanoma.

6.3.3. Optimized Dumbbell- based ddPCR based assay allowed to quantify isomiR in melanoma cell lines and FFPE samples

To date, there are no commercial kits able to quantify a specific variant of a miRNA. Recently, Honda et al. described the Dumbbell-PCR (Db-PCR), which is a TaqMan RT-PCR-based method able to distinctively quantify a specific small RNA variant with single-nucleotide resolution at terminal sequences. The main advantage of this methods is to perform a quantitative analysis of RNA terminal heterogeneity without performing NGS [563].

We used and optimized the Db-PCR for the quantification of canonical miR-125a-5p and miR-125a-5p|0|–2 isomiR by using synthetic oligonucleotides to verify the specificity of the assay. In order to have a more sensitive method able to also quantify few copies of isomiRs, we decided to replace the last step (qPCR quantification) with a droplet digital PCR (ddPCR) quantification. In addition, we introduced some variations in order to be able to use a lower RNA amount, since the amount of RNA supplied by patient samples is often limited. To simplify the annotation, we named our optimized method: Dumbbell based droplet digital PCR assay (Db-ddPCR) **(Figure 28)**.

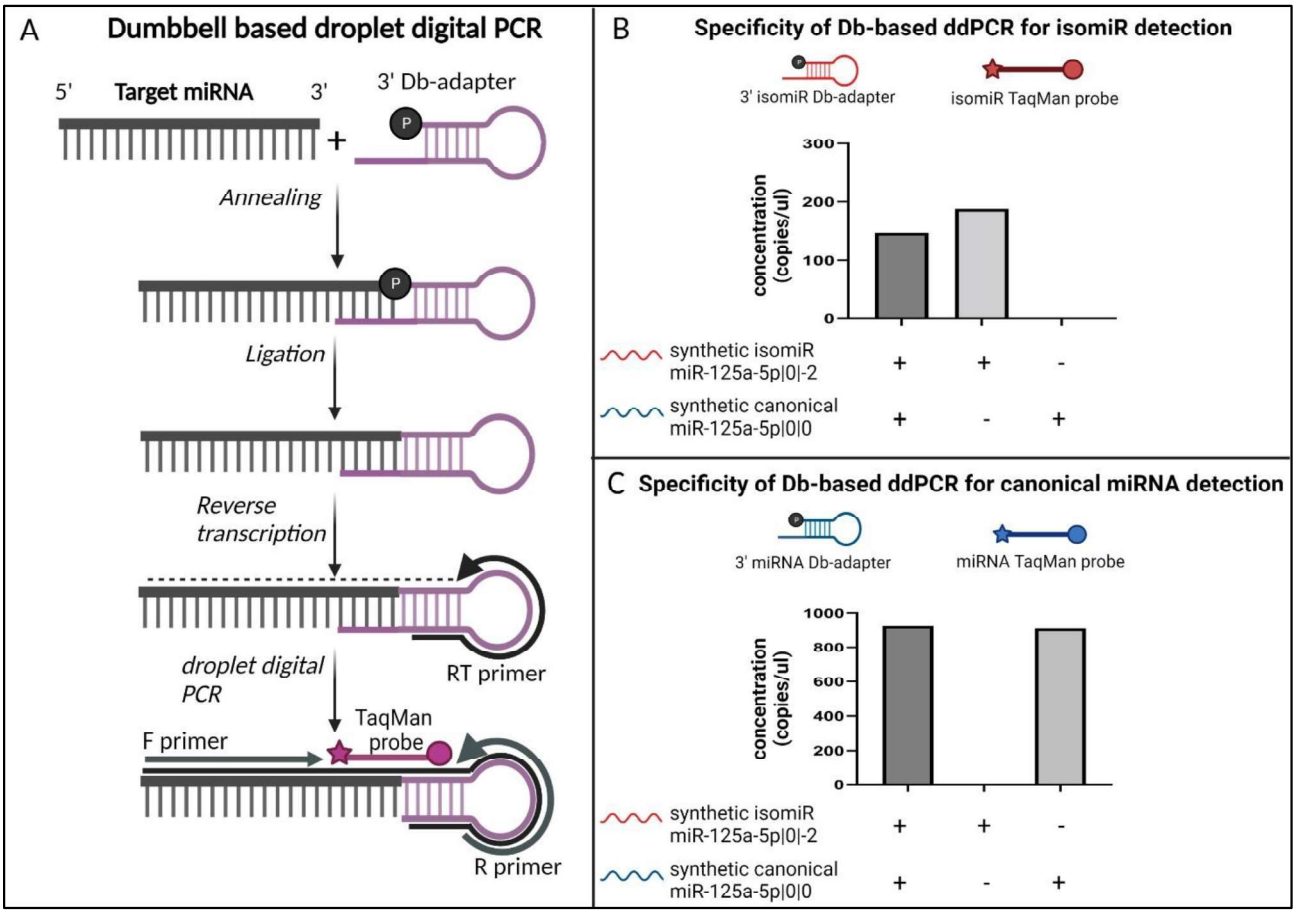

Figure 28.Dumbbell based droplet digital PCR (Db-based ddPCR). A Schematic representation of Db-based ddPCR, which consists in 4 steps: annealing of a specific 3'Db-adapter, the ligation, the reverse transcription and the quantification by ddPCR. B IsomiR specific assay uses specific 3'adapter and TaqMan probe. Box plot shows that the assay is specific for the detection of the isomiR, and the presence of the miRNA

did not affect the isomiR quantification. CB Canonical miRNA specific assay uses specific 3'adapter and TaqMan probe. Box plot shows that the assay is specific for the detection of the canonical miRNA, and the presence of the isomiR did not affect the canonical miRNA quantification. Figure created with Biorender.com.

Successively, we test the optimized Db-PCR in biological samples, namely in a melanoma cell line, SKMEL-28 cells. Finally, we used the Db-ddPCR assay to quantify canonical and isomiR expression level in 11 FFPE melanoma samples. We compared the expression of miRNA and isomiR with a paired t test. Results showed that the expression of the miR-125a-5p|0|–2 isomiR is statistically higher compared to the canonical form (*p value* = 0.0469) with a mean ratio of 1.27 (**Figure 29**).

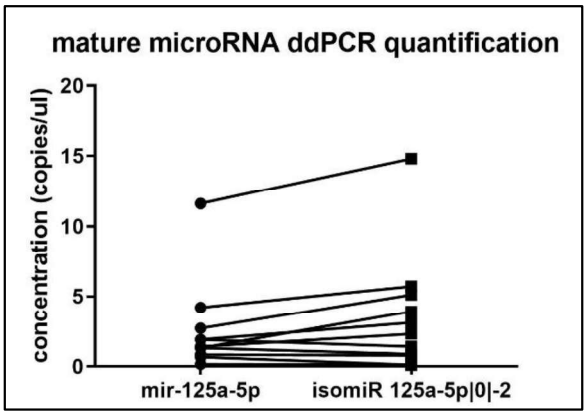

Figure 29. Differential expression of canonical miR-125a-5p and isomiR miR-125a-5p|0|–2 in SSM melanomas. Before-after plot showing the differential expression of canonical and isomiR of miR-125a-5p in 11 superficial spreading melanomas (SSM). isomiR is significant upregulated compared to the canonical miRNA (*p value* =0.0469). miRNA and isomiR expression was quantified with Db-ddPCR.

6.3.4. Functional analysis of a specific isomiR of miR-125a-5p in melanoma

6.3.4.1. miR-125a-5p miRNA and isomiR regulated different target genes

In order to investigate the role of miR-125a-5p|0|–2, we ran a bioinformatics analysis to predict the impact of the lack of 2nts in target gene binding. We used RNA22 algorithm to obtain the list of putative pairing sites for miR-125a-5p canonical form (N = 1342) and its miR-125a-5p|0|−2 isomiR (N = 971) (Supplementary Table 4 from Dika et al. [576]). miR-125a-5p|0|−2 loses the ability to bind a fraction of canonical miR-125a-5p|0|0 targets (Supplementary Table 5 from Dika et al. [576]). The list of predicted target genes was submitted for enrichment analysis to MetaCore software. We identified the significantly enrichment pathways and networks for common and specific targets of canonical and isomiR (Supplementary Table 6 from Dika et al. [576]). We observed that miR-125a-5p|0|−2 lost target genes involved in nervous system development, neurogenesis, and neuronal differentiation. In addition, the isomiR form no longer targets key genes involved in cell adhesion and migration (Ephrin receptors, Netrin 1) or intracellular signaling (Phosphatidylinositol-4-Phosphate 3-Kinase Catalytic Subunit Type 2 Beta (PIK3C2B)).

Unexpectedly, we observed that isoform showed new 5 targets, which were not in common with canonical miR-125a: T Cell Leukemia Homeobox 1 (TLX1, also known as HOX11), Glycine-N-Acyltransferase Like 1 (GLYATL1), SWI/SNF Related, Matrix Associated, Actin Dependent Regulator of Chromatin, Subfamily E, Member 1 (SMARCE1. also known as BAF57), Trimethyllysine Hydroxylase, Epsilon (TMLHE) and Claudin 2 (CLDN2). Interestingly, three of the specific targets of the miR-125a-5p isoform are involved also in nervous system processes (TLX11, SMARCE1 and TMLHE). The other two specific targets of the isoform of miR-125a-5p are not components of nervous system development, but there are linked to cancer.

We analyzed the mRNA expression of these five genes in melanoma and the correlation with the survival on Human Protein Atlas. Melanoma patients (n=102) were divided based on level of expression into one of the two groups "low" (under cut off) or "high" (over cut off): for SMARCE1 there were 43 patients with low expression and 59 with high expression (cut-off=4.93), for TLX1 there were 43 patients with low expression and 59 with high expression (cut-off=0.0041), for CDL2 there were 71 patients with low expression and 31 with high expression (cut-off=0.03), for GLYATL1 there were 47 patients with low expression and 55 with high expression (cut-off=0.0044), and for TLMHE there were 52 patients with low expression and 50 with high expression (cut-off=2.07). Fragments Per Kilobase of transcript per Million mapped reads (FRKM) average expression were reported for all targets: 5.5 for SMARCE1, 0.1 for TLX1, <0.1 for CDL2 and GLYATL1 and 2.1 for TMLHE. We observed that patients with lower expression of SMARCE1, TLX1 and GLYATL1 have a better survival, while a low expression of TMLHE and CLDN2 is associated with a worst survival. Specifically, only SMARCE1 and TLX1 show a significant difference between high and low expression, with *p value* =0.022 and *p value*=0.021, respectively (**Figure 30**).

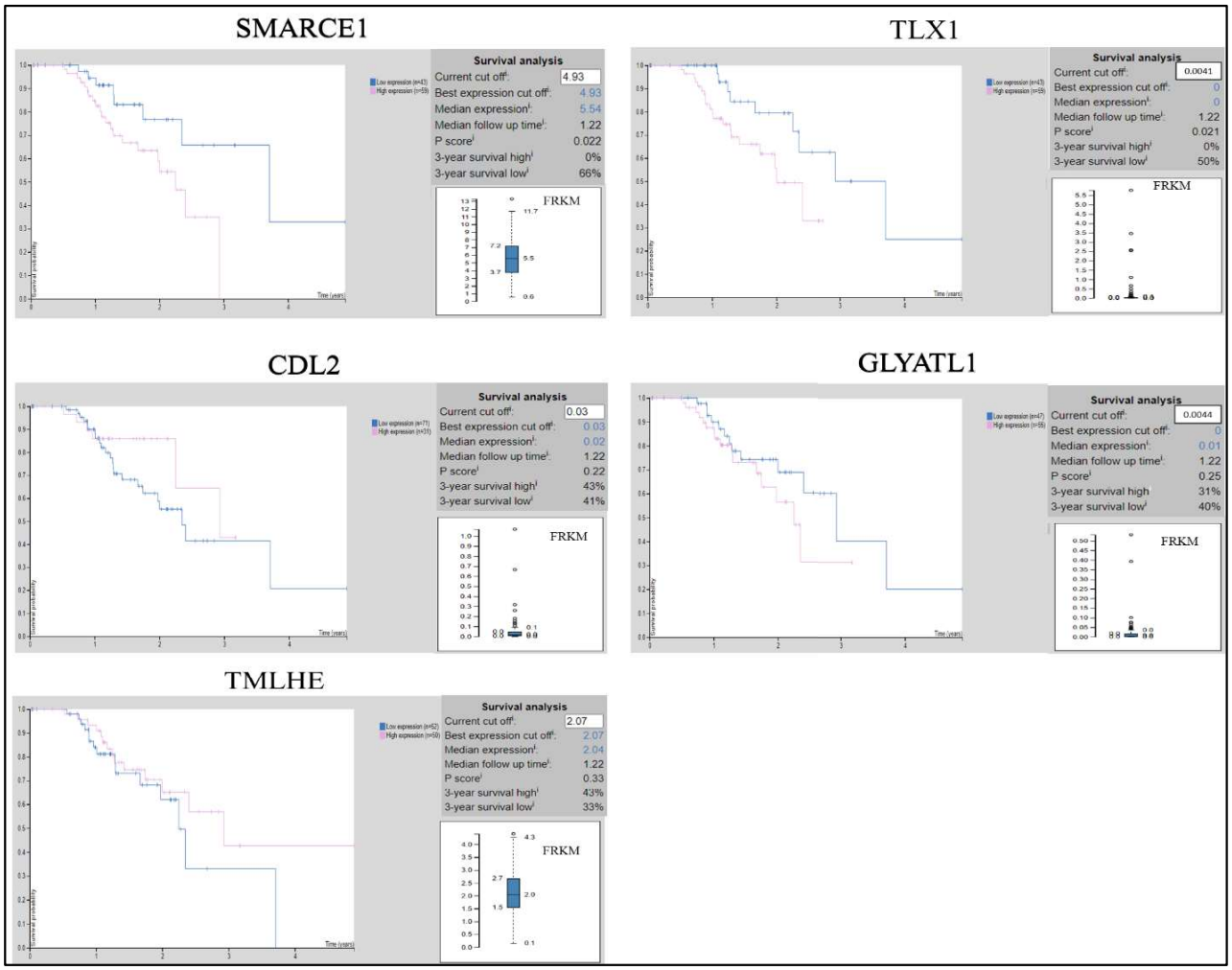

Figure 30. Association of isomiR predicted target mRNA expression in melanoma and overall survival. Kaplan-Meier plots summarize results from analysis of correlation between mRNA expression level (SMARCE1, TLX1, CDL2, GLYATL1 and TMLHE) and patient survival. Melanoma patients (n=102) were divided based on level of expression into one of the two groups "low" (under cut off) or "high" (over cut off). X-axis shows time for survival (years) and y-axis shows the probability of survival, where 1.0 corresponds to 100 percent. FRKM average was reported for all targets. FRKM= Fragments Per Kilobase of transcript per Million mapped reads.

6.3.4.2. SMARCE1 is specifically targeted by the isomiR form of miR-125a-5p

Since the protein level of TLX1 was very low in melanoma, we decided to study and focus on SMARCE1. We analyzed the expression of SMARCE1 in a melanoma cell line, namely SKMEL28. We examined the target in terms of mRNA and protein after 24h, 48h, 72h, and 96h of isomiR and canonical miRNA transfection. SMARCE mRNA did not change between the different conditions. On the other hand, we observed a reduction of the protein level after 48h of the isomiR transfection. These results suggested that SMARCE1 could be a specific target of the isomiR vs the canonical miRNA (**Figure 31**).

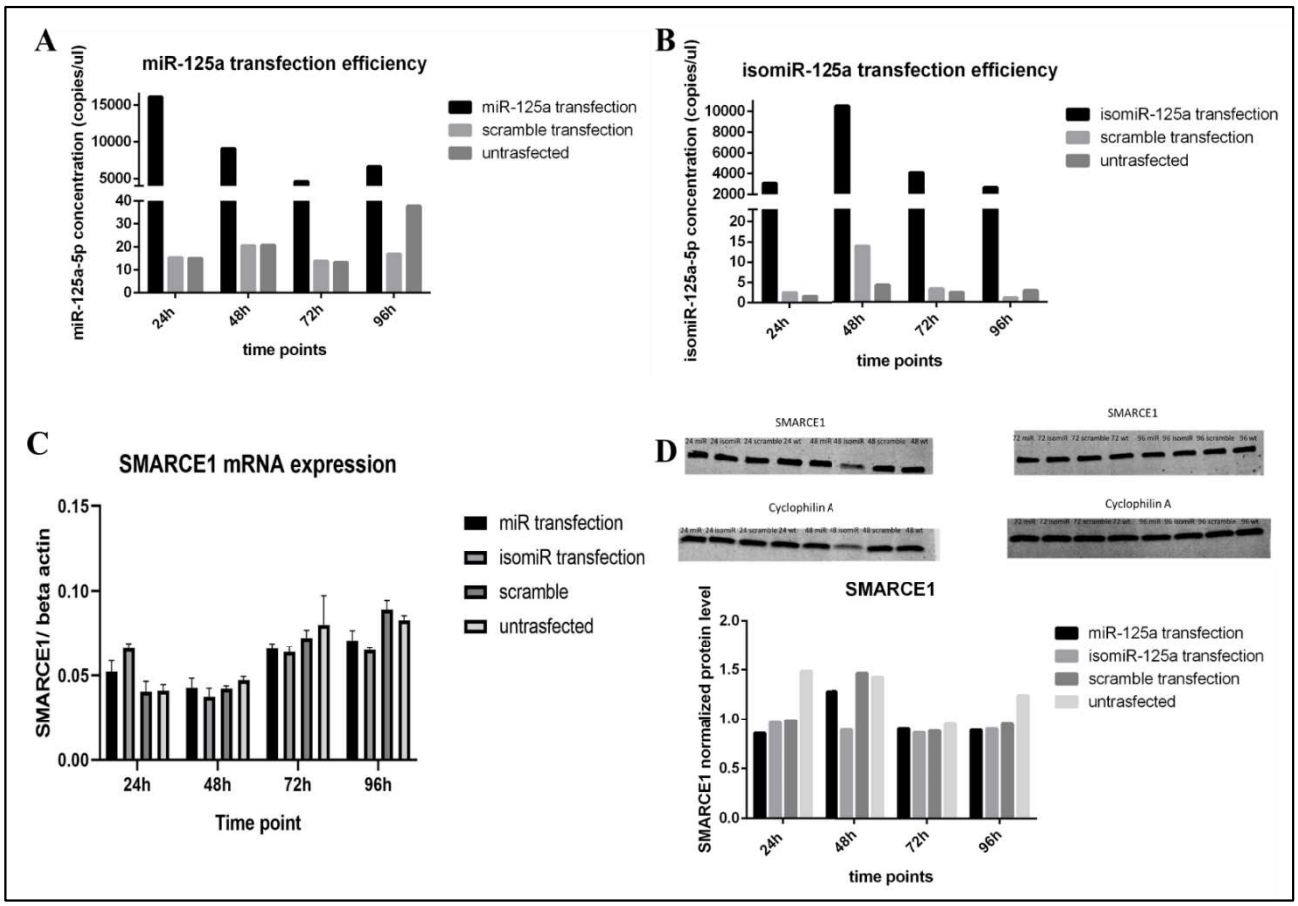

Figure 31. Validation of SMARCE1 as specific target of isomiR miR-125a-5p|0|–2. A) Bar graph reported canonical miR-125a-5p transfection efficiency in SK-Mel-28 cell at four time points: 24h, 48h, 72h and 96h. B) Bar graph reported isomiR miR-125a-5p|0|–2 transfection efficiency in SK-Mel-28 cell at four time points: 24h, 48h, 72h and 96h. C) Bar graph showed mRNA expression level of SMARCE1 (normalized with beta actin expression) in SK-Mel-28 cell at four time points after transfection: 24h, 48h, 72h and 96h. D) Figure show western blot membrane and normalized SMARCE1 protein level (SMARCE1/Cyclophilin A) in SK-Mel-28 cell at four time points after transfection: 24h, 48h, 72h and 96h. A reduction of SMARCE1 level are observed in SK-Mel-28 cell in 48h after isomiR transfection.

6.4. MiRNA isoforms contribution to melanoma pathogenesis

The identification and the study of miR-125a-5p|0|–2 isoform suggested that the analysis of canonical miRNAs and their isomiRs could give new and more complete information about melanoma, instead to focus only on canonical miRNA. We decided to investigate all isomiRs in melanoma in order to find the isomiR contribution to melanoma pathogenesis. For this purpose, we analyzed our NGS data with the isoMiRmap pipeline to find differential expressed isomiRs in melanoma compared to benign nevi. In addition, to identify isomiRs potentially associated with tumor progression, we used SKCM cohort of TCGA database, which collects clinical and molecular data from fresh-frozen tissues, including small RNA-seq data, to compare isomiR profile in primary melanoma and melanoma metastasis [530].

In what follows, the sum of canonical miRNAs, namely the sequence of the miRNA reported in miRBase, and their isomiRs, namely all the miRNA variants-isoforms, has been grouped and called "mature miRNAs".

6.4.1. Mature miRNA profile and miRNA variants characterization in early-stage melanoma samples

We investigated the global mature miRNA (canonical and isomiR) profile of 23 FFPE samples, namely 3 BN and 20 early-stage CM, by using isoMiRmap. We identified 494 mature miRNAs, including 130 canonical miRNAs and 364 miRNA isoforms that passed quality trimming and filtering. Precisely, we found 90 canonical miRNAs with at least one isomiR, for a total of 324 isomiRs with a detectable canonical form. On the other hand, 40 expressed canonical miRNAs did not have any isomiR in our data. In addition, some canonical miRNA sequences were not detected in our dataset for about 11% of the identified. In this case, the corresponding isomiRs are called "orphan" isomiRs.

IsomiRs were classified into five categories according to their variation from the canonical sequence: start-site isomiR, end-site isomiR, 3' non-templated addition isomiR, shifted isomiR and the remaining "mixed" isomiR. The first and second groups exhibit nts addition or deletion respectively at the 5' and at the 3' end of the canonical sequence. In these two groups, added nucleotides "match" with stem loop sequence. On the contrary, when the added nucleotides in 5' or 3' end differ from those in the stem loop sequence, the isomiRs were defined 5' non-templated addition and 3' non-templated addition, respectively. No 5' non-templated addition isomiR was identified in our dataset. Among the 3' non-templated additions, the most frequent consists in uridylation, namely addition of one or more uracils. Shifted isomiRs are long as the canonical sequence, but their start-sites and,

consequently, their end-sites are shifted to the left (in 5' direction) or to the right (in 3' direction) to one or more positions. Finally, the mixed isomiR group includes miRNA variants that manifest at least two of these differences compared to the canonical counterpart (**Table 15**).

Table 15. Mature microRNA classification in 23 formalin-fixed paraffin-embedded (FFPE) samples

Mature miRNAs from small RNA-seq			
Type	***Sub-type***	***Total***	
"canonical" miRNAs	miRNA with isomiR	90 (18.2%)	130 (26.3%)
	miRNA without isomiR	40 (8.1%)	
isomiRs	isomiR with canonical miRNA	324 (65.6%)	364 (73.7%)
	orphan isomiR	40 (8.1%)	
	Total		494 (100%)
Classification miRNAs with isomiRs			
Groups	***Sub-groups***	***Total***	
miRNAs with 1 isomiR		25 (27.8%)	25 (27.8%)
miRNA with 2-3 isomiRs	2 isomiRs	14 (15.6%)	27 (30.0%)
	3 isomiRs	13 (14.4%)	
miRNA with 4-5 isomiRs	4 isomiRs	10 (11.1%)	21 (23.3%)
	5 isomiRs	11 (12.2%)	
miRNA with 6-13 isomiRs	6 isomiRs	6 (6.7%)	17 (18.9%)
	7 isomiRs	2 (2.2%)	
	8 isomiRs	2 (2.2%)	
	9 isomiRs	3 (3.4%)	
	10 isomiRs	2 (2.2%)	
	11 isomiRs	1 (1.1%)	
	13 isomiRs	1 (1.1%)	
	Total		90 (100%)
Classification isomiRs with canonical miRNA			
Groups	***Sub-groups***	***Total***	
End-site isomiRs		199 (61.4%)	199 (61.4%)
Start-site isomiRs		19 (5.9%)	19 (5.9%)
Shifted isomiRs		9 (2.8%)	9 (2.8%)
3' non-templated addition isomiRs		43 (13.2%)	43 (13.2%)
Mixed isomiRs	End-site + start-site	13 (4.0%)	54 (16.7%)
	End-site + 3' non-templated addition	34 (10.5%)	
	Start-site + 3' non-templated addition	6 (1.9%)	
	Shifted + 3' non-templated addition	1 (0.3%)	
	Total		324 (100%)

6.4.2. End-site isomiRs are the most abundant and expressed isomiRs in FFPE samples

The most represented class of isomiR is the end-site class (61.4%). Looking at the normalized expression of all isomiRs in the early-stage melanomas, we observed that they can vary between 5-6 to over 2300. We selected the isomiR with a normalized expression > 20 and obtained a list of 126 isomiRs (Supplementary Table S2 from Broseghini et al. [530]). Among them, the majority of isomiRs (about 75%) belong to the end-site group. The ten most expressed isomiRs include 9 end-site isomiRs (hsa-miR-10b-5p|0|–1, hsa-miR-205-5p|0|+1, hsa-miR-27b-3p|0|–1, hsa-miR-125a-5p|0|–2, has-miR-10a-5p|0|–1, hsa-miR-181a-5p|0|–1, hsa-miR-30d-5p|0|+2, hsa-miR-143-3p|0|–1, hsa-let-7a-5p|0|–1) and one 3' non-template addition isomiR (hsa-miR-143-3p|0|0(+1U)) (**Table 16**).

Table 16. List of ten isomiRs more expressed in 20 early-stage melanoma samples

IsomiR name	isomiR group	*isomiR expression in melanoma (average, n=20)*
hsa-miR-10b-5p|0|-1	end-site	2368.09
hsa-miR-205-5p|0|+1	end-site	1221.77
hsa-miR-27b-3p|0|-1	end-site	845.19
hsa-miR-125a-5p|0|-2	end-site	623.96
hsa-miR-10a-5p|0|-1	end-site	594.23
hsa-miR-181a-5p|0|-1	end-site	546.38
hsa-miR-143-3p|0|0(+1U)	3' non-templated addition	509.64
hsa-miR-30d-5p|0|+2	end-site	462.00
hsa-miR-143-3p|0|-1	end-site	382.90
hsa-let-7a-5p|0|-1	end-site	321.81

6.4.3. Enrichment of isomiRs belonging the cancer-related miRNA family in BN and CM samples

We calculated the average expression of each isomiR in all sequenced samples (BN and CM) and the ratio between each isomiR and its canonical miRNA. We focused on highly expressed isomiRs that could potentially affect the target gene regulation of the canonical miRNA. A panel of 17 isomiRs that are 3- to 10-fold more abundant than their canonical forms is reported in **Table 17**. We observed an enrichment of isomiRs belonging to three important miRNA families, namely miR-30 family, miR-200 family, and miR-10 family.

Table 17. IsomiRs most represented in melanoma and nevi small RNA-sequencing data

IsomiR	Type	IsomiR expression (mean)	Canonical miRNA expression (mean)	Ratio isomiR/canonical miRNA
hsa-miR-141-3p|0|–1	end-site isomiR	200.33	8.65	23.15
hsa-miR-222-3p|0|+3	end-site isomiR	154.64	9.05	17.08
hsa-miR-30a-5p|0|+2	end-site isomiR	211.95	13.33	15.9

hsa-miR-125a-5p|0|–2	end-site isomiR	765.69	56.46	13.56
hsa-miR-30d-5p|0|+2	end-site isomiR	416.87	41.32	10.09
hsa-miR-10b-5p|0|–1	end-site isomiR	2950.88	357.98	8.24
hsa-miR-27a-3p|0|–1	end-site isomiR	167.78	30.55	5.49
hsa-miR-30a-5p|0|–2	end-site isomiR	72.12	13.33	5.41
hsa-miR-222-3p|0|+4	end-site isomiR	46.98	9.05	5.19
hsa-miR-19b-3p|0|–1	end-site isomiR	52.06	11.59	4.49
hsa-miR-30c-5p|0|+1	end-site isomiR	151.53	34.28	4.42
hsa-miR-26b-5p|0|+1	end-site isomiR	172.47	39.32	4.39
hsa-miR-222-3p|0|+2	end-site isomiR	36.83	9.05	4.07
hsa-miR-10a-5p|0|–1	end-site isomiR	636.58	184.52	3.45
hsa-miR-30a-5p|0|+1	end-site isomiR	45.68	13.33	3.43
hsa-miR-30d-5p|0|+1	end-site isomiR	140.07	41.32	3.39
hsa-miR-200b-3p|0|+1	end-site isomiR	44.86	13.26	3.38

We analyzed the expression of isomiRs and canonical forms for each family member (**Figure 32-34**). The most representative miR-30 family isomiRs are 3′ isoforms with the addiction of 1 and 2 nts (**Figure 32**). miR-200 family presented highly expressed 3′ isoforms, with addiction or deletion of nts (**Figure 33**). Finally, the most expressed miR-10 family isomiRs are shorter 3′-isoforms (deletion of 1 or 2 nts in the 3’ end) (**Figure 34**).

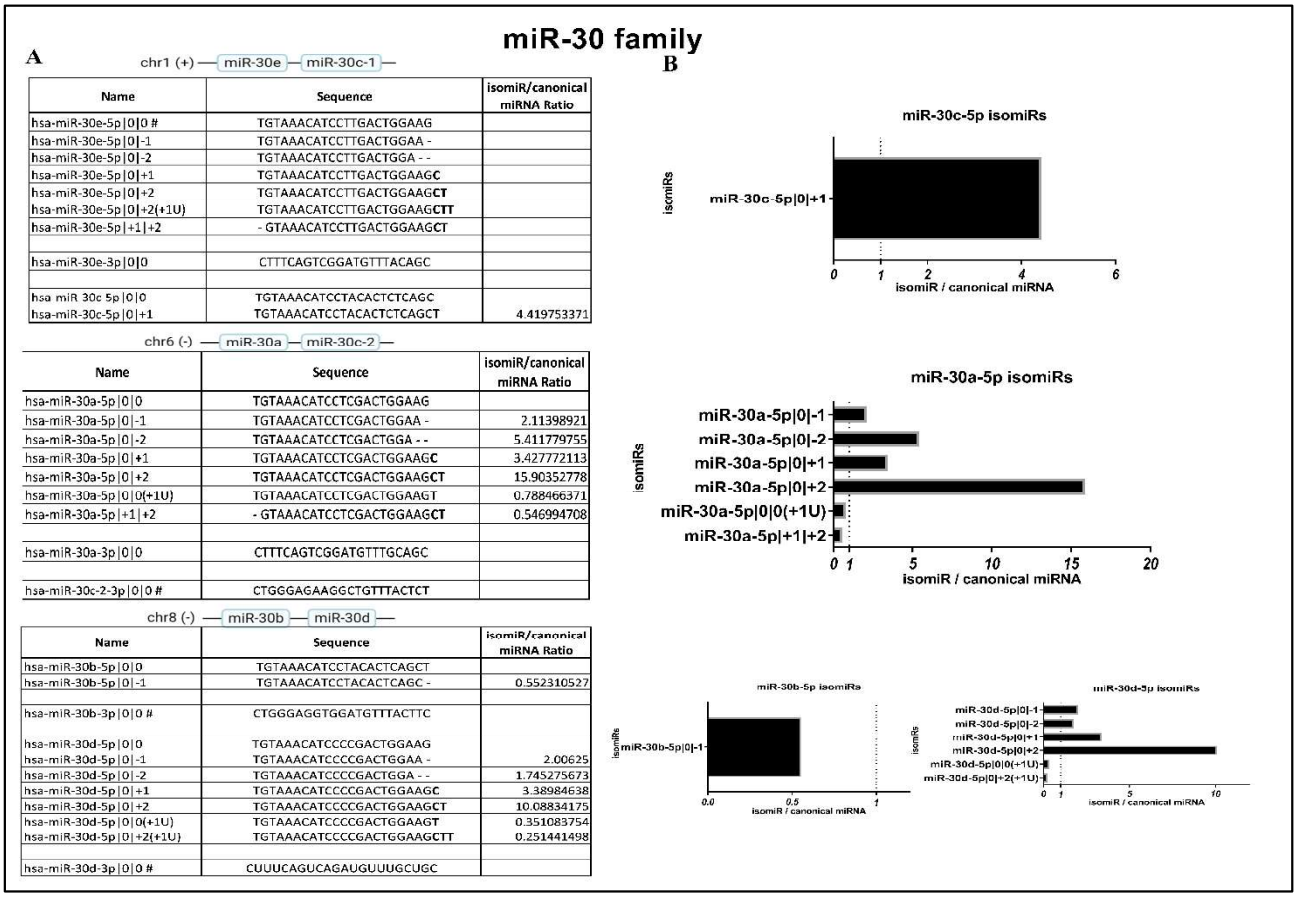

Figure 32. Representation of miR-30 family isoforms in all samples from small RNA-seq data. A) miR-30 family contains 5 members and 6 mature microRNA molecules encoded by 6 genes distributed on three different chromosomes: miR-30e and miR-30c-1 (chr1), miR-30a and miR-30c-2 (chr6), miR-30b and miR-30d (chr8). Tables report the canonical microRNAs and all detected isomiRs, their sequences and the expression ratio between each isomiR and the canonical miRNA (if the sequence was detected). #: the canonical miRNA is not detected in our small RNA-seq data. B) Expression ratio of each isomiR/miRNA is illustrated with bar chart. The most expressed isoform is a longer 3' isomiR for miR-30c-1, miR-30a and miR30d. miR-30b isomiR is less expressed if compared to the canonical miRNA (ratio < 1). miR-30c-2 and miR30e canonical miRNAs were not detected in these samples. miR-30e isomiRs can be considered "orphan isomiRs" in this dataset.

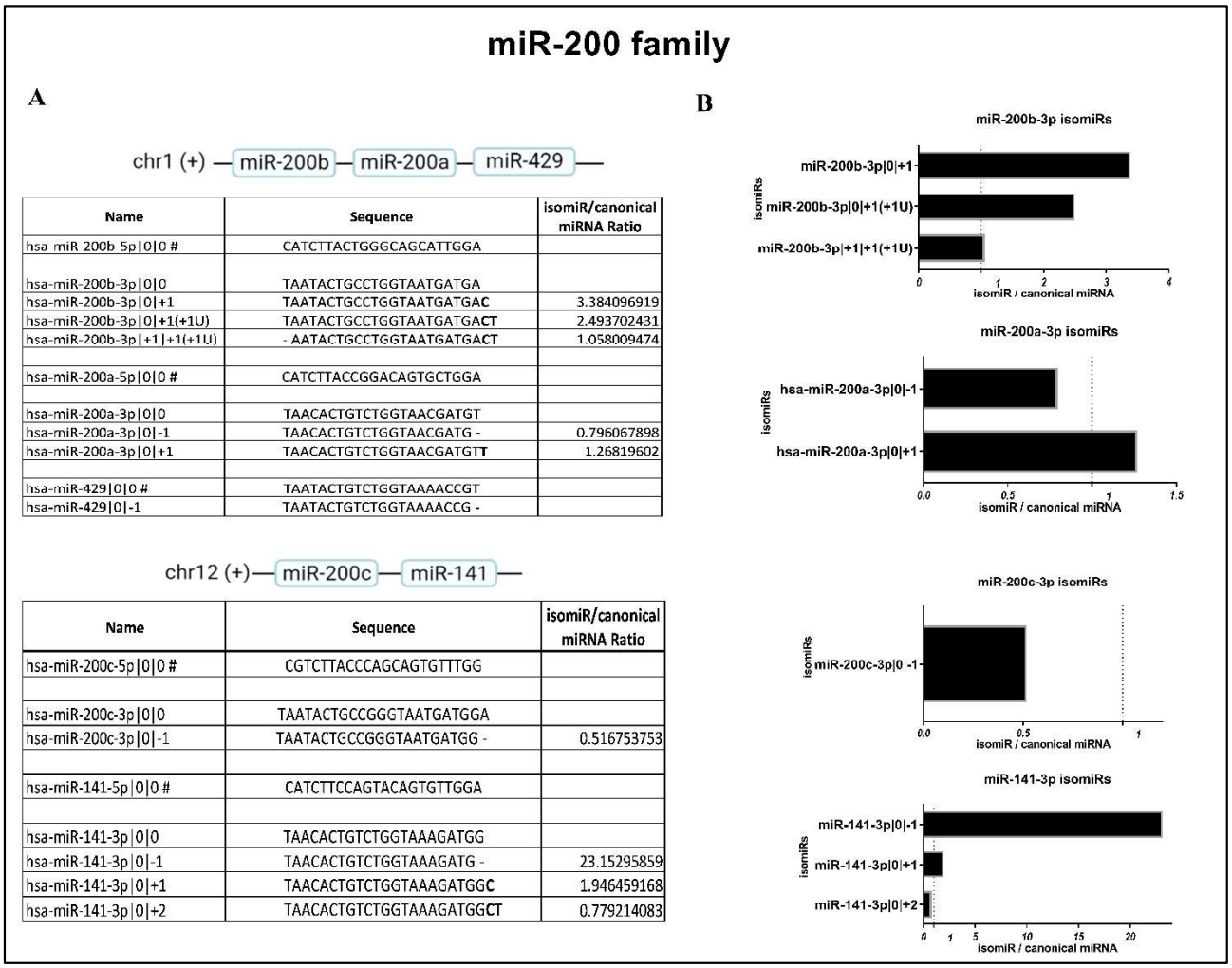

Figure 33. Representation of miR-200 family isoforms in all samples from small RNA-seq data. A) miR-200 family contains 5 mature microRNA molecules encoded by 5 genes distributed on two different chromosomes: miR-200b, miR-200a and miR-429 (chr1), miR-200c and miR-141 (chr12). Tables report the canonical microRNAs and all detected isomiRs, their sequences and the expression ratio between each isomiR and the canonical miRNA (if the sequence was detected). #: the canonical miRNA is not detected in our small RNA-seq data. B) Expression ratio of each isomiR/miRNA is illustrated with bar chart. The most expressed isoform is a longer 3'isomiR for miR-200b and miR200a, while a shorter 3'isomiR for miR-141. miR-200c isomiR is less expressed if compared to the canonical miRNA (ratio < 1). miR-429 canonical miRNA was not detected in these samples, and its isomiR can be considered "orphan isomiRs" in this dataset.

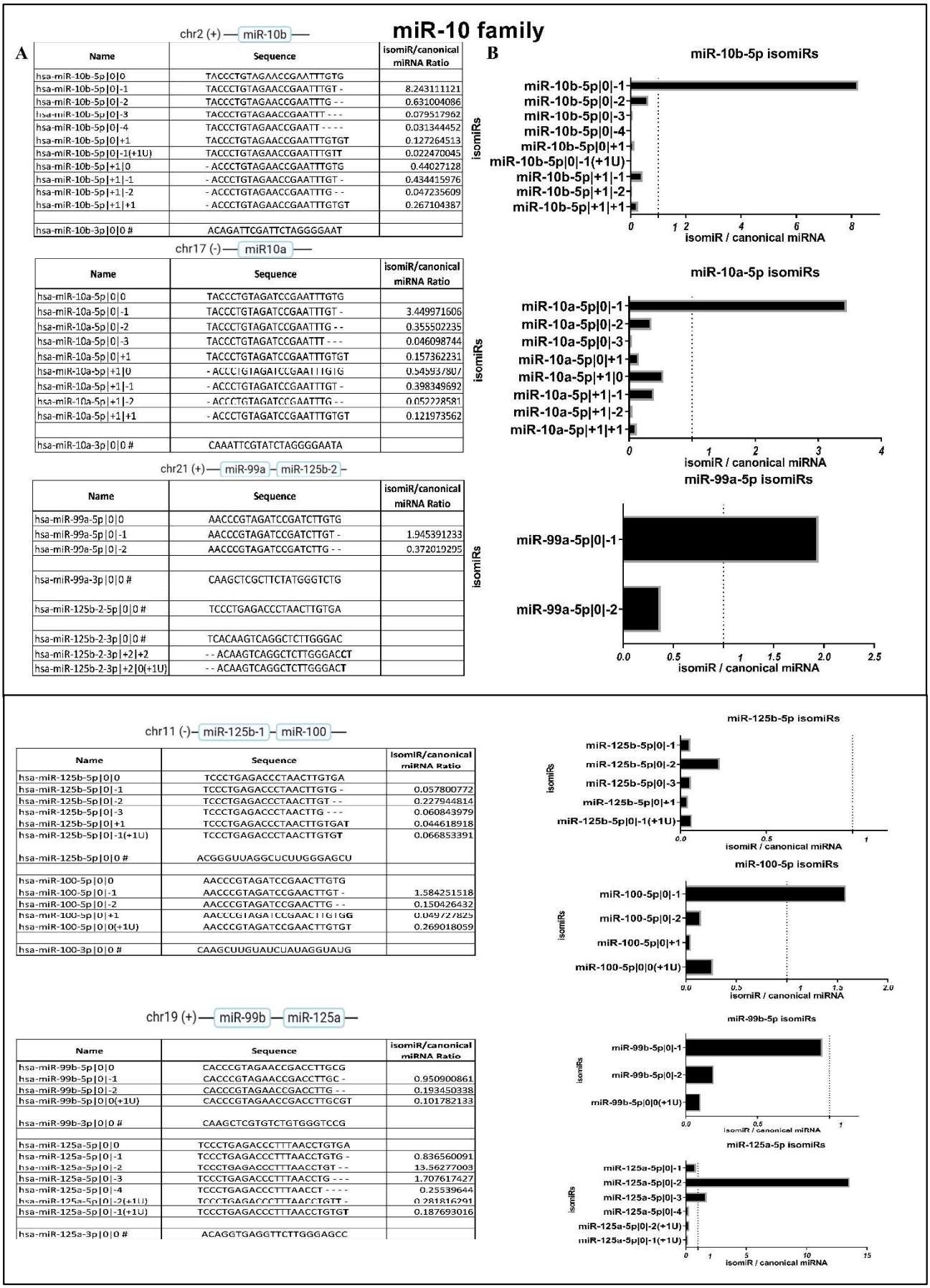

Figure 34. Representation of miR-10 family isoforms in all samples from small RNA-seq data. A) miR-10 family consists of miR-10a and miR-10b (encoded in Hox clusters, chr17 and chr2 respectively), and the more distantly related miR-99a/b, miR-100 and miR-125 (chr21, chr11 and chr19). Tables report the canonical

microRNAs and all detected isomiRs, their sequences and the expression ratio between each isomiR and the canonical miRNA (if the sequence was detected). #: the canonical miRNA is not detected in our small RNA-seq data. B) Expression ratio of each isomiR/miRNA is illustrated with bar chart. The most expressed isoform is a shorter 3' isomiR for miR-10a, miR-10a, miR-99a, miR-100, miR-125a. miR-125b and miR-99b isomiRs are less expressed if compared to the canonical miRNA (ratio < 1). miR-125b-2 canonical miRNA was not detected in these samples, and its isomiRs can be considered "orphan isomiRs" in this dataset.

6.4.4. Identification of isomiRs more expressed than the canonical form in early-stage melanoma

We focused on isomiRs that showed a higher or an equal expression level than the corresponding canonical mRNA form in melanomas to identify the most relevant isomiRs specifically in early-stage melanomas. The expression ratio between all isomiRs and canonical miRNA was calculated, excluding miRNAs without isomiRs and orphan isomiRs. We used the average expression of the selected 412 mature miRNAs in 20 early-stage melanomas and calculated the expression ratio for each isomiR obtaining a wide set of ratios: from 3000 times less expressed than the canonical miRNAs to 50 times more expressed. 39 isomiRs with a ratio isomiR/miRNA >1 were obtained (**Figure 35A**).

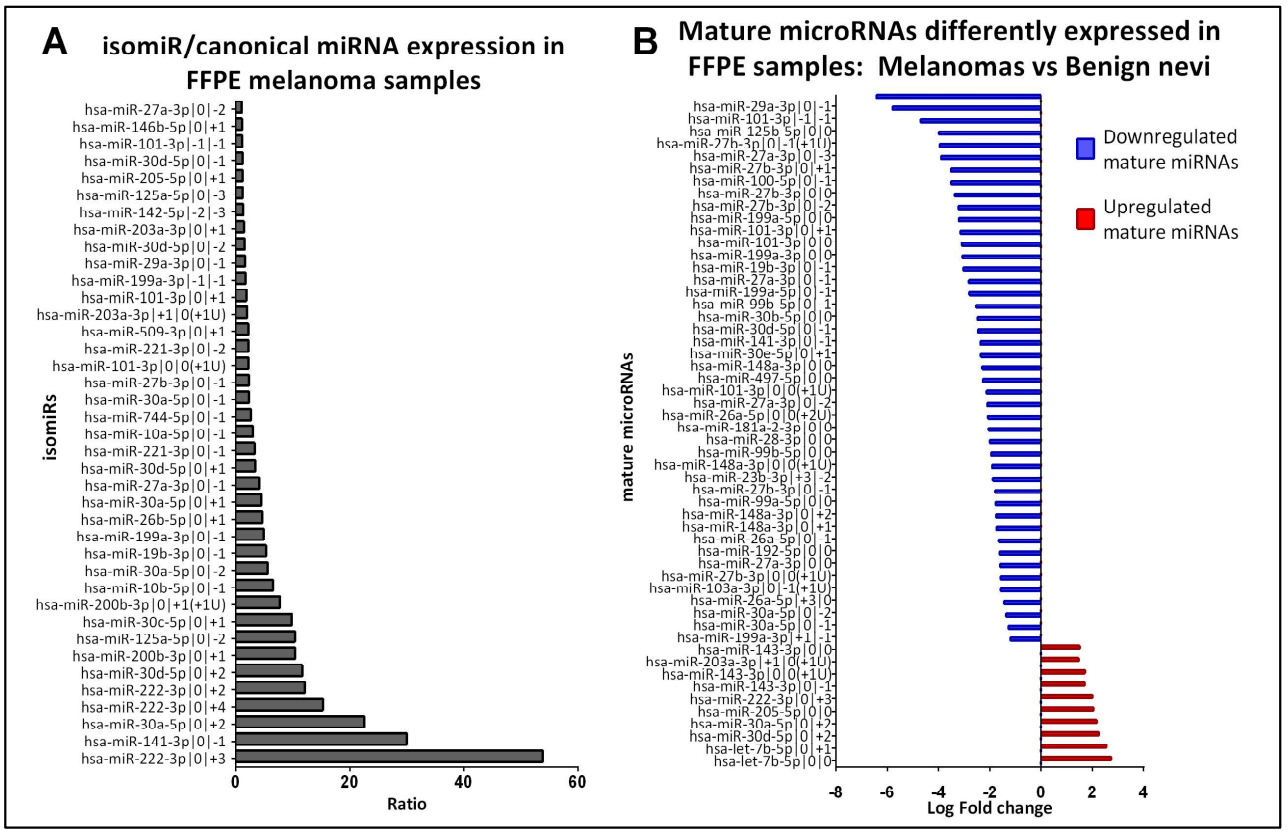

Figure 35. Expression of mature microRNAs in FFPE samples. A) IsomiR/canonical miRNA expression in 20 FFPE melanoma samples. Bar graph representing isomiR/miRNA ratios in 20 FFPE early-stage melanoma samples greater than 1 for isomiR with an average normalized expression >20 (n = 39). B) List of 55 mature microRNAs differently expressed in 20 FFPE early-stage melanoma compared to 3 FFPE benign nevi samples. Interleaved bar charts showing the average log FC in CM vs. BN. We identified 10 upregulated (in red) and 45 downregulated mature microRNAs with FC >2 and adjusted *p value* < 0.05.

Interestingly, many of these isomiRs belonged to the same miRNA family: 9 isomiRs belong to miR-30 family (3 to miR-30a-5p, 1 to miR-30c-5p, and 3 to miR-30d-5p); 5 isomiRs belong to miR-221/222 family (3 to miR-221-3p and 2 to miR-222-3p); 4 isomiRs belong to miR-10 family (1 to miR-10a-5p, 1 to miR-10b-5p, and 2 to miR-125a-5p) 3 isomiRs belong to miR-101 family (all to miR-101-3p), 3 isomiRs belong to miR-200 family (1 to miR-141-3p and 2 to miR-200b-3p), and 3 isomiRs belong to miR-27 family (1 to miR-27a-3p and 2 to miR-27b-3p).

6.4.5. Benign nevi and early-stage melanoma present a different mature miRNA expression profile

Mature miRNA expression profile of 3 BN and 20 early-stage CM was analyzed and compared. 55 mature miRNAs (18 canonical and 37 isomiRs) were identified as differentially expressed between early-stage CM and BN (adjusted *p value* < 0.05, **Figure 35B**): 45 are downregulated in melanoma, while 10 are upregulated (**Table 18**).

Table 18. List of differentially expressed mature microRNAs in primary melanoma (CM) and benign nevi (BN) samples

Mature miRNAs differently expressed in CM vs BN			
Name	***p value* (Corr)**	**Regulation**	**Log FC**
canonical miRNAs			
hsa-let-7b-5p|0|0	1.0E-02	up	2.73
hsa-miR-205-5p|0|0	9.3E-03	up	2.04
hsa-miR-143-3p|0|0	4.2E-02	up	1.50
hsa-miR-27a-3p|0|0	7.1E-03	down	-1.60
hsa-miR-192-5p|0|0	3.9E-02	down	-1.61
hsa-miR-99a-5p|0|0	2.1E-02	down	-1.77
hsa-miR-99b-5p|0|0	3.6E-02	down	-1.94
hsa-miR-28-3p|0|0	1.1E-02	down	-1.99
hsa-miR-181a-2-3p|0|0	5.8E-04	down	-2.05
hsa-miR-497-5p|0|0	3.4E-04	down	-2.27
hsa-miR-148a-3p|0|0	2.7E-03	down	-2.29
hsa-miR-30b-5p|0|0	3.3E-03	down	-2.47
hsa-miR-199a-3p|0|0	1.5E-05	down	-3.07
hsa-miR-101-3p|0|0	4.2E-05	down	-3.08
hsa-miR-199a-5p|0|0	8.9E-07	down	-3.21
hsa-miR-27b-3p|0|0	3.2E-06	down	-3.38
hsa-miR-125b-5p|0|0	9.6E-07	down	-3.98
hsa-miR-29a-3p|0|0	8.6E-09	down	-6.42
isomiRs			
hsa-let-7b-5p|0|+1	5.6E-03	up	2.54
hsa-miR-30d-5p|0|+2	7.2E-03	up	2.25
hsa-miR-30a-5p|0|+2	1.3E-03	up	2.17
hsa-miR-222-3p|0|+3	9.0E-03	up	2.00

hsa-miR-143-3p|0|0(+1U)	2.6E-02	up	1.71
hsa-miR-143-3p|0|-1	4.5E-02	up	1.70
hsa-miR-203a-3p|+1|0(+1U)	4.2E-02	up	1.46
hsa-miR-199a-3p|+1|-1	2.0E-02	down	-1.19
hsa-miR-30a-5p|0|-1	1.7E-02	down	-1.28
hsa-miR-30a-5p|0|-2	4.5E-02	down	-1.36
hsa-miR-26a-5p|+3|0	4.3E-02	down	-1.44
hsa-miR-103a-3p|0|-1(+1U)	3.2E-02	down	-1.57
hsa-miR-27b-3p|0|0(+1U)	5.0E-02	down	-1.57
hsa-miR-26a-5p|0|-1	2.0E-02	down	-1.64
hsa-miR-148a-3p|0|+1	3.2E-02	down	-1.73
hsa-miR-148a-3p|0|+2	1.7E-02	down	-1.75
hsa-miR-27b-3p|0|-1	2.7E-02	down	-1.78
hsa-miR-23b-3p|+3|-2	6.8E-03	down	-1.87
hsa-miR-148a-3p|0|0(+1U)	1.2E-02	down	-1.90
hsa-miR-26a-5p|0|0(+2U)	1.6E-04	down	-2.06
hsa-miR-27a-3p|0|-2	3.1E-03	down	-2.10
hsa-miR-101-3p|0|0(+1U)	2.7E-03	down	-2.12
hsa-miR-30e-5p|0|+1	4.8E-04	down	-2.35
hsa-miR-141-3p|0|-1	3.8E-03	down	-2.36
hsa-miR-30d-5p|0|-1	8.5E-03	down	-2.46
hsa-miR-99b-5p|0|-1	1.1E-02	down	-2.53
hsa-miR-199a-5p|0|-1	6.1E-06	down	-2.79
hsa-miR-27a-3p|0|-1	1.3E-03	down	-2.81
hsa-miR-19b-3p|0|-1	2.6E-04	down	-3.02
hsa-miR-101-3p|0|+1	3.4E-05	down	-3.15
hsa-miR-27b-3p|0|-2	3.4E-05	down	-3.23
hsa-miR-100-5p|0|-1	1.3E-03	down	-3.50
hsa-miR-27b-3p|0|+1	4.7E-06	down	-3.51
hsa-miR-27a-3p|0|-3	9.6E-07	down	-3.89
hsa-miR-27b-3p|0|-1(+1U)	1.2E-06	down	-3.95
hsa-miR-101-3p|-1|-1	1.2E-06	down	-4.70
hsa-miR-29a-3p|0|-1	4.0E-08	down	-5.79

10 differentially expressed canonical miRNAs have at least one isomiR in this list of 55 mature miRNAs ((let-7b-5p, miR-101-3p, miR-143-3p, miR-148a-3p, miR-199a-3p, miR-199a-5p, miR-27a-3p, miR-27b-3p, miR-29a-3p, miR-99b-5p), while 8 do not have any isomiR in the list (miR-125b-5p, miR-181a-2-3p, miR-192-5p, miR-205-5p, miR-28-3p, miR-30b-5p, miR-497-5p, miR-99a-5p). 16 isomiRs do not have the canonical miRNA in the list, meaning that these isomiRs are differently expressed in early-stage CM vs. BN, but not the corresponding canonical miRNAs. The other 21 isomiRs have the canonical miRNA in the list. In most cases, isomiRs show the same expression variation than the canonical miRNA, namely isomiR(s) and the corresponding canonical

miRNA are all downregulated or upregulated in the CM compared to BN. Despite this, there are exceptions: some isomiRs of the same canonical miRNA, such as miR-30a-5p and miR-30d-5p, present opposite trends: miR-30a-5p|0|+2 and miR-30d-5p|0|+2 are upregulated in early-stage CM, while miR-30a-5p|0|–1, miR-30a-5p|0|–2 and miR-30d-5p|0|–1 are downregulated compared to BN. Their canonical forms are not differentially expressed between CM and BN.

In the 55 mature miRNA list, there are 16 isomiR with a ratio isomiR/miRNA > 1, namely hsa-miR-101-3p|0|+1 (ratio = 1.83), hsa-miR-101-3p|0|0(+1U) (ratio = 2.2), hsa-miR-101-3p|–1|–1 (ratio = 1.8), hsa-miR-141-3p|0|–1 (ratio = 30.1), hsa-miR-19b-3p|0|–1 (ratio = 5.31), hsa-miR-203a-3p|+1|0(+1U) (ratio = 1.99), hsa-miR-222-3p|0|+3 (ratio = 53.84), hsa-miR-27a-3p|0|–1 (ratio = 4.08), hsa-miR-27a-3p|0|–2 (ratio = 1.02), hsa-miR-27b-3p|0|–1 (ratio = 2.29), hsa-miR-29a-3p|0|–1 (ratio = 1.57), hsa-miR-30a-5p|0|–1 (ratio = 2.30), hsa-miR-30a-5p|0|+2 (ratio = 22.55), hsa-miR-30a-5p|0|–2 (ratio = 5.54), and hsa-miR-30d-5p|0|–1 (ratio = 1.15), and hsa-miR-30d-5p|0|+2 (ratio = 11.64).

6.4.6. Classification of isomiRs with a potentially relevant role in early-stage melanoma

We selected mature miRNAs showing two characteristics: i) at least one isoform is differentially expressed between early-stage CM and BN; ii) at least one isoform is more expressed than the canonical form. We obtained a list of 10 miRNAs, which were further divided into four classes (**Figure 36**):

(a) isomiRs with a similar trend in early-stage CM vs. BN and similar relative abundance;
(b) isomiRs with a similar trend in early-stage CM vs. BN and different relative abundance;
(c) isomiRs with opposite trend in early-stage CM vs. BN and similar relative abundance;
(d) isomiRs with opposite trend in early-stage CM vs. BN and different relative abundance.

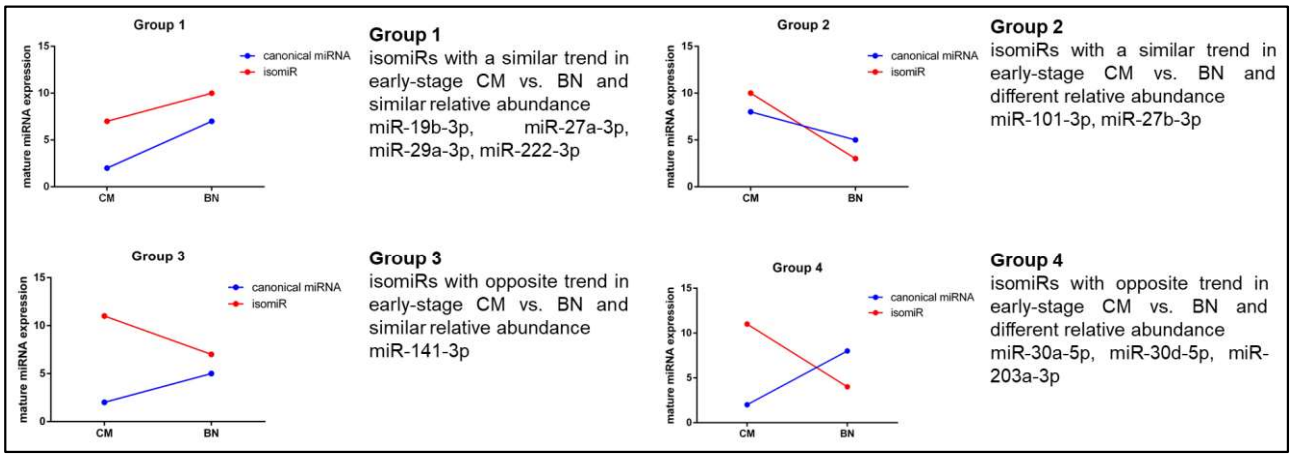

Figure 36. Classification of mature miRNAs based on differential expression in melanoma (CM) and benign nevi (BN) and on relative abundance.

6.4.6.1. IsomiRs with a similar trend in early-stage CM vs. BN and similar relative abundance

miR-19b-3p, miR-27a-3p, miR-29a-3p and miR-222-3p belong to the first class, which includes canonical miRNAs and corresponding isomiRs with the same trend of variation between early-stage CM and BN and similar abundance distribution. Canonical miRNAs and the isomiRs of miR-19b-3p, miR-27a-3p, miR-29a-3p are downregulated in CM, while mature miRNAs of miR-222-3p are upregulated in CM. Also the relative abundance is similar in CM and BN, in both the most expressed isomiRs are miR-19b-3p|0|–1, 27a-3p|0|–1, miR-29a-3p|0|– 1 followed by the canonical miR-29a-3p, and miR-222-3p|0|+3 (**Figure 37**).

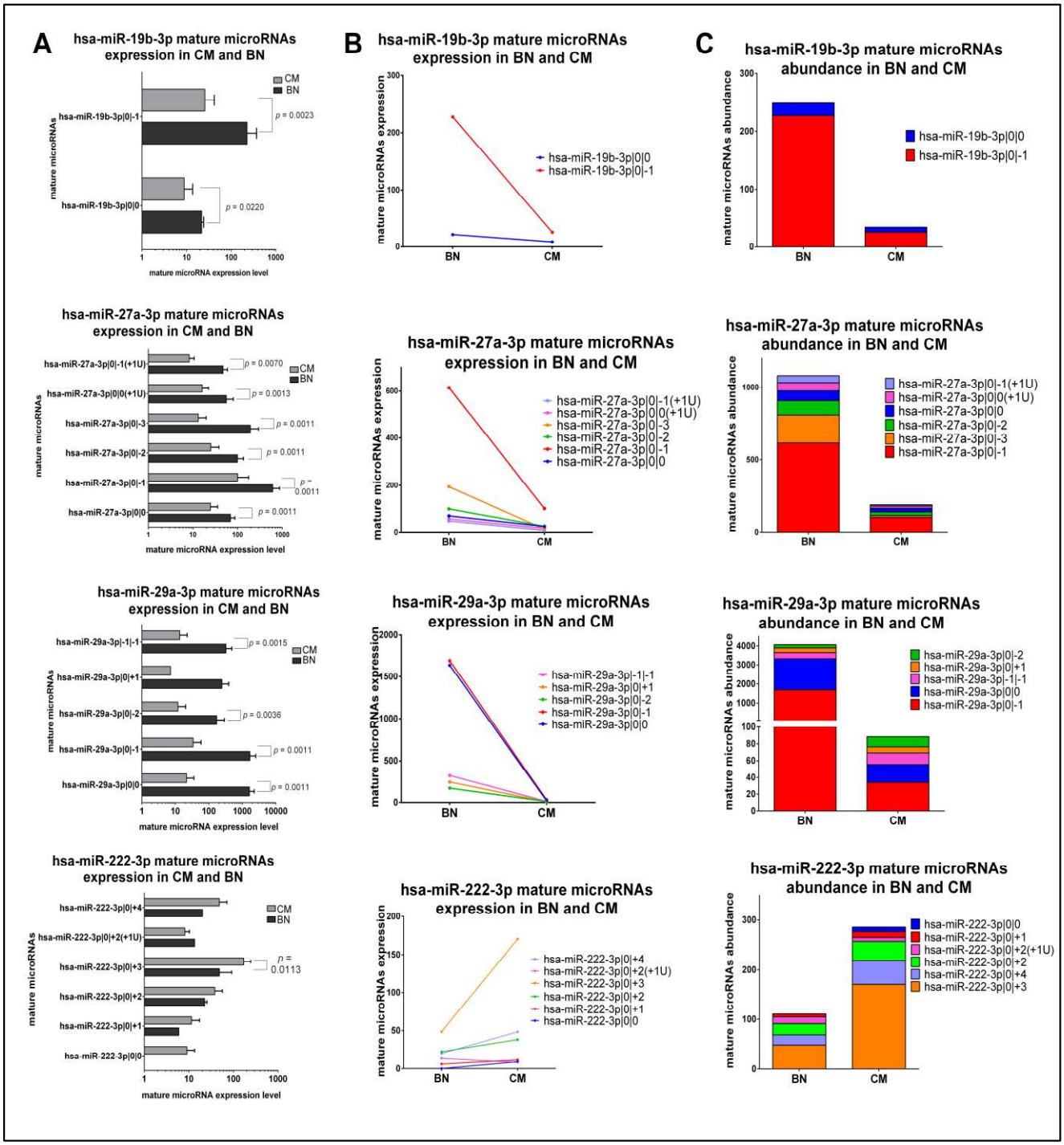

Figure 37. Group 1: IsomiRs with a similar trend in 20 FFPE CM vs. 3 FFPE BN and similar relative abundance. (A) Mature microRNA expression in BN and CM. All mature microRNAs are represented in a separated bar chart (mean ± standard deviation). A Mann-Whitney test was performed to compare the expression level in BN and CM. P values are shown when the difference is statistically significant. (B) Expression trend of mature microRNAs in BN and primary CM. Before-after blot shown the same expression trend between mature microRNAs. (C) Mature microRNA abundance distribution microRNAs in BN and CM. Stacked bar chart illustrates the same mature microRNA abundance distribution between BN and CM. Mature microRNAs are sorting based on their expression in BN.

6.4.6.2. IsomiRs with a similar trend in CM vs. BN and different relative abundance

miR-101-3p and miR-27b-3p belong to the second class, where miRNAs have the same trend of variation for all their isomiRs in CM vs. BN, but there is different abundance distribution between CM and BN. Almost all isomiRs and canonical miR-101-3p are significantly downregulated in CM. However, there is a difference in relative abundance distribution. We observed that the major expressed isomiR is miR-101-3p|0|0(+1U) in CM and miR-101-3p|–1|–1 in BN. The 9 isomiRs and canonical form of miR-27b-3p are lower expressed in CM compared to BN with a significant difference in most of the cases. Looking at the abundance distribution, miR-27b-3p|0|–1 is the most expressed form in CM, while the canonical miRNA is the most expressed mature miRNA in BN (**Figure 38**).

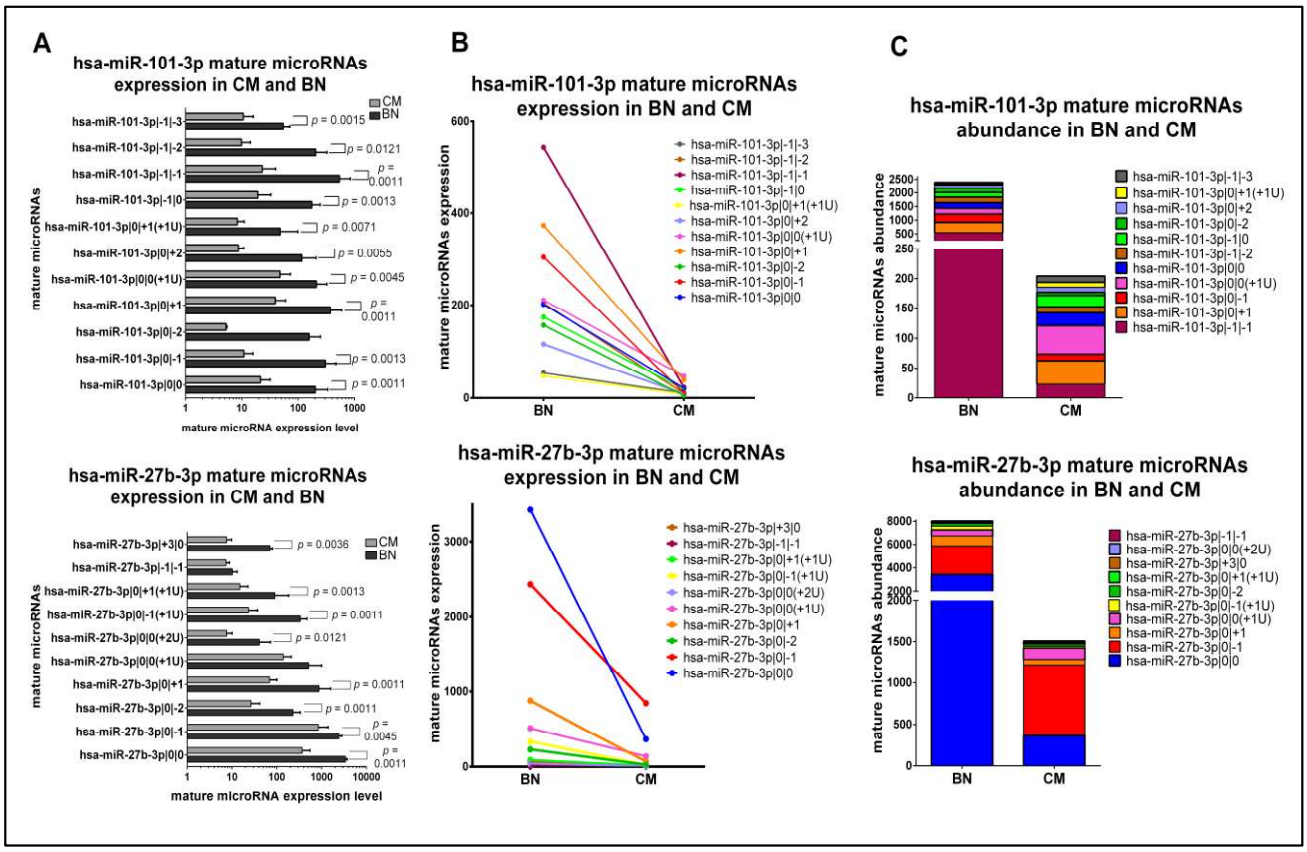

Figure 38. Group 2: IsomiRs with a similar trend in 20 CM vs. 3 BN and different relative abundance. (A) Mature microRNA in BN and CM. All mature microRNAs are represented in a separated bar chart (mean). Bar indicates standard deviation. Mann-Whitney t test was performed to compared expression level in BN and CM. p values are shown when the difference is statistically significant. (B) Expression trend of mature microRNAs in BN and CM. Before-after blot shown the same expression trend between mature microRNAs. (C). Mature microRNA abundance distribution in BN and CM. A stacked bar chart illustrates a different mature microRNA abundance distribution between BN and CM. Mature microRNAs are sorting based on their expression in BN.

6.4.6.3. IsomiRs with opposite trend in CM vs. BN and similar relative abundance

miR-141-3p is the only miRNA of the third class. miR-141-3p|0|–1 is downregulated in CM compared to BN (*p value* = 0.0023), while the canonical miRNA and miR-141-3p|0|+1 have a comparable expression in CM and BN. miR-141-3p|0|+2 is only detectable in CM samples. The abundance distribution is similar between CM and BN: miR-141-3p|0|–1 is the most expressed mature miRNA in both groups (**Figure 39**).

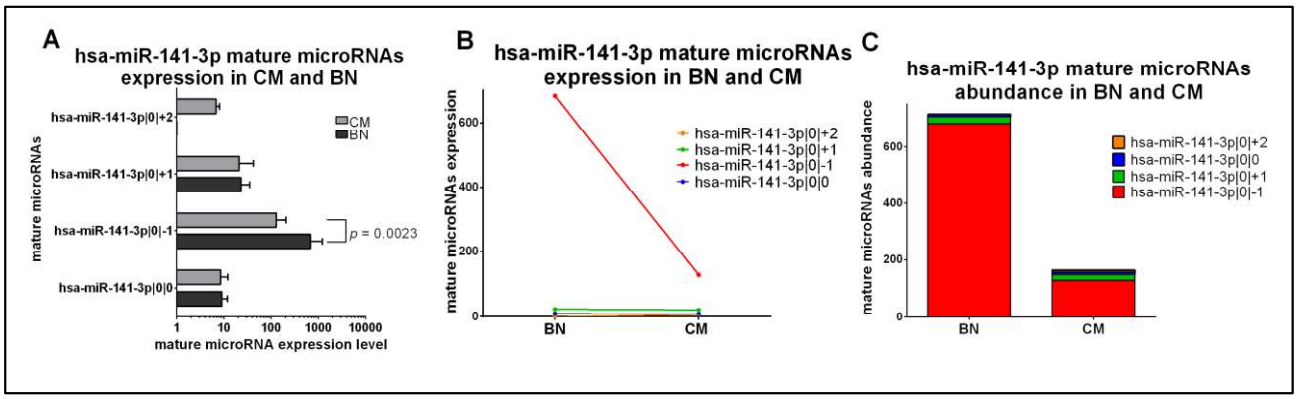

Figure 39. Group 3: IsomiRs with opposite trends in 20 CM vs. 3 BN and similar relative abundance. (A) Mature microRNA expression in BN and CM. All mature microRNAs are represented in a separated bar chart (mean). Bar indicates standard deviation. Mann-Whitney t test was performed to compared expression level in BN and CM. p values are shown when the difference is statistically significant. (B) Expression trend of mature microRNAs in BN and CM. Before-after blot shown a different expression trend between mature microRNAs. (C) Mature microRNA abundance distribution in BN and CM. The stacked bar chart illustrates the same mature microRNA abundance distribution between BN and CM. Mature microRNAs are sorting based on their expression in BN.

6.4.6.4. IsomiRs with opposite trend in CM vs. BN and different relative abundance

Finally, the last class includes three miRNAs, namely miR-30a-5p, miR-30d-5p and miR-203a-3p, which show different expression trend between isomiRs and the canonical form and a different isomiRs abundance distribution in CM and BN.

We identified six different isomiRs of miR-30a-5p that are expressed in CM and BN. One isomiR is upregulated (miR-30a-5p|0|+2), while two are downregulated (miR-30a-5p|0|–1, miR-30a-5p|0|0(+1U)) in CM. The most expressed mature miRNA in CM is miR-30a-5p|0|+2, while in BN is miR-30a-5p|0|–2.

Similarly, miR-30d-5p have six detected isomiRs: the canonical form and several isomiRs do not show differences between CM and BN, and one isomiR is detected only in CM (miR-30d-5p|0|+2(+1U)). However, there are two isomiRs that have a significant and opposite trend: miR-30d-5p|0|–1 is downregulated in CM, while miR-30d-5p|0|+2 is upregulated in CM. Furthermore, miR-30d-5p|0|–1 and miR-30d-5p|0|+2 are also the most expressed isomiR in CM and BN, respectively.

We found nine isomiRs of miR-203a-3p, but only three of them have different expression. MiR-203a-3p|0|–1 and miR-203a-3p|0|+1 are under expressed in CM, while miR-203a-3p|+1|0(+1U) is overexpressed in CM. Moreover, isomiR abundance distribution is different: the most expressed isomiR in BN is miR-203a-3p|0|+1, while in CM is miR-203a-3p|+1|0(+1U) (**Figure 40**).

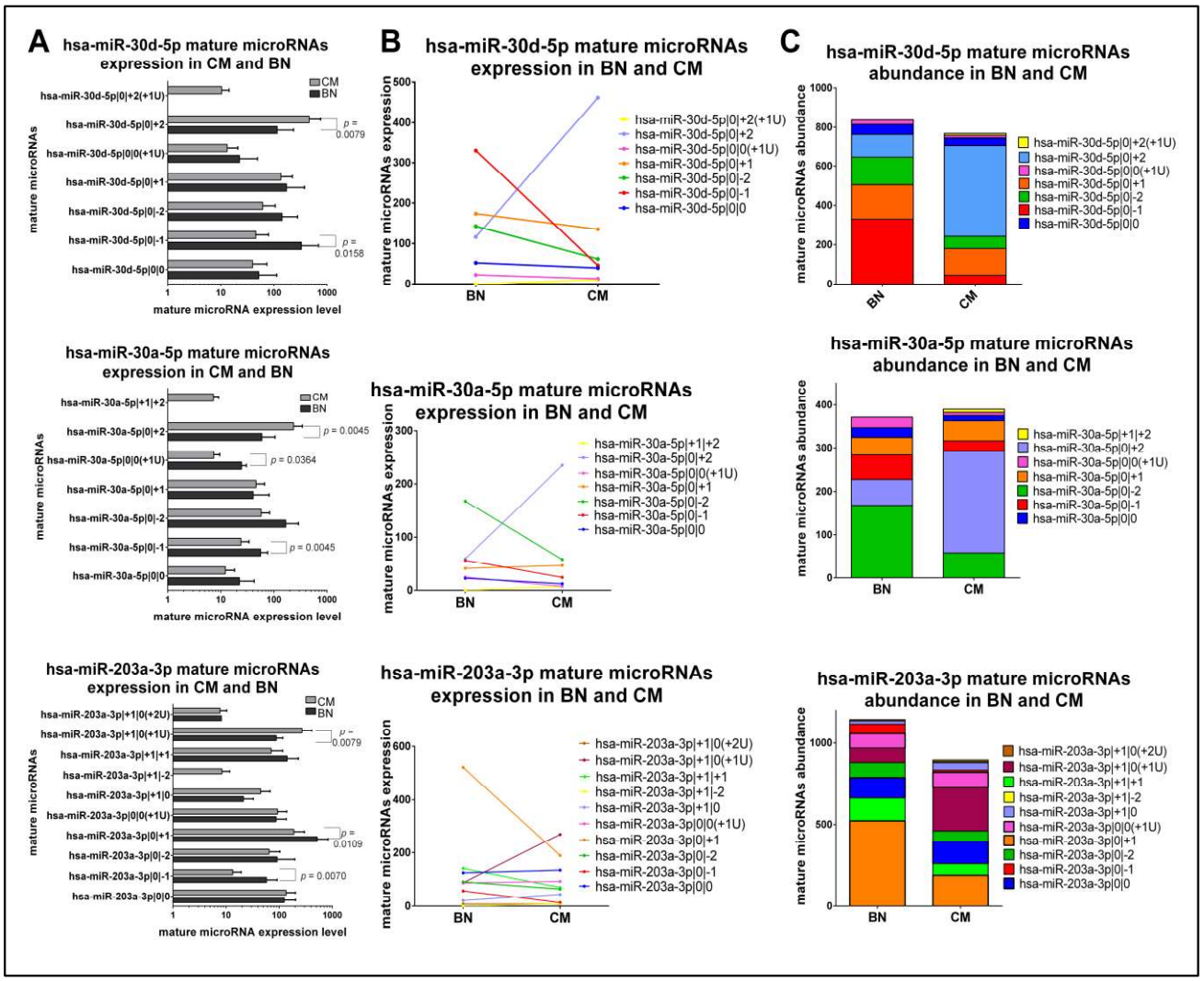

Figure 40. Group 4: IsomiRs with the opposite trend in 20 CM vs. 3 BN and different relative abundance. (A) Mature microRNA expression in BN and CM. All mature microRNAs are represented in a separated bar chart (mean). Bar indicates standard deviation. A Mann-Whitney t test was performed to compared expression level in BN and CM. p values are shown when the difference is statistically significant. (B) Expression trend of mature microRNAs in BN and CM. Before-after blot shown a different expression trend between mature microRNAs. (C) Mature microRNA abundance distribution in BN and CM. The stacked bar chart illustrates a different mature microRNA abundance distribution between BN and CM. Mature microRNAs are sorting based on their expression in BN.

6.4.7. IsomiR classification in fresh-frozen primary melanoma and metastasis from TCGA database

We studied the contribution of the isomiRs in 323 melanoma patients, including 63 primary cutaneous melanomas (CM), and 260 melanoma metastases (MM), and we analyzed the association of isomiR

expression with melanoma mutated genes. 3690 mature miRNAs were detected, including 474 canonical miRNAs and 3216 isomiRs (Supplementary Table S4 from Broseghini et al. [530]).

The majority of canonical miRNA (n=389) had at least one co-expressed isomiR, while 85 miRNAs did not have any detected isomiR. Again, we detected the presence of orphan isomiRs (n = 258), while 2958 isomiRs present a detectable canonical miRNA. In the isomiRs list, we showed the presence of 5' non-templated addition group, namely isomiRs with the addition of one or more nucleotides in the 5' end, which did not match with the stem-loop sequence. End-site type is the most frequent isomiR group. Finally, we detected four novel miRNAs and three isomiRs of novel miRNAs, which have been previously detected by examining small RNA-seq samples [587] (**Table 19**).

Table 19. Mature microRNA classification in 323 fresh-frozen melanoma from TCGA SKCM cohort.

Mature miRNAs from small RNA-seq			
Type	***Sub-type***		***Total***
"canonical" miRNAs	miRNA with isomiR	90 (18.2%)	130 (26.3%)
	miRNA without isomiR	40 (8.1%)	
isomiRs	isomiR with canonical miRNA	324 (65.6%)	364 (73.7%)
	orphan isomiR	40 (8.1%)	
	Total		494 (100%)
Classification miRNAs with isomiRs			
Groups	***Sub-groups***		***Total***
miRNAs with 1 isomiR		25 (27.8%)	25 (27.8%)
miRNA with 2-3 isomiRs	2 isomiRs	14 (15.6%)	27 (30.0%)
	3 isomiRs	13 (14.4%)	
miRNA with 4-5 isomiRs	4 isomiRs	10 (11.1%)	21 (23.3%)
	5 isomiRs	11 (12.2%)	
miRNA with 6-13 isomiRs	6 isomiRs	6 (6.7%)	17 (18.9%)
	7 isomiRs	2 (2.2%)	
	8 isomiRs	2 (2.2%)	
	9 isomiRs	3 (3.4%)	
	10 isomiRs	2 (2.2%)	
	11 isomiRs	1 (1.1%)	
	13 isomiRs	1 (1.1%)	
	Total		90 (100%)
Classification isomiRs with canonical miRNA			
Groups	***Sub-groups***		***Total***
End-site isomiRs		199 (61.4%)	199 (61.4%)
Start-site isomiRs		19 (5.9%)	19 (5.9%)
Shifted isomiRs		9 (2.8%)	9 (2.8%)
3' non-templated addition isomiRs		43 (13.2%)	43 (13.2%)

Mixed isomiRs	End-site + start-site	13 (4.0%)	54 (16.7%)
	End-site + 3' non-templated addition	34 (10.5%)	
	Start-site + 3' non-templated addition	6 (1.9%)	
	Shifted + 3' non-templated addition	1 (0.3%)	
	Total		324 (100%)

6.4.8. Identification of the isomiRs more expressed more expressed than the canonical form in fresh primary melanoma samples from TCGA

We investigated isomiRs that showed a higher or an equal expression level than canonical mRNA in primary melanomas from the TCGA SKCM cohort, which includes mostly stage II and stage III fresh primary melanoma. We calculated the expression ratio between 2958 isomiRs and the corresponding canonical miRNA in 63 CM and we found 1373 isomiR with a ratio > 1. Among them, there were 21 isomiRs already identified in early-stage FFPE melanomas (mostly stage I melanomas) (**Figure 35A**), confirming the identification of these isomiRs also in fresh melanoma tissue and late-stage melanomas (**Table 20**).

Table 20. List of isomiRs with an isomiR/canonical miRNA ratio greater than 1 in 63 fresh-frozen and 20 FFPE primary melanoma samples at different stages

Mature microRNA name	Ratio isomiR/canonical miRNA in 63 late-stage CM samples	Ratio isomiR/canonical miRNA in 20 early-stage CM sample
hsa-miR-101-3p|0|0(+1U)	1.21	2.22
hsa-miR-125a-5p|0|–2	2.22	10.35
hsa-miR-141-3p|0|–1	506.45	30.01
hsa-miR-142-5p|–2|–3	137.60	1.28
hsa-miR-146b-5p|0|+1	2.68	1.07
hsa-miR-199a-3p|0|–1	5.22	4.89
hsa-miR-199a-3p|–1|–1	1.14	1.66
hsa-miR-200b-3p|0|+1	2.41	10.39
hsa-miR-200b-3p|0|+1(+1U)	67983.34	7.76
hsa-miR-203a-3p|+1|0(+1U)	16.12	1.99
hsa-miR-203a-3p|0|+1	6.59	1.40
hsa-miR-222-3p|0|+3	3.80	53.84
hsa-miR-222-3p|0|+4	57.90	15.25
hsa-miR-26b-5p|0|+1	15.51	4.61
hsa-miR-27a-3p|0|–1	2.53	4.08
hsa-miR-27a-3p|0|–2	1.68	1.02
hsa-miR-27b-3p|0|–1	522.43	2.29
hsa-miR-29a-3p|0|–1	9.61	1.57

hsa-miR-30c-5p|0|+1	18.70	9.81
hsa-miR-30d-5p|0|–1	1.37	1.15
hsa-miR-30d-5p|0|–2	33.78	1.55

6.4.9. IsomiR expression contributes to distinguish primary melanoma and metastasis

The mature miRNA profiles of 63 fresh-frozen CM and 260 MM samples from the TCGA database were compared using an unpaired t-test (Benjamini-Hochberg correction, FC > 1.5, adjusted *p value* < 0.05), and we found 332 mature miRNAs differentially expressed: 211 are upregulated and 121 are downregulated in MM vs. CM (Supplementary Figure S1, Supplementary Table S6 from Broseghini et al. [530]). Looking at the type of mature miRNAs, 36 are canonical miRNAs, while the remaining 296 are isomiR variants. The most representative isomiR type is end-site group (n=175).

We found isomiRs that showed opposite trend in CMs and MMs compared to their canonical miRNA. Specifically, miR-101-3p, miR-146b-3p, miR-148a-3p, miR-15a-5p, miR-16-5p, miR-181a-5p, miR-181a-2-3p, miR-181b-5p, miR-21-5p, miR-22-3p, miR-23a-5p, miR-23b-3p, miR-24-3p, miR-30e-5p, miR-361-3p, and miR-500a-3p have at least two variants with opposite trends (Supplementary Table S5, Supplementary Figure S2 from Broseghini et al. [530]).

Three isomiR variants of miR-101-3p showed three differently expressed isomiRs: miR-101-3p|0|–2 and miR-101-3p|–1|–2 are upregulated, while miR-101-3p|0|0(+2U) is downregulated in MM compared to CM.

MMs showed high level of miR-146b-3p|0|–1 and a low level of miR-146b-3p|–1|–2 compared to CM. miR-15a-5p, miR-16-5p and miR-181a-5p have an upregulated isomiR (miR-15a-5p|0|–2, miR-16-5p|0|–2, miR-181a-5p|0|–3, respectively), and a downregulated isomiR (miR-15a-5p|0|+2, miR-16-5p|0|+3, miR-181a-5p|0|+2, respectively).

There are several differentially expressed of miR-148a-3p: two are downregulated (miR-148a-3p|0|+2, miR-148a-3p|0|0(+2U)), while five are upregulated: (miR-148a-3p|+1|0, miR-148a-3p|+1|–1, miR-148a-3p|0|–1, miR-148a-3p|0|–2, and miR-148a-3p|0|–3)) in MM compared to CM. The majority of the mature miRNAs of miR-181a-2-3p and miR-181b-5p are downregulated in MM (miR-181a-2-3p|0|+1, miR-181a-2-3p|–1|0, miR-181a-2-3p|–1|–1; miR-181b-5p|0|+1, miR-181b-5p|0|+2(+1U), miR-181b-5p|0|0), while only one is upregulated (miR-181a-2-3p|0|–3, miR-181b-5p|0|–3).

miR-21-5p, miR-22-3p, miR-24-3p and miR-30e-5p present mostly upregulated isomiRs (miR-21-5p|+2|0, miR-21-5p|+4|0, miR-21-5p|0|–2, miR-21-5p|0|–3, miR-21-5p|0|–4; miR-22-3p|+2|0, miR-

22-3p|0|–2, miR-22-3p|0|–3, miR-22-3p|0|–4; miR-24-3p|0|–3, miR-24-3p|0|–3(+1U); miR-24-3p|0|–4, miR-30e-5p|+1|–2, miR-30e-5p|0|–2, miR-30e-5p|0|–3) and only one downregulated (miR-21-5p|0|+2, miR-22-3p|0|+1(+1U), miR-24-3p|0|0(+2U), miR-30e-5p|+1|+4, respectively) in MM compared with CM. miR-23a-3p has two downregulated isomiRs (miR-23a-3p|0|+1(+2U), miR-23a-3p|0|+2(+1U)) and three upregulated isomiRs (miR-23a-3p|+1|–1, miR-23a-3p|0|–2, miR-23a-3p|0|–3) in MM vs. CM. miR-23b-3p and miR-500a-3p have only one upregulated mature miRNA (miR-23b-3p|0|–4, miR-500a-3p|–1|–3), while all the others are downregulated in MM (miR-23b-3p|+1|0, miR-23b-3p|+1|0(+1U), miR-23b-3p|0|0, miR-23b-3p|0|0(+1U), miR-23b-3p|0|–1(+1U), miR-23b-3p|0|–1(+2U); miR-500a-3p|0|+1(+1U), miR-500a-3p|–1|+1, miR-500a-3p|–1|0, miR-500a-3p|–1|–4). Finally, we found two downregulated isomiRs (miR-361-3p|+1|+2, miR-361-3p|0|+2) and two upregulated isomiRs of miR-361-3p (miR-361-3p|0|–2, miR-361-3p|0|–3) in MM vs. CM.

6.4.10 Identification of isomiRs associated with driver gene mutations in TCGA samples

Mutation status of BRAF, NRAS and NF1 for the melanoma samples was collected from the TCGA database (Supplementary Table S7 from Broseghini et al. [530]). For BRAF, the most frequent mutation is the missense mutation V600E, which is present in 145 samples. Among them, 21 melanomas have also the mutation V600M. For NRAS, there are frequently missense mutations in Q61- position. Specifically, 33 samples with Q61R, 28 samples with Q61K, 11 samples with Q61L and five samples with Q61H have been found. There is a wide variety of different mutations and different types of mutations of NF1, including missense, stop codon, frameshift, and splice mutations. We investigate the isomiR differential expression in mutated NF1, BRAF and NRAS compared to wild type (WT) samples.

6.4.10.1. Identification of mature miRNAs associated with mutated NF1

We collected the NF1 mutation status for 66 melanoma samples: 51 with at least one mutation in NF1, while 15 with wild type NF1. Mature miRNA expression was compared in melanomas with NF1mut vs. NF1wt (t Test unpaired unequal variance (Welch), adjusted *p value* < 0.01), and it emerged that five mature miRNAs were differentially expressed mature miRNAs (**Table 21**).

Table 21. List of mature microRNAs associated with NF1 mutation in TCGA SKCM samples

Comparison between NF1 mutated and NF1 WT samples					
Name	**Sequence**	**Type**	***p value* (Corr)**	**Regulation**	**FC**
hsa-miR-378a-3p|–1|–1(+1U)	CACTGGACTTGGAGTCAGAAGGT	mixed: shifted + 3'non-templated addition	7.77E-02	down	-2.55

hsa-let-7d-5p|+1|–1	GAGGTAGTAGGTTGCATAGT	mixed: start-site + end-site	9.29E-02	up	1.62
hsa-miR-148a-3p|+3|–1	GTGCACTACAGAACTTTG	mixed: start-site + end-site	7.77E-02	up	2.04
hsa-miR-584-5p|–1|–2	ATTATGGTTTGCCTGGGACTG	mixed: start-site + end-site	8.38E-02	up	2.75
hsa-miR-766-3p|0|–2	ACTCCAGCCCCACAGCCTCA	end-site	7.77E-02	up	2.26

6.4.10.2. Identification of mature miRNAs associated with mutated BRAF

TCGA provided BRAF mutation status of 187 melanoma samples: 168 had at least one mutation in BRAF while 19 are without BRAF mutations. The most frequent mutation of BRAF is in V600-position (149 patients): V600E (n= 118), V600E + V600M (n=21), V600M + V600G (n=3), V600E + V660V (n=2), V600E + other mutations (n=5). The association between isomiR expression and BRAF mutation, comparing mutated *vs*. wild type BRAF, was assessed and it resulted in a list 44 differentially expressed mature miRNAs. Most of them (n=42) are upregulated in BRAF mutated melanoma patients, while only two isomiRs are downregulated (hsa-miR-181a-2-3p|0|+1, hsa-miR-92a-3p|0|+1(+1U)) (**Table 22**).

Successively, we analyzed mature miRNAs that are specifically altered in BRAF (V600E) melanoma. Melanomas with exclusively V600E mutation and melanomas with both V600E and V600M BRAF mutations showed a different mature miRNA profile. There are 7 differentially expressed mature miRNAs: let-7b-3p|0|–1(+1U), miR-100-5p|0|0(+1U), miR-125b-5p|0|0, miR-221-3p|0|–1 are downregulated, while let-7a-5p|+1|–2, miR-1247-5p|0|–1, miR-219a-1-3p|0|0 are upregulated in V600E|V600M BRAF mutated melanomas compared to V600E BRAF mutated melanomas (**Table 22**).

Table 22. List of mature microRNAs associated with BRAF mutation in TCGA SKCM samples

IsomiRs differentially expressed in mutated vs. wild type (WT) BRAF melanoma samples

Name	Sequence	Type	*p value* (Corr)	Regulation	FC
hsa-miR-181a-2-3p|0|+1	ACCACTGACCGTTGACTGTACCT	end-site	2.17E-02	down	-1.57
hsa-miR-92a-3p|0|+1(+1U)	TATTGCACTTGTCCCGGCCTGTGT	mixed: end-site + 3' non-templated addition	2.14E-02	down	-1.31

hsa-let-7d-3p|0|–2(+2U)	CTATACGACCTGCTGCCTTTTT	mixed: end-site + 3' non-templated addition	4.40E-02	up	0.76
hsa-let-7i-3p|0|–2	CTGCGCAAGCTACTGCCTTG	end-site	2.12E-02	up	1.75
hsa-miR-100-5p|+1|–1	ACCCGTAGATCCGAACTTGT	mixed: start-site + end-site	2.14E-02	up	1.96
hsa-miR-100-5p|0|–1	AACCCGTAGATCCGAACTTGT	end-site	2.02E-02	up	2.00
hsa-miR-100-5p|0|–1(+2U)	AACCCGTAGATCCGAACTTGTTT	mixed: end-site + 3' non-templated addition	7.63E-07	up	1.39
hsa-miR-106b-3p|+1|–1	CGCACTGTGGGTACTTGCTG	mixed: start-site + end-site	4.49E-03	up	0.81
hsa-miR-1247-5p|0|–1	ACCCGTCCCGTTCGTCCCCGG	end-site	2.02E-02	up	0.96
hsa-miR-125b-5p|0|+1	TCCCTGAGACCCTAACTTGTGAG	end-site	2.44E-04	up	0.86
hsa-miR-1307-3p|0|–2	ACTCGGCGTGGCGTCGGTCG	end-site	3.05E-02	up	0.80
hsa-miR-143-3p|0|–3(+1U)	TGAGATGAAGCACTGTAGT	mixed: end-site + 3' non-templated addition	3.95E-02	up	1.06
hsa-miR-143-3p|–1|–1	CTGAGATGAAGCACTGTAGCT	shifted	4.64E-02	up	1.03
hsa-miR-143-3p|–1|–3	CTGAGATGAAGCACTGTAG	mixed: start-site + end-site	2.59E-02	up	1.21
hsa-miR-146a-5p|0|–4	TGAGAACTGAATTCCATG	end-site	3.11E-02	up	0.87
hsa-miR-154-5p|0|0	TAGGTTATCCGTGTTGCCTTCG	canonical	8.45E-03	up	0.94
hsa-miR-181c-5p|0|0	AACATTCAACCTGTCGGTGAGT	canonical	8.45E-03	up	-1.57
hsa-miR-199a-3p|+3|–1	GTAGTCTGCACATTGGTT	mixed: start-site + end-site	4.49E-03	up	1.07
hsa-miR-204-5p|0|0	TTCCCTTTGTCATCCTATGCCT	canonical	1.91E-02	up	0.82
hsa-miR-204-5p|0|0(+2U)	TTCCCTTTGTCATCCTATGCCTTT	3' non-templated addition	2.46E-02	up	1.95
hsa-miR-204-5p|0|–1	TTCCCTTTGTCATCCTATGCC	end-site	1.40E-02	up	0.87

hsa-miR-204-5p|0|–2	TTCCCTTTGTCATCCTATGC	end-site	1.60E-02	up	2.09
hsa-miR-214-5p|+1|0	GCCTGTCTACACTTGCTGTGC	start-site	2.59E-02	up	1.76
hsa-miR-296-3p|0|–2	GAGGGTTGGGTGGAGGCTCT	end-site	3.53E-05	up	0.96
hsa-miR-29a-3p|0|–4(+2U)	TAGCACCATCTGAAATCGTT	mixed: end-site + 3' non-templated addition	4.15E-03	up	0.98
hsa-miR-30c-2-3p|0|–2	CTGGGAGAAGGCTGTTTACT	end-site	1.39E-02	up	0.85
hsa-miR-330-5p|0|–1	TCTCTGGGCCTGTGTCTTAGG	end-site	2.54E-02	up	0.72
hsa-miR-342-3p|0|0(+1U)	TCTCACACAGAAATCGCACCCGTT	3' non-templated addition	4.49E-03	up	0.78
hsa-miR-342-5p|+1|+2	GGGGTGCTATCTGTGATTGAGG	mixed: start-site + end-site	1.09E-02	up	0.70
hsa-miR-381-3p|0|0	TATACAAGGGCAAGCTCTCTGT	canonical	2.52E-02	up	0.61
hsa-miR-409-5p|0|0	AGGTTACCCGAGCAACTTTGCAT	canonical	4.97E-02	up	0.94
hsa-miR-423-5p|0|–2	TGAGGGGCAGAGAGCGAGACT	end-site	2.54E-02	up	0.93
hsa-miR-432-5p|0|–1(+1U)	TCTTGGAGTAGGTCATTGGGTGT	mixed: end-site + 3' non-templated addition	4.64E-02	up	1.06
hsa-miR-485-3p|0|0	GTCATACACGGCTCTCCTCTCT	canonical	3.05E-02	up	1.00
hsa-miR-493-3p|0|–1	TGAAGGTCTACTGTGTGCCAG	end-site	9.25E-03	up	0.90
hsa-miR-495-3p|0|0	AAACAAACATGGTGCACTTCTT	canonical	8.45E-03	up	0.92
hsa-miR-518a-3p|0|0	GAAAGCGCTTCCCTTTGCTGGA	canonical	1.91E-02	up	0.89
hsa-miR-519a-5p|–1|–1	ACTCTAGAGGGAAGCGCTTTCT	shifted	2.44E-04	up	2.55
hsa-miR-625-3p|+1|–1(+1U)	ACTATAGAACTTTCCCCCTCT	mixed: start-site + end-site + 3' non-templated addition	3.90E-02	up	3.59

hsa-miR-671-3p|0|0	TCCGGTTCTCAGGGCTCCAC C	canonical	3.95E-02	up	0.85
hsa-miR-6892-5p|0|–1	GTAAGGGACCGGAGAGTAG G	end-site	2.44E-04	up	0.84
hsa-miR-758-5p|+2|+1	TGGTTGACCAGAGAGCACA CG	mixed: start-site + end-site	1.90E-03	up	0.89
hsa-miR-937-3p|0|–2	ATCCGCGCTCTGACTCTCTG	end-site	6.44E-03	up	0.91
hsa-miR-942-5p|0|–2	TCTTCTCTGTTTTGGCCATG	end-site	7.63E-07	up	1.09

Comparison between BRAF V600E and BRAF WT samples

Name	Sequence	Type	*p value* (Corr)	Regulation	FC
hsa-miR-181a-2-3p|0|+1	ACCACTGACCGTTGACTGTA CCT	end-site	0.0241	down	-2.91
hsa-miR-181a-2-3p|–1|–1	AACCACTGACCGTTGACTGT AC	shifted	0.0483	down	-2.29
hsa-let-7b-5p|0|–1	TGAGGTAGTAGGTTGTGTGG T	end-site	0.0289	up	2.13
hsa-let-7b-5p|0|–2	TGAGGTAGTAGGTTGTGTGG	end-site	0.0262	up	2.32
hsa-miR-100-5p|+1|–1	ACCCGTAGATCCGAACTTGT	mixed: start-site + end-site	0.0234	up	4.35
hsa-miR-100-5p|0|0	AACCCGTAGATCCGAACTTG TG	canonical	0.0262	up	3.62
hsa-miR-100-5p|0|–1	AACCCGTAGATCCGAACTTG T	end-site	0.0089	up	4.59
hsa-miR-125b-5p|0|0	TCCCTGAGACCCTAACTTGT GA	canonical	0.0323	up	2.70
hsa-miR-125b-5p|0|–1	TCCCTGAGACCCTAACTTGT G	end-site	0.0262	up	3.02
hsa-miR-146b-3p|0|0	GCCCTGTGGACTCAGTTCTG GT	canonical	0.0146	up	2.33
hsa-miR-181c-5p|0|0	AACATTCAACCTGTCGGTGA GT	canonical	0.0262	up	2.22
hsa-miR-204-5p|0|0	TTCCCTTTGTCATCCTATGCC T	canonical	0.0289	up	4.63

Comparison between BRAF V600E-V600M and BRAF V600E samples

Name	Sequence	Type	*p value* (Corr)	Regulation	FC
hsa-let-7b-3p|0|–1(+1U)	CTATACAACCTACTGCCTTC CT	mixed: end-site + 3' non-	0.03969	down	-2.30

		template addition			
hsa-miR-100-5p|0|0(+1U)	AACCCGTAGATCCGAACTTGTGT	3' non-template addition	0.03969	down	-4.14
hsa-miR-125b-5p|0|0	TCCCTGAGACCCTAACTTGTGA	canonical	0.03969	down	-2.77
hsa-miR-221-3p|0|–1	AGCTACATTGTCTGCTGGGTTT	end-site	0.03969	down	-2.29
hsa-let-7a-5p|+1|–2	GAGGTAGTAGGTTGTATAG	mixed: start-site + end-site	0.03969	up	2.14
hsa-miR-1247-5p|0|–1	ACCCGTCCCGTTCGTCCCCGG	end-site	0.03969	up	4.07
hsa-miR-219a-1-3p|0|0	AGAGTTGAGTCTGGACGTCCCG	canonical	0.03969	up	1.75

6.4.10.3. Identification of mature miRNAs associated with mutated NRAS

From the TCGA database, we obtained information about NRAS mutation status of 111 melanoma samples: 85 have at least one mutation in NRAS, while 26 melanomas have wild type NRAS. We identified six differentially expressed mature miRNAs by the comparison of mature miRNA expression profile (miR-17-3p|0|0, miR-17-3p|+1|0, miR-19b-3p|0|–1, miR-20a-5p|0|–2, miR-3614-5p|0|–1, and miR-509-3p|+4|+1) (**Table 23**).

Table 23. List of mature microRNAs associated with NRAS mutation in TCGA SKCM samples

Comparison between mutated NRAS and wild type (WT) NRAS					
Name	**Sequence**	**Type**	***p value* (Corr)**	**Regulation**	**FC**
hsa-miR-509-3p|+4|+1	TGGTACGTCTGTGGGTAGA	mixed: start-site + end-site	4.66E-02	down	-2.15
hsa-miR-17-3p|+1|0	CTGCAGTGAAGGCACTTGTAG	start-site	8.11E-02	up	1.90
hsa-miR-17-3p|0|0	ACTGCAGTGAAGGCACTTGTAG	canonical	2.11E-02	up	1.81
hsa-miR-19b-3p|0|–1	TGTGCAAATCCATGCAAAACTG	end-site	8.11E-02	up	1.73
hsa-miR-20a-5p|0|–2	TAAAGTGCTTATAGTGCAGGT	end-site	7.26E-02	up	1.80
hsa-miR-3614-5p|0|–1	CCACTTGGATCTGAAGGCTGCC	end-site	8.11E-02	up	1.80

7. DISCUSSION

7.1. Combined assessment of miR-21-5p and miR-146a-5p expression can be associated with BT measurement for SSM staging

Cutaneous melanoma is a potentially lethal form of skin cancer, and its incidence is constantly increasing. SSM and NM remain the two most common histologic subtypes and make up steady rates of about 65-70% and 20%, respectively, of all primary melanomas diagnosed [133,588]. Histologically, these two subtypes present relevant differences. On one hand, SSM is characterized by a predominantly epidermal component with a slow RGP that can be followed by a VGP when the diagnosis is delayed. On the other hand, NM frequently presents higher BT, lack of clinically significant intraepidermal involvement, and rapid VGP since onset.

BT is the most important histopathologic factor for primary melanoma staging and is an independent prognostic factor [589-591], specifically in SSM. In the last edition of AJCC, T1a and T1b subgroups were established using a BT of 0.8 mm as cut-off [140], in fact, this cut-off value has been accepted as the optimal value to separate patients with high and low risk in OS. Moreover, the survival rate of melanoma patients decreases more rapidly at BT ranging from 0.8 to 0.9mm than for BT above 0.9mm. Therefore, the correct evaluation of BT is necessary to obtain disease staging, to determinate eventual margins of excision, to decide if SNL biopsy should be performed and to guide follow-up and management of the patient [144].

However, several studies noticed imprecisions in BT measurements and describe significant impact on staging and patient management [146,592]. The failure to follow standardized thickness measurement guidelines and the wrong rounding of terminal decimal digits when BT values are registered, are potential sources of imprecision [592]. The clinical impact of inter-observer variability in the assessment of the histologic parameters of CM, based on the 7th edition AJCC staging system, showed discordance rate of 87% in any variable, and specifically 14% rate of discordance in BT measurement [146]. Another limitation of the exact BT determination in CM specimens is the sequential serial sectioning that can increase the BT in almost 50% of melanomas [593]. Upon this evidence, BT measurement can be a limitative parameter in CM staging and potentially leads to melanoma misclassification and subsequently incorrect or inappropriate management and follow-up [146].

Moreover, the use of BT is limited for NM. In fact, independently from BT on initial diagnosis, NM is associated with a worse prognosis. The increased aggressiveness of NM may be due to a different biological and genetic background compared to SSM: NM are associated with higher rate of

mutations in *NRAS* (*p value* <0.001) and in other NM-specific genes, such as Notch Receptor 4 (*NOTCH4*), Ankyrin 3 (*ANK3*) and Zinc Finger Protein 560 (*ZNF560*). NM histopathologic subtype has been proved to be an independent risk factor for survival [594].

This study aimed at investigating a molecular parameter with a smaller margin of error to support tumor stage evaluation. miRNAs expression can represent a valid molecular biomarker with a predictive role in assessment of tumoral staging that reinforces the BT determination.

We identified two miRNAs, namely miR-21-5p and miR-146a-5p, that display a strong, significant linear correlation with BT in SSM but not in NM subtype. Correlation between miRNA dysregulation and melanoma prognosis has been described by several studies [312]. miRNA levels are frequently compared in primary and metastatic melanoma, and the use of miRNA panels has been proposed in the general assessment of melanoma prognosis in terms of TTR and/or progression-free survival or OS. Moreover, a putative role of specific miRNAs in immune or target therapy resistance has been reported, demonstrating the interaction of these simple molecules in important pathogenetic pathways [491,595]. Recently, a meta-analysis identified a panel of diagnostic miRNAs able to distinguish melanoma to benign nevi with a receiver operating characteristic curve of 0.98 [596]. The potential use of miRNAs as prognostic biomarkers in melanoma is supported also by our data.

We focused on SSM histopathologic subtype to test the performance of a molecular parameter, namely miRNA expression, that objectively identifies high-risk SSM patients, thus potentially complementing BT assessment. The correlation between miR-21-5p and miR-146a-5p combined expression and BT was accurate and highly significant in our dataset of 90 SSMs provided by two different hospitals in Italy (Torino and Bologna). None of the previously identified high-risk subjects with BT determination was misclassified using miRNA parameter. Moreover, the miRNA parameter has shown the potential to reduce the overallocation of patients to the high-risk group. However, this hypothesis needs to be further confirmed in a larger, multicentric study. In addition, when we analyzed the OS and TTR of SSM, a significant difference in prognosis was associated with of 0.8mm BT cut-off value and 1.5 miRNA cut-off value. Patients with combined miRNA expression greater than 1.5 have a worse prognosis than patients with expression below 1.5.

miR-21-5p and miR-146a-5p were chosen based on their strong linear correlation with BT in a pilot group of samples. These two miRNAs are known to have a relevant role in melanoma.

miR-21-5p is an important cancer related miRNA. miR-21-5p has been found upregulated in primary lesions with histological atypia and mitotic activity [597], in melanoma cell lines compared to melanocytes [598], and in primary melanomas compared to benign nevi [597]. miR-21-5p expression

is an important prognostic factor in melanoma, in fact, it correlates with advanced clinical stage and poor survival [400]. miR-21-5p affects several cellular processes, including proliferation, migration, and apoptosis. In fact, the depletion of miR-21-5p in melanoma cells increases programmed cell death 4 (PDCD4), PTEN and BTG2 expression resulting in inhibition of proliferation and migration and in promotion of apoptosis [340]. Moreover, miR-21-5p upregulation promotes tumor growth and invasiveness through the downregulation of the tissue inhibitor of metalloproteinase-3 (TIMP3) [420] and inhibits apoptosis by affecting BCL-2 and Akt [400]. Consistent with our findings, it has been shown that miR-21 expression in higher in melanoma with BT > 1mm and advanced clinical stage [400].

Also miR-146a-5p plays an oncogenic role in melanoma. It was observed that miR-146a is upregulated by oncogenic BRAF and NRAS, and its overexpression in melanoma cell lines promotes proliferation and leads to tumor formation in mice [599]. miR-146a-5p induces melanoma cell growth by directly targeting lunatic fringe (LFNG) and Protein numb homolog (NUMB), which represses the NOTCH/PTEN/Akt pathway [337]. It was observed that miR-146a-5p can promote cell migration and invasion in melanoma by directly targeting SMAD Family Member 4 (SMAD4) [600]. Both miRNAs are largely involved in inflammatory processes [601].

The strong correlation that we observed between these two miRNAs and BT in SSM could be linked to their role in the promotion of the vertical growth phase. Since the fraction of tumor cells in all melanoma samples was microscopically estimated to be at least 70%, it is plausible that the increased expression of miR-21-5p and 146a-5p is an intrinsic feature of the tumor, with the main impact on tumor depth.

miRNA expression can be extremely useful in cases where the validation is required or where there is uncertainty surrounding the measurement of BT. miRNAs have shown the ability to replicate the accuracy of BT in identifying the lesions that subsequently metastasized. An advantage to use a molecular parameter, such as miRNA expression, is that it is objective and not susceptible to inter-operator variability or other confounding histopathologic factors, including the presence of regression. Regression indicates the loss of the thickness of the lesions with scarring fibrosis, increased vascularity, lymphocytic infiltrate, and accumulation of melanophages (melanin-containing macrophages found in pigmented skin lesions) [146,602]. Regression is a relatively common event and has been identified in up to 58% of thin melanomas [603], but its relationship with prognosis is controversial. The presence of regression can lead to an under or overestimated of BT when measured conventionally. We did not find any issue in estimating BT in samples with regression, and there was

not significant difference in miRNA expression between SSM with and without regression, thus supporting the utility of our molecular parameter in this subgroup of samples.

7.2. Comprehensive characterization of miRNA expression and regulatory network highlights mechanisms of tumor development and molecular features differentiating MPMs from single CMs.

Environmental and genetic factors can influence the risk of melanoma development [131]. A family history of melanoma has been widely correlated with an increased melanoma risk [8]. Also a personal history of melanoma is an important risk factor to develop CM: during their lifetime about 8% of patients with single melanoma will develop MPM [29,71-74]. This risk is higher in the first year after the first diagnosis and remained increased for at least 20 years [75]. Suggested predisposing factors involved in the development of MPM are high percentage of atypical nevi, family history of melanoma and an early onset of the disease (young age) [74].

Germline mutations that confer hereditary susceptibility can be present in families with history of CM, especially families where more than one member develop MPMs [604,605]. However, a very low prevalence of mutations in *CDKN2A* and *CDK4* genes has been reported in MPM patients [76]. Moreover, MPM patients without a family history have also been reported and in these cases germline mutations in melanoma predisposing genes are rarely detected [29,76,77]. Therefore, there are some other genetic or epigenetic factors active in MPM that promote multiple events of melanocytic transformation.

With a small RNA-seq approach, we provide the first comprehensive molecular characterization of MPMs by analyzing their miRNome. The global miRNA expression profile faithfully reflects the mRNA expression of cells and tissues, with the advantage to be obtainable also from FFPE samples, which is the typical available tissue for thin melanomas [606,607]. A specific expression pattern of MPM tumors were observed when compared to single CM. MPM miRNome is more similar to BN, thus suggesting a less aggressive and more differentiated phenotype. Family history of melanoma seems to have no impact in miRNA pattern, in fact, we observed no distinct miRNA pattern in MPMs with or without a recognized family history of melanoma. We validated a panel of miRNAs differently expressed between MPM and CM in a larger cohort. In addition, we obtained a panel of miRNAs differentially expressed in tumors from the same patient.

The prognosis of MPM patients is still controversial with studies stating that developing multiple melanomas is associated with worse prognosis or the opposite [608-610]. Analyzing with proper

multivariate statistical analysis, the Surveillance, Epidemiology, and End Results (SEER) data showed that there is no substantial difference among single CM and MPM patients [611].

From a biological point of view, we observed that MPMs have a less invasive phenotype as pointed out by the main regulatory pathways activated in these tumors, thus providing further elements of discussion to support a less aggressive behavior of MPM.

MPMs present higher expression levels of miRNAs known to inhibit EMT (e.g., miR-200 family, miR-205, miR-149) [584-586] compared to single CM. Tumor cells use EMT to escape from their microenvironment and migrate to new locations to form metastases [612]. Despite the neural crest origin of the melanocytes, EMT has been reported in melanoma cells, where it promotes the metastatic phenotype of malignant melanocytes [413,613]. E-cadherin is generally expressed by melanocytes and it mediates the adhesion between melanocytes and keratinocytes [614]. However, many studies in melanoma observed the loss of E-cadherin [615,616], which is the major hallmark of EMT.

We examined the cellular hubs regulated by specific miRNAs of MPM. We noticed that the main cellular hubs are centered in ITGA6, BTG2 and TLR4 proteins. The majority of the miRNAs that regulate these hubs are downregulated in MPM compared to CM, and high expression of these three genes is associated with a better prognosis in TCGA SKCM cohort.

ITGA6, (also named CD49f) is a transmembrane glycoprotein adhesion receptor that mediates cell-matrix and cell-cell interactions. ITGA6 is an important stem cell biomarker: it is the only common gene expressed in embryonic stem cells, neural stem cells, and hematopoietic stem cells [617,618]. More than 30 stem cell populations expressed ITGA6, including cancer stem cells [619]. The role of ITGA6 in melanoma is not clear. However, our observation point toward its high level in MPMs due to the miR-25 and miR-29 downregulation.

BTG2 is an anti-proliferative protein of the BTG/TOB family and its expression is p53 dependent [620]. However, its role can change based on the cell type [621]: BTG2 inhibits proliferation and migration in gastric cancer cells [622] and in lung cancer cells [623], while it promotes cancer cell migration in bladder cancer [624]. In B16 melanoma cells, miR-21 induces a metastatic behavior by suppressing many tumor suppressor proteins, including PTEN, PDCD4, and BTG2 [340]. MPMs shown downregulated levels of several miRNAs targeting BTG2, including miR-132-3p, miR-146a-5p and miR-15a-5p and miR-21-5p. Therefore, an upregulation of BTG2 expression is to be expected.

TLR4 plays an important role in inflammation and cancer. According to Human Protein Atlas, TLR4 protein is expressed at very low levels in melanoma cells *in vivo*. However, TLR4 activation has been

reported to promote an inflammatory microenvironment and tumor progression *in vitro* [625]. TLR4 promotes proliferation and migration of melanoma cells [626]. TLR4 also interacts with Tripartite Motif Containing 44 (TRIM44), which is a negative prognostic factor in melanoma [627]. This biological role for TLR4 in melanoma is partially in contrast with our observation of a better survival in MPM patients that have higher TLR4 levels.

7.3 A specific 3'isomiRs of miR-125a-5p is more expressed and presents different target genes compared to the canonical miRNAs

NGS data show a differential expression of miR-125a-5p between 1st and 2nd tumor in MPM patients, specifically, the expression was higher in the 2nd melanomas. However, qPCR technology did not confirm expected data. Investigating and observing the reads generated by the small RNA-seq experiment and referred to miR-125a-5p following the standard matching pipeline, we noticed that in all samples, most of the reads were shorter by 2nts. This specific isomiR, miR-125a-5p|0|–2 is highly expressed in our dataset and it is also the most expressed isoform of miR-125a-5p. NGS data showed a different expression trend in our groups (BN, CM, and MPM) of this isomiR if compared to its canonical form and resulted to be significantly differentially expressed in MPMs. The higher expression of the isomiR compared to the canonical form was confirmed in 11 FFPE melanoma samples by Db-ddPCR assay. This data needs to be further confirmed in a larger cohort. In addition, the differentially expression of miR-125a-5p|0|–2 between 1st and 2nd tumors in MPM patients need to be validated with Db-ddPCR assay.

We showed that this isomiR is highly abundant also in other tumors, as we confirmed by analyzing its levels across 32 tumor types from the TCGA database. This isomiR was also reported as more expressed compared to the canonical miRNA in colorectal cancer [528].

The bioinformatic analyses showed that miR-125a-5p|0|–2 putatively loses the ability to target and regulate a group of genes specifically involved in cell adhesion and cell differentiation of the canonical miRNA. In details, it seems that this 3' shorter isoform loses target genes involved in neuronal differentiation. Interestingly, miR-125 has specific role in adult nervous system development and neuronal differentiation [628,629]. The imbalance between major miR-125 variants in melanocytes could mean that miR-125 has a role in melanocyte development and differentiation from the neural crest [630], differentiating this lineage from other common ancestor cells. Consequently, its role can be reflected in melanoma development and progression.

Nevertheless, the isomiR lost many target of the canonical miRNA, miR-125a-5p|0|–2 gains 5 novel targets, namely TLX1 (HOX11), GLYATL1, SMARCE1 (BAF57), TMLHE and CLDN2.

Interestingly, three of the specific targets of the miR-125a-5p isomiR (SMARCE1, TLX1 and TMLHE) are involved also in nervous system processes.

SMARCE1 (BAF57) is a subunit of the ATP-dependent chromatin remodeling complex SWI/SNF, which is required to activate gene transcription normally repressed by chromatin [631]. In non-neuronal cell, it was observed that C-terminus of BAF57 interacts with CoREST to participate in REST/NRSF-mediated repression of neuronal traits [632]. Kazantseva et al. observed that in neurons there is an alternative splicing of BAF57 mRNA that led to deletions of exon 3 or exons 3-4 and results in N-terminally truncated BAF57 (N-BAF57) isoforms. These N-BAF57 isoforms are exclusively expressed in the brain. Functional studied confirmed that N-BAF57 proteins are associated with SWI/SNF complex in neuron and it was suggested that their role is to support neuronal phenotypes by regulating the expression of some neuron restrictive silencer element (NRSE)-containing genes [633].

Studied showed different roles of SMARCE1 in cancer development [634-638]. Interestingly, germline mutations in SMARCE1 have been found in uveal melanoma [639,640]. Finally, small interfering RNA (siRNA) against SMARCE1 is able to sensitize melanoma cells to cisplatin at low doses [641].

The second target involved in neurogenesis is the nuclear transcription factor TLX1, also named HOX11. TLX1 has been shown to be involved in many biological processes, including neurogenesis. The expression of TLX in adult neural stem cells leads to an undifferentiated and proliferative state [642,643]. In addition, TLX1 was described as post-mitotic selector gene that promotes with T Cell Leukemia Homeobox 3 (TLX3) the glutamatergic versus GABAergic cell fates in dorsal spinal cord during embryogenesis [644]. TLX1 was therefore associated to proliferation and self-renewing of neural stem cells. However, expression of TLX1 is not exclusive to neural stem cells, in fact, also rapidly dividing neural progenitor cells in the subventricular zone showed high TLX1 expression level [645]. It was also demonstrated that TLX1 plays a role also in hippocampal neurogenesis [646]. In addition, several studies support a role of this homeobox gene in oncogenesis [647-649].

TMLHE is a mitochondrial trimehyllysine dioxygenase, it catalyzes the first step of the biosynthesis of endogenous carnitine. Through an analysis of chromosome X exome, it emerged that TMLHE is linked to autism spectrum disorders and intellectual disability [650]. In addition, Ferreira et al. suggested that carnitine play an important role in neuroprotection during the development of the brain [651]. Melone et al. proposed that one of the main factor in metabolic cancer flexibility to adaption and survival used by cancer cell is the carnitine system [652].

The other two specific targets of the isoform of miR-125a-5p are not components of nervous system development, however they are linked to cancer. GLYATL1 was characterized in prostate cancer, where it is overexpressed and it is regulated by androgen and transcription factor ETS Variant Transcription Factor 1 (ETV1) [653]. The critical role of GLYATL1 in prostate cancer was confirmed through a meta-analysis of prostate cancer gene expression data [654].

CLDN2 is a tight junction involved in apical cell-cell adhesion and is fundament for epithelial cell polarity. It belongs to the group of claudins that are altered in several cancers. In particular, it was observed that CLDN2 is upregulated in endometrial endometrioid carcinoma, hepatoblastoma (fetal) and is downregulated in endometrial seropapillary carcinoma and in prostate carcinoma [655]. In addition, it was observed that CLDN2 is a strong negative prognostic factors in colorectal cancer [656], where it promotes self-renewal of cancer stem-like cells [657], and in breast cancer, where its high expression predicts early liver recurrences [658]. In osteosarcoma, CLDN2 seems to have a protective role, in fact it was suggested that it inhibits metastasis development by downregulating the afadin/ERK signaling pathway [659].

Human Protein Atlas has been used to investigate the association with these 5 proteins and melanoma patient survival. Lower expression levels of SMARCE1, TLX1 and GLYATL1 are associated with a better survival, while a low expression of TMLHE and CLDN2 are associated with a worst survival. However, only SMARCE1 and TLX1 show a significant difference between high and low expression.

In order to observe a possible effect of the isomiR in the regulation of the candidate target, we chose the protein associated to survival with the higher expression in melanoma, namely SMARCE1. In addition, SMARCE1 is the only of these five targets already described in melanoma. Interestingly, our computational analysis suggested that isoform miR-125a-5p targets and binds a nucleotides sequence located in exon 4 of SMARCE1 mRNA, which is the same exon that is normally removed in neuronal cells. Preliminary data showed a downregulation of protein level of SMARCE1 after 48h transfection of the isomiR. On the other hand, canonical miRNA seems to do not affect protein level, suggesting that SMARCE1 is a specific target of the 3' isoform miR-125a-5p. These results need to be validated; however they serve as the basis for further functional studies.

7.4. Non-random dysregulation of specific isomiRs contributes to the understanding of the complex melanoma pathogenesis

A single mature sequence for each miRNA is provide by miRBase database. This sequence is usually the sequence with the highest coverage reported in small RNA-seq experiment. According to the recent observation that isomiRs can discriminate human cancers [570], we detected a relevant number

of miRNA isoforms in our dataset of melanoma and benign nevi samples, and in primary melanoma and melanoma metastasis from SKCM TCGA dataset. We expected the canonical miRNAs to be the most abundant compared to its isomiRs. However, we found that in both FFPE and fresh-frozen melanoma samples several isomiRs are more abundant than the canonical forms, being up to 50 times more expressed in FFPE early-stage melanoma samples.

End-site isomiRs are the most represented group in both dataset, in according also with what has been observed in colon cancer [528]. Most of the highly expressed isomiRs belong to three important cancer-related miRNA families, namely miR-30 family, miR-200 family, and miR-10 family. Canonical miRNAs from these family were thoroughly described as key regulators in cancer and melanoma [660-663], while the functional role of their isomiRs is still unknown. We speculate that isomiRs could have relevant functional roles, similar to protein-coding gene isoforms, which were discovered to play an important role in biological diversity and evolution [664]. Cloonan et al. suggested that canonical miRNA works together with its isomiRs to increase the signal-to-noise ratio in miRNA-mRNA targeting [527].

Despite there is a concern in the literature about the fact that sequencing and/or mapping artefacts may result in an overrepresentation of isomiRs [558], it have been shown that isomiRs represent actual molecules rather than sequencing artifacts. In fact, most categories of isomiRs are detected at levels above thresholds comparable to their canonical miRNA sequence despite the use of aggressive filtering. Moreover, isomiRs can show increased levels as compared to the canonical miRNAs [527].

Different tissues present different isomiR profiles: the most abundant isoform does differ across tissues and disease states, suggesting that isomiR biogenesis may be a regulated process [665]. Sequence library preparation could cause miRNA degradation at the miRNA ends leading to the identification of miRNA variants. If true, these effects cannot explain the bias of the heterogeneity between the two miRNA ends in which the 3'-ends are usually more frequent than the 5'-ends [529]. Finally, it was observed that there is a significant number of isomiRs longer and more abundant than the canonical miRNA. These observations suggest that isomiRs are not experimental artifacts but rather true biological events. In this study, we used isoMiRmap pipeline, which comprehensively reports all isomiRs whose sequences exist within known miRNA sequences in a deterministic and exhaustive manner. This approach can identify also 3' non-templated isomiRs [582].

In addition to be able to discriminate human cancers, isomiRs could be used as diagnostic and prognostic biomarkers in several cancers and related subtypes; in fact, they can differentiate between healthy and non-healthy individuals [666].

In order to investigate the contribution of isomiRs to melanoma pathogenesis, we compared the isomiR profile of benign nevi and early-stage primary cutaneous melanoma FFPE samples, and of primary cutaneous melanoma and melanoma metastasis of fresh-frozen samples. We found 55 mature miRNAs (including canonical forms and isoforms) that were differently expressed between BN and early-stage melanoma. In some case, only the isomiR, and not the corresponding canonical miRNA, was differently expressed. Among these 55 mature miRNAs, we found 16 isomiRs that were more abundant than their canonical counterpart. These 16 miRNA variants were classified in four groups according to the expression trend in tumors compared to benign nevi and miRNA/isomiR relative abundance distribution.

Mature miRNAs with similar expression trends and similar abundance distribution in nevi and early-stage melanomas, include miR-19b-3p, miR-27a-3p, miR-29a-3p and miR-222-3p. Our data showed that canonical and isomiR of miR-19b-3p are downregulated in early-stage FFPE melanoma. However, *in vitro* study showed that miR-19b-3p expression is higher in most melanoma cell lines compared to normal melanocytes and promotes cell proliferation [338]. The expression of miR-27a-3p in melanoma seems to be positively correlated with tumor stage and lymph node metastasis of melanoma tissues. The downregulation of miR-27a-3p induces autophagy and apoptosis of melanoma cells [408]. However, there are no data about its differential expression between nevi and melanoma. We observed lower level of miR-29a-3p in early-stage melanoma, and this data seems in agreement with the literature that suggests a tumor suppressive role of this miRNA: its overexpression inhibits proliferation, migration, and invasion, and promotes apoptosis by blocking Wnt/β-catenin and NF-κB pathways [382]. miR-222-3p belongs to the miR-221 family, which is an important oncogenic miRNA family involved in the progression of melanoma and has a key role in EMT [341]. According to the literature, we found higher level of canonical and isomiRs of miR-222-3p in early-stage melanoma compared to benign nevi suggesting an oncogenic role. For this class of isomiRs, we hypothesized a cooperative effect of the isomiRs on the target genes.

The second class consists of canonical and isomiRs of miR-101-3p and miR-27b-3p, which have the same expression trend but different abundance distribution in benign nevi and early-stage melanomas. All mature miRNAs of miR-101-3p and miR-27b-3p are downregulated in melanoma. Our data agreed with previous studies describing these two canonical miRNAs as tumor suppressor miRNAs. miR-101-3p directly targets MITF and Enhancer of zeste homolog 2 (EZH2) leading to inhibition of invasion and proliferation. In addition, low expression of miR-101-3p has been associated to a poor survival in stage IV melanoma patients [321]. Canonical miR-27b-3p inhibits the melanoma development by targeting MYC [667].

The third class includes only canonical and isomiRs of miR-141-3p. A specific isomiR of miR-141-3p (miR-141-3p|0|–1) is downregulated in early-stage melanoma, while the canonical miRNA is not differentially expressed. In both benign nevi and early-stage melanoma, this specific isomiR is the most abundant variant. This seems to suggest that only this isomiR could have a protective role, and not the canonical form or the other variants. The canonical miR-141-3p has been found to inhibit the proliferation of melanoma cells [668].

Finally, the last class includes mature miRNAs of miR-30a-5p, miR-30d-5p and miR-203a-3p. This group showed different expression trend for at least two isoforms, and a different mature miRNA prevalence in benign nevi and early-stage melanomas. All these three canonical miRNAs have been extensively studied in melanoma.

In melanoma, miR-30a-5p acts as tumor suppressor miRNA. In fact, miR-30a-5p is generally downregulated in melanoma tissues and cell lines. The overexpression of miR-30a-5p results in a significant inhibition of proliferation, migration, and invasion *in vitro.* Moreover, overexpression of miR-30a-5p delays tumor growth [383] and inhibits metastasis [440] *in vivo*. In our analysis, although the difference is not statistically significant, canonical miR-30a-5p is more expressed in benign nevi than early-stage melanomas. We speculate that tumor suppressor effects may derive from the cumulative activity of all the isoforms.

On the other hand, miR-30d-5p is an oncomiR in melanoma. High level of miR-30d-5p in melanoma correlates with stage, metastatic potential, shorter time to recurrence, and reduced overall survival. Moreover, miR-30d-5p promotes metastatic behavior of melanoma cells [422]. In this analysis, BN and melanomas show similar expression levels of canonical miR-30d-5p, which is probably linked to the early stages of the melanomas. However, several isoforms of miR-30d-5p are significantly downregulated in melanoma.

MiR-203a-5p is an important tumor suppressor miRNA in melanoma, which is involved in the regulation of proliferation, cell cycle, migration, and invasion [372,373]. The expression of canonical miR-203a-3p is generally downregulated in melanoma, especially in metastatic melanoma. Low miR-203a-3p expression is associated with poor overall survival [435]. Also in this case, our data shown BN and melanomas with similar expression levels of canonical miR-203a-5p.

We took advantage of data available from TCGA to study the isomiR contribution to melanoma progression. TCGA database provides clinical and molecular data from fresh tumor tissues, including small RNA-seq data from primary melanoma and melanoma metastasis. SKCM cohort includes mostly advanced stages primary melanomas (stage II and stage III). Primary melanoma and

melanoma metastasis present strong differences in the isomiR profile: 121 mature miRNAs are downregulated and 211 are upregulated in melanoma metastases compared with primary melanomas. Among the differently expressed mature miRNAs there are miR-101-3p, miR-146b-3p, miR-148a-3p, miR-15a-5p, miR-16-5p, miR-181a-2-3p, miR-181a-5p, miR-181b-5p, miR-21-5p, miR-22-3p, miR-23a-5p, miR-23b-3p, miR-24-3p, miR-30e-5p, miR-361-3p, and miR-500a-3p that have at least two variants with opposite trends in primary melanoma and metastasis.

Molecular classification of melanoma is based on presence of mutations in key genes of the MAPK/ERK pathway, namely *NF1, NRAS* and *BRAF*. Many miRNAs are known to affect or to be affected by the altered activation of MAPK/ERK pathway in melanoma, and some of them are responsible for drug resistance [488]. In the literature, there is no study that analyzed the isomiR expression with mutation status of these genes. Thus, we focused on the different isomiR profiles associated with the mutation status of NF1, BRAF and NRAS. Information on the mutation status of BRAF, NRAS and NF1 for SKCM TCGA samples have been collected and used to investigate the association between isomiR expression and the most clinically relevant mutations in melanoma. Somatic mutations of BRAF are found in almost 47% of sporadic CM, and the most frequent mutation is the V600E (56%), while other activating mutation at codons 600 and 601, such as V600K V600R V600D K601E, were less frequent (20%, 2%, 1%, 2% respectively). NRAS mutations are found in 28% of the melanomas and almost all of them occurred at “hotspot” codons 12, 13 or 61 (6%, 4%, 86% respectively) [669]. In NF1, BRAF and NRAS mutation groups, several isomiRs differentially expressed have been identified suggesting that the identified isomiRs could have a suppressive, promotive or cooperative role in the MAPK pathway.

Several canonical miRNAs of isomiRs that are differently expressed in mutated BRAF samples have been already associated to BRAF. It was observed that vemurafenib (BRAFi) alters the miRNA expression in melanoma cells, leading to an upregulation of miR-181a-2-3p [670]. MiR-181c-5p is associated with the BRAF mutation in thyroid follicular adenomas, where it is found upregulated in RAS- or BRAF mutated follicular adenomas compared to wild-type tumors [671]. However, its role in melanoma needs to be established.

Among the miRNAs whose isoforms are associated with BRAF mutations, we found let-7a-5p and let-7b-5p, which are well known important tumor suppressor miRNAs in melanoma, where they inhibit proliferation and migration. Their expression is usually downregulated in melanomas [672]. miR-143-3p inhibits migration and proliferation and induces apoptosis *in vitro* [673]. Similarly, miR-330-5p, miR-342-5p, and miR-942-5p inhibit cell proliferation and invasion in cutaneous malignant melanoma [390,674,675]. miR-154-5p represses cell proliferation and metastasis in melanoma [676].

MAPK/ERK pathway can upregulate miRNAs in melanoma cells, specifically the miR-17-92 miRNA family [677]. We observed a remarkable upregulation of several isomiRs from the miR-17-92 cluster in NRAS mutant melanomas.

8. CONCLUSION

In conclusion, this study showed that miR-146a-5p and miR-21-5p expression significantly correlates with BT in SSM and their measurement in archive samples can complement and support standard BT assessment. The use of molecular marker as miRNAs may aid pathologists to deal with difficult cases where the BT is uncertain. Despite our results dataset has showed the potential prognostic role of miRNAs, it is relatively small. To validate these results, a multicentric study should be carried out. In addition, the correlation between miRNA expression and BT will be verified in other sample types, including atypical nevi and other histopathologic subtypes of melanoma, thereby broadening the spectrum of potential applications.

Then, we provide a comprehensive characterization of miRNA dysregulation and regulatory network in single primary CM and MPMs. A less aggressive phenotype of MPMs is supported by the pattern of miRNA alterations thus confirming the relevance of small noncoding RNA alterations in this fascinating—but poorly studied—melanoma subtype.

Focusing only on canonical miRNAs has the risk to overlook and lose important information that could improve our understanding of cancer pathogenesis. Indeed, we described isomiR dysregulation in benign nevi, melanoma at different stages and sources, and melanoma metastasis. IsomiRs can be more expressed than their canonical miRNA and different miRNA variants are modulated in different and sometimes opposite ways in normal and tumor samples, a fact that was not expected. Preliminary data confirm the higher expression of a specific isoform of miR-125a-5p compared to the canonical form. In addition, the results suggest that this isomiR acts differently compared to the canonical counterpart by targeting different proteins. Our results have provided a prospective functional role for isomiRs, although functional studies need to be performed for definitive confirmation. We also reported that isomiRs can be associated with tumor mutation status, sometimes diverging from the trend of the canonical miRNAs. Our results and observations about a non-random dysregulation of specific isomiRs in melanoma serve as the basis for further functional studies.

9. BIBLIOGRAPHY

1. Gershenwald, J.E.; Scolyer, R.A. Melanoma Staging: American Joint Committee on Cancer (AJCC) 8th Edition and Beyond. *Ann Surg Oncol* **2018**, *25*, 2105-2110, doi:10.1245/s10434-018-6513-7.
2. Erdmann, F.; Lortet-Tieulent, J.; Schuz, J.; Zeeb, H.; Greinert, R.; Breitbart, E.W.; Bray, F. International trends in the incidence of malignant melanoma 1953-2008--are recent generations at higher or lower risk? *Int J Cancer* **2013**, *132*, 385-400, doi:10.1002/ijc.27616.
3. NIH. SEER Cancer Stat Facts: Melanoma of the Skin. **2019**.
4. Matthews, N.H., Li Wen-Qing Li, Qureshi A. A., Weinstock M. A., and Eunyoung Cho. CUTANEOUS MELANOMA. Etiology and Therapy. Chapter I: Epidemiology of Melanoma. **2017**.
5. WHO. Cancer fact sheet: Melanoma of skin. *Cancer Today* **2018**.
6. Weir, H.K.; Marrett, L.D.; Cokkinides, V.; Barnholtz-Sloan, J.; Patel, P.; Tai, E.; Jemal, A.; Li, J.; Kim, J.; Ekwueme, D.U. Melanoma in adolescents and young adults (ages 15-39 years): United States, 1999-2006. *J Am Acad Dermatol* **2011**, *65*, S38-49, doi:10.1016/j.jaad.2011.04.038.
7. Rastrelli, M.; Tropea, S.; Pigozzo, J.; Bezzon, E.; Campana, L.G.; Stramare, R.; Alaibac, M.; Rossi, C.R. Melanoma m1: diagnosis and therapy. *In Vivo* **2014**, *28*, 273-285.
8. Gandini, S.; Sera, F.; Cattaruzza, M.S.; Pasquini, P.; Zanetti, R.; Masini, C.; Boyle, P.; Melchi, C.F. Meta-analysis of risk factors for cutaneous melanoma: III. Family history, actinic damage and phenotypic factors. *Eur J Cancer* **2005**, *41*, 2040-2059, doi:10.1016/j.ejca.2005.03.034.
9. Chaudru, V.; Chompret, A.; Bressac-de Paillerets, B.; Spatz, A.; Avril, M.F.; Demenais, F. Influence of genes, nevi, and sun sensitivity on melanoma risk in a family sample unselected by family history and in melanoma-prone families. *J Natl Cancer Inst* **2004**, *96*, 785-795, doi:10.1093/jnci/djh136.
10. Elwood, J.M.; Koh, H.K. Etiology, epidemiology, risk factors, and public health issues of melanoma. *Curr Opin Oncol* **1994**, *6*, 179-187, doi:10.1097/00001622-199403000-00011.
11. Newton-Bishop, J.A.; Chang, Y.M.; Elliott, F.; Chan, M.; Leake, S.; Karpavicius, B.; Haynes, S.; Fitzgibbon, E.; Kukalizch, K.; Randerson-Moor, J.; et al. Relationship between sun exposure and melanoma risk for tumours in different body sites in a large case-control study in a temperate climate. *Eur J Cancer* **2011**, *47*, 732-741, doi:10.1016/j.ejca.2010.10.008.
12. Bais, A.F.; Lucas, R.M.; Bornman, J.F.; Williamson, C.E.; Sulzberger, B.; Austin, A.T.; Wilson, S.R.; Andrady, A.L.; Bernhard, G.; McKenzie, R.L.; et al. Environmental effects of ozone depletion, UV radiation and interactions with climate change: UNEP Environmental Effects Assessment Panel, update 2017. *Photochem Photobiol Sci* **2018**, *17*, 127-179, doi:10.1039/c7pp90043k.
13. Gilchrest, B.A.; Eller, M.S.; Geller, A.C.; Yaar, M. The pathogenesis of melanoma induced by ultraviolet radiation. *N Engl J Med* **1999**, *340*, 1341-1348, doi:10.1056/NEJM199904293401707.
14. Gandini, S.; Sera, F.; Cattaruzza, M.S.; Pasquini, P.; Picconi, O.; Boyle, P.; Melchi, C.F. Meta-analysis of risk factors for cutaneous melanoma: II. Sun exposure. *Eur J Cancer* **2005**, *41*, 45-60, doi:10.1016/j.ejca.2004.10.016.
15. Wojcik, K.Y.; Escobedo, L.A.; Wysong, A.; Heck, J.E.; Ritz, B.; Hamilton, A.S.; Milam, J.; Cockburn, M.G. High Birth Weight, Early UV Exposure, and Melanoma Risk in Children, Adolescents, and Young Adults. *Epidemiology* **2019**, *30*, 278-284, doi:10.1097/EDE.0000000000000963.
16. Arnold, M.; Kvaskoff, M.; Thuret, A.; Guenel, P.; Bray, F.; Soerjomataram, I. Cutaneous melanoma in France in 2015 attributable to solar ultraviolet radiation and the use of sunbeds. *J Eur Acad Dermatol Venereol* **2018**, *32*, 1681-1686, doi:10.1111/jdv.15022.

17. Naldi, L.; Lorenzo Imberti, G.; Parazzini, F.; Gallus, S.; La Vecchia, C. Pigmentary traits, modalities of sun reaction, history of sunburns, and melanocytic nevi as risk factors for cutaneous malignant melanoma in the Italian population: results of a collaborative case-control study. *Cancer* **2000**, *88*, 2703-2710, doi:10.1002/1097-0142(20000615)88:12<2703::aid-cncr8>3.0.co;2-q.
18. Bliss, J.M.; Ford, D.; Swerdlow, A.J.; Armstrong, B.K.; Cristofolini, M.; Elwood, J.M.; Green, A.; Holly, E.A.; Mack, T.; MacKie, R.M.; et al. Risk of cutaneous melanoma associated with pigmentation characteristics and freckling: systematic overview of 10 case-control studies. The International Melanoma Analysis Group (IMAGE). *Int J Cancer* **1995**, *62*, 367-376, doi:10.1002/ijc.2910620402.
19. Titus-Ernstoff, L.; Perry, A.E.; Spencer, S.K.; Gibson, J.J.; Cole, B.F.; Ernstoff, M.S. Pigmentary characteristics and moles in relation to melanoma risk. *Int J Cancer* **2005**, *116*, 144-149, doi:10.1002/ijc.21001.
20. Haenssle, H.A.; Mograby, N.; Ngassa, A.; Buhl, T.; Emmert, S.; Schon, M.P.; Rosenberger, A.; Bertsch, H.P. Association of Patient Risk Factors and Frequency of Nevus-Associated Cutaneous Melanomas. *JAMA Dermatol* **2016**, *152*, 291-298, doi:10.1001/jamadermatol.2015.3775.
21. Purdue, M.P.; From, L.; Armstrong, B.K.; Kricker, A.; Gallagher, R.P.; McLaughlin, J.R.; Klar, N.S.; Marrett, L.D.; Genes, E.; Melanoma Study, G. Etiologic and other factors predicting nevus-associated cutaneous malignant melanoma. *Cancer Epidemiol Biomarkers Prev* **2005**, *14*, 2015-2022, doi:10.1158/1055-9965.EPI-05-0097.
22. Gandini, S.; Sera, F.; Cattaruzza, M.S.; Pasquini, P.; Abeni, D.; Boyle, P.; Melchi, C.F. Meta-analysis of risk factors for cutaneous melanoma: I. Common and atypical naevi. *Eur J Cancer* **2005**, *41*, 28-44, doi:10.1016/j.ejca.2004.10.015.
23. Anderson, D.E.; Badzioch, M.D. Hereditary cutaneous malignant melanoma: a 20-year family update. *Anticancer Res* **1991**, *11*, 433-437.
24. Colombino, M.; Sini, M.; Lissia, A.; De Giorgi, V.; Stanganelli, I.; Ayala, F.; Massi, D.; Rubino, C.; Manca, A.; Paliogiannis, P.; et al. Discrepant alterations in main candidate genes among multiple primary melanomas. *J Transl Med* **2014**, *12*, 117, doi:10.1186/1479-5876-12-117.
25. Pasquali, E.; Garcia-Borron, J.C.; Fargnoli, M.C.; Gandini, S.; Maisonneuve, P.; Bagnardi, V.; Specchia, C.; Liu, F.; Kayser, M.; Nijsten, T.; et al. MC1R variants increased the risk of sporadic cutaneous melanoma in darker-pigmented Caucasians: a pooled-analysis from the M-SKIP project. *Int J Cancer* **2015**, *136*, 618-631, doi:10.1002/ijc.29018.
26. Shain, A.H.; Yeh, I.; Kovalyshyn, I.; Sriharan, A.; Talevich, E.; Gagnon, A.; Dummer, R.; North, J.; Pincus, L.; Ruben, B.; et al. The Genetic Evolution of Melanoma from Precursor Lesions. *N Engl J Med* **2015**, *373*, 1926-1936, doi:10.1056/NEJMoa1502583.
27. Potrony, M.; Badenas, C.; Aguilera, P.; Puig-Butille, J.A.; Carrera, C.; Malvehy, J.; Puig, S. Update in genetic susceptibility in melanoma. *Ann Transl Med* **2015**, *3*, 210, doi:10.3978/j.issn.2305-5839.2015.08.11.
28. Badenas, C.; Aguilera, P.; Puig-Butille, J.A.; Carrera, C.; Malvehy, J.; Puig, S. Genetic counseling in melanoma. *Dermatol Ther* **2012**, *25*, 397-402, doi:10.1111/j.1529-8019.2012.01499.x.
29. Helgadottir, H.; Tuominen, R.; Olsson, H.; Hansson, J.; Hoiom, V. Cancer risks and survival in patients with multiple primary melanomas: Association with family history of melanoma and germline CDKN2A mutation status. *J Am Acad Dermatol* **2017**, *77*, 893-901, doi:10.1016/j.jaad.2017.05.050.
30. Tsao, H.; Niendorf, K. Genetic testing in hereditary melanoma. *J Am Acad Dermatol* **2004**, *51*, 803-808, doi:10.1016/j.jaad.2004.04.045.
31. Read, J.; Wadt, K.A.; Hayward, N.K. Melanoma genetics. *J Med Genet* **2016**, *53*, 1-14, doi:10.1136/jmedgenet-2015-103150.

32. Zocchi, L.; Lontano, A.; Merli, M.; Dika, E.; Nagore, E.; Quaglino, P.; Puig, S.; Ribero, S. Familial Melanoma and Susceptibility Genes: A Review of the Most Common Clinical and Dermoscopic Phenotypic Aspect, Associated Malignancies and Practical Tips for Management. *J Clin Med* **2021**, *10*, doi:10.3390/jcm10163760.
33. Aoude, L.G.; Wadt, K.A.; Pritchard, A.L.; Hayward, N.K. Genetics of familial melanoma: 20 years after CDKN2A. *Pigment Cell Melanoma Res* **2015**, *28*, 148-160, doi:10.1111/pcmr.12333.
34. Goldstein, A.M.; Chan, M.; Harland, M.; Hayward, N.K.; Demenais, F.; Bishop, D.T.; Azizi, E.; Bergman, W.; Bianchi-Scarra, G.; Bruno, W.; et al. Features associated with germline CDKN2A mutations: a GenoMEL study of melanoma-prone families from three continents. *J Med Genet* **2007**, *44*, 99-106, doi:10.1136/jmg.2006.043802.
35. Goldstein, A.M.; Chan, M.; Harland, M.; Gillanders, E.M.; Hayward, N.K.; Avril, M.F.; Azizi, E.; Bianchi-Scarra, G.; Bishop, D.T.; Bressac-de Paillerets, B.; et al. High-risk melanoma susceptibility genes and pancreatic cancer, neural system tumors, and uveal melanoma across GenoMEL. *Cancer Res* **2006**, *66*, 9818-9828, doi:10.1158/0008-5472.CAN-06-0494.
36. Helgadottir, H.; Hoiom, V.; Jonsson, G.; Tuominen, R.; Ingvar, C.; Borg, A.; Olsson, H.; Hansson, J. High risk of tobacco-related cancers in CDKN2A mutation-positive melanoma families. *J Med Genet* **2014**, *51*, 545-552, doi:10.1136/jmedgenet-2014-102320.
37. McWilliams, R.R.; Wieben, E.D.; Rabe, K.G.; Pedersen, K.S.; Wu, Y.; Sicotte, H.; Petersen, G.M. Prevalence of CDKN2A mutations in pancreatic cancer patients: implications for genetic counseling. *Eur J Hum Genet* **2011**, *19*, 472-478, doi:10.1038/ejhg.2010.198.
38. Goldstein, A.M.; Chaudru, V.; Ghiorzo, P.; Badenas, C.; Malvehy, J.; Pastorino, L.; Laud, K.; Hulley, B.; Avril, M.F.; Puig-Butille, J.A.; et al. Cutaneous phenotype and MC1R variants as modifying factors for the development of melanoma in CDKN2A G101W mutation carriers from 4 countries. *Int J Cancer* **2007**, *121*, 825-831, doi:10.1002/ijc.22712.
39. Nikolaou, V.; Kang, X.; Stratigos, A.; Gogas, H.; Latorre, M.C.; Gabree, M.; Plaka, M.; Njauw, C.N.; Kypreou, K.; Mirmigi, I.; et al. Comprehensive mutational analysis of CDKN2A and CDK4 in Greek patients with cutaneous melanoma. *Br J Dermatol* **2011**, *165*, 1219-1222, doi:10.1111/j.1365-2133.2011.10551.x.
40. Puntervoll, H.E.; Yang, X.R.; Vetti, H.H.; Bachmann, I.M.; Avril, M.F.; Benfodda, M.; Catricala, C.; Dalle, S.; Duval-Modeste, A.B.; Ghiorzo, P.; et al. Melanoma prone families with CDK4 germline mutation: phenotypic profile and associations with MC1R variants. *J Med Genet* **2013**, *50*, 264-270, doi:10.1136/jmedgenet-2012-101455.
41. Horn, S.; Figl, A.; Rachakonda, P.S.; Fischer, C.; Sucker, A.; Gast, A.; Kadel, S.; Moll, I.; Nagore, E.; Hemminki, K.; et al. TERT promoter mutations in familial and sporadic melanoma. *Science* **2013**, *339*, 959-961, doi:10.1126/science.1230062.
42. Carbone, M.; Yang, H.; Pass, H.I.; Krausz, T.; Testa, J.R.; Gaudino, G. BAP1 and cancer. *Nat Rev Cancer* **2013**, *13*, 153-159, doi:10.1038/nrc3459.
43. Wadt, K.A.; Aoude, L.G.; Johansson, P.; Solinas, A.; Pritchard, A.; Crainic, O.; Andersen, M.T.; Kiilgaard, J.F.; Heegaard, S.; Sunde, L.; et al. A recurrent germline BAP1 mutation and extension of the BAP1 tumor predisposition spectrum to include basal cell carcinoma. *Clin Genet* **2015**, *88*, 267-272, doi:10.1111/cge.12501.
44. Wiesner, T.; Obenauf, A.C.; Murali, R.; Fried, I.; Griewank, K.G.; Ulz, P.; Windpassinger, C.; Wackernagel, W.; Loy, S.; Wolf, I.; et al. Germline mutations in BAP1 predispose to melanocytic tumors. *Nat Genet* **2011**, *43*, 1018-1021, doi:10.1038/ng.910.
45. Wiesner, T.; Fried, I.; Ulz, P.; Stacher, E.; Popper, H.; Murali, R.; Kutzner, H.; Lax, S.; Smolle-Juttner, F.; Geigl, J.B.; et al. Toward an improved definition of the tumor spectrum associated with BAP1 germline mutations. *J Clin Oncol* **2012**, *30*, e337-340, doi:10.1200/JCO.2011.41.2965.

46. Murali, R.; Wilmott, J.S.; Jakrot, V.; Al-Ahmadie, H.A.; Wiesner, T.; McCarthy, S.W.; Thompson, J.F.; Scolyer, R.A. BAP1 expression in cutaneous melanoma: a pilot study. *Pathology* **2013**, *45*, 606-609, doi:10.1097/PAT.0b013e3283653818.
47. Yang, X.R.; Brown, K.; Landi, M.T.; Ghiorzo, P.; Badenas, C.; Xu, M.; Hayward, N.K.; Calista, D.; Landi, G.; Bruno, W.; et al. Duplication of CXC chemokine genes on chromosome 4q13 in a melanoma-prone family. *Pigment Cell Melanoma Res* **2012**, *25*, 243-247, doi:10.1111/j.1755-148X.2012.00969.x.
48. Han, J.; Qureshi, A.A.; Prescott, J.; Guo, Q.; Ye, L.; Hunter, D.J.; De Vivo, I. A prospective study of telomere length and the risk of skin cancer. *J Invest Dermatol* **2009**, *129*, 415-421, doi:10.1038/jid.2008.238.
49. Iles, M.M.; Bishop, D.T.; Taylor, J.C.; Hayward, N.K.; Brossard, M.; Cust, A.E.; Dunning, A.M.; Lee, J.E.; Moses, E.K.; Akslen, L.A.; et al. The effect on melanoma risk of genes previously associated with telomere length. *J Natl Cancer Inst* **2014**, *106*, doi:10.1093/jnci/dju267.
50. Palm, W.; de Lange, T. How shelterin protects mammalian telomeres. *Annu Rev Genet* **2008**, *42*, 301-334, doi:10.1146/annurev.genet.41.110306.130350.
51. Flynn, R.L.; Zou, L. Oligonucleotide/oligosaccharide-binding fold proteins: a growing family of genome guardians. *Crit Rev Biochem Mol Biol* **2010**, *45*, 266-275, doi:10.3109/10409238.2010.488216.
52. Robles-Espinoza, C.D.; Harland, M.; Ramsay, A.J.; Aoude, L.G.; Quesada, V.; Ding, Z.; Pooley, K.A.; Pritchard, A.L.; Tiffen, J.C.; Petljak, M.; et al. POT1 loss-of-function variants predispose to familial melanoma. *Nat Genet* **2014**, *46*, 478-481, doi:10.1038/ng.2947.
53. Aoude, L.G.; Pritchard, A.L.; Robles-Espinoza, C.D.; Wadt, K.; Harland, M.; Choi, J.; Gartside, M.; Quesada, V.; Johansson, P.; Palmer, J.M.; et al. Nonsense mutations in the shelterin complex genes ACD and TERF2IP in familial melanoma. *J Natl Cancer Inst* **2015**, *107*, doi:10.1093/jnci/dju408.
54. Williams, P.F.; Olsen, C.M.; Hayward, N.K.; Whiteman, D.C. Melanocortin 1 receptor and risk of cutaneous melanoma: a meta-analysis and estimates of population burden. *Int J Cancer* **2011**, *129*, 1730-1740, doi:10.1002/ijc.25804.
55. Flanagan, N.; Healy, E.; Ray, A.; Philips, S.; Todd, C.; Jackson, I.J.; Birch-Machin, M.A.; Rees, J.L. Pleiotropic effects of the melanocortin 1 receptor (MC1R) gene on human pigmentation. *Hum Mol Genet* **2000**, *9*, 2531-2537, doi:10.1093/hmg/9.17.2531.
56. Raimondi, S.; Sera, F.; Gandini, S.; Iodice, S.; Caini, S.; Maisonneuve, P.; Fargnoli, M.C. MC1R variants, melanoma and red hair color phenotype: a meta-analysis. *Int J Cancer* **2008**, *122*, 2753-2760, doi:10.1002/ijc.23396.
57. Cordoba-Lanus, E.; Hernandez-Jimenez, J.G.; Medina-Coello, C.; Espinoza-Jimenez, A.; Gonzalez, A.; Rodriguez-Perez, M.D.; Carretero-Hernandez, G.; Almeida, P.; Suarez-Hernandez, J.; Perera-Molinero, A.; et al. MC1R gene variants and sporadic malignant melanoma susceptibility in the Canary Islands population. *Arch Dermatol Res* **2014**, *306*, 51-58, doi:10.1007/s00403-013-1420-z.
58. Puig-Butille, J.A.; Carrera, C.; Kumar, R.; Garcia-Casado, Z.; Badenas, C.; Aguilera, P.; Malvehy, J.; Nagore, E.; Puig, S. Distribution of MC1R variants among melanoma subtypes: p.R163Q is associated with lentigo maligna melanoma in a Mediterranean population. *Br J Dermatol* **2013**, *169*, 804-811, doi:10.1111/bjd.12418.
59. Fargnoli, M.C.; Gandini, S.; Peris, K.; Maisonneuve, P.; Raimondi, S. MC1R variants increase melanoma risk in families with CDKN2A mutations: a meta-analysis. *Eur J Cancer* **2010**, *46*, 1413-1420, doi:10.1016/j.ejca.2010.01.027.
60. Moller, K.; Sigurbjornsdottir, S.; Arnthorsson, A.O.; Pogenberg, V.; Dilshat, R.; Fock, V.; Brynjolfsdottir, S.H.; Bindesboll, C.; Bessadottir, M.; Ogmundsdottir, H.M.; et al. MITF has a central role in regulating starvation-induced autophagy in melanoma. *Sci Rep* **2019**, *9*, 1055, doi:10.1038/s41598-018-37522-6.

61. Bertolotto, C.; Lesueur, F.; Giuliano, S.; Strub, T.; de Lichy, M.; Bille, K.; Dessen, P.; d'Hayer, B.; Mohamdi, H.; Remenieras, A.; et al. Corrigendum: A SUMOylation-defective MITF germline mutation predisposes to melanoma and renal carcinoma. *Nature* **2016**, *531*, 126, doi:10.1038/nature16158.
62. Sturm, R.A.; Fox, C.; McClenahan, P.; Jagirdar, K.; Ibarrola-Villava, M.; Banan, P.; Abbott, N.C.; Ribas, G.; Gabrielli, B.; Duffy, D.L.; et al. Phenotypic characterization of nevus and tumor patterns in MITF E318K mutation carrier melanoma patients. *J Invest Dermatol* **2014**, *134*, 141-149, doi:10.1038/jid.2013.272.
63. Ward, K.A.; Lazovich, D.; Hordinsky, M.K. Germline melanoma susceptibility and prognostic genes: a review of the literature. *J Am Acad Dermatol* **2012**, *67*, 1055-1067, doi:10.1016/j.jaad.2012.02.042.
64. Fernandez, L.P.; Milne, R.L.; Pita, G.; Floristan, U.; Sendagorta, E.; Feito, M.; Aviles, J.A.; Martin-Gonzalez, M.; Lazaro, P.; Benitez, J.; et al. Pigmentation-related genes and their implication in malignant melanoma susceptibility. *Exp Dermatol* **2009**, *18*, 634-642, doi:10.1111/j.1600-0625.2009.00846.x.
65. Ogbah, Z.; Badenas, C.; Harland, M.; Puig-Butille, J.A.; Elliot, F.; Bonifaci, N.; Guino, E.; Randerson-Moor, J.; Chan, M.; Iles, M.M.; et al. Evaluation of PAX3 genetic variants and nevus number. *Pigment Cell Melanoma Res* **2013**, *26*, 666-676, doi:10.1111/pcmr.12130.
66. Planelles, D.; Nagore, E.; Moret, A.; Botella-Estrada, R.; Vila, E.; Guillen, C.; Montoro, J.A. HLA class II polymorphisms in Spanish melanoma patients: homozygosity for HLA-DQA1 locus can be a potential melanoma risk factor. *Br J Dermatol* **2006**, *154*, 261-266, doi:10.1111/j.1365-2133.2005.06896.x.
67. Pena-Chilet, M.; Blanquer-Maceiras, M.; Ibarrola-Villava, M.; Martinez-Cadenas, C.; Martin-Gonzalez, M.; Gomez-Fernandez, C.; Mayor, M.; Aviles, J.A.; Lluch, A.; Ribas, G. Genetic variants in PARP1 (rs3219090) and IRF4 (rs12203592) genes associated with melanoma susceptibility in a Spanish population. *BMC Cancer* **2013**, *13*, 160, doi:10.1186/1471-2407-13-160.
68. Ibarrola-Villava, M.; Martin-Gonzalez, M.; Lazaro, P.; Pizarro, A.; Lluch, A.; Ribas, G. Role of glutathione S-transferases in melanoma susceptibility: association with GSTP1 rs1695 polymorphism. *Br J Dermatol* **2012**, *166*, 1176-1183, doi:10.1111/j.1365-2133.2012.10831.x.
69. Iles, M.M.; Law, M.H.; Stacey, S.N.; Han, J.; Fang, S.; Pfeiffer, R.; Harland, M.; Macgregor, S.; Taylor, J.C.; Aben, K.K.; et al. A variant in FTO shows association with melanoma risk not due to BMI. *Nat Genet* **2013**, *45*, 428-432, 432e421, doi:10.1038/ng.2571.
70. Tsao, H.; Chin, L.; Garraway, L.A.; Fisher, D.E. Melanoma: from mutations to medicine. *Genes Dev* **2012**, *26*, 1131-1155, doi:10.1101/gad.191999.112.
71. De Simone, P.; Valiante, M.; Silipo, V. Familial melanoma and multiple primary melanoma. *G Ital Dermatol Venereol* **2017**, *152*, 262-265, doi:10.23736/S0392-0488.17.05554-7.
72. Johnson, T.M.; Hamilton, T.; Lowe, L. Multiple primary melanomas. *J Am Acad Dermatol* **1998**, *39*, 422-427, doi:10.1016/s0190-9622(98)70318-4.
73. Levi, F.; Randimbison, L.; Te, V.C.; La Vecchia, C. High constant incidence rates of second cutaneous melanomas. *Int J Cancer* **2005**, *117*, 877-879, doi:10.1002/ijc.21262.
74. Ferrone, C.R.; Ben Porat, L.; Panageas, K.S.; Berwick, M.; Halpern, A.C.; Patel, A.; Coit, D.G. Clinicopathological features of and risk factors for multiple primary melanomas. *JAMA* **2005**, *294*, 1647-1654, doi:10.1001/jama.294.13.1647.
75. Adler, N.R.; Kelly, J.W.; Haydon, A.; McLean, C.A.; Mar, V.J. Clinicopathological characteristics and prognosis of patients with multiple primary melanomas. *Br J Dermatol* **2018**, *178*, e44-e45, doi:10.1111/bjd.15855.
76. Casula, M.; Paliogiannis, P.; Ayala, F.; De Giorgi, V.; Stanganelli, I.; Mandala, M.; Colombino, M.; Manca, A.; Sini, M.C.; Caraco, C.; et al. Germline and somatic mutations in

patients with multiple primary melanomas: a next generation sequencing study. *BMC Cancer* **2019**, *19*, 772, doi:10.1186/s12885-019-5984-7.

77. Bruno, W.; Pastorino, L.; Ghiorzo, P.; Andreotti, V.; Martinuzzi, C.; Menin, C.; Elefanti, L.; Stagni, C.; Vecchiato, A.; Rodolfo, M.; et al. Multiple primary melanomas (MPMs) and criteria for genetic assessment: MultiMEL, a multicenter study of the Italian Melanoma Intergroup. *J Am Acad Dermatol* **2016**, *74*, 325-332, doi:10.1016/j.jaad.2015.09.053.
78. Blackwood, M.A.; Holmes, R.; Synnestvedt, M.; Young, M.; George, C.; Yang, H.; Elder, D.E.; Schuchter, L.M.; Guerry, D.; Ganguly, A. Multiple primary melanoma revisited. *Cancer* **2002**, *94*, 2248-2255, doi:10.1002/cncr.10454.
79. Puig, S.; Malvehy, J.; Badenas, C.; Ruiz, A.; Jimenez, D.; Cuellar, F.; Azon, A.; Gonzalez, U.; Castel, T.; Campoy, A.; et al. Role of the CDKN2A locus in patients with multiple primary melanomas. *J Clin Oncol* **2005**, *23*, 3043-3051, doi:10.1200/JCO.2005.08.034.
80. Maubec, E.; Chaudru, V.; Mohamdi, H.; Blondel, C.; Margaritte-Jeannin, P.; Forget, S.; Corda, E.; Boitier, F.; Dalle, S.; Vabres, P.; et al. Familial melanoma: clinical factors associated with germline CDKN2A mutations according to the number of patients affected by melanoma in a family. *J Am Acad Dermatol* **2012**, *67*, 1257-1264, doi:10.1016/j.jaad.2012.05.014.
81. Potrony, M.; Puig-Butille, J.A.; Aguilera, P.; Badenas, C.; Carrera, C.; Malvehy, J.; Puig, S. Increased prevalence of lung, breast, and pancreatic cancers in addition to melanoma risk in families bearing the cyclin-dependent kinase inhibitor 2A mutation: implications for genetic counseling. *J Am Acad Dermatol* **2014**, *71*, 888-895, doi:10.1016/j.jaad.2014.06.036.
82. Auroy, S.; Avril, M.F.; Chompret, A.; Pham, D.; Goldstein, A.M.; Bianchi-Scarra, G.; Frebourg, T.; Joly, P.; Spatz, A.; Rubino, C.; et al. Sporadic multiple primary melanoma cases: CDKN2A germline mutations with a founder effect. *Genes Chromosomes Cancer* **2001**, *32*, 195-202, doi:10.1002/gcc.1183.
83. Harland, M.; Cust, A.E.; Badenas, C.; Chang, Y.M.; Holland, E.A.; Aguilera, P.; Aitken, J.F.; Armstrong, B.K.; Barrett, J.H.; Carrera, C.; et al. Prevalence and predictors of germline CDKN2A mutations for melanoma cases from Australia, Spain and the United Kingdom. *Hered Cancer Clin Pract* **2014**, *12*, 20, doi:10.1186/1897-4287-12-20.
84. Psaty, E.L.; Scope, A.; Halpern, A.C.; Marghoob, A.A. Defining the patient at high risk for melanoma. *Int J Dermatol* **2010**, *49*, 362-376, doi:10.1111/j.1365-4632.2010.04381.x.
85. Doubrovsky, A.; Menzies, S.W. Enhanced survival in patients with multiple primary melanoma. *Arch Dermatol* **2003**, *139*, 1013-1018, doi:10.1001/archderm.139.8.1013.
86. El Sharouni, M.A.; Witkamp, A.J.; Sigurdsson, V.; van Diest, P.J. Comparison of Survival Between Patients With Single vs Multiple Primary Cutaneous Melanomas. *JAMA Dermatol* **2019**, doi:10.1001/jamadermatol.2019.1134.
87. Sommer, L. Generation of melanocytes from neural crest cells. *Pigment Cell Melanoma Res* **2011**, *24*, 411-421, doi:10.1111/j.1755-148X.2011.00834.x.
88. Raman, M.; Chen, W.; Cobb, M.H. Differential regulation and properties of MAPKs. *Oncogene* **2007**, *26*, 3100-3112, doi:10.1038/sj.onc.1210392.
89. Xie, Y.; Shi, X.; Sheng, K.; Han, G.; Li, W.; Zhao, Q.; Jiang, B.; Feng, J.; Li, J.; Gu, Y. PI3K/Akt signaling transduction pathway, erythropoiesis and glycolysis in hypoxia (Review). *Mol Med Rep* **2019**, *19*, 783-791, doi:10.3892/mmr.2018.9713.
90. Carlino, M.S.; Long, G.V.; Kefford, R.F.; Rizos, H. Targeting oncogenic BRAF and aberrant MAPK activation in the treatment of cutaneous melanoma. *Crit Rev Oncol Hematol* **2015**, *96*, 385-398, doi:10.1016/j.critrevonc.2015.08.021.
91. Ponti, G.; Manfredini, M.; Greco, S.; Pellacani, G.; Depenni, R.; Tomasi, A.; Maccaferri, M.; Cascinu, S. BRAF, NRAS and C-KIT Advanced Melanoma: Clinico-pathological Features, Targeted-Therapy Strategies and Survival. *Anticancer Res* **2017**, *37*, 7043-7048, doi:10.21873/anticanres.12175.

92. Cheng, L.; Lopez-Beltran, A.; Massari, F.; MacLennan, G.T.; Montironi, R. Molecular testing for BRAF mutations to inform melanoma treatment decisions: a move toward precision medicine. *Mod Pathol* **2018**, *31*, 24-38, doi:10.1038/modpathol.2017.104.
93. Pratilas, C.A.; Taylor, B.S.; Ye, Q.; Viale, A.; Sander, C.; Solit, D.B.; Rosen, N. (V600E)BRAF is associated with disabled feedback inhibition of RAF-MEK signaling and elevated transcriptional output of the pathway. *Proc Natl Acad Sci U S A* **2009**, *106*, 4519-4524, doi:10.1073/pnas.0900780106.
94. Maurer, G.; Tarkowski, B.; Baccarini, M. Raf kinases in cancer-roles and therapeutic opportunities. *Oncogene* **2011**, *30*, 3477-3488, doi:10.1038/onc.2011.160.
95. Poynter, J.N.; Elder, J.T.; Fullen, D.R.; Nair, R.P.; Soengas, M.S.; Johnson, T.M.; Redman, B.; Thomas, N.E.; Gruber, S.B. BRAF and NRAS mutations in melanoma and melanocytic nevi. *Melanoma Res* **2006**, *16*, 267-273, doi:10.1097/01.cmr.0000222600.73179.f3.
96. Shain, A.H.; Bastian, B.C. From melanocytes to melanomas. *Nat Rev Cancer* **2016**, *16*, 345-358, doi:10.1038/nrc.2016.37.
97. Shain, A.H.; Bastian, B.C. The Genetic Evolution of Melanoma. *N Engl J Med* **2016**, *374*, 995-996, doi:10.1056/NEJMc1515834.
98. Seitz-Alghrouz, R.; Hidalgo, J.V.; Kayser, C.; Kreutz, C.; Technau-Hafsi, K.; Diaz, C.; von Deimling, A.; Timmer, J.; Werner, M.; Malkovsky, M.; et al. BRAF V600E Mutations in Nevi and Melanocytic Tumors of Uncertain Malignant Potential. *J Invest Dermatol* **2018**, *138*, 2489-2491, doi:10.1016/j.jid.2018.04.035.
99. Uribe, P.; Wistuba, II; Gonzalez, S. BRAF mutation: a frequent event in benign, atypical, and malignant melanocytic lesions of the skin. *Am J Dermatopathol* **2003**, *25*, 365-370, doi:10.1097/00000372-200310000-00001.
100. Long, G.V.; Menzies, A.M.; Nagrial, A.M.; Haydu, L.E.; Hamilton, A.L.; Mann, G.J.; Hughes, T.M.; Thompson, J.F.; Scolyer, R.A.; Kefford, R.F. Prognostic and clinicopathologic associations of oncogenic BRAF in metastatic melanoma. *J Clin Oncol* **2011**, *29*, 1239-1246, doi:10.1200/JCO.2010.32.4327.
101. van Dijk, M.C.; Bernsen, M.R.; Ruiter, D.J. Analysis of mutations in B-RAF, N-RAS, and H-RAS genes in the differential diagnosis of Spitz nevus and spitzoid melanoma. *Am J Surg Pathol* **2005**, *29*, 1145-1151.
102. Jakob, J.A.; Bassett, R.L., Jr.; Ng, C.S.; Curry, J.L.; Joseph, R.W.; Alvarado, G.C.; Rohlfs, M.L.; Richard, J.; Gershenwald, J.E.; Kim, K.B.; et al. NRAS mutation status is an independent prognostic factor in metastatic melanoma. *Cancer* **2012**, *118*, 4014-4023, doi:10.1002/cncr.26724.
103. Omholt, K.; Karsberg, S.; Platz, A.; Kanter, L.; Ringborg, U.; Hansson, J. Screening of N-ras codon 61 mutations in paired primary and metastatic cutaneous melanomas: mutations occur early and persist throughout tumor progression. *Clin Cancer Res* **2002**, *8*, 3468-3474.
104. Burd, C.E.; Liu, W.; Huynh, M.V.; Waqas, M.A.; Gillahan, J.E.; Clark, K.S.; Fu, K.; Martin, B.L.; Jeck, W.R.; Souroullas, G.P.; et al. Mutation-specific RAS oncogenicity explains NRAS codon 61 selection in melanoma. *Cancer Discov* **2014**, *4*, 1418-1429, doi:10.1158/2159-8290.CD-14-0729.
105. Hodis, E.; Watson, I.R.; Kryukov, G.V.; Arold, S.T.; Imielinski, M.; Theurillat, J.P.; Nickerson, E.; Auclair, D.; Li, L.; Place, C.; et al. A landscape of driver mutations in melanoma. *Cell* **2012**, *150*, 251-263, doi:10.1016/j.cell.2012.06.024.
106. Munoz-Couselo, E.; Adelantado, E.Z.; Ortiz, C.; Garcia, J.S.; Perez-Garcia, J. NRAS-mutant melanoma: current challenges and future prospect. *Onco Targets Ther* **2017**, *10*, 3941-3947, doi:10.2147/OTT.S117121.
107. Goel, V.K.; Lazar, A.J.; Warneke, C.L.; Redston, M.S.; Haluska, F.G. Examination of mutations in BRAF, NRAS, and PTEN in primary cutaneous melanoma. *J Invest Dermatol* **2006**, *126*, 154-160, doi:10.1038/sj.jid.5700026.

108. Omholt, K.; Platz, A.; Kanter, L.; Ringborg, U.; Hansson, J. NRAS and BRAF mutations arise early during melanoma pathogenesis and are preserved throughout tumor progression. *Clin Cancer Res* **2003**, *9*, 6483-6488.
109. Ellerhorst, J.A.; Greene, V.R.; Ekmekcioglu, S.; Warneke, C.L.; Johnson, M.M.; Cooke, C.P.; Wang, L.E.; Prieto, V.G.; Gershenwald, J.E.; Wei, Q.; et al. Clinical correlates of NRAS and BRAF mutations in primary human melanoma. *Clin Cancer Res* **2011**, *17*, 229-235, doi:10.1158/1078-0432.CCR-10-2276.
110. Maertens, O.; Johnson, B.; Hollstein, P.; Frederick, D.T.; Cooper, Z.A.; Messiaen, L.; Bronson, R.T.; McMahon, M.; Granter, S.; Flaherty, K.; et al. Elucidating distinct roles for NF1 in melanomagenesis. *Cancer Discov* **2013**, *3*, 338-349, doi:10.1158/2159-8290.CD-12-0313.
111. Manzano, J.L.; Layos, L.; Buges, C.; de Los Llanos Gil, M.; Vila, L.; Martinez-Balibrea, E.; Martinez-Cardus, A. Resistant mechanisms to BRAF inhibitors in melanoma. *Ann Transl Med* **2016**, *4*, 237, doi:10.21037/atm.2016.06.07.
112. Cirenajwis, H.; Lauss, M.; Ekedahl, H.; Torngren, T.; Kvist, A.; Saal, L.H.; Olsson, H.; Staaf, J.; Carneiro, A.; Ingvar, C.; et al. NF1-mutated melanoma tumors harbor distinct clinical and biological characteristics. *Mol Oncol* **2017**, *11*, 438-451, doi:10.1002/1878-0261.12050.
113. Shtivelman, E.; Davies, M.Q.; Hwu, P.; Yang, J.; Lotem, M.; Oren, M.; Flaherty, K.T.; Fisher, D.E. Pathways and therapeutic targets in melanoma. *Oncotarget* **2014**, *5*, 1701-1752, doi:10.18632/oncotarget.1892.
114. Vita, M.; Tisserand, J.C.; Chauvot de Beauchene, I.; Panel, N.; Tchertanov, L.; Agopian, J.; Mescam-Mancini, L.; Fouet, B.; Fournier, B.; Dubreuil, P.; et al. Characterization of S628N: a novel KIT mutation found in a metastatic melanoma. *JAMA Dermatol* **2014**, *150*, 1345-1349, doi:10.1001/jamadermatol.2014.1437.
115. Carvajal, R.D.; Lawrence, D.P.; Weber, J.S.; Gajewski, T.F.; Gonzalez, R.; Lutzky, J.; O'Day, S.J.; Hamid, O.; Wolchok, J.D.; Chapman, P.B.; et al. Phase II Study of Nilotinib in Melanoma Harboring KIT Alterations Following Progression to Prior KIT Inhibition. *Clin Cancer Res* **2015**, *21*, 2289-2296, doi:10.1158/1078-0432.CCR-14-1630.
116. Curtin, J.A.; Busam, K.; Pinkel, D.; Bastian, B.C. Somatic activation of KIT in distinct subtypes of melanoma. *J Clin Oncol* **2006**, *24*, 4340-4346, doi:10.1200/JCO.2006.06.2984.
117. Giles, K.M.; Rosenbaum, B.E.; Berger, M.; Izsak, A.; Li, Y.; Illa Bochaca, I.; Vega-Saenz de Miera, E.; Wang, J.; Darvishian, F.; Zhong, H.; et al. Revisiting the Clinical and Biologic Relevance of Partial PTEN Loss in Melanoma. *J Invest Dermatol* **2019**, *139*, 430-438, doi:10.1016/j.jid.2018.07.031.
118. Wu, H.; Goel, V.; Haluska, F.G. PTEN signaling pathways in melanoma. *Oncogene* **2003**, *22*, 3113-3122, doi:10.1038/sj.onc.1206451.
119. Tsao, H.; Goel, V.; Wu, H.; Yang, G.; Haluska, F.G. Genetic interaction between NRAS and BRAF mutations and PTEN/MMAC1 inactivation in melanoma. *J Invest Dermatol* **2004**, *122*, 337-341, doi:10.1046/j.0022-202X.2004.22243.x.
120. Nogueira, C.; Kim, K.H.; Sung, H.; Paraiso, K.H.; Dannenberg, J.H.; Bosenberg, M.; Chin, L.; Kim, M. Cooperative interactions of PTEN deficiency and RAS activation in melanoma metastasis. *Oncogene* **2010**, *29*, 6222-6232, doi:10.1038/onc.2010.349.
121. Mirmohammadsadegh, A.; Marini, A.; Nambiar, S.; Hassan, M.; Tannapfel, A.; Ruzicka, T.; Hengge, U.R. Epigenetic silencing of the PTEN gene in melanoma. *Cancer Res* **2006**, *66*, 6546-6552, doi:10.1158/0008-5472.CAN-06-0384.
122. Wellbrock, C.; Arozarena, I. Microphthalmia-associated transcription factor in melanoma development and MAP-kinase pathway targeted therapy. *Pigment Cell Melanoma Res* **2015**, *28*, 390-406, doi:10.1111/pcmr.12370.
123. Lister, J.A.; Capper, A.; Zeng, Z.; Mathers, M.E.; Richardson, J.; Paranthaman, K.; Jackson, I.J.; Elizabeth Patton, E. A conditional zebrafish MITF mutation reveals MITF levels are

critical for melanoma promotion vs. regression in vivo. *J Invest Dermatol* **2014**, *134*, 133-140, doi:10.1038/jid.2013.293.

124. Clark, W.H., Jr.; Elder, D.E.; Guerry, D.t.; Epstein, M.N.; Greene, M.H.; Van Horn, M. A study of tumor progression: the precursor lesions of superficial spreading and nodular melanoma. *Hum Pathol* **1984**, *15*, 1147-1165, doi:10.1016/s0046-8177(84)80310-x.
125. Hussussian, C.J.; Struewing, J.P.; Goldstein, A.M.; Higgins, P.A.; Ally, D.S.; Sheahan, M.D.; Clark, W.H., Jr.; Tucker, M.A.; Dracopoli, N.C. Germline p16 mutations in familial melanoma. *Nat Genet* **1994**, *8*, 15-21, doi:10.1038/ng0994-15.
126. Bennett, D.C. Genetics of melanoma progression: the rise and fall of cell senescence. *Pigment Cell Melanoma Res* **2016**, *29*, 122-140, doi:10.1111/pcmr.12422.
127. Miller, A.J.; Mihm, M.C., Jr. Melanoma. *N Engl J Med* **2006**, *355*, 51-65, doi:10.1056/NEJMra052166.
128. Schatton, T.; Frank, M.H. Cancer stem cells and human malignant melanoma. *Pigment Cell Melanoma Res* **2008**, *21*, 39-55, doi:10.1111/j.1755-148X.2007.00427.x.
129. Scatena, C.; Murtas, D.; Tomei, S. Cutaneous Melanoma Classification: The Importance of High-Throughput Genomic Technologies. *Front Oncol* **2021**, *11*, 635488, doi:10.3389/fonc.2021.635488.
130. Trindade, F.M.; de Freitas, M.L.P.; Bittencourt, F.V. Dermoscopic evaluation of superficial spreading melanoma. *An Bras Dermatol* **2021**, *96*, 139-147, doi:10.1016/j.abd.2020.06.012.
131. Rastrelli, M.; Tropea, S.; Rossi, C.R.; Alaibac, M. Melanoma: epidemiology, risk factors, pathogenesis, diagnosis and classification. *In Vivo* **2014**, *28*, 1005-1011.
132. Elder, D.E.; Bastian, B.C.; Cree, I.A.; Massi, D.; Scolyer, R.A. The 2018 World Health Organization Classification of Cutaneous, Mucosal, and Uveal Melanoma: Detailed Analysis of 9 Distinct Subtypes Defined by Their Evolutionary Pathway. *Arch Pathol Lab Med* **2020**, *144*, 500-522, doi:10.5858/arpa.2019-0561-RA.
133. Greenwald, H.S.; Friedman, E.B.; Osman, I. Superficial spreading and nodular melanoma are distinct biological entities: a challenge to the linear progression model. *Melanoma Res* **2012**, *22*, 1-8, doi:10.1097/CMR.0b013e32834e6aa0.
134. Kalkhoran, S.; Milne, O.; Zalaudek, I.; Puig, S.; Malvehy, J.; Kelly, J.W.; Marghoob, A.A. Historical, clinical, and dermoscopic characteristics of thin nodular melanoma. *Arch Dermatol* **2010**, *146*, 311-318, doi:10.1001/archdermatol.2009.369.
135. Xiong, M.; Charifa, A.; Chen, C.S.J. Lentigo Maligna Melanoma. In *StatPearls*; Treasure Island (FL), 2021.
136. Darmawan, C.C.; Jo, G.; Montenegro, S.E.; Kwak, Y.; Cheol, L.; Cho, K.H.; Mun, J.H. Early detection of acral melanoma: A review of clinical, dermoscopic, histopathologic, and molecular characteristics. *J Am Acad Dermatol* **2019**, *81*, 805-812, doi:10.1016/j.jaad.2019.01.081.
137. Bello, D.M.; Chou, J.F.; Panageas, K.S.; Brady, M.S.; Coit, D.G.; Carvajal, R.D.; Ariyan, C.E. Prognosis of acral melanoma: a series of 281 patients. *Ann Surg Oncol* **2013**, *20*, 3618-3625, doi:10.1245/s10434-013-3089-0.
138. Cancer Genome Atlas, N. Genomic Classification of Cutaneous Melanoma. *Cell* **2015**, *161*, 1681-1696, doi:10.1016/j.cell.2015.05.044.
139. Elder, D.E., Massi D., Scoyler R. A., Willemze R. WHO classification of skin tumor. **2017**.
140. Amin, M.B.; Greene, F.L.; Edge, S.B.; Compton, C.C.; Gershenwald, J.E.; Brookland, R.K.; Meyer, L.; Gress, D.M.; Byrd, D.R.; Winchester, D.P. The Eighth Edition AJCC Cancer Staging Manual: Continuing to build a bridge from a population-based to a more "personalized" approach to cancer staging. *CA Cancer J Clin* **2017**, *67*, 93-99, doi:10.3322/caac.21388.
141. Green, A.C.; Baade, P.; Coory, M.; Aitken, J.F.; Smithers, M. Population-based 20-year survival among people diagnosed with thin melanomas in Queensland, Australia. *J Clin Oncol* **2012**, *30*, 1462-1467, doi:10.1200/JCO.2011.38.8561.

142. Gimotty, P.A.; Elder, D.E.; Fraker, D.L.; Botbyl, J.; Sellers, K.; Elenitsas, R.; Ming, M.E.; Schuchter, L.; Spitz, F.R.; Czerniecki, B.J.; et al. Identification of high-risk patients among those diagnosed with thin cutaneous melanomas. *J Clin Oncol* **2007**, *25*, 1129-1134, doi:10.1200/JCO.2006.08.1463.
143. Spatz, A.; Cook, M.G.; Elder, D.E.; Piepkorn, M.; Ruiter, D.J.; Barnhill, R.L. Interobserver reproducibility of ulceration assessment in primary cutaneous melanomas. *Eur J Cancer* **2003**, *39*, 1861-1865, doi:10.1016/s0959-8049(03)00325-3.
144. Lo, S.N.; Scolyer, R.A.; Thompson, J.F. Long-Term Survival of Patients with Thin (T1) Cutaneous Melanomas: A Breslow Thickness Cut Point of 0.8 mm Separates Higher-Risk and Lower-Risk Tumors. *Ann Surg Oncol* **2018**, *25*, 894-902, doi:10.1245/s10434-017-6325-1.
145. Gershenwald, J.E.; Scolyer, R.A.; Hess, K.R.; Sondak, V.K.; Long, G.V.; Ross, M.I.; Lazar, A.J.; Faries, M.B.; Kirkwood, J.M.; McArthur, G.A.; et al. Melanoma staging: Evidence-based changes in the American Joint Committee on Cancer eighth edition cancer staging manual. *CA Cancer J Clin* **2017**, *67*, 472-492, doi:10.3322/caac.21409.
146. Bhoyrul, B.; Brent, G.; Elliott, F.; McLorinan, J.; Wilson, A.; Peach, H.; Mathew, B.; Mitra, A. Pathological review of primary cutaneous malignant melanoma by a specialist skin cancer multidisciplinary team improves patient care in the UK. *J Clin Pathol* **2019**, *72*, 482-486, doi:10.1136/jclinpath-2019-205767.
147. Rigel, D.S.; Russak, J.; Friedman, R. The evolution of melanoma diagnosis: 25 years beyond the ABCDs. *CA Cancer J Clin* **2010**, *60*, 301-316, doi:10.3322/caac.20074.
148. Robinson, J.K.; Turrisi, R. Skills training to learn discrimination of ABCDE criteria by those at risk of developing melanoma. *Arch Dermatol* **2006**, *142*, 447-452, doi:10.1001/archderm.142.4.447.
149. Neila, J.; Soyer, H.P. Key points in dermoscopy for diagnosis of melanomas, including difficult to diagnose melanomas, on the trunk and extremities. *J Dermatol* **2011**, *38*, 3-9, doi:10.1111/j.1346-8138.2010.01131.x.
150. Rayner, J.E.; Laino, A.M.; Nufer, K.L.; Adams, L.; Raphael, A.P.; Menzies, S.W.; Soyer, H.P. Clinical Perspective of 3D Total Body Photography for Early Detection and Screening of Melanoma. *Front Med (Lausanne)* **2018**, *5*, 152, doi:10.3389/fmed.2018.00152.
151. Branzan, A.L.; Landthaler, M.; Szeimies, R.M. In vivo confocal scanning laser microscopy in dermatology. *Lasers Med Sci* **2007**, *22*, 73-82, doi:10.1007/s10103-006-0416-8.
152. Smoller, B.R. Histologic criteria for diagnosing primary cutaneous malignant melanoma. *Mod Pathol* **2006**, *19 Suppl 2*, S34-40, doi:10.1038/modpathol.3800508.
153. Kim, R.H.; Meehan, S.A. Immunostain use in the diagnosis of melanomas referred to a tertiary medical center: a 15-year retrospective review (2001-2015). *J Cutan Pathol* **2017**, *44*, 221-227, doi:10.1111/cup.12867.
154. Davis, L.E.; Shalin, S.C.; Tackett, A.J. Current state of melanoma diagnosis and treatment. *Cancer Biol Ther* **2019**, *20*, 1366-1379, doi:10.1080/15384047.2019.1640032.
155. Palmer, S.R.; Erickson, L.A.; Ichetovkin, I.; Knauer, D.J.; Markovic, S.N. Circulating serologic and molecular biomarkers in malignant melanoma. *Mayo Clin Proc* **2011**, *86*, 981-990, doi:10.4065/mcp.2011.0287.
156. McGovern, V.J.; Shaw, H.M.; Milton, G.W.; McCarthy, W.H. Ulceration and prognosis in cutaneous malignant melanoma. *Histopathology* **1982**, *6*, 399-407, doi:10.1111/j.1365-2559.1982.tb02737.x.
157. Sprakel, B.; Stenschke, F.; Unnewehr, M.; Ladas, A.; Senninger, N. [Prognosis of malignant melanoma following dissection regional lymph node metastases]. *Chirurg* **2003**, *74*, 55-60, doi:10.1007/s00104-002-0548-8.
158. Vollmer, R.T.; Seigler, H.F. Using a continuous transformation of the Breslow thickness for prognosis in cutaneous melanoma. *Am J Clin Pathol* **2001**, *115*, 205-212, doi:10.1309/WAVR-560R-NU5E-4Q96.

159. Breslow, A. Tumor thickness, level of invasion and node dissection in stage I cutaneous melanoma. *Ann Surg* **1975**, *182*, 572-575, doi:10.1097/00000658-197511000-00007.
160. Balch, C.M.; Wilkerson, J.A.; Murad, T.M.; Soong, S.J.; Ingalls, A.L.; Maddox, W.A. The prognostic significance of ulceration of cutaneous melanoma. *Cancer* **1980**, *45*, 3012-3017, doi:10.1002/1097-0142(19800615)45:12<3012::aid-cncr2820451223>3.0.co;2-o.
161. Zurac, S.; Negroiu, G.; Petrescu, S.; Andrei, R.; Tebeica, T.; Popp, C.; Mustata, R.; Neagu, M.; Constantin, C.; Solovan, C.; et al. Spectrum of morphologic alterations of regression in cutaneous melanoma--potential for improving disease prognosis. *Rom J Intern Med* **2012**, *50*, 145-153.
162. Sinnamon, A.J.; Sharon, C.E.; Song, Y.; Neuwirth, M.G.; Elder, D.E.; Xu, X.; Chu, E.Y.; Ming, M.E.; Fraker, D.L.; Gimotty, P.A.; et al. The prognostic significance of tumor-infiltrating lymphocytes for primary melanoma varies by sex. *J Am Acad Dermatol* **2018**, *79*, 245-251, doi:10.1016/j.jaad.2018.02.066.
163. Faries, M.B.; Thompson, J.F.; Cochran, A.J.; Andtbacka, R.H.; Mozzillo, N.; Zager, J.S.; Jahkola, T.; Bowles, T.L.; Testori, A.; Beitsch, P.D.; et al. Completion Dissection or Observation for Sentinel-Node Metastasis in Melanoma. *N Engl J Med* **2017**, *376*, 2211-2222, doi:10.1056/NEJMoa1613210.
164. Wong, S.L.; Faries, M.B.; Kennedy, E.B.; Agarwala, S.S.; Akhurst, T.J.; Ariyan, C.; Balch, C.M.; Berman, B.S.; Cochran, A.; Delman, K.A.; et al. Sentinel Lymph Node Biopsy and Management of Regional Lymph Nodes in Melanoma: American Society of Clinical Oncology and Society of Surgical Oncology Clinical Practice Guideline Update. *J Clin Oncol* **2018**, *36*, 399-413, doi:10.1200/JCO.2017.75.7724.
165. Domingues, B.; Lopes, J.M.; Soares, P.; Populo, H. Melanoma treatment in review. *Immunotargets Ther* **2018**, *7*, 35-49, doi:10.2147/ITT.S134842.
166. Strojan, P. Role of radiotherapy in melanoma management. *Radiol Oncol* **2010**, *44*, 1-12, doi:10.2478/v10019-010-0008-x.
167. Franke, V.; van Akkooi, A.C.J. The extent of surgery for stage III melanoma: how much is appropriate? *Lancet Oncol* **2019**, *20*, e167-e174, doi:10.1016/S1470-2045(19)30099-3.
168. Bhatia, S.; Tykodi, S.S.; Thompson, J.A. Treatment of metastatic melanoma: an overview. *Oncology (Williston Park)* **2009**, *23*, 488-496.
169. Varrone, F.; Caputo, E. The miRNAs Role in Melanoma and in Its Resistance to Therapy. *International journal of molecular sciences* **2020**, *21*, doi:10.3390/ijms21030878.
170. Grimaldi, A.M.; Simeone, E.; Festino, L.; Vanella, V.; Strudel, M.; Ascierto, P.A. MEK Inhibitors in the Treatment of Metastatic Melanoma and Solid Tumors. *Am J Clin Dermatol* **2017**, *18*, 745-754, doi:10.1007/s40257-017-0292-y.
171. Kakadia, S.; Yarlagadda, N.; Awad, R.; Kundranda, M.; Niu, J.; Naraev, B.; Mina, L.; Dragovich, T.; Gimbel, M.; Mahmoud, F. Mechanisms of resistance to BRAF and MEK inhibitors and clinical update of US Food and Drug Administration-approved targeted therapy in advanced melanoma. *Onco Targets Ther* **2018**, *11*, 7095-7107, doi:10.2147/OTT.S182721.
172. Koelblinger, P.; Thuerigen, O.; Dummer, R. Development of encorafenib for BRAF-mutated advanced melanoma. *Curr Opin Oncol* **2018**, *30*, 125-133, doi:10.1097/CCO.0000000000000426.
173. Topalian, S.L.; Drake, C.G.; Pardoll, D.M. Immune checkpoint blockade: a common denominator approach to cancer therapy. *Cancer Cell* **2015**, *27*, 450-461, doi:10.1016/j.ccell.2015.03.001.
174. Abdel-Wahab, N.; Shah, M.; Suarez-Almazor, M.E. Adverse Events Associated with Immune Checkpoint Blockade in Patients with Cancer: A Systematic Review of Case Reports. *PLoS One* **2016**, *11*, e0160221, doi:10.1371/journal.pone.0160221.
175. Brahmer, J.R.; Lacchetti, C.; Schneider, B.J.; Atkins, M.B.; Brassil, K.J.; Caterino, J.M.; Chau, I.; Ernstoff, M.S.; Gardner, J.M.; Ginex, P.; et al. Management of Immune-Related Adverse Events in Patients Treated With Immune Checkpoint Inhibitor Therapy: American

Society of Clinical Oncology Clinical Practice Guideline. *J Clin Oncol* **2018**, *36*, 1714-1768, doi:10.1200/JCO.2017.77.6385.
176. Homet Moreno, B.; Mok, S.; Comin-Anduix, B.; Hu-Lieskovan, S.; Ribas, A. Combined treatment with dabrafenib and trametinib with immune-stimulating antibodies for BRAF mutant melanoma. *Oncoimmunology* **2016**, *5*, e1052212, doi:10.1080/2162402X.2015.1052212.
177. Deken, M.A.; Gadiot, J.; Jordanova, E.S.; Lacroix, R.; van Gool, M.; Kroon, P.; Pineda, C.; Geukes Foppen, M.H.; Scolyer, R.; Song, J.Y.; et al. Targeting the MAPK and PI3K pathways in combination with PD1 blockade in melanoma. *Oncoimmunology* **2016**, *5*, e1238557, doi:10.1080/2162402X.2016.1238557.
178. Ha, M.; Kim, V.N. Regulation of microRNA biogenesis. *Nat Rev Mol Cell Biol* **2014**, *15*, 509-524, doi:10.1038/nrm3838.
179. Broughton, J.P.; Lovci, M.T.; Huang, J.L.; Yeo, G.W.; Pasquinelli, A.E. Pairing beyond the Seed Supports MicroRNA Targeting Specificity. *Molecular cell* **2016**, *64*, 320-333, doi:10.1016/j.molcel.2016.09.004.
180. Vasudevan, S. Posttranscriptional upregulation by microRNAs. *Wiley Interdiscip Rev RNA* **2012**, *3*, 311-330, doi:10.1002/wrna.121.
181. Makarova, J.A.; Shkurnikov, M.U.; Wicklein, D.; Lange, T.; Samatov, T.R.; Turchinovich, A.A.; Tonevitsky, A.G. Intracellular and extracellular microRNA: An update on localization and biological role. *Prog Histochem Cytochem* **2016**, *51*, 33-49, doi:10.1016/j.proghi.2016.06.001.
182. Fu, G.; Brkic, J.; Hayder, H.; Peng, C. MicroRNAs in Human Placental Development and Pregnancy Complications. *International journal of molecular sciences* **2013**, *14*, 5519-5544, doi:10.3390/ijms14035519.
183. Tufekci, K.U.; Oner, M.G.; Meuwissen, R.L.; Genc, S. The role of microRNAs in human diseases. *Methods Mol Biol* **2014**, *1107*, 33-50, doi:10.1007/978-1-62703-748-8_3.
184. Paul, P.; Chakraborty, A.; Sarkar, D.; Langthasa, M.; Rahman, M.; Bari, M.; Singha, R.S.; Malakar, A.K.; Chakraborty, S. Interplay between miRNAs and human diseases. *J Cell Physiol* **2018**, *233*, 2007-2018, doi:10.1002/jcp.25854.
185. Negrini, M.; Ferracin, M.; Sabbioni, S.; Croce, C.M. MicroRNAs in human cancer: from research to therapy. *J Cell Sci* **2007**, *120*, 1833-1840, doi:10.1242/jcs.03450.
186. Hayes, J.; Peruzzi, P.P.; Lawler, S. MicroRNAs in cancer: biomarkers, functions and therapy. *Trends Mol Med* **2014**, *20*, 460-469, doi:10.1016/j.molmed.2014.06.005.
187. Huang, W. MicroRNAs: Biomarkers, Diagnostics, and Therapeutics. *Methods Mol Biol* **2017**, *1617*, 57-67, doi:10.1007/978-1-4939-7046-9_4.
188. Wang, J.; Chen, J.; Sen, S. MicroRNA as Biomarkers and Diagnostics. *J Cell Physiol* **2016**, *231*, 25-30, doi:10.1002/jcp.25056.
189. de Rie, D.; Abugessaisa, I.; Alam, T.; Arner, E.; Arner, P.; Ashoor, H.; Astrom, G.; Babina, M.; Bertin, N.; Burroughs, A.M.; et al. An integrated expression atlas of miRNAs and their promoters in human and mouse. *Nat Biotechnol* **2017**, *35*, 872-878, doi:10.1038/nbt.3947.
190. Kim, Y.K.; Kim, V.N. Processing of intronic microRNAs. *EMBO J* **2007**, *26*, 775-783, doi:10.1038/sj.emboj.7601512.
191. Tanzer, A.; Stadler, P.F. Molecular evolution of a microRNA cluster. *J Mol Biol* **2004**, *339*, 327-335, doi:10.1016/j.jmb.2004.03.065.
192. O'Brien, J.; Hayder, H.; Zayed, Y.; Peng, C. Overview of MicroRNA Biogenesis, Mechanisms of Actions, and Circulation. *Front Endocrinol (Lausanne)* **2018**, *9*, 402, doi:10.3389/fendo.2018.00402.
193. Denli, A.M.; Tops, B.B.; Plasterk, R.H.; Ketting, R.F.; Hannon, G.J. Processing of primary microRNAs by the Microprocessor complex. *Nature* **2004**, *432*, 231-235, doi:10.1038/nature03049.

194. Alarcon, C.R.; Lee, H.; Goodarzi, H.; Halberg, N.; Tavazoie, S.F. N6-methyladenosine marks primary microRNAs for processing. *Nature* **2015**, *519*, 482-485, doi:10.1038/nature14281.
195. Han, J.; Lee, Y.; Yeom, K.H.; Kim, Y.K.; Jin, H.; Kim, V.N. The Drosha-DGCR8 complex in primary microRNA processing. *Genes Dev* **2004**, *18*, 3016-3027, doi:10.1101/gad.1262504.
196. Okada, C.; Yamashita, E.; Lee, S.J.; Shibata, S.; Katahira, J.; Nakagawa, A.; Yoneda, Y.; Tsukihara, T. A high-resolution structure of the pre-microRNA nuclear export machinery. *Science* **2009**, *326*, 1275-1279, doi:10.1126/science.1178705.
197. Zhang, H.; Kolb, F.A.; Jaskiewicz, L.; Westhof, E.; Filipowicz, W. Single processing center models for human Dicer and bacterial RNase III. *Cell* **2004**, *118*, 57-68, doi:10.1016/j.cell.2004.06.017.
198. Yoda, M.; Kawamata, T.; Paroo, Z.; Ye, X.; Iwasaki, S.; Liu, Q.; Tomari, Y. ATP-dependent human RISC assembly pathways. *Nat Struct Mol Biol* **2010**, *17*, 17-23, doi:10.1038/nsmb.1733.
199. Meijer, H.A.; Smith, E.M.; Bushell, M. Regulation of miRNA strand selection: follow the leader? *Biochem Soc Trans* **2014**, *42*, 1135-1140, doi:10.1042/BST20140142.
200. Ruby, J.G.; Jan, C.H.; Bartel, D.P. Intronic microRNA precursors that bypass Drosha processing. *Nature* **2007**, *448*, 83-86, doi:10.1038/nature05983.
201. Babiarz, J.E.; Ruby, J.G.; Wang, Y.; Bartel, D.P.; Blelloch, R. Mouse ES cells express endogenous shRNAs, siRNAs, and other Microprocessor-independent, Dicer-dependent small RNAs. *Genes Dev* **2008**, *22*, 2773-2785, doi:10.1101/gad.1705308.
202. Xie, M.; Li, M.; Vilborg, A.; Lee, N.; Shu, M.D.; Yartseva, V.; Sestan, N.; Steitz, J.A. Mammalian 5'-capped microRNA precursors that generate a single microRNA. *Cell* **2013**, *155*, 1568-1580, doi:10.1016/j.cell.2013.11.027.
203. Yang, J.S.; Maurin, T.; Robine, N.; Rasmussen, K.D.; Jeffrey, K.L.; Chandwani, R.; Papapetrou, E.P.; Sadelain, M.; O'Carroll, D.; Lai, E.C. Conserved vertebrate mir-451 provides a platform for Dicer-independent, Ago2-mediated microRNA biogenesis. *Proc Natl Acad Sci U S A* **2010**, *107*, 15163-15168, doi:10.1073/pnas.1006432107.
204. Cheloufi, S.; Dos Santos, C.O.; Chong, M.M.; Hannon, G.J. A dicer-independent miRNA biogenesis pathway that requires Ago catalysis. *Nature* **2010**, *465*, 584-589, doi:10.1038/nature09092.
205. Huntzinger, E.; Izaurralde, E. Gene silencing by microRNAs: contributions of translational repression and mRNA decay. *Nat Rev Genet* **2011**, *12*, 99-110, doi:10.1038/nrg2936.
206. Ipsaro, J.J.; Joshua-Tor, L. From guide to target: molecular insights into eukaryotic RNA-interference machinery. *Nat Struct Mol Biol* **2015**, *22*, 20-28, doi:10.1038/nsmb.2931.
207. Xu, W.; San Lucas, A.; Wang, Z.; Liu, Y. Identifying microRNA targets in different gene regions. *BMC bioinformatics* **2014**, *15 Suppl 7*, S4, doi:10.1186/1471-2105-15-S7-S4.
208. Forman, J.J.; Legesse-Miller, A.; Coller, H.A. A search for conserved sequences in coding regions reveals that the let-7 microRNA targets Dicer within its coding sequence. *Proc Natl Acad Sci U S A* **2008**, *105*, 14879-14884, doi:10.1073/pnas.0803230105.
209. Zhang, J.; Zhou, W.; Liu, Y.; Liu, T.; Li, C.; Wang, L. Oncogenic role of microRNA-532-5p in human colorectal cancer via targeting of the 5'UTR of RUNX3. *Oncol Lett* **2018**, *15*, 7215-7220, doi:10.3892/ol.2018.8217.
210. Dharap, A.; Pokrzywa, C.; Murali, S.; Pandi, G.; Vemuganti, R. MicroRNA miR-324-3p induces promoter-mediated expression of RelA gene. *PLoS One* **2013**, *8*, e79467, doi:10.1371/journal.pone.0079467.
211. Kawamata, T.; Tomari, Y. Making RISC. *Trends Biochem Sci* **2010**, *35*, 368-376, doi:10.1016/j.tibs.2010.03.009.
212. Jo, M.H.; Shin, S.; Jung, S.R.; Kim, E.; Song, J.J.; Hohng, S. Human Argonaute 2 Has Diverse Reaction Pathways on Target RNAs. *Molecular cell* **2015**, *59*, 117-124, doi:10.1016/j.molcel.2015.04.027.

213. Krutzfeldt, J.; Rajewsky, N.; Braich, R.; Rajeev, K.G.; Tuschl, T.; Manoharan, M.; Stoffel, M. Silencing of microRNAs in vivo with 'antagomirs'. *Nature* **2005**, *438*, 685-689, doi:10.1038/nature04303.
214. Ameres, S.L.; Horwich, M.D.; Hung, J.H.; Xu, J.; Ghildiyal, M.; Weng, Z.; Zamore, P.D. Target RNA-directed trimming and tailing of small silencing RNAs. *Science* **2010**, *328*, 1534-1539, doi:10.1126/science.1187058.
215. Ellwanger, D.C.; Buttner, F.A.; Mewes, H.W.; Stumpflen, V. The sufficient minimal set of miRNA seed types. *Bioinformatics* **2011**, *27*, 1346-1350, doi:10.1093/bioinformatics/btr149.
216. Behm-Ansmant, I.; Rehwinkel, J.; Doerks, T.; Stark, A.; Bork, P.; Izaurralde, E. mRNA degradation by miRNAs and GW182 requires both CCR4:NOT deadenylase and DCP1:DCP2 decapping complexes. *Genes Dev* **2006**, *20*, 1885-1898, doi:10.1101/gad.1424106.
217. Jonas, S.; Izaurralde, E. Towards a molecular understanding of microRNA-mediated gene silencing. *Nat Rev Genet* **2015**, *16*, 421-433, doi:10.1038/nrg3965.
218. Christie, M.; Boland, A.; Huntzinger, E.; Weichenrieder, O.; Izaurralde, E. Structure of the PAN3 pseudokinase reveals the basis for interactions with the PAN2 deadenylase and the GW182 proteins. *Molecular cell* **2013**, *51*, 360-373, doi:10.1016/j.molcel.2013.07.011.
219. Braun, J.E.; Truffault, V.; Boland, A.; Huntzinger, E.; Chang, C.T.; Haas, G.; Weichenrieder, O.; Coles, M.; Izaurralde, E. A direct interaction between DCP1 and XRN1 couples mRNA decapping to 5' exonucleolytic degradation. *Nat Struct Mol Biol* **2012**, *19*, 1324-1331, doi:10.1038/nsmb.2413.
220. Vasudevan, S.; Steitz, J.A. AU-rich-element-mediated upregulation of translation by FXR1 and Argonaute 2. *Cell* **2007**, *128*, 1105-1118, doi:10.1016/j.cell.2007.01.038.
221. Truesdell, S.S.; Mortensen, R.D.; Seo, M.; Schroeder, J.C.; Lee, J.H.; LeTonqueze, O.; Vasudevan, S. MicroRNA-mediated mRNA translation activation in quiescent cells and oocytes involves recruitment of a nuclear microRNP. *Sci Rep* **2012**, *2*, 842, doi:10.1038/srep00842.
222. Orom, U.A.; Nielsen, F.C.; Lund, A.H. MicroRNA-10a binds the 5'UTR of ribosomal protein mRNAs and enhances their translation. *Molecular cell* **2008**, *30*, 460-471, doi:10.1016/j.molcel.2008.05.001.
223. Bukhari, S.I.A.; Truesdell, S.S.; Lee, S.; Kollu, S.; Classon, A.; Boukhali, M.; Jain, E.; Mortensen, R.D.; Yanagiya, A.; Sadreyev, R.I.; et al. A Specialized Mechanism of Translation Mediated by FXR1a-Associated MicroRNP in Cellular Quiescence. *Molecular cell* **2016**, *61*, 760-773, doi:10.1016/j.molcel.2016.02.013.
224. Nishi, K.; Nishi, A.; Nagasawa, T.; Ui-Tei, K. Human TNRC6A is an Argonaute-navigator protein for microRNA-mediated gene silencing in the nucleus. *RNA* **2013**, *19*, 17-35, doi:10.1261/rna.034769.112.
225. Benhamed, M.; Herbig, U.; Ye, T.; Dejean, A.; Bischof, O. Senescence is an endogenous trigger for microRNA-directed transcriptional gene silencing in human cells. *Nat Cell Biol* **2012**, *14*, 266-275, doi:10.1038/ncb2443.
226. Pitchiaya, S.; Heinicke, L.A.; Park, J.I.; Cameron, E.L.; Walter, N.G. Resolving Subcellular miRNA Trafficking and Turnover at Single-Molecule Resolution. *Cell Rep* **2017**, *19*, 630-642, doi:10.1016/j.celrep.2017.03.075.
227. Cernilogar, F.M.; Onorati, M.C.; Kothe, G.O.; Burroughs, A.M.; Parsi, K.M.; Breiling, A.; Lo Sardo, F.; Saxena, A.; Miyoshi, K.; Siomi, H.; et al. Chromatin-associated RNA interference components contribute to transcriptional regulation in Drosophila. *Nature* **2011**, *480*, 391-395, doi:10.1038/nature10492.
228. Bottini, S.; Hamouda-Tekaya, N.; Mategot, R.; Zaragosi, L.E.; Audebert, S.; Pisano, S.; Grandjean, V.; Mauduit, C.; Benahmed, M.; Barbry, P.; et al. Post-transcriptional gene silencing mediated by microRNAs is controlled by nucleoplasmic Sfpq. *Nat Commun* **2017**, *8*, 1189, doi:10.1038/s41467-017-01126-x.

229. Allo, M.; Agirre, E.; Bessonov, S.; Bertucci, P.; Gomez Acuna, L.; Buggiano, V.; Bellora, N.; Singh, B.; Petrillo, E.; Blaustein, M.; et al. Argonaute-1 binds transcriptional enhancers and controls constitutive and alternative splicing in human cells. *Proc Natl Acad Sci U S A* **2014**, *111*, 15622-15629, doi:10.1073/pnas.1416858111.
230. Havens, M.A.; Reich, A.A.; Hastings, M.L. Drosha promotes splicing of a pre-microRNA-like alternative exon. *PLoS Genet* **2014**, *10*, e1004312, doi:10.1371/journal.pgen.1004312.
231. Miao, L.; Yao, H.; Li, C.; Pu, M.; Yao, X.; Yang, H.; Qi, X.; Ren, J.; Wang, Y. A dual inhibition: microRNA-552 suppresses both transcription and translation of cytochrome P450 2E1. *Biochim Biophys Acta* **2016**, *1859*, 650-662, doi:10.1016/j.bbagrm.2016.02.016.
232. Hanniford, D.; Segura, M.F.; Zhong, J.; Philips, E.; Jirau-Serrano, X.; Darvishian, F.; Berman, R.S.; Shapiro, R.L.; Pavlick, A.C.; Brown, B.; et al. Identification of metastasis-suppressive microRNAs in primary melanoma. *J Natl Cancer Inst* **2015**, *107*, doi:10.1093/jnci/dju494.
233. Howell, P.M., Jr.; Li, X.; Riker, A.I.; Xi, Y. MicroRNA in Melanoma. *Ochsner J* **2010**, *10*, 83-92.
234. Philippidou, D.; Schmitt, M.; Moser, D.; Margue, C.; Nazarov, P.V.; Muller, A.; Vallar, L.; Nashan, D.; Behrmann, I.; Kreis, S. Signatures of microRNAs and selected microRNA target genes in human melanoma. *Cancer Res* **2010**, *70*, 4163-4173, doi:10.1158/0008-5472.CAN-09-4512.
235. Balkwill, F.R.; Capasso, M.; Hagemann, T. The tumor microenvironment at a glance. *J Cell Sci* **2012**, *125*, 5591-5596, doi:10.1242/jcs.116392.
236. Zhang, B.; Pan, X.; Cobb, G.P.; Anderson, T.A. microRNAs as oncogenes and tumor suppressors. *Dev Biol* **2007**, *302*, 1-12, doi:10.1016/j.ydbio.2006.08.028.
237. Peng, Y.; Croce, C.M. The role of MicroRNAs in human cancer. *Signal Transduct Target Ther* **2016**, *1*, 15004, doi:10.1038/sigtrans.2015.4.
238. Calin, G.A.; Dumitru, C.D.; Shimizu, M.; Bichi, R.; Zupo, S.; Noch, E.; Aldler, H.; Rattan, S.; Keating, M.; Rai, K.; et al. Frequent deletions and down-regulation of micro- RNA genes miR15 and miR16 at 13q14 in chronic lymphocytic leukemia. *Proc Natl Acad Sci U S A* **2002**, *99*, 15524-15529, doi:10.1073/pnas.242606799.
239. Calin, G.A.; Croce, C.M. MicroRNAs and chromosomal abnormalities in cancer cells. *Oncogene* **2006**, *25*, 6202-6210, doi:10.1038/sj.onc.1209910.
240. Ota, A.; Tagawa, H.; Karnan, S.; Tsuzuki, S.; Karpas, A.; Kira, S.; Yoshida, Y.; Seto, M. Identification and characterization of a novel gene, C13orf25, as a target for 13q31-q32 amplification in malignant lymphoma. *Cancer Res* **2004**, *64*, 3087-3095, doi:10.1158/0008-5472.can-03-3773.
241. Tagawa, H.; Seto, M. A microRNA cluster as a target of genomic amplification in malignant lymphoma. *Leukemia* **2005**, *19*, 2013-2016, doi:10.1038/sj.leu.2403942.
242. Hayashita, Y.; Osada, H.; Tatematsu, Y.; Yamada, H.; Yanagisawa, K.; Tomida, S.; Yatabe, Y.; Kawahara, K.; Sekido, Y.; Takahashi, T. A polycistronic microRNA cluster, miR-17-92, is overexpressed in human lung cancers and enhances cell proliferation. *Cancer Res* **2005**, *65*, 9628-9632, doi:10.1158/0008-5472.CAN-05-2352.
243. Mavrakis, K.J.; Wolfe, A.L.; Oricchio, E.; Palomero, T.; de Keersmaecker, K.; McJunkin, K.; Zuber, J.; James, T.; Khan, A.A.; Leslie, C.S.; et al. Genome-wide RNA-mediated interference screen identifies miR-19 targets in Notch-induced T-cell acute lymphoblastic leukaemia. *Nat Cell Biol* **2010**, *12*, 372-379, doi:10.1038/ncb2037.
244. Zhang, L.; Huang, J.; Yang, N.; Greshock, J.; Megraw, M.S.; Giannakakis, A.; Liang, S.; Naylor, T.L.; Barchetti, A.; Ward, M.R.; et al. microRNAs exhibit high frequency genomic alterations in human cancer. *Proc Natl Acad Sci U S A* **2006**, *103*, 9136-9141, doi:10.1073/pnas.0508889103.
245. Calin, G.A.; Sevignani, C.; Dumitru, C.D.; Hyslop, T.; Noch, E.; Yendamuri, S.; Shimizu, M.; Rattan, S.; Bullrich, F.; Negrini, M.; et al. Human microRNA genes are frequently located

at fragile sites and genomic regions involved in cancers. *Proc Natl Acad Sci U S A* **2004**, *101*, 2999-3004, doi:10.1073/pnas.0307323101.

246. O'Donnell, K.A.; Wentzel, E.A.; Zeller, K.I.; Dang, C.V.; Mendell, J.T. c-Myc-regulated microRNAs modulate E2F1 expression. *Nature* **2005**, *435*, 839-843, doi:10.1038/nature03677.
247. Chang, T.C.; Yu, D.; Lee, Y.S.; Wentzel, E.A.; Arking, D.E.; West, K.M.; Dang, C.V.; Thomas-Tikhonenko, A.; Mendell, J.T. Widespread microRNA repression by Myc contributes to tumorigenesis. *Nat Genet* **2008**, *40*, 43-50, doi:10.1038/ng.2007.30.
248. Wang, B.; Hsu, S.H.; Wang, X.; Kutay, H.; Bid, H.K.; Yu, J.; Ganju, R.K.; Jacob, S.T.; Yuneva, M.; Ghoshal, K. Reciprocal regulation of microRNA-122 and c-Myc in hepatocellular cancer: role of E2F1 and transcription factor dimerization partner 2. *Hepatology* **2014**, *59*, 555-566, doi:10.1002/hep.26712.
249. Han, H.; Sun, D.; Li, W.; Shen, H.; Zhu, Y.; Li, C.; Chen, Y.; Lu, L.; Li, W.; Zhang, J.; et al. A c-Myc-MicroRNA functional feedback loop affects hepatocarcinogenesis. *Hepatology* **2013**, *57*, 2378-2389, doi:10.1002/hep.26302.
250. He, L.; He, X.; Lim, L.P.; de Stanchina, E.; Xuan, Z.; Liang, Y.; Xue, W.; Zender, L.; Magnus, J.; Ridzon, D.; et al. A microRNA component of the p53 tumour suppressor network. *Nature* **2007**, *447*, 1130-1134, doi:10.1038/nature05939.
251. Hermeking, H. The miR-34 family in cancer and apoptosis. *Cell Death Differ* **2010**, *17*, 193-199, doi:10.1038/cdd.2009.56.
252. Raver-Shapira, N.; Marciano, E.; Meiri, E.; Spector, Y.; Rosenfeld, N.; Moskovits, N.; Bentwich, Z.; Oren, M. Transcriptional activation of miR-34a contributes to p53-mediated apoptosis. *Molecular cell* **2007**, *26*, 731-743, doi:10.1016/j.molcel.2007.05.017.
253. Chang, T.C.; Wentzel, E.A.; Kent, O.A.; Ramachandran, K.; Mullendore, M.; Lee, K.H.; Feldmann, G.; Yamakuchi, M.; Ferlito, M.; Lowenstein, C.J.; et al. Transactivation of miR-34a by p53 broadly influences gene expression and promotes apoptosis. *Molecular cell* **2007**, *26*, 745-752, doi:10.1016/j.molcel.2007.05.010.
254. Yamakuchi, M.; Lowenstein, C.J. MiR-34, SIRT1 and p53: the feedback loop. *Cell Cycle* **2009**, *8*, 712-715, doi:10.4161/cc.8.5.7753.
255. Xiao, J.; Lin, H.; Luo, X.; Luo, X.; Wang, Z. miR-605 joins p53 network to form a p53:miR-605:Mdm2 positive feedback loop in response to stress. *EMBO J* **2011**, *30*, 524-532, doi:10.1038/emboj.2010.347.
256. Zhang, Y.; Liao, J.M.; Zeng, S.X.; Lu, H. p53 downregulates Down syndrome-associated DYRK1A through miR-1246. *EMBO Rep* **2011**, *12*, 811-817, doi:10.1038/embor.2011.98.
257. Yamakuchi, M.; Lotterman, C.D.; Bao, C.; Hruban, R.H.; Karim, B.; Mendell, J.T.; Huso, D.; Lowenstein, C.J. P53-induced microRNA-107 inhibits HIF-1 and tumor angiogenesis. *Proc Natl Acad Sci U S A* **2010**, *107*, 6334-6339, doi:10.1073/pnas.0911082107.
258. Han, L.; Witmer, P.D.; Casey, E.; Valle, D.; Sukumar, S. DNA methylation regulates MicroRNA expression. *Cancer Biol Ther* **2007**, *6*, 1284-1288, doi:10.4161/cbt.6.8.4486.
259. Saito, Y.; Jones, P.A. Epigenetic activation of tumor suppressor microRNAs in human cancer cells. *Cell Cycle* **2006**, *5*, 2220-2222, doi:10.4161/cc.5.19.3340.
260. Fazi, F.; Racanicchi, S.; Zardo, G.; Starnes, L.M.; Mancini, M.; Travaglini, L.; Diverio, D.; Ammatuna, E.; Cimino, G.; Lo-Coco, F.; et al. Epigenetic silencing of the myelopoiesis regulator microRNA-223 by the AML1/ETO oncoprotein. *Cancer Cell* **2007**, *12*, 457-466, doi:10.1016/j.ccr.2007.09.020.
261. Saito, Y.; Liang, G.; Egger, G.; Friedman, J.M.; Chuang, J.C.; Coetzee, G.A.; Jones, P.A. Specific activation of microRNA-127 with downregulation of the proto-oncogene BCL6 by chromatin-modifying drugs in human cancer cells. *Cancer Cell* **2006**, *9*, 435-443, doi:10.1016/j.ccr.2006.04.020.
262. Lujambio, A.; Calin, G.A.; Villanueva, A.; Ropero, S.; Sanchez-Cespedes, M.; Blanco, D.; Montuenga, L.M.; Rossi, S.; Nicoloso, M.S.; Faller, W.J.; et al. A microRNA DNA

methylation signature for human cancer metastasis. *Proc Natl Acad Sci U S A* **2008**, *105*, 13556-13561, doi:10.1073/pnas.0803055105.

263. Lehmann, U.; Hasemeier, B.; Christgen, M.; Muller, M.; Romermann, D.; Langer, F.; Kreipe, H. Epigenetic inactivation of microRNA gene hsa-mir-9-1 in human breast cancer. *J Pathol* **2008**, *214*, 17-24, doi:10.1002/path.2251.
264. Lujambio, A.; Esteller, M. CpG island hypermethylation of tumor suppressor microRNAs in human cancer. *Cell Cycle* **2007**, *6*, 1455-1459.
265. Donzelli, S.; Mori, F.; Bellissimo, T.; Sacconi, A.; Casini, B.; Frixa, T.; Roscilli, G.; Aurisicchio, L.; Facciolo, F.; Pompili, A.; et al. Epigenetic silencing of miR-145-5p contributes to brain metastasis. *Oncotarget* **2015**, *6*, 35183-35201, doi:10.18632/oncotarget.5930.
266. Walz, A.L.; Ooms, A.; Gadd, S.; Gerhard, D.S.; Smith, M.A.; Guidry Auvil, J.M.; Meerzaman, D.; Chen, Q.R.; Hsu, C.H.; Yan, C.; et al. Recurrent DGCR8, DROSHA, and SIX homeodomain mutations in favorable histology Wilms tumors. *Cancer Cell* **2015**, *27*, 286-297, doi:10.1016/j.ccell.2015.01.003.
267. Iliou, M.S.; da Silva-Diz, V.; Carmona, F.J.; Ramalho-Carvalho, J.; Heyn, H.; Villanueva, A.; Munoz, P.; Esteller, M. Impaired DICER1 function promotes stemness and metastasis in colon cancer. *Oncogene* **2014**, *33*, 4003-4015, doi:10.1038/onc.2013.398.
268. Merritt, W.M.; Lin, Y.G.; Han, L.Y.; Kamat, A.A.; Spannuth, W.A.; Schmandt, R.; Urbauer, D.; Pennacchio, L.A.; Cheng, J.F.; Nick, A.M.; et al. Dicer, Drosha, and outcomes in patients with ovarian cancer. *N Engl J Med* **2008**, *359*, 2641-2650, doi:10.1056/NEJMoa0803785.
269. Pampalakis, G.; Diamandis, E.P.; Katsaros, D.; Sotiropoulou, G. Down-regulation of dicer expression in ovarian cancer tissues. *Clin Biochem* **2010**, *43*, 324-327, doi:10.1016/j.clinbiochem.2009.09.014.
270. Faggad, A.; Budczies, J.; Tchernitsa, O.; Darb-Esfahani, S.; Sehouli, J.; Muller, B.M.; Wirtz, R.; Chekerov, R.; Weichert, W.; Sinn, B.; et al. Prognostic significance of Dicer expression in ovarian cancer-link to global microRNA changes and oestrogen receptor expression. *J Pathol* **2010**, *220*, 382-391, doi:10.1002/path.2658.
271. Karube, Y.; Tanaka, H.; Osada, H.; Tomida, S.; Tatematsu, Y.; Yanagisawa, K.; Yatabe, Y.; Takamizawa, J.; Miyoshi, S.; Mitsudomi, T.; et al. Reduced expression of Dicer associated with poor prognosis in lung cancer patients. *Cancer Sci* **2005**, *96*, 111-115, doi:10.1111/j.1349-7006.2005.00015.x.
272. Dome, J.S.; Coppes, M.J. Recent advances in Wilms tumor genetics. *Curr Opin Pediatr* **2002**, *14*, 5-11, doi:10.1097/00008480-200202000-00002.
273. Zhang, J.; Fan, X.S.; Wang, C.X.; Liu, B.; Li, Q.; Zhou, X.J. Up-regulation of Ago2 expression in gastric carcinoma. *Med Oncol* **2013**, *30*, 628, doi:10.1007/s12032-013-0628-2.
274. Voller, D.; Reinders, J.; Meister, G.; Bosserhoff, A.K. Strong reduction of AGO2 expression in melanoma and cellular consequences. *Br J Cancer* **2013**, *109*, 3116-3124, doi:10.1038/bjc.2013.646.
275. Melo, S.A.; Moutinho, C.; Ropero, S.; Calin, G.A.; Rossi, S.; Spizzo, R.; Fernandez, A.F.; Davalos, V.; Villanueva, A.; Montoya, G.; et al. A genetic defect in exportin-5 traps precursor microRNAs in the nucleus of cancer cells. *Cancer Cell* **2010**, *18*, 303-315, doi:10.1016/j.ccr.2010.09.007.
276. Hanahan, D.; Weinberg, R.A. Hallmarks of cancer: the next generation. *Cell* **2011**, *144*, 646-674, doi:10.1016/j.cell.2011.02.013.
277. Trimarchi, J.M.; Lees, J.A. Sibling rivalry in the E2F family. *Nat Rev Mol Cell Biol* **2002**, *3*, 11-20, doi:10.1038/nrm714.
278. Sylvestre, Y.; De Guire, V.; Querido, E.; Mukhopadhyay, U.K.; Bourdeau, V.; Major, F.; Ferbeyre, G.; Chartrand, P. An E2F/miR-20a autoregulatory feedback loop. *J Biol Chem* **2007**, *282*, 2135-2143, doi:10.1074/jbc.M608939200.

279. Woods, K.; Thomson, J.M.; Hammond, S.M. Direct regulation of an oncogenic micro-RNA cluster by E2F transcription factors. *J Biol Chem* **2007**, *282*, 2130-2134, doi:10.1074/jbc.C600252200.
280. Du, B.; Wang, Z.; Zhang, X.; Feng, S.; Wang, G.; He, J.; Zhang, B. MicroRNA-545 suppresses cell proliferation by targeting cyclin D1 and CDK4 in lung cancer cells. *PLoS One* **2014**, *9*, e88022, doi:10.1371/journal.pone.0088022.
281. Gillies, J.K.; Lorimer, I.A. Regulation of p27Kip1 by miRNA 221/222 in glioblastoma. *Cell Cycle* **2007**, *6*, 2005-2009, doi:10.4161/cc.6.16.4526.
282. Galardi, S.; Mercatelli, N.; Giorda, E.; Massalini, S.; Frajese, G.V.; Ciafre, S.A.; Farace, M.G. miR-221 and miR-222 expression affects the proliferation potential of human prostate carcinoma cell lines by targeting p27Kip1. *J Biol Chem* **2007**, *282*, 23716-23724, doi:10.1074/jbc.M701805200.
283. le Sage, C.; Nagel, R.; Egan, D.A.; Schrier, M.; Mesman, E.; Mangiola, A.; Anile, C.; Maira, G.; Mercatelli, N.; Ciafre, S.A.; et al. Regulation of the p27(Kip1) tumor suppressor by miR-221 and miR-222 promotes cancer cell proliferation. *EMBO J* **2007**, *26*, 3699-3708, doi:10.1038/sj.emboj.7601790.
284. Visone, R.; Russo, L.; Pallante, P.; De Martino, I.; Ferraro, A.; Leone, V.; Borbone, E.; Petrocca, F.; Alder, H.; Croce, C.M.; et al. MicroRNAs (miR)-221 and miR-222, both overexpressed in human thyroid papillary carcinomas, regulate p27Kip1 protein levels and cell cycle. *Endocr Relat Cancer* **2007**, *14*, 791-798, doi:10.1677/ERC-07-0129.
285. Hussein, M.R.; Haemel, A.K.; Wood, G.S. Apoptosis and melanoma: molecular mechanisms. *J Pathol* **2003**, *199*, 275-288, doi:10.1002/path.1300.
286. Pichiorri, F.; Suh, S.S.; Rocci, A.; De Luca, L.; Taccioli, C.; Santhanam, R.; Zhou, W.; Benson, D.M., Jr.; Hofmainster, C.; Alder, H.; et al. Downregulation of p53-inducible microRNAs 192, 194, and 215 impairs the p53/MDM2 autoregulatory loop in multiple myeloma development. *Cancer Cell* **2010**, *18*, 367-381, doi:10.1016/j.ccr.2010.09.005.
287. Zhang, C.Z.; Zhang, J.X.; Zhang, A.L.; Shi, Z.D.; Han, L.; Jia, Z.F.; Yang, W.D.; Wang, G.X.; Jiang, T.; You, Y.P.; et al. MiR-221 and miR-222 target PUMA to induce cell survival in glioblastoma. *Mol Cancer* **2010**, *9*, 229, doi:10.1186/1476-4598-9-229.
288. Cimmino, A.; Calin, G.A.; Fabbri, M.; Iorio, M.V.; Ferracin, M.; Shimizu, M.; Wojcik, S.E.; Aqeilan, R.I.; Zupo, S.; Dono, M.; et al. miR-15 and miR-16 induce apoptosis by targeting BCL2. *Proc Natl Acad Sci U S A* **2005**, *102*, 13944-13949, doi:10.1073/pnas.0506654102.
289. Sacconi, A.; Biagioni, F.; Canu, V.; Mori, F.; Di Benedetto, A.; Lorenzon, L.; Ercolani, C.; Di Agostino, S.; Cambria, A.M.; Germoni, S.; et al. miR-204 targets Bcl-2 expression and enhances responsiveness of gastric cancer. *Cell Death Dis* **2012**, *3*, e423, doi:10.1038/cddis.2012.160.
290. Zhang, H.; Li, Y.; Huang, Q.; Ren, X.; Hu, H.; Sheng, H.; Lai, M. MiR-148a promotes apoptosis by targeting Bcl-2 in colorectal cancer. *Cell Death Differ* **2011**, *18*, 1702-1710, doi:10.1038/cdd.2011.28.
291. Nie, J.; Liu, L.; Zheng, W.; Chen, L.; Wu, X.; Xu, Y.; Du, X.; Han, W. microRNA-365, down-regulated in colon cancer, inhibits cell cycle progression and promotes apoptosis of colon cancer cells by probably targeting Cyclin D1 and Bcl-2. *Carcinogenesis* **2012**, *33*, 220-225, doi:10.1093/carcin/bgr245.
292. Denoyelle, C.; Lambert, B.; Meryet-Figuiere, M.; Vigneron, N.; Brotin, E.; Lecerf, C.; Abeilard, E.; Giffard, F.; Louis, M.H.; Gauduchon, P.; et al. miR-491-5p-induced apoptosis in ovarian carcinoma depends on the direct inhibition of both BCL-XL and EGFR leading to BIM activation. *Cell Death Dis* **2014**, *5*, e1445, doi:10.1038/cddis.2014.389.
293. Hatley, M.E.; Patrick, D.M.; Garcia, M.R.; Richardson, J.A.; Bassel-Duby, R.; van Rooij, E.; Olson, E.N. Modulation of K-Ras-dependent lung tumorigenesis by MicroRNA-21. *Cancer Cell* **2010**, *18*, 282-293, doi:10.1016/j.ccr.2010.08.013.

294. Kalluri, R.; Weinberg, R.A. The basics of epithelial-mesenchymal transition. *J Clin Invest* **2009**, *119*, 1420-1428, doi:10.1172/JCI39104.
295. Kong, W.; Yang, H.; He, L.; Zhao, J.J.; Coppola, D.; Dalton, W.S.; Cheng, J.Q. MicroRNA-155 is regulated by the transforming growth factor beta/Smad pathway and contributes to epithelial cell plasticity by targeting RhoA. *Mol Cell Biol* **2008**, *28*, 6773-6784, doi:10.1128/MCB.00941-08.
296. Ma, L.; Teruya-Feldstein, J.; Weinberg, R.A. Tumour invasion and metastasis initiated by microRNA-10b in breast cancer. *Nature* **2007**, *449*, 682-688, doi:10.1038/nature06174.
297. Ma, L.; Young, J.; Prabhala, H.; Pan, E.; Mestdagh, P.; Muth, D.; Teruya-Feldstein, J.; Reinhardt, F.; Onder, T.T.; Valastyan, S.; et al. miR-9, a MYC/MYCN-activated microRNA, regulates E-cadherin and cancer metastasis. *Nat Cell Biol* **2010**, *12*, 247-256, doi:10.1038/ncb2024.
298. Hurteau, G.J.; Carlson, J.A.; Spivack, S.D.; Brock, G.J. Overexpression of the microRNA hsa-miR-200c leads to reduced expression of transcription factor 8 and increased expression of E-cadherin. *Cancer Res* **2007**, *67*, 7972-7976, doi:10.1158/0008-5472.CAN-07-1058.
299. Korpal, M.; Lee, E.S.; Hu, G.; Kang, Y. The miR-200 family inhibits epithelial-mesenchymal transition and cancer cell migration by direct targeting of E-cadherin transcriptional repressors ZEB1 and ZEB2. *J Biol Chem* **2008**, *283*, 14910-14914, doi:10.1074/jbc.C800074200.
300. Ding, X.; Park, S.I.; McCauley, L.K.; Wang, C.Y. Signaling between transforming growth factor beta (TGF-beta) and transcription factor SNAI2 represses expression of microRNA miR-203 to promote epithelial-mesenchymal transition and tumor metastasis. *J Biol Chem* **2013**, *288*, 10241-10253, doi:10.1074/jbc.M112.443655.
301. Zhang, Z.; Zhang, B.; Li, W.; Fu, L.; Fu, L.; Zhu, Z.; Dong, J.T. Epigenetic Silencing of miR-203 Upregulates SNAI2 and Contributes to the Invasiveness of Malignant Breast Cancer Cells. *Genes Cancer* **2011**, *2*, 782-791, doi:10.1177/1947601911429743.
302. Meng, X.; Wu, J.; Pan, C.; Wang, H.; Ying, X.; Zhou, Y.; Yu, H.; Zuo, Y.; Pan, Z.; Liu, R.Y.; et al. Genetic and epigenetic down-regulation of microRNA-212 promotes colorectal tumor metastasis via dysregulation of MnSOD. *Gastroenterology* **2013**, *145*, 426-436 e421-426, doi:10.1053/j.gastro.2013.04.004.
303. Ferrara, N. VEGF and the quest for tumour angiogenesis factors. *Nat Rev Cancer* **2002**, *2*, 795-803, doi:10.1038/nrc909.
304. Camps, C.; Buffa, F.M.; Colella, S.; Moore, J.; Sotiriou, C.; Sheldon, H.; Harris, A.L.; Gleadle, J.M.; Ragoussis, J. hsa-miR-210 Is induced by hypoxia and is an independent prognostic factor in breast cancer. *Clin Cancer Res* **2008**, *14*, 1340-1348, doi:10.1158/1078-0432.CCR-07-1755.
305. Fasanaro, P.; D'Alessandra, Y.; Di Stefano, V.; Melchionna, R.; Romani, S.; Pompilio, G.; Capogrossi, M.C.; Martelli, F. MicroRNA-210 modulates endothelial cell response to hypoxia and inhibits the receptor tyrosine kinase ligand Ephrin-A3. *J Biol Chem* **2008**, *283*, 15878-15883, doi:10.1074/jbc.M800731200.
306. Lou, Y.L.; Guo, F.; Liu, F.; Gao, F.L.; Zhang, P.Q.; Niu, X.; Guo, S.C.; Yin, J.H.; Wang, Y.; Deng, Z.F. miR-210 activates notch signaling pathway in angiogenesis induced by cerebral ischemia. *Mol Cell Biochem* **2012**, *370*, 45-51, doi:10.1007/s11010-012-1396-6.
307. Liu, F.; Lou, Y.L.; Wu, J.; Ruan, Q.F.; Xie, A.; Guo, F.; Cui, S.P.; Deng, Z.F.; Wang, Y. Upregulation of microRNA-210 regulates renal angiogenesis mediated by activation of VEGF signaling pathway under ischemia/perfusion injury in vivo and in vitro. *Kidney Blood Press Res* **2012**, *35*, 182-191, doi:10.1159/000331054.
308. Ghosh, G.; Subramanian, I.V.; Adhikari, N.; Zhang, X.; Joshi, H.P.; Basi, D.; Chandrashekhar, Y.S.; Hall, J.L.; Roy, S.; Zeng, Y.; et al. Hypoxia-induced microRNA-424 expression in human endothelial cells regulates HIF-alpha isoforms and promotes angiogenesis. *J Clin Invest* **2010**, *120*, 4141-4154, doi:10.1172/JCI42980.

309. Liu, L.Z.; Li, C.; Chen, Q.; Jing, Y.; Carpenter, R.; Jiang, Y.; Kung, H.F.; Lai, L.; Jiang, B.H. MiR-21 induced angiogenesis through AKT and ERK activation and HIF-1alpha expression. *PLoS One* **2011**, *6*, e19139, doi:10.1371/journal.pone.0019139.
310. Lei, Z.; Li, B.; Yang, Z.; Fang, H.; Zhang, G.M.; Feng, Z.H.; Huang, B. Regulation of HIF-1alpha and VEGF by miR-20b tunes tumor cells to adapt to the alteration of oxygen concentration. *PLoS One* **2009**, *4*, e7629, doi:10.1371/journal.pone.0007629.
311. Cha, S.T.; Chen, P.S.; Johansson, G.; Chu, C.Y.; Wang, M.Y.; Jeng, Y.M.; Yu, S.L.; Chen, J.S.; Chang, K.J.; Jee, S.H.; et al. MicroRNA-519c suppresses hypoxia-inducible factor-1alpha expression and tumor angiogenesis. *Cancer Res* **2010**, *70*, 2675-2685, doi:10.1158/0008-5472.CAN-09-2448.
312. Riefolo, M.; Porcellini, E.; Dika, E.; Broseghini, E.; Ferracin, M. Interplay between small and long non-coding RNAs in cutaneous melanoma: a complex jigsaw puzzle with missing pieces. *Mol Oncol* **2019**, *13*, 74-98, doi:10.1002/1878-0261.12412.
313. Levy, C.; Khaled, M.; Fisher, D.E. MITF: master regulator of melanocyte development and melanoma oncogene. *Trends Mol Med* **2006**, *12*, 406-414, doi:10.1016/j.molmed.2006.07.008.
314. Kawakami, A.; Fisher, D.E. The master role of microphthalmia-associated transcription factor in melanocyte and melanoma biology. *Lab Invest* **2017**, *97*, 649-656, doi:10.1038/labinvest.2017.9.
315. Hsiao, J.J.; Fisher, D.E. The roles of microphthalmia-associated transcription factor and pigmentation in melanoma. *Arch Biochem Biophys* **2014**, *563*, 28-34, doi:10.1016/j.abb.2014.07.019.
316. Uzdensky, A.B.; Demyanenko, S.V.; Bibov, M.Y. Signal transduction in human cutaneous melanoma and target drugs. *Curr Cancer Drug Targets* **2013**, *13*, 843-866, doi:10.2174/15680096113130080004.
317. Vitiello, M.; Tuccoli, A.; D'Aurizio, R.; Sarti, S.; Giannecchini, L.; Lubrano, S.; Marranci, A.; Evangelista, M.; Peppicelli, S.; Ippolito, C.; et al. Context-dependent miR-204 and miR-211 affect the biological properties of amelanotic and melanotic melanoma cells. *Oncotarget* **2017**, *8*, 25395-25417, doi:10.18632/oncotarget.15915.
318. Levy, C.; Khaled, M.; Iliopoulos, D.; Janas, M.M.; Schubert, S.; Pinner, S.; Chen, P.H.; Li, S.; Fletcher, A.L.; Yokoyama, S.; et al. Intronic miR-211 assumes the tumor suppressive function of its host gene in melanoma. *Molecular cell* **2010**, *40*, 841-849, doi:10.1016/j.molcel.2010.11.020.
319. Mazar, J.; DeYoung, K.; Khaitan, D.; Meister, E.; Almodovar, A.; Goydos, J.; Ray, A.; Perera, R.J. The regulation of miRNA-211 expression and its role in melanoma cell invasiveness. *PLoS One* **2010**, *5*, e13779, doi:10.1371/journal.pone.0013779.
320. Xu, Y.; Brenn, T.; Brown, E.R.; Doherty, V.; Melton, D.W. Differential expression of microRNAs during melanoma progression: miR-200c, miR-205 and miR-211 are downregulated in melanoma and act as tumour suppressors. *Br J Cancer* **2012**, *106*, 553-561, doi:10.1038/bjc.2011.568.
321. Luo, C.; Merz, P.R.; Chen, Y.; Dickes, E.; Pscherer, A.; Schadendorf, D.; Eichmuller, S.B. MiR-101 inhibits melanoma cell invasion and proliferation by targeting MITF and EZH2. *Cancer Lett* **2013**, *341*, 240-247, doi:10.1016/j.canlet.2013.08.021.
322. Bemis, L.T.; Chen, R.; Amato, C.M.; Classen, E.H.; Robinson, S.E.; Coffey, D.G.; Erickson, P.F.; Shellman, Y.G.; Robinson, W.A. MicroRNA-137 targets microphthalmia-associated transcription factor in melanoma cell lines. *Cancer Res* **2008**, *68*, 1362-1368, doi:10.1158/0008-5472.CAN-07-2912.
323. Haflidadottir, B.S.; Bergsteinsdottir, K.; Praetorius, C.; Steingrimsson, E. miR-148 regulates Mitf in melanoma cells. *PLoS One* **2010**, *5*, e11574, doi:10.1371/journal.pone.0011574.
324. Luo, C.; Tetteh, P.W.; Merz, P.R.; Dickes, E.; Abukiwan, A.; Hotz-Wagenblatt, A.; Holland-Cunz, S.; Sinnberg, T.; Schittek, B.; Schadendorf, D.; et al. miR-137 inhibits the invasion of

melanoma cells through downregulation of multiple oncogenic target genes. *J Invest Dermatol* **2013**, *133*, 768-775, doi:10.1038/jid.2012.357.

325. Ozsolak, F.; Poling, L.L.; Wang, Z.; Liu, H.; Liu, X.S.; Roeder, R.G.; Zhang, X.; Song, J.S.; Fisher, D.E. Chromatin structure analyses identify miRNA promoters. *Genes Dev* **2008**, *22*, 3172-3183, doi:10.1101/gad.1706508.
326. Arts, N.; Cane, S.; Hennequart, M.; Lamy, J.; Bommer, G.; Van den Eynde, B.; De Plaen, E. microRNA-155, induced by interleukin-1ss, represses the expression of microphthalmia-associated transcription factor (MITF-M) in melanoma cells. *PLoS One* **2015**, *10*, e0122517, doi:10.1371/journal.pone.0122517.
327. Segura, M.F.; Hanniford, D.; Menendez, S.; Reavie, L.; Zou, X.; Alvarez-Diaz, S.; Zakrzewski, J.; Blochin, E.; Rose, A.; Bogunovic, D.; et al. Aberrant miR-182 expression promotes melanoma metastasis by repressing FOXO3 and microphthalmia-associated transcription factor. *Proc Natl Acad Sci U S A* **2009**, *106*, 1814-1819, doi:10.1073/pnas.0808263106.
328. Guo, J.; Zhang, J.F.; Wang, W.M.; Cheung, F.W.; Lu, Y.F.; Ng, C.F.; Kung, H.F.; Liu, W.K. MicroRNA-218 inhibits melanogenesis by directly suppressing microphthalmia-associated transcription factor expression. *RNA Biol* **2014**, *11*, 732-741, doi:10.4161/rna.28865.
329. Qian, H.; Yang, C.; Yang, Y. MicroRNA-26a inhibits the growth and invasiveness of malignant melanoma and directly targets on MITF gene. *Cell Death Discov* **2017**, *3*, 17028, doi:10.1038/cddiscovery.2017.28.
330. Goswami, S.; Tarapore, R.S.; Poenitzsch Strong, A.M.; TeSlaa, J.J.; Grinblat, Y.; Setaluri, V.; Spiegelman, V.S. MicroRNA-340-mediated degradation of microphthalmia-associated transcription factor (MITF) mRNA is inhibited by coding region determinant-binding protein (CRD-BP). *J Biol Chem* **2015**, *290*, 384-395, doi:10.1074/jbc.M114.590158.
331. Pierard, G.E. Cell proliferation in cutaneous malignant melanoma: relationship with neoplastic progression. *ISRN Dermatol* **2012**, *2012*, 828146, doi:10.5402/2012/828146.
332. Bueno, M.J.; Malumbres, M. MicroRNAs and the cell cycle. *Biochim Biophys Acta* **2011**, *1812*, 592-601, doi:10.1016/j.bbadis.2011.02.002.
333. Wang, S.; Wu, Y.; Xu, Y.; Tang, X. miR-10b promoted melanoma progression through Wnt/beta-catenin pathway by repressing ITCH expression. *Gene* **2019**, *710*, 39-47, doi:10.1016/j.gene.2019.05.043.
334. Lin, N.; Zhou, Y.; Lian, X.; Tu, Y. Expression of microRNA-106b and its clinical significance in cutaneous melanoma. *Genet Mol Res* **2015**, *14*, 16379-16385, doi:10.4238/2015.December.9.6.
335. Chen, X.; Chen, P.; Chen, S.S.; Ma, T.; Shi, G.; Zhou, Y.; Li, J.; Sheng, L. miR106b5p promotes cell cycle progression of malignant melanoma by targeting PTEN. *Oncol Rep* **2018**, *39*, 331-337, doi:10.3892/or.2017.6099.
336. Ren, J.W.; Li, Z.J.; Tu, C. MiR-135 post-transcriptionally regulates FOXO1 expression and promotes cell proliferation in human malignant melanoma cells. *Int J Clin Exp Pathol* **2015**, *8*, 6356-6366.
337. Raimo, M.; Orso, F.; Grassi, E.; Cimino, D.; Penna, E.; De Pitta, C.; Stadler, M.B.; Primo, L.; Calautti, E.; Quaglino, P.; et al. miR-146a Exerts Differential Effects on Melanoma Growth and Metastatization. *Mol Cancer Res* **2016**, *14*, 548-562, doi:10.1158/1541-7786.MCR-15-0425-T.
338. Ohira, T.; Naohiro, S.; Nakayama, Y.; Osaki, M.; Okada, F.; Oshimura, M.; Kugoh, H. miR-19b regulates hTERT mRNA expression through targeting PITX1 mRNA in melanoma cells. *Sci Rep* **2015**, *5*, 8201, doi:10.1038/srep08201.
339. Greenberg, E.; Hajdu, S.; Nemlich, Y.; Cohen, R.; Itzhaki, O.; Jacob-Hirsch, J.; Besser, M.J.; Schachter, J.; Markel, G. Differential regulation of aggressive features in melanoma cells by members of the miR-17-92 complex. *Open Biol* **2014**, *4*, 140030, doi:10.1098/rsob.140030.

340. Yang, C.H.; Yue, J.; Pfeffer, S.R.; Handorf, C.R.; Pfeffer, L.M. MicroRNA miR-21 regulates the metastatic behavior of B16 melanoma cells. *J Biol Chem* **2011**, *286*, 39172-39178, doi:10.1074/jbc.M111.285098.
341. Felicetti, F.; Errico, M.C.; Bottero, L.; Segnalini, P.; Stoppacciaro, A.; Biffoni, M.; Felli, N.; Mattia, G.; Petrini, M.; Colombo, M.P.; et al. The promyelocytic leukemia zinc finger-microRNA-221/-222 pathway controls melanoma progression through multiple oncogenic mechanisms. *Cancer Res* **2008**, *68*, 2745-2754, doi:10.1158/0008-5472.CAN-07-2538.
342. Huo, J.; Zhang, Y.; Li, R.; Wang, Y.; Wu, J.; Zhang, D. Upregulated MicroRNA-25 Mediates the Migration of Melanoma Cells by Targeting DKK3 through the WNT/beta-Catenin Pathway. *International journal of molecular sciences* **2016**, *17*, doi:10.3390/ijms17111124.
343. Jiang, Q.Q.; Liu, W.B. miR-25 Promotes Melanoma Progression by regulating RNA binding motif protein 47. *Med Sci (Paris)* **2018**, *34 Focus issue F1*, 59-65, doi:10.1051/medsci/201834f111.
344. Komina, A.; Palkina, N.; Aksenenko, M.; Tsyrenzhapova, S.; Ruksha, T. Antiproliferative and Pro-Apoptotic Effects of MiR-4286 Inhibition in Melanoma Cells. *PLoS One* **2016**, *11*, e0168229, doi:10.1371/journal.pone.0168229.
345. Hua, K.T.; Hong, J.B.; Sheen, Y.S.; Huang, H.Y.; Huang, Y.L.; Chen, J.S.; Liao, Y.H. miR-519d Promotes Melanoma Progression by Downregulating EphA4. *Cancer Res* **2018**, *78*, 216-229, doi:10.1158/0008-5472.CAN-17-1933.
346. Kitago, M.; Martinez, S.R.; Nakamura, T.; Sim, M.S.; Hoon, D.S. Regulation of RUNX3 tumor suppressor gene expression in cutaneous melanoma. *Clin Cancer Res* **2009**, *15*, 2988-2994, doi:10.1158/1078-0432.CCR-08-3172.
347. Zhao, C.C.; Guo, H.; Wang, Y.; Li, J.H. Comprehensive upstream and downstream regulatory analyses identify miR-675-3p as a potential prognostic biomarker in melanoma. *Hum Cell* **2021**, *34*, 654-666, doi:10.1007/s13577-020-00473-0.
348. Schultz, J.; Lorenz, P.; Gross, G.; Ibrahim, S.; Kunz, M. MicroRNA let-7b targets important cell cycle molecules in malignant melanoma cells and interferes with anchorage-independent growth. *Cell Res* **2008**, *18*, 549-557, doi:10.1038/cr.2008.45.
349. Shen, C.; Hua, H.; Gu, L.; Cao, S.; Cai, H.; Yao, X.; Chen, X. miR-124 Functions As A Melanoma Tumor Suppressor By Targeting RACK1. *Onco Targets Ther* **2019**, *12*, 9975-9986, doi:10.2147/OTT.S225120.
350. Yang, P.; Bu, P.; Li, C. miR-124 inhibits proliferation, migration and invasion of malignant melanoma cells via targeting versican. *Exp Ther Med* **2017**, *14*, 3555-3562, doi:10.3892/etm.2017.4998.
351. Zhang, Z.; Zhang, S.; Ma, P.; Jing, Y.; Peng, H.; Gao, W.Q.; Zhuang, G. Lin28B promotes melanoma growth by mediating a microRNA regulatory circuit. *Carcinogenesis* **2015**, *36*, 937-945, doi:10.1093/carcin/bgv085.
352. Nyholm, A.M.; Lerche, C.M.; Manfe, V.; Biskup, E.; Johansen, P.; Morling, N.; Thomsen, B.M.; Glud, M.; Gniadecki, R. miR-125b induces cellular senescence in malignant melanoma. *BMC Dermatol* **2014**, *14*, 8, doi:10.1186/1471-5945-14-8.
353. Felli, N.; Felicetti, F.; Lustri, A.M.; Errico, M.C.; Bottero, L.; Cannistraci, A.; De Feo, A.; Petrini, M.; Pedini, F.; Biffoni, M.; et al. miR-126&126* restored expressions play a tumor suppressor role by directly regulating ADAM9 and MMP7 in melanoma. *PLoS One* **2013**, *8*, e56824, doi:10.1371/journal.pone.0056824.
354. Wang, J.J.; Li, Z.F.; Li, X.J.; Han, Z.; Zhang, L.; Liu, Z.J. Effects of microRNA-136 on melanoma cell proliferation, apoptosis, and epithelial-mesenchymal transition by targetting PMEL through the Wnt signaling pathway. *Biosci Rep* **2017**, *37*, doi:10.1042/BSR20170743.
355. Lv, N.; Hao, S.; Luo, C.; Abukiwan, A.; Hao, Y.; Gai, F.; Huang, W.; Huang, L.; Xiao, X.; Eichmuller, S.B.; et al. miR-137 inhibits melanoma cell proliferation through downregulation of GLO1. *Sci China Life Sci* **2018**, *61*, 541-549, doi:10.1007/s11427-017-9138-9.

356. Hao, S.; Luo, C.; Abukiwan, A.; Wang, G.; He, J.; Huang, L.; Weber, C.E.; Lv, N.; Xiao, X.; Eichmuller, S.B.; et al. miR-137 inhibits proliferation of melanoma cells by targeting PAK2. *Exp Dermatol* **2015**, *24*, 947-952, doi:10.1111/exd.12812.
357. Chen, Y.; Cao, K.E.; Wang, S.; Chen, J.; He, B.; He, G.U.; Chen, Y.; Peng, B.; Zhou, J. MicroRNA-138 suppresses proliferation, invasion and glycolysis in malignant melanoma cells by targeting HIF-1alpha. *Exp Ther Med* **2016**, *11*, 2513-2518, doi:10.3892/etm.2016.3220.
358. Meng, F.; Zhang, Y.; Li, X.; Wang, J.; Wang, Z. Clinical significance of miR-138 in patients with malignant melanoma through targeting of PDK1 in the PI3K/AKT autophagy signaling pathway. *Oncol Rep* **2017**, *38*, 1655-1662, doi:10.3892/or.2017.5838.
359. Noguchi, S.; Mori, T.; Hoshino, Y.; Yamada, N.; Nakagawa, T.; Sasaki, N.; Akao, Y.; Maruo, K. Comparative study of anti-oncogenic microRNA-145 in canine and human malignant melanoma. *J Vet Med Sci* **2012**, *74*, 1-8.
360. Biroccio, A.; Amodei, S.; Antonelli, A.; Benassi, B.; Zupi, G. Inhibition of c-Myc oncoprotein limits the growth of human melanoma cells by inducing cellular crisis. *J Biol Chem* **2003**, *278*, 35693-35701, doi:10.1074/jbc.M304597200.
361. Levati, L.; Alvino, E.; Pagani, E.; Arcelli, D.; Caporaso, P.; Bondanza, S.; Di Leva, G.; Ferracin, M.; Volinia, S.; Bonmassar, E.; et al. Altered expression of selected microRNAs in melanoma: antiproliferative and proapoptotic activity of miRNA-155. *Int J Oncol* **2009**, *35*, 393-400.
362. Levati, L.; Pagani, E.; Romani, S.; Castiglia, D.; Piccinni, E.; Covaciu, C.; Caporaso, P.; Bondanza, S.; Antonetti, F.R.; Bonmassar, E.; et al. MicroRNA-155 targets the SKI gene in human melanoma cell lines. *Pigment Cell Melanoma Res* **2011**, *24*, 538-550, doi:10.1111/j.1755-148X.2011.00857.x.
363. Chen, J.; Feilotter, H.E.; Pare, G.C.; Zhang, X.; Pemberton, J.G.; Garady, C.; Lai, D.; Yang, X.; Tron, V.A. MicroRNA-193b represses cell proliferation and regulates cyclin D1 in melanoma. *Am J Pathol* **2010**, *176*, 2520-2529, doi:10.2353/ajpath.2010.091061.
364. Chen, J.; Zhang, X.; Lentz, C.; Abi-Daoud, M.; Pare, G.C.; Yang, X.; Feilotter, H.E.; Tron, V.A. miR-193b Regulates Mcl-1 in Melanoma. *Am J Pathol* **2011**, *179*, 2162-2168, doi:10.1016/j.ajpath.2011.07.010.
365. Bai, M.; Zhang, M.; Long, F.; Yu, N.; Zeng, A.; Zhao, R. Circulating microRNA-194 regulates human melanoma cells via PI3K/AKT/FoxO3a and p53/p21 signaling pathway. *Oncol Rep* **2017**, *37*, 2702-2710, doi:10.3892/or.2017.5537.
366. Yang, X.; Lei, S.; Long, J.; Liu, X.; Wu, Q. MicroRNA-199a-5p inhibits tumor proliferation in melanoma by mediating HIF-1alpha. *Mol Med Rep* **2016**, *13*, 5241-5247, doi:10.3892/mmr.2016.5202.
367. Chen, W.Y.; Xu, Y.Y.; Zhang, X.Y. Targeting GOLM1 by microRNA-200a in melanoma suppresses cell proliferation, invasion and migration via regulating PI3K/Akt signaling pathway and epithelial-mesenchymal transition. *Eur Rev Med Pharmacol Sci* **2019**, *23*, 6997-7007, doi:10.26355/eurrev_201908_18740.
368. Bustos, M.A.; Ono, S.; Marzese, D.M.; Oyama, T.; Iida, Y.; Cheung, G.; Nelson, N.; Hsu, S.C.; Yu, Q.; Hoon, D.S.B. MiR-200a Regulates CDK4/6 Inhibitor Effect by Targeting CDK6 in Metastatic Melanoma. *J Invest Dermatol* **2017**, *137*, 1955-1964, doi:10.1016/j.jid.2017.03.039.
369. Zhou, W.J.; Wang, H.Y.; Zhang, J.; Dai, H.Y.; Yao, Z.X.; Zheng, Z.; Meng-Yan, S.; Wu, K. NEAT1/miR-200b-3p/SMAD2 axis promotes progression of melanoma. *Aging (Albany NY)* **2020**, *12*, 22759-22775, doi:10.18632/aging.103909.
370. Liu, S.; Tetzlaff, M.T.; Cui, R.; Xu, X. miR-200c inhibits melanoma progression and drug resistance through down-regulation of BMI-1. *Am J Pathol* **2012**, *181*, 1823-1835, doi:10.1016/j.ajpath.2012.07.009.

371. Huang, D.; Wang, F.; Wu, W.; Lian, C.; Liu, E. MicroRNA-429 inhibits cancer cell proliferation and migration by targeting the AKT1 in melanoma. *Cancer Biomark* **2019**, *26*, 63-68, doi:10.3233/CBM-190289.
372. Chang, X.; Sun, Y.; Han, S.; Zhu, W.; Zhang, H.; Lian, S. MiR-203 inhibits melanoma invasive and proliferative abilities by targeting the polycomb group gene BMI1. *Biochem Biophys Res Commun* **2015**, *456*, 361-366, doi:10.1016/j.bbrc.2014.11.087.
373. Noguchi, S.; Mori, T.; Otsuka, Y.; Yamada, N.; Yasui, Y.; Iwasaki, J.; Kumazaki, M.; Maruo, K.; Akao, Y. Anti-oncogenic microRNA-203 induces senescence by targeting E2F3 protein in human melanoma cells. *J Biol Chem* **2012**, *287*, 11769-11777, doi:10.1074/jbc.M111.325027.
374. Franken, N.A.; Rodermond, H.M.; Stap, J.; Haveman, J.; van Bree, C. Clonogenic assay of cells in vitro. *Nat Protoc* **2006**, *1*, 2315-2319, doi:10.1038/nprot.2006.339.
375. Liu, S.; Tetzlaff, M.T.; Liu, A.; Liegl-Atzwanger, B.; Guo, J.; Xu, X. Loss of microRNA-205 expression is associated with melanoma progression. *Lab Invest* **2012**, *92*, 1084-1096, doi:10.1038/labinvest.2012.62.
376. Dar, A.A.; Majid, S.; de Semir, D.; Nosrati, M.; Bezrookove, V.; Kashani-Sabet, M. miRNA-205 suppresses melanoma cell proliferation and induces senescence via regulation of E2F1 protein. *J Biol Chem* **2011**, *286*, 16606-16614, doi:10.1074/jbc.M111.227611.
377. Georgantas, R.W., 3rd; Streicher, K.; Luo, X.; Greenlees, L.; Zhu, W.; Liu, Z.; Brohawn, P.; Morehouse, C.; Higgs, B.W.; Richman, L.; et al. MicroRNA-206 induces G1 arrest in melanoma by inhibition of CDK4 and Cyclin D. *Pigment Cell Melanoma Res* **2014**, *27*, 275-286, doi:10.1111/pcmr.12200.
378. Wei, Y.; Du, Y.; Chen, X.; Li, P.; Wang, Y.; Zang, W.; Zhao, L.; Li, Z.; Zhao, G. Expression patterns of microRNA-218 and its potential functions by targeting CIP2A and BMI1 genes in melanoma. *Tumour Biol* **2014**, *35*, 8007-8015, doi:10.1007/s13277-014-2079-6.
379. Shi, L.; Huo, J.W.; Chen, S.S.; Xue, J.X.; Gao, W.Y.; Li, X.Y.; Song, Y.H.; Xu, H.T.; Zhu, X.W.; Chen, K. MicroRNA-22 targets FMNL2 to inhibit melanoma progression via the regulation of the Wnt/beta-catenin signaling pathway and epithelial-mesenchymal transition. *Eur Rev Med Pharmacol Sci* **2019**, *23*, 5332-5342, doi:10.26355/eurrev_201906_18200.
380. Gao, J.; Zeng, K.; Liu, Y.; Gao, L.; Liu, L. LncRNA SNHG5 promotes growth and invasion in melanoma by regulating the miR-26a-5p/TRPC3 pathway. *Onco Targets Ther* **2019**, *12*, 169-179, doi:10.2147/OTT.S184078.
381. Schmitt, M.J.; Philippidou, D.; Reinsbach, S.E.; Margue, C.; Wienecke-Baldacchino, A.; Nashan, D.; Behrmann, I.; Kreis, S. Interferon-gamma-induced activation of Signal Transducer and Activator of Transcription 1 (STAT1) up-regulates the tumor suppressing microRNA-29 family in melanoma cells. *Cell Commun Signal* **2012**, *10*, 41, doi:10.1186/1478-811X-10-41.
382. Xiong, Y.; Liu, L.; Qiu, Y.; Liu, L. MicroRNA-29a Inhibits Growth, Migration and Invasion of Melanoma A375 Cells in Vitro by Directly Targeting BMI1. *Cell Physiol Biochem* **2018**, *50*, 385-397, doi:10.1159/000494015.
383. Liu, E.; Sun, X.; Li, J.; Zhang, C. miR30a5p inhibits the proliferation, migration and invasion of melanoma cells by targeting SOX4. *Mol Med Rep* **2018**, *18*, 2492-2498, doi:10.3892/mmr.2018.9166.
384. Zheng, Y.; Sun, Y.; Liu, Y.; Zhang, X.; Li, F.; Li, L.; Wang, J. The miR-31-SOX10 axis regulates tumor growth and chemotherapy resistance of melanoma via PI3K/AKT pathway. *Biochem Biophys Res Commun* **2018**, doi:10.1016/j.bbrc.2018.06.175.
385. Tian, F.; Wei, H.; Tian, H.; Qiu, Y.; Xu, J. miR-33a is downregulated in melanoma cells and modulates cell proliferation by targeting PCTAIRE1. *Oncol Lett* **2016**, *11*, 2741-2746, doi:10.3892/ol.2016.4321.

386. Zhou, J.; Xu, D.; Xie, H.; Tang, J.; Liu, R.; Li, J.; Wang, S.; Chen, X.; Su, J.; Zhou, X.; et al. miR-33a functions as a tumor suppressor in melanoma by targeting HIF-1alpha. *Cancer Biol Ther* **2015**, *16*, 846-855, doi:10.1080/15384047.2015.1030545.
387. Zhang, C.; Li, H.; Wang, J.; Zhang, J.; Hou, X. MicroRNA-338-3p suppresses cell proliferation, migration and invasion in human malignant melanoma by targeting MACC1. *Exp Ther Med* **2019**, *18*, 997-1004, doi:10.3892/etm.2019.7644.
388. Yamazaki, H.; Chijiwa, T.; Inoue, Y.; Abe, Y.; Suemizu, H.; Kawai, K.; Wakui, M.; Furukawa, D.; Mukai, M.; Kuwao, S.; et al. Overexpression of the miR-34 family suppresses invasive growth of malignant melanoma with the wild-type p53 gene. *Exp Ther Med* **2012**, *3*, 793-796, doi:10.3892/etm.2012.497.
389. Poenitzsch Strong, A.M.; Setaluri, V.; Spiegelman, V.S. MicroRNA-340 as a modulator of RAS-RAF-MAPK signaling in melanoma. *Arch Biochem Biophys* **2014**, *563*, 118-124, doi:10.1016/j.abb.2014.07.012.
390. Shi, Q.; He, Q.; Wei, J. MicroRNA-342 Prohibits Proliferation and Invasion of Melanoma Cells by Directly Targeting Zinc-Finger E-Box-Binding Homeobox 1. *Oncol Res* **2018**, *26*, 1447-1455, doi:10.3727/096504018X15193823766141.
391. Zhu, Y.; Wen, X.; Zhao, P. MicroRNA-365 Inhibits Cell Growth and Promotes Apoptosis in Melanoma by Targeting BCL2 and Cyclin D1 (CCND1). *Med Sci Monit* **2018**, *24*, 3679-3692, doi:10.12659/MSM.909633.
392. Wu, J.; Li, J.; Ren, J.; Zhang, D. MicroRNA-485-5p represses melanoma cell invasion and proliferation by suppressing Frizzled7. *Biomed Pharmacother* **2017**, *90*, 303-310, doi:10.1016/j.biopha.2017.03.064.
393. Liu, S.M.; Lu, J.; Lee, H.C.; Chung, F.H.; Ma, N. miR-524-5p suppresses the growth of oncogenic BRAF melanoma by targeting BRAF and ERK2. *Oncotarget* **2014**, *5*, 9444-9459, doi:10.18632/oncotarget.2452.
394. Chen, L.; Cao, Y.; Rong, D.; Wang, Y.; Cao, Y. MicroRNA-605 functions as a tumor suppressor by targeting INPP4B in melanoma. *Oncol Rep* **2017**, *38*, 1276-1286, doi:10.3892/or.2017.5740.
395. Liu, K.; Jin, J.; Rong, K.; Zhuo, L.; Li, P. MicroRNA675 inhibits cell proliferation and invasion in melanoma by directly targeting metadherin. *Mol Med Rep* **2018**, *17*, 3372-3379, doi:10.3892/mmr.2017.8264.
396. Bu, P.; Luo, C.; He, Q.; Yang, P.; Li, X.; Xu, D. MicroRNA-9 inhibits the proliferation and migration of malignant melanoma cells via targeting sirituin 1. *Exp Ther Med* **2017**, *14*, 931-938, doi:10.3892/etm.2017.4595.
397. Feng, Z.; Zhang, C.; Wu, R.; Hu, W. Tumor suppressor p53 meets microRNAs. *J Mol Cell Biol* **2011**, *3*, 44-50, doi:10.1093/jmcb/mjq040.
398. Liu, J.; Zhang, C.; Zhao, Y.; Feng, Z. MicroRNA Control of p53. *J Cell Biochem* **2017**, *118*, 7-14, doi:10.1002/jcb.25609.
399. Satzger, I.; Mattern, A.; Kuettler, U.; Weinspach, D.; Voelker, B.; Kapp, A.; Gutzmer, R. MicroRNA-15b represents an independent prognostic parameter and is correlated with tumor cell proliferation and apoptosis in malignant melanoma. *Int J Cancer* **2010**, *126*, 2553-2562, doi:10.1002/ijc.24960.
400. Jiang, L.; Lv, X.; Li, J.; Li, J.; Li, X.; Li, W.; Li, Y. The status of microRNA-21 expression and its clinical significance in human cutaneous malignant melanoma. *Acta Histochem* **2012**, *114*, 582-588, doi:10.1016/j.acthis.2011.11.001.
401. Dar, A.A.; Majid, S.; Rittsteuer, C.; de Semir, D.; Bezrookove, V.; Tong, S.; Nosrati, M.; Sagebiel, R.; Miller, J.R., 3rd; Kashani-Sabet, M. The role of miR-18b in MDM2-p53 pathway signaling and melanoma progression. *J Natl Cancer Inst* **2013**, *105*, 433-442, doi:10.1093/jnci/djt003.
402. Reuland, S.N.; Smith, S.M.; Bemis, L.T.; Goldstein, N.B.; Almeida, A.R.; Partyka, K.A.; Marquez, V.E.; Zhang, Q.; Norris, D.A.; Shellman, Y.G. MicroRNA-26a is strongly

downregulated in melanoma and induces cell death through repression of silencer of death domains (SODD). *J Invest Dermatol* **2013**, *133*, 1286-1293, doi:10.1038/jid.2012.400.
403. Wu, X.; Bao, H. Tumor suppressive microRNA-485-5p targets PRRX1 in human skin melanoma cells, regulating epithelial-mesenchymal transition and apoptosis. *Cell Biol Int* **2021**, doi:10.1002/cbin.11575.
404. Russell, R.C.; Yuan, H.X.; Guan, K.L. Autophagy regulation by nutrient signaling. *Cell Res* **2014**, *24*, 42-57, doi:10.1038/cr.2013.166.
405. Ndoye, A.; Weeraratna, A.T. Autophagy- An emerging target for melanoma therapy. *F1000Res* **2016**, *5*, doi:10.12688/f1000research.8347.1.
406. Luo, M.; Wu, L.; Zhang, K.; Wang, H.; Wu, S.; O'Connell, D.; Gao, T.; Zhong, H.; Yang, Y. miR-216b enhances the efficacy of vemurafenib by targeting Beclin-1, UVRAG and ATG5 in melanoma. *Cell Signal* **2018**, *42*, 30-43, doi:10.1016/j.cellsig.2017.09.024.
407. Chen, Y.; Liersch, R.; Detmar, M. The miR-290-295 cluster suppresses autophagic cell death of melanoma cells. *Sci Rep* **2012**, *2*, 808, doi:10.1038/srep00808.
408. Tang, H.; Xu, X.; Xiao, W.; Liao, Y.; Xiao, X.; Li, L.; Li, K.; Jia, X.; Feng, H. Silencing of microRNA-27a facilitates autophagy and apoptosis of melanoma cells through the activation of the SYK-dependent mTOR signaling pathway. *J Cell Biochem* **2019**, *120*, 13262-13274, doi:10.1002/jcb.28600.
409. Bhattacharya, A.; Schmitz, U.; Raatz, Y.; Schonherr, M.; Kottek, T.; Schauer, M.; Franz, S.; Saalbach, A.; Anderegg, U.; Wolkenhauer, O.; et al. miR-638 promotes melanoma metastasis and protects melanoma cells from apoptosis and autophagy. *Oncotarget* **2015**, *6*, 2966-2980, doi:10.18632/oncotarget.3070.
410. Xiao, Y.; Diao, Q.; Liang, Y.; Peng, Y.; Zeng, K. MicroRNA2415p promotes malignant melanoma cell autophagy and apoptosis via regulating ubiquitin D. *Mol Med Rep* **2017**, *16*, 8448-8454, doi:10.3892/mmr.2017.7614.
411. Luo, M.; Wu, L.; Zhang, K.; Wang, H.; Zhang, T.; Gutierrez, L.; O'Connell, D.; Zhang, P.; Li, Y.; Gao, T.; et al. miR-137 regulates ferroptosis by targeting glutamine transporter SLC1A5 in melanoma. *Cell Death Differ* **2018**, *25*, 1457-1472, doi:10.1038/s41418-017-0053-8.
412. Zhang, K.; Wu, L.; Zhang, P.; Luo, M.; Du, J.; Gao, T.; O'Connell, D.; Wang, G.; Wang, H.; Yang, Y. miR-9 regulates ferroptosis by targeting glutamic-oxaloacetic transaminase GOT1 in melanoma. *Mol Carcinog* **2018**, *57*, 1566-1576, doi:10.1002/mc.22878.
413. Alonso, S.R.; Tracey, L.; Ortiz, P.; Perez-Gomez, B.; Palacios, J.; Pollan, M.; Linares, J.; Serrano, S.; Saez-Castillo, A.I.; Sanchez, L.; et al. A high-throughput study in melanoma identifies epithelial-mesenchymal transition as a major determinant of metastasis. *Cancer Res* **2007**, *67*, 3450-3460, doi:10.1158/0008-5472.CAN-06-3481.
414. Luan, W.; Ding, Y.; Xi, H.; Ruan, H.; Lu, F.; Ma, S.; Wang, J. Exosomal miR-106b-5p derived from melanoma cell promotes primary melanocytes epithelial-mesenchymal transition through targeting EphA4. *J Exp Clin Cancer Res* **2021**, *40*, 107, doi:10.1186/s13046-021-01906-w.
415. Yu, Y.; Yu, F.; Sun, P. MicroRNA-1246 Promotes Melanoma Progression Through Targeting FOXA2. *Onco Targets Ther* **2020**, *13*, 1245-1253, doi:10.2147/OTT.S234276.
416. Pencheva, N.; Tran, H.; Buss, C.; Huh, D.; Drobnjak, M.; Busam, K.; Tavazoie, S.F. Convergent multi-miRNA targeting of ApoE drives LRP1/LRP8-dependent melanoma metastasis and angiogenesis. *Cell* **2012**, *151*, 1068-1082, doi:10.1016/j.cell.2012.10.028.
417. Cohen, R.; Greenberg, E.; Nemlich, Y.; Schachter, J.; Markel, G. miR-17 regulates melanoma cell motility by inhibiting the translation of ETV1. *Oncotarget* **2015**, *6*, 19006-19016, doi:10.18632/oncotarget.4147.
418. Weber, C.E.; Luo, C.; Hotz-Wagenblatt, A.; Gardyan, A.; Kordass, T.; Holland-Letz, T.; Osen, W.; Eichmuller, S.B. miR-339-3p Is a Tumor Suppressor in Melanoma. *Cancer Res* **2016**, *76*, 3562-3571, doi:10.1158/0008-5472.CAN-15-2932.

419. Orso, F.; Quirico, L.; Virga, F.; Penna, E.; Dettori, D.; Cimino, D.; Coppo, R.; Grassi, E.; Elia, A.R.; Brusa, D.; et al. miR-214 and miR-148b Targeting Inhibits Dissemination of Melanoma and Breast Cancer. *Cancer Res* **2016**, *76*, 5151-5162, doi:10.1158/0008-5472.CAN-15-1322.
420. Martin del Campo, S.E.; Latchana, N.; Levine, K.M.; Grignol, V.P.; Fairchild, E.T.; Jaime-Ramirez, A.C.; Dao, T.V.; Karpa, V.I.; Carson, M.; Ganju, A.; et al. MiR-21 enhances melanoma invasiveness via inhibition of tissue inhibitor of metalloproteinases 3 expression: in vivo effects of MiR-21 inhibitor. *PLoS One* **2015**, *10*, e0115919, doi:10.1371/journal.pone.0115919.
421. Knoll, S.; Furst, K.; Kowtharapu, B.; Schmitz, U.; Marquardt, S.; Wolkenhauer, O.; Martin, H.; Putzer, B.M. E2F1 induces miR-224/452 expression to drive EMT through TXNIP downregulation. *EMBO Rep* **2014**, *15*, 1315-1329, doi:10.15252/embr.201439392.
422. Gaziel-Sovran, A.; Segura, M.F.; Di Micco, R.; Collins, M.K.; Hanniford, D.; Vega-Saenz de Miera, E.; Rakus, J.F.; Dankert, J.F.; Shang, S.; Kerbel, R.S.; et al. miR-30b/30d regulation of GalNAc transferases enhances invasion and immunosuppression during metastasis. *Cancer Cell* **2011**, *20*, 104-118, doi:10.1016/j.ccr.2011.05.027.
423. Bai, X.; Yang, M.; Xu, Y. MicroRNA-373 promotes cell migration via targeting salt-inducible kinase 1 expression in melanoma. *Exp Ther Med* **2018**, *16*, 4759-4764, doi:10.3892/etm.2018.6784.
424. Kordass, T.; Weber, C.E.M.; Eisel, D.; Pane, A.A.; Osen, W.; Eichmuller, S.B. miR-193b and miR-30c-1(*) inhibit, whereas miR-576-5p enhances melanoma cell invasion in vitro. *Oncotarget* **2018**, *9*, 32507-32522, doi:10.18632/oncotarget.25986.
425. Muller, D.W.; Bosserhoff, A.K. Integrin beta 3 expression is regulated by let-7a miRNA in malignant melanoma. *Oncogene* **2008**, *27*, 6698-6706, doi:10.1038/onc.2008.282.
426. Caporali, S.; Amaro, A.; Levati, L.; Alvino, E.; Lacal, P.M.; Mastroeni, S.; Ruffini, F.; Bonmassar, L.; Antonini Cappellini, G.C.; Felli, N.; et al. miR-126-3p down-regulation contributes to dabrafenib acquired resistance in melanoma by up-regulating ADAM9 and VEGF-A. *J Exp Clin Cancer Res* **2019**, *38*, 272, doi:10.1186/s13046-019-1238-4.
427. Qi, J.; Wang, W.W.; Chen, W.; Lu, W.Y.; Shang, A.Q. Mechanism of miR-137 regulating migration and invasion of melanoma cells by targeting PIK3R3 gene. *J Cell Biochem* **2018**, doi:10.1002/jcb.28124.
428. Qiu, H.; Chen, F.; Chen, M. MicroRNA-138 negatively regulates the hypoxia-inducible factor 1alpha to suppress melanoma growth and metastasis. *Biol Open* **2019**, *8*, doi:10.1242/bio.042937.
429. Jin, C.; Wang, A.; Liu, L.; Wang, G.; Li, G.; Han, Z. miR-145-5p inhibits tumor occurrence and metastasis through the NF-kappaB signaling pathway by targeting TLR4 in malignant melanoma. *J Cell Biochem* **2019**, doi:10.1002/jcb.28388.
430. Sun, R.; Guo, M.; Fan, X.; Meng, Q.; Yuan, D.; Yang, X.; Yan, K.; Deng, H. MicroRNA-148b Inhibits the Malignant Biological Behavior of Melanoma by Reducing Sirtuin 7 Expression Levels. *Biomed Res Int* **2020**, *2020*, 9568976, doi:10.1155/2020/9568976.
431. Sun, X.; Zhang, C.; Cao, Y.; Liu, E. miR-150 Suppresses Tumor Growth in Melanoma Through Downregulation of MYB. *Oncol Res* **2019**, *27*, 317-323, doi:10.3727/096504018X15228863026239.
432. Yang, X.; Zhao, H.; Yang, J.; Ma, Y.; Liu, Z.; Li, C.; Wang, T.; Yan, Z.; Du, N. MiR-150-5p regulates melanoma proliferation, invasion and metastasis via SIX1-mediated Warburg Effect. *Biochem Biophys Res Commun* **2019**, *515*, 85-91, doi:10.1016/j.bbrc.2019.05.111.
433. Zeng, H.F.; Yan, S.; Wu, S.F. MicroRNA-153-3p suppress cell proliferation and invasion by targeting SNAI1 in melanoma. *Biochem Biophys Res Commun* **2017**, *487*, 140-145, doi:10.1016/j.bbrc.2017.04.032.
434. Guo, B.; Hui, Q.; Zhang, Y.; Chang, P.; Tao, K. miR-194 is a negative regulator of GEF-H1 pathway in melanoma. *Oncol Rep* **2016**, *36*, 2412-2420, doi:10.3892/or.2016.5020.

435. Lohcharoenkal, W.; Das Mahapatra, K.; Pasquali, L.; Crudden, C.; Kular, L.; Akkaya Ulum, Y.Z.; Zhang, L.; Xu Landen, N.; Girnita, L.; Jagodic, M.; et al. Genome-Wide Screen for MicroRNAs Reveals a Role for miR-203 in Melanoma Metastasis. *J Invest Dermatol* **2018**, doi:10.1016/j.jid.2017.09.049.
436. Bell, R.E.; Khaled, M.; Netanely, D.; Schubert, S.; Golan, T.; Buxbaum, A.; Janas, M.M.; Postolsky, B.; Goldberg, M.S.; Shamir, R.; et al. Transcription factor/microRNA axis blocks melanoma invasion program by miR-211 targeting NUAK1. *J Invest Dermatol* **2014**, *134*, 441-451, doi:10.1038/jid.2013.340.
437. Boyle, G.M.; Woods, S.L.; Bonazzi, V.F.; Stark, M.S.; Hacker, E.; Aoude, L.G.; Dutton-Regester, K.; Cook, A.L.; Sturm, R.A.; Hayward, N.K. Melanoma cell invasiveness is regulated by miR-211 suppression of the BRN2 transcription factor. *Pigment Cell Melanoma Res* **2011**, *24*, 525-537, doi:10.1111/j.1755-148X.2011.00849.x.
438. Luan, W.; Li, L.; Shi, Y.; Bu, X.; Xia, Y.; Wang, J.; Djangmah, H.S.; Liu, X.; You, Y.; Xu, B. Long non-coding RNA MALAT1 acts as a competing endogenous RNA to promote malignant melanoma growth and metastasis by sponging miR-22. *Oncotarget* **2016**, *7*, 63901-63912, doi:10.18632/oncotarget.11564.
439. Nemlich, Y.; Baruch, E.N.; Besser, M.J.; Shoshan, E.; Bar-Eli, M.; Anafi, L.; Barshack, I.; Schachter, J.; Ortenberg, R.; Markel, G. ADAR1-mediated regulation of melanoma invasion. *Nat Commun* **2018**, *9*, 2154, doi:10.1038/s41467-018-04600-2.
440. Noori, J.; Sharifi, M.; Haghjooy Javanmard, S. miR-30a Inhibits Melanoma Tumor Metastasis by Targeting the E-cadherin and Zinc Finger E-box Binding Homeobox 2. *Adv Biomed Res* **2018**, *7*, 143, doi:10.4103/abr.abr_146_18.
441. Liu, R.; Xie, H.; Luo, C.; Chen, Z.; Zhou, X.; Xia, K.; Chen, X.; Zhou, M.; Cao, P.; Cao, K.; et al. Identification of FLOT2 as a novel target for microRNA-34a in melanoma. *J Cancer Res Clin Oncol* **2015**, *141*, 993-1006, doi:10.1007/s00432-014-1874-1.
442. Migliore, C.; Petrelli, A.; Ghiso, E.; Corso, S.; Capparuccia, L.; Eramo, A.; Comoglio, P.M.; Giordano, S. MicroRNAs impair MET-mediated invasive growth. *Cancer Res* **2008**, *68*, 10128-10136, doi:10.1158/0008-5472.CAN-08-2148.
443. Zehavi, L.; Avraham, R.; Barzilai, A.; Bar-Ilan, D.; Navon, R.; Sidi, Y.; Avni, D.; Leibowitz-Amit, R. Silencing of a large microRNA cluster on human chromosome 14q32 in melanoma: biological effects of mir-376a and mir-376c on insulin growth factor 1 receptor. *Mol Cancer* **2012**, *11*, 44, doi:10.1186/1476-4598-11-44.
444. Velazquez-Torres, G.; Shoshan, E.; Ivan, C.; Huang, L.; Fuentes-Mattei, E.; Paret, H.; Kim, S.J.; Rodriguez-Aguayo, C.; Xie, V.; Brooks, D.; et al. A-to-I miR-378a-3p editing can prevent melanoma progression via regulation of PARVA expression. *Nat Commun* **2018**, *9*, 461, doi:10.1038/s41467-018-02851-7.
445. Shoshan, E.; Mobley, A.K.; Braeuer, R.R.; Kamiya, T.; Huang, L.; Vasquez, M.E.; Salameh, A.; Lee, H.J.; Kim, S.J.; Ivan, C.; et al. Reduced adenosine-to-inosine miR-455-5p editing promotes melanoma growth and metastasis. *Nat Cell Biol* **2015**, *17*, 311-321, doi:10.1038/ncb3110.
446. Rang, Z.; Yang, G.; Wang, Y.W.; Cui, F. miR-542-3p suppresses invasion and metastasis by targeting the proto-oncogene serine/threonine protein kinase, PIM1, in melanoma. *Biochem Biophys Res Commun* **2016**, *474*, 315-320, doi:10.1016/j.bbrc.2016.04.093.
447. Fang, W.; Fan, Y.; Fa, Z.; Xu, J.; Yu, H.; Li, P.; Gu, J. microRNA-625 inhibits tumorigenicity by suppressing proliferation, migration and invasion in malignant melanoma. *Oncotarget* **2017**, *8*, 13253-13263, doi:10.18632/oncotarget.14710.
448. Giles, K.M.; Brown, R.A.; Epis, M.R.; Kalinowski, F.C.; Leedman, P.J. miRNA-7-5p inhibits melanoma cell migration and invasion. *Biochem Biophys Res Commun* **2013**, *430*, 706-710, doi:10.1016/j.bbrc.2012.11.086.

449. Liu, S.; Kumar, S.M.; Lu, H.; Liu, A.; Yang, R.; Pushparajan, A.; Guo, W.; Xu, X. MicroRNA-9 up-regulates E-cadherin through inhibition of NF-kappaB1-Snail1 pathway in melanoma. *J Pathol* **2012**, *226*, 61-72, doi:10.1002/path.2964.
450. Carmeliet, P. Mechanisms of angiogenesis and arteriogenesis. *Nat Med* **2000**, *6*, 389-395, doi:10.1038/74651.
451. Mahabeleshwar, G.H.; Byzova, T.V. Angiogenesis in melanoma. *Semin Oncol* **2007**, *34*, 555-565, doi:10.1053/j.seminoncol.2007.09.009.
452. Tupone, M.G.; D'Aguanno, S.; Di Martile, M.; Valentini, E.; Desideri, M.; Trisciuoglio, D.; Donzelli, S.; Sacconi, A.; Buglioni, S.; Ercolani, C.; et al. microRNA-378a-5p iS a novel positive regulator of melanoma progression. *Oncogenesis* **2020**, *9*, 22, doi:10.1038/s41389-020-0203-6.
453. Lv, R.; Yu, J.; Sun, Q. Anti-angiogenic role of microRNA-23b in melanoma by disturbing NF-kappaB signaling pathway via targeted inhibition of NAMPT. *Future Oncol* **2020**, *16*, 541-458, doi:10.2217/fon-2019-0699.
454. Ramirez-Montagut, T.; Turk, M.J.; Wolchok, J.D.; Guevara-Patino, J.A.; Houghton, A.N. Immunity to melanoma: unraveling the relation of tumor immunity and autoimmunity. *Oncogene* **2003**, *22*, 3180-3187, doi:10.1038/sj.onc.1206462.
455. Postow, M.A.; Chesney, J.; Pavlick, A.C.; Robert, C.; Grossmann, K.; McDermott, D.; Linette, G.P.; Meyer, N.; Giguere, J.K.; Agarwala, S.S.; et al. Nivolumab and ipilimumab versus ipilimumab in untreated melanoma. *N Engl J Med* **2015**, *372*, 2006-2017, doi:10.1056/NEJMoa1414428.
456. Audrito, V.; Serra, S.; Stingi, A.; Orso, F.; Gaudino, F.; Bologna, C.; Neri, F.; Garaffo, G.; Nassini, R.; Baroni, G.; et al. PD-L1 up-regulation in melanoma increases disease aggressiveness and is mediated through miR-17-5p. *Oncotarget* **2017**, *8*, 15894-15911, doi:10.18632/oncotarget.15213.
457. Li, Q.; Johnston, N.; Zheng, X.; Wang, H.; Zhang, X.; Gao, D.; Min, W. miR-28 modulates exhaustive differentiation of T cells through silencing programmed cell death-1 and regulating cytokine secretion. *Oncotarget* **2016**, *7*, 53735-53750, doi:10.18632/oncotarget.10731.
458. Mahmoud, F.; Shields, B.; Makhoul, I.; Avaritt, N.; Wong, H.K.; Hutchins, L.F.; Shalin, S.; Tackett, A.J. Immune surveillance in melanoma: From immune attack to melanoma escape and even counterattack. *Cancer Biol Ther* **2017**, *18*, 451-469, doi:10.1080/15384047.2017.1323596.
459. Mathsyaraja, H.; Thies, K.; Taffany, D.A.; Deighan, C.; Liu, T.; Yu, L.; Fernandez, S.A.; Shapiro, C.; Otero, J.; Timmers, C.; et al. CSF1-ETS2-induced microRNA in myeloid cells promote metastatic tumor growth. *Oncogene* **2015**, *34*, 3651-3661, doi:10.1038/onc.2014.294.
460. Nachmani, D.; Lankry, D.; Wolf, D.G.; Mandelboim, O. The human cytomegalovirus microRNA miR-UL112 acts synergistically with a cellular microRNA to escape immune elimination. *Nat Immunol* **2010**, *11*, 806-813, doi:10.1038/ni.1916.
461. Heinemann, A.; Zhao, F.; Pechlivanis, S.; Eberle, J.; Steinle, A.; Diederichs, S.; Schadendorf, D.; Paschen, A. Tumor suppressive microRNAs miR-34a/c control cancer cell expression of ULBP2, a stress-induced ligand of the natural killer cell receptor NKG2D. *Cancer Res* **2012**, *72*, 460-471, doi:10.1158/0008-5472.CAN-11-1977.
462. Chen, S.; Wang, L.; Fan, J.; Ye, C.; Dominguez, D.; Zhang, Y.; Curiel, T.J.; Fang, D.; Kuzel, T.M.; Zhang, B. Host miR155 promotes tumor growth through a myeloid-derived suppressor cell-dependent mechanism. *Cancer Res* **2015**, *75*, 519-531, doi:10.1158/0008-5472.CAN-14-2331.
463. Liu, Y.; Lai, L.; Chen, Q.; Song, Y.; Xu, S.; Ma, F.; Wang, X.; Wang, J.; Yu, H.; Cao, X.; et al. MicroRNA-494 is required for the accumulation and functions of tumor-expanded myeloid-derived suppressor cells via targeting of PTEN. *J Immunol* **2012**, *188*, 5500-5510, doi:10.4049/jimmunol.1103505.

464. Zhao, E.; Maj, T.; Kryczek, I.; Li, W.; Wu, K.; Zhao, L.; Wei, S.; Crespo, J.; Wan, S.; Vatan, L.; et al. Cancer mediates effector T cell dysfunction by targeting microRNAs and EZH2 via glycolysis restriction. *Nat Immunol* **2016**, *17*, 95-103, doi:10.1038/ni.3313.
465. Noman, M.Z.; Messai, Y.; Carre, T.; Akalay, I.; Meron, M.; Janji, B.; Hasmim, M.; Chouaib, S. Microenvironmental hypoxia orchestrating the cell stroma cross talk, tumor progression and antitumor response. *Crit Rev Immunol* **2011**, *31*, 357-377.
466. Noman, M.Z.; Buart, S.; Romero, P.; Ketari, S.; Janji, B.; Mari, B.; Mami-Chouaib, F.; Chouaib, S. Hypoxia-inducible miR-210 regulates the susceptibility of tumor cells to lysis by cytotoxic T cells. *Cancer Res* **2012**, *72*, 4629-4641, doi:10.1158/0008-5472.CAN-12-1383.
467. Sha, J.; Gastman, B.R.; Morris, N.; Mesinkovska, N.A.; Baron, E.D.; Cooper, K.D.; McCormick, T.; Arbesman, J.; Harter, M.L. The Response of microRNAs to Solar UVR in Skin-Resident Melanocytes Differs between Melanoma Patients and Healthy Persons. *PLoS One* **2016**, *11*, e0154915, doi:10.1371/journal.pone.0154915.
468. Kulshreshtha, R.; Ferracin, M.; Wojcik, S.E.; Garzon, R.; Alder, H.; Agosto-Perez, F.J.; Davuluri, R.; Liu, C.G.; Croce, C.M.; Negrini, M.; et al. A microRNA signature of hypoxia. *Mol Cell Biol* **2007**, *27*, 1859-1867, doi:10.1128/MCB.01395-06.
469. Zhang, Z.; Sun, H.; Dai, H.; Walsh, R.M.; Imakura, M.; Schelter, J.; Burchard, J.; Dai, X.; Chang, A.N.; Diaz, R.L.; et al. MicroRNA miR-210 modulates cellular response to hypoxia through the MYC antagonist MNT. *Cell Cycle* **2009**, *8*, 2756-2768, doi:10.4161/cc.8.17.9387.
470. Wozniak, M.; Sztiller-Sikorska, M.; Czyz, M. Diminution of miR-340-5p levels is responsible for increased expression of ABCB5 in melanoma cells under oxygen-deprived conditions. *Exp Mol Pathol* **2015**, *99*, 707-716, doi:10.1016/j.yexmp.2015.11.014.
471. Chen, Y.; Zhang, Z.; Luo, C.; Chen, Z.; Zhou, J. MicroRNA-18b inhibits the growth of malignant melanoma via inhibition of HIF-1alpha-mediated glycolysis. *Oncol Rep* **2016**, *36*, 471-479, doi:10.3892/or.2016.4824.
472. Serguienko, A.; Grad, I.; Wennerstrom, A.B.; Meza-Zepeda, L.A.; Thiede, B.; Stratford, E.W.; Myklebost, O.; Munthe, E. Metabolic reprogramming of metastatic breast cancer and melanoma by let-7a microRNA. *Oncotarget* **2015**, *6*, 2451-2465, doi:10.18632/oncotarget.3235.
473. Zhang, H.; Feng, C.; Zhang, M.; Zeng, A.; Si, L.; Yu, N.; Bai, M. miR-625-5p/PKM2 negatively regulates melanoma glycolysis state. *J Cell Biochem* **2019**, *120*, 2964-2972, doi:10.1002/jcb.26917.
474. Mazar, J.; Qi, F.; Lee, B.; Marchica, J.; Govindarajan, S.; Shelley, J.; Li, J.L.; Ray, A.; Perera, R.J. MicroRNA 211 Functions as a Metabolic Switch in Human Melanoma Cells. *Mol Cell Biol* **2016**, *36*, 1090-1108, doi:10.1128/MCB.00762-15.
475. Qin, J.Z.; Xin, H.; Nickoloff, B.J. Targeting glutamine metabolism sensitizes melanoma cells to TRAIL-induced death. *Biochem Biophys Res Commun* **2010**, *398*, 146-152, doi:10.1016/j.bbrc.2010.06.057.
476. Luan, W.; Zhou, Z.; Zhu, Y.; Xia, Y.; Wang, J.; Xu, B. miR-137 inhibits glutamine catabolism and growth of malignant melanoma by targeting glutaminase. *Biochem Biophys Res Commun* **2018**, *495*, 46-52, doi:10.1016/j.bbrc.2017.10.152.
477. Lu, R.; Zhang, X.; Li, X.; Wan, X. Circ_0016418 promotes melanoma development and glutamine catabolism by regulating the miR-605-5p/GLS axis. *Int J Clin Exp Pathol* **2020**, *13*, 1791-1801.
478. Vergani, E.; Di Guardo, L.; Dugo, M.; Rigoletto, S.; Tragni, G.; Ruggeri, R.; Perrone, F.; Tamborini, E.; Gloghini, A.; Arienti, F.; et al. Overcoming melanoma resistance to vemurafenib by targeting CCL2-induced miR-34a, miR-100 and miR-125b. *Oncotarget* **2016**, *7*, 4428-4441, doi:10.18632/oncotarget.6599.
479. Stark, M.S.; Bonazzi, V.F.; Boyle, G.M.; Palmer, J.M.; Symmons, J.; Lanagan, C.M.; Schmidt, C.W.; Herington, A.C.; Ballotti, R.; Pollock, P.M.; et al. miR-514a regulates the

tumour suppressor NF1 and modulates BRAFi sensitivity in melanoma. *Oncotarget* **2015**, *6*, 17753-17763, doi:10.18632/oncotarget.3924.

480. Kim, J.H.; Ahn, J.H.; Lee, M. Upregulation of MicroRNA-1246 Is Associated with BRAF Inhibitor Resistance in Melanoma Cells with Mutant BRAF. *Cancer Res Treat* **2017**, *49*, 947-959, doi:10.4143/crt.2016.280.
481. Fattore, L.; Ruggiero, C.F.; Pisanu, M.E.; Liguoro, D.; Cerri, A.; Costantini, S.; Capone, F.; Acunzo, M.; Romano, G.; Nigita, G.; et al. Reprogramming miRNAs global expression orchestrates development of drug resistance in BRAF mutated melanoma. *Cell Death Differ* **2019**, *26*, 1267-1282, doi:10.1038/s41418-018-0205-5.
482. Liu, S.; Tetzlaff, M.T.; Wang, T.; Yang, R.; Xie, L.; Zhang, G.; Krepler, C.; Xiao, M.; Beqiri, M.; Xu, W.; et al. miR-200c/Bmi1 axis and epithelial-mesenchymal transition contribute to acquired resistance to BRAF inhibitor treatment. *Pigment Cell Melanoma Res* **2015**, *28*, 431-441, doi:10.1111/pcmr.12379.
483. Nguyen, M.T.; Lin, C.H.; Liu, S.M.; Miyashita, A.; Ihn, H.; Lin, H.; Ng, C.H.; Tsai, J.C.; Chen, M.H.; Tsai, M.S.; et al. miR-524-5p reduces the progression of the BRAF inhibitor-resistant melanoma. *Neoplasia* **2020**, *22*, 789-799, doi:10.1016/j.neo.2020.10.009.
484. Choe, M.H.; Yoon, Y.; Kim, J.; Hwang, S.G.; Han, Y.H.; Kim, J.S. miR-550a-3-5p acts as a tumor suppressor and reverses BRAF inhibitor resistance through the direct targeting of YAP. *Cell Death Dis* **2018**, *9*, 640, doi:10.1038/s41419-018-0698-3.
485. Fattore, L.; Mancini, R.; Acunzo, M.; Romano, G.; Lagana, A.; Pisanu, M.E.; Malpicci, D.; Madonna, G.; Mallardo, D.; Capone, M.; et al. miR-579-3p controls melanoma progression and resistance to target therapy. *Proc Natl Acad Sci U S A* **2016**, *113*, E5005-5013, doi:10.1073/pnas.1607753113.
486. Sun, X.; Li, J.; Sun, Y.; Zhang, Y.; Dong, L.; Shen, C.; Yang, L.; Yang, M.; Li, Y.; Shen, G.; et al. miR-7 reverses the resistance to BRAFi in melanoma by targeting EGFR/IGF-1R/CRAF and inhibiting the MAPK and PI3K/AKT signaling pathways. *Oncotarget* **2016**, *7*, 53558-53570, doi:10.18632/oncotarget.10669.
487. Mishra, P.J.; Mishra, P.J.; Merlino, G. Integrated Genomics Identifies miR-32/MCL-1 Pathway as a Critical Driver of Melanomagenesis: Implications for miR-Replacement and Combination Therapy. *PLoS One* **2016**, *11*, e0165102, doi:10.1371/journal.pone.0165102.
488. Motti, M.L.; Minopoli, M.; Di Carluccio, G.; Ascierto, P.A.; Carriero, M.V. MicroRNAs as Key Players in Melanoma Cell Resistance to MAPK and Immune Checkpoint Inhibitors. *International journal of molecular sciences* **2020**, *21*, doi:10.3390/ijms21124544.
489. Galore-Haskel, G.; Nemlich, Y.; Greenberg, E.; Ashkenazi, S.; Hakim, M.; Itzhaki, O.; Shoshani, N.; Shapira-Fromer, R.; Ben-Ami, E.; Ofek, E.; et al. A novel immune resistance mechanism of melanoma cells controlled by the ADAR1 enzyme. *Oncotarget* **2015**, *6*, 28999-29015, doi:10.18632/oncotarget.4905.
490. Martinez-Usatorre, A.; Sempere, L.F.; Carmona, S.J.; Carretero-Iglesia, L.; Monnot, G.; Speiser, D.E.; Rufer, N.; Donda, A.; Zehn, D.; Jandus, C.; et al. MicroRNA-155 Expression Is Enhanced by T-cell Receptor Stimulation Strength and Correlates with Improved Tumor Control in Melanoma. *Cancer Immunol Res* **2019**, *7*, 1013-1024, doi:10.1158/2326-6066.CIR-18-0504.
491. Huber, V.; Vallacchi, V.; Fleming, V.; Hu, X.; Cova, A.; Dugo, M.; Shahaj, E.; Sulsenti, R.; Vergani, E.; Filipazzi, P.; et al. Tumor-derived microRNAs induce myeloid suppressor cells and predict immunotherapy resistance in melanoma. *J Clin Invest* **2018**, *128*, 5505-5516, doi:10.1172/JCI98060.
492. Wagenseller, A.G.; Shada, A.; D'Auria, K.M.; Murphy, C.; Sun, D.; Molhoek, K.R.; Papin, J.A.; Dutta, A.; Slingluff, C.L., Jr. MicroRNAs induced in melanoma treated with combination targeted therapy of Temsirolimus and Bevacizumab. *J Transl Med* **2013**, *11*, 218, doi:10.1186/1479-5876-11-218.

493. Li, Y.; Zhang, J.; Liu, Y.; Zhang, B.; Zhong, F.; Wang, S.; Fang, Z. MiR-30a-5p confers cisplatin resistance by regulating IGF1R expression in melanoma cells. *BMC Cancer* **2018**, *18*, 404, doi:10.1186/s12885-018-4233-9.
494. Li, N.; Liu, Y.; Pang, H.; Lee, D.; Zhou, Y.; Xiao, Z. Methylation-Mediated Silencing of MicroRNA-211 Decreases the Sensitivity of Melanoma Cells to Cisplatin. *Med Sci Monit* **2019**, *25*, 1590-1599, doi:10.12659/MSM.911862.
495. Chang, X.; Zhu, W.; Zhang, H.; Lian, S. Sensitization of melanoma cells to temozolomide by overexpression of microRNA 203 through direct targeting of glutaminase-mediated glutamine metabolism. *Clin Exp Dermatol* **2017**, *42*, 614-621, doi:10.1111/ced.13119.
496. Villaruz, L.C.; Huang, G.; Romkes, M.; Kirkwood, J.M.; Buch, S.C.; Nukui, T.; Flaherty, K.T.; Lee, S.J.; Wilson, M.A.; Nathanson, K.L.; et al. MicroRNA expression profiling predicts clinical outcome of carboplatin/paclitaxel-based therapy in metastatic melanoma treated on the ECOG-ACRIN trial E2603. *Clin Epigenetics* **2015**, *7*, 58, doi:10.1186/s13148-015-0092-2.
497. Cheng, L.; Sharples, R.A.; Scicluna, B.J.; Hill, A.F. Exosomes provide a protective and enriched source of miRNA for biomarker profiling compared to intracellular and cell-free blood. *J Extracell Vesicles* **2014**, *3*, doi:10.3402/jev.v3.23743.
498. Mitchell, P.S.; Parkin, R.K.; Kroh, E.M.; Fritz, B.R.; Wyman, S.K.; Pogosova-Agadjanyan, E.L.; Peterson, A.; Noteboom, J.; O'Briant, K.C.; Allen, A.; et al. Circulating microRNAs as stable blood-based markers for cancer detection. *Proc Natl Acad Sci U S A* **2008**, *105*, 10513-10518, doi:10.1073/pnas.0804549105

0804549105 [pii].
499. Ferracin, M.; Negrini, M. Micromarkers 2.0: an update on the role of microRNAs in cancer diagnosis and prognosis. *Expert Rev Mol Diagn* **2015**, *15*, 1369-1381, doi:10.1586/14737159.2015.1081058.
500. Leidinger, P.; Keller, A.; Borries, A.; Reichrath, J.; Rass, K.; Jager, S.U.; Lenhof, H.P.; Meese, E. High-throughput miRNA profiling of human melanoma blood samples. *BMC Cancer* **2010**, *10*, 262, doi:10.1186/1471-2407-10-262.
501. Heneghan, H.M.; Miller, N.; Kelly, R.; Newell, J.; Kerin, M.J. Systemic miRNA-195 differentiates breast cancer from other malignancies and is a potential biomarker for detecting noninvasive and early stage disease. *Oncologist* **2010**, *15*, 673-682, doi:10.1634/theoncologist.2010-0103.
502. Ferracin, M.; Lupini, L.; Salamon, I.; Saccenti, E.; Zanzi, M.V.; Rocchi, A.; Da Ros, L.; Zagatti, B.; Musa, G.; Bassi, C.; et al. Absolute quantification of cell-free microRNAs in cancer patients. *Oncotarget* **2015**, *6*, 14545-14555, doi:10.18632/oncotarget.3859.
503. Fogli, S.; Polini, B.; Carpi, S.; Pardini, B.; Naccarati, A.; Dubbini, N.; Lanza, M.; Breschi, M.C.; Romanini, A.; Nieri, P. Identification of plasma microRNAs as new potential biomarkers with high diagnostic power in human cutaneous melanoma. *Tumour Biol* **2017**, *39*, 1010428317701646, doi:10.1177/1010428317701646.
504. Armand-Labit, V.; Meyer, N.; Casanova, A.; Bonnabau, H.; Platzer, V.; Tournier, E.; Sansas, B.; Verdun, S.; Thouvenot, B.; Hilselberger, B.; et al. Identification of a Circulating MicroRNA Profile as a Biomarker of Metastatic Cutaneous Melanoma. *Acta Derm Venereol* **2016**, *96*, 29-34, doi:10.2340/00015555-2156.
505. Van Laar, R.; Lincoln, M.; Van Laar, B. Development and validation of a plasma-based melanoma biomarker suitable for clinical use. *Br J Cancer* **2018**, doi:10.1038/bjc.2017.477.
506. Greenberg, E.; Besser, M.J.; Ben-Ami, E.; Shapira-Frommer, R.; Itzhaki, O.; Zikich, D.; Levy, D.; Kubi, A.; Eyal, E.; Onn, A.; et al. A comparative analysis of total serum miRNA profiles identifies novel signature that is highly indicative of metastatic melanoma: a pilot study. *Biomarkers* **2013**, *18*, 502-508, doi:10.3109/1354750X.2013.816777.
507. Margue, C.; Reinsbach, S.; Philippidou, D.; Beaume, N.; Walters, C.; Schneider, J.G.; Nashan, D.; Behrmann, I.; Kreis, S. Comparison of a healthy miRNome with melanoma

patient miRNomes: are microRNAs suitable serum biomarkers for cancer? *Oncotarget* **2015**, *6*, 12110-12127, doi:10.18632/oncotarget.3661.

508. Pfeffer, S.R.; Grossmann, K.F.; Cassidy, P.B.; Yang, C.H.; Fan, M.; Kopelovich, L.; Leachman, S.A.; Pfeffer, L.M. Detection of Exosomal miRNAs in the Plasma of Melanoma Patients. *J Clin Med* **2015**, *4*, 2012-2027, doi:10.3390/jcm4121957.
509. Alegre, E.; Sanmamed, M.F.; Rodriguez, C.; Carranza, O.; Martin-Algarra, S.; Gonzalez, A. Study of circulating microRNA-125b levels in serum exosomes in advanced melanoma. *Arch Pathol Lab Med* **2014**, *138*, 828-832, doi:10.5858/arpa.2013-0134-OA.
510. Friedman, E.B.; Shang, S.; de Miera, E.V.; Fog, J.U.; Teilum, M.W.; Ma, M.W.; Berman, R.S.; Shapiro, R.L.; Pavlick, A.C.; Hernando, E.; et al. Serum microRNAs as biomarkers for recurrence in melanoma. *J Transl Med* **2012**, *10*, 155, doi:10.1186/1479-5876-10-155.
511. Shiiyama, R.; Fukushima, S.; Jinnin, M.; Yamashita, J.; Miyashita, A.; Nakahara, S.; Kogi, A.; Aoi, J.; Masuguchi, S.; Inoue, Y.; et al. Sensitive detection of melanoma metastasis using circulating microRNA expression profiles. *Melanoma Res* **2013**, *23*, 366-372, doi:10.1097/CMR.0b013e328363e485.
512. Fleming, N.H.; Zhong, J.; da Silva, I.P.; Vega-Saenz de Miera, E.; Brady, B.; Han, S.W.; Hanniford, D.; Wang, J.; Shapiro, R.L.; Hernando, E.; et al. Serum-based miRNAs in the prediction and detection of recurrence in melanoma patients. *Cancer* **2015**, *121*, 51-59, doi:10.1002/cncr.28981.
513. Bai, M.; Zhang, H.; Si, L.; Yu, N.; Zeng, A.; Zhao, R. Upregulation of Serum miR-10b Is Associated with Poor Prognosis in Patients with Melanoma. *J Cancer* **2017**, *8*, 2487-2491, doi:10.7150/jca.18824.
514. Saldanha, G.; Potter, L.; Shendge, P.; Osborne, J.; Nicholson, S.; Yii, N.; Varma, S.; Aslam, M.I.; Elshaw, S.; Papadogeorgakis, E.; et al. Plasma microRNA-21 is associated with tumor burden in cutaneous melanoma. *J Invest Dermatol* **2013**, *133*, 1381-1384, doi:10.1038/jid.2012.477.
515. Ono, S.; Oyama, T.; Lam, S.; Chong, K.; Foshag, L.J.; Hoon, D.S. A direct plasma assay of circulating microRNA-210 of hypoxia can identify early systemic metastasis recurrence in melanoma patients. *Oncotarget* **2015**, *6*, 7053-7064, doi:10.18632/oncotarget.3142.
516. Guo, S.; Guo, W.; Li, S.; Dai, W.; Zhang, N.; Zhao, T.; Wang, H.; Ma, J.; Yi, X.; Ge, R.; et al. Serum miR-16: A Potential Biomarker for Predicting Melanoma Prognosis. *J Invest Dermatol* **2016**, *136*, 985-993, doi:10.1016/j.jid.2015.12.041.
517. Tian, R.; Liu, T.; Qiao, L.; Gao, M.; Li, J. Decreased serum microRNA-206 level predicts unfavorable prognosis in patients with melanoma. *Int J Clin Exp Pathol* **2015**, *8*, 3097-3103.
518. Kanemaru, H.; Fukushima, S.; Yamashita, J.; Honda, N.; Oyama, R.; Kakimoto, A.; Masuguchi, S.; Ishihara, T.; Inoue, Y.; Jinnin, M.; et al. The circulating microRNA-221 level in patients with malignant melanoma as a new tumor marker. *J Dermatol Sci* **2011**, *61*, 187-193, doi:10.1016/j.jdermsci.2010.12.010.
519. Li, P.; He, Q.Y.; Luo, C.Q.; Qian, L.Y. Circulating miR-221 expression level and prognosis of cutaneous malignant melanoma. *Med Sci Monit* **2014**, *20*, 2472-2477, doi:10.12659/MSM.891327.
520. Stark, M.S.; Klein, K.; Weide, B.; Haydu, L.E.; Pflugfelder, A.; Tang, Y.H.; Palmer, J.M.; Whiteman, D.C.; Scolyer, R.A.; Mann, G.J.; et al. The Prognostic and Predictive Value of Melanoma-related MicroRNAs Using Tissue and Serum: A MicroRNA Expression Analysis. *EBioMedicine* **2015**, *2*, 671-680, doi:10.1016/j.ebiom.2015.05.011.
521. Tengda, L.; Shuping, L.; Mingli, G.; Jie, G.; Yun, L.; Weiwei, Z.; Anmei, D. Serum exosomal microRNAs as potent circulating biomarkers for melanoma. *Melanoma Res* **2018**, *28*, 295-303, doi:10.1097/CMR.0000000000000450.
522. Zelli, V.; Compagnoni, C.; Capelli, R.; Corrente, A.; Cornice, J.; Vecchiotti, D.; Di Padova, M.; Zazzeroni, F.; Alesse, E.; Tessitore, A. Emerging Role of isomiRs in Cancer: State of the Art and Recent Advances. *Genes (Basel)* **2021**, *12*, doi:10.3390/genes12091447.

523. Griffiths-Jones, S.; Grocock, R.J.; van Dongen, S.; Bateman, A.; Enright, A.J. miRBase: microRNA sequences, targets and gene nomenclature. *Nucleic Acids Res* **2006**, *34*, D140-144, doi:10.1093/nar/gkj112.
524. Landgraf, P.; Rusu, M.; Sheridan, R.; Sewer, A.; Iovino, N.; Aravin, A.; Pfeffer, S.; Rice, A.; Kamphorst, A.O.; Landthaler, M.; et al. A mammalian microRNA expression atlas based on small RNA library sequencing. *Cell* **2007**, *129*, 1401-1414, doi:10.1016/j.cell.2007.04.040.
525. Morin, R.D.; O'Connor, M.D.; Griffith, M.; Kuchenbauer, F.; Delaney, A.; Prabhu, A.L.; Zhao, Y.; McDonald, H.; Zeng, T.; Hirst, M.; et al. Application of massively parallel sequencing to microRNA profiling and discovery in human embryonic stem cells. *Genome Res* **2008**, *18*, 610-621, doi:10.1101/gr.7179508.
526. Tan, G.C.; Chan, E.; Molnar, A.; Sarkar, R.; Alexieva, D.; Isa, I.M.; Robinson, S.; Zhang, S.; Ellis, P.; Langford, C.F.; et al. 5' isomiR variation is of functional and evolutionary importance. *Nucleic Acids Res* **2014**, *42*, 9424-9435, doi:10.1093/nar/gku656.
527. Cloonan, N.; Wani, S.; Xu, Q.; Gu, J.; Lea, K.; Heater, S.; Barbacioru, C.; Steptoe, A.L.; Martin, H.C.; Nourbakhsh, E.; et al. MicroRNAs and their isomiRs function cooperatively to target common biological pathways. *Genome Biol* **2011**, *12*, R126, doi:10.1186/gb-2011-12-12-r126.
528. Wu, C.W.; Evans, J.M.; Huang, S.; Mahoney, D.W.; Dukek, B.A.; Taylor, W.R.; Yab, T.C.; Smyrk, T.C.; Jen, J.; Kisiel, J.B.; et al. A Comprehensive Approach to Sequence-oriented IsomiR annotation (CASMIR): demonstration with IsomiR profiling in colorectal neoplasia. *BMC Genomics* **2018**, *19*, 401, doi:10.1186/s12864-018-4794-7.
529. Loher, P.; Londin, E.R.; Rigoutsos, I. IsomiR expression profiles in human lymphoblastoid cell lines exhibit population and gender dependencies. *Oncotarget* **2014**, *5*, 8790-8802, doi:10.18632/oncotarget.2405.
530. Broseghini, E.; Dika, E.; Londin, E.; Ferracin, M. MicroRNA Isoforms Contribution to Melanoma Pathogenesis. *Non-Coding RNA* **2021**, *7*, 63.
531. Kim, V.N. MicroRNA biogenesis: coordinated cropping and dicing. *Nat Rev Mol Cell Biol* **2005**, *6*, 376-385, doi:10.1038/nrm1644.
532. Burroughs, A.M.; Ando, Y.; de Hoon, M.J.; Tomaru, Y.; Nishibu, T.; Ukekawa, R.; Funakoshi, T.; Kurokawa, T.; Suzuki, H.; Hayashizaki, Y.; et al. A comprehensive survey of 3' animal miRNA modification events and a possible role for 3' adenylation in modulating miRNA targeting effectiveness. *Genome Res* **2010**, *20*, 1398-1410, doi:10.1101/gr.106054.110.
533. Chiang, H.R.; Schoenfeld, L.W.; Ruby, J.G.; Auyeung, V.C.; Spies, N.; Baek, D.; Johnston, W.K.; Russ, C.; Luo, S.; Babiarz, J.E.; et al. Mammalian microRNAs: experimental evaluation of novel and previously annotated genes. *Genes Dev* **2010**, *24*, 992-1009, doi:10.1101/gad.1884710.
534. Westholm, J.O.; Ladewig, E.; Okamura, K.; Robine, N.; Lai, E.C. Common and distinct patterns of terminal modifications to mirtrons and canonical microRNAs. *RNA* **2012**, *18*, 177-192, doi:10.1261/rna.030627.111.
535. van der Kwast, R.; Quax, P.H.A.; Nossent, A.Y. An Emerging Role for isomiRs and the microRNA Epitranscriptome in Neovascularization. *Cells* **2019**, *9*, doi:10.3390/cells9010061.
536. Tomasello, L.; Distefano, R.; Nigita, G.; Croce, C.M. The MicroRNA Family Gets Wider: The IsomiRs Classification and Role. *Front Cell Dev Biol* **2021**, *9*, 668648, doi:10.3389/fcell.2021.668648.
537. Kuchenbauer, F.; Morin, R.D.; Argiropoulos, B.; Petriv, O.I.; Griffith, M.; Heuser, M.; Yung, E.; Piper, J.; Delaney, A.; Prabhu, A.L.; et al. In-depth characterization of the microRNA transcriptome in a leukemia progression model. *Genome Res* **2008**, *18*, 1787-1797, doi:10.1101/gr.077578.108.

538. Wu, H.; Ye, C.; Ramirez, D.; Manjunath, N. Alternative processing of primary microRNA transcripts by Drosha generates 5' end variation of mature microRNA. *PLoS One* **2009**, *4*, e7566, doi:10.1371/journal.pone.0007566.
539. Zhou, H.; Arcila, M.L.; Li, Z.; Lee, E.J.; Henzler, C.; Liu, J.; Rana, T.M.; Kosik, K.S. Deep annotation of mouse iso-miR and iso-moR variation. *Nucleic Acids Res* **2012**, *40*, 5864-5875, doi:10.1093/nar/gks247.
540. Galka-Marciniak, P.; Urbanek-Trzeciak, M.O.; Nawrocka, P.M.; Kozlowski, P. A pan-cancer atlas of somatic mutations in miRNA biogenesis genes. *Nucleic Acids Res* **2021**, *49*, 601-620, doi:10.1093/nar/gkaa1223.
541. Han, B.W.; Hung, J.H.; Weng, Z.; Zamore, P.D.; Ameres, S.L. The 3'-to-5' exoribonuclease Nibbler shapes the 3' ends of microRNAs bound to Drosophila Argonaute1. *Curr Biol* **2011**, *21*, 1878-1887, doi:10.1016/j.cub.2011.09.034.
542. Berezikov, E.; Robine, N.; Samsonova, A.; Westholm, J.O.; Naqvi, A.; Hung, J.H.; Okamura, K.; Dai, Q.; Bortolamiol-Becet, D.; Martin, R.; et al. Deep annotation of Drosophila melanogaster microRNAs yields insights into their processing, modification, and emergence. *Genome Res* **2011**, *21*, 203-215, doi:10.1101/gr.116657.110.
543. Burroughs, A.M.; Ando, Y. Identifying and characterizing functional 3' nucleotide addition in the miRNA pathway. *Methods* **2019**, *152*, 23-30, doi:10.1016/j.ymeth.2018.08.006.
544. Yang, W.; Chendrimada, T.P.; Wang, Q.; Higuchi, M.; Seeburg, P.H.; Shiekhattar, R.; Nishikura, K. Modulation of microRNA processing and expression through RNA editing by ADAR deaminases. *Nat Struct Mol Biol* **2006**, *13*, 13-21, doi:10.1038/nsmb1041.
545. Li, L.; Song, Y.; Shi, X.; Liu, J.; Xiong, S.; Chen, W.; Fu, Q.; Huang, Z.; Gu, N.; Zhang, R. The landscape of miRNA editing in animals and its impact on miRNA biogenesis and targeting. *Genome Res* **2018**, *28*, 132-143, doi:10.1101/gr.224386.117.
546. Kawahara, Y.; Zinshteyn, B.; Sethupathy, P.; Iizasa, H.; Hatzigeorgiou, A.G.; Nishikura, K. Redirection of silencing targets by adenosine-to-inosine editing of miRNAs. *Science* **2007**, *315*, 1137-1140, doi:10.1126/science.1138050.
547. Glogovitis, I.; Yahubyan, G.; Wurdinger, T.; Koppers-Lalic, D.; Baev, V. isomiRs-Hidden Soldiers in the miRNA Regulatory Army, and How to Find Them? *Biomolecules* **2020**, *11*, doi:10.3390/biom11010041.
548. Yue, C.; Wang, M.; Ding, B.; Wang, W.; Fu, S.; Zhou, D.; Zhang, Z.; Han, S. Polymorphism of the pre-miR-146a is associated with risk of cervical cancer in a Chinese population. *Gynecol Oncol* **2011**, *122*, 33-37, doi:10.1016/j.ygyno.2011.03.032.
549. van der Kwast, R.; Woudenberg, T.; Quax, P.H.A.; Nossent, A.Y. MicroRNA-411 and Its 5'-IsomiR Have Distinct Targets and Functions and Are Differentially Regulated in the Vasculature under Ischemia. *Mol Ther* **2020**, *28*, 157-170, doi:10.1016/j.ymthe.2019.10.002.
550. Moore, M.J.; Scheel, T.K.; Luna, J.M.; Park, C.Y.; Fak, J.J.; Nishiuchi, E.; Rice, C.M.; Darnell, R.B. miRNA-target chimeras reveal miRNA 3'-end pairing as a major determinant of Argonaute target specificity. *Nat Commun* **2015**, *6*, 8864, doi:10.1038/ncomms9864.
551. Sheu-Gruttadauria, J.; Xiao, Y.; Gebert, L.F.; MacRae, I.J. Beyond the seed: structural basis for supplementary microRNA targeting by human Argonaute2. *EMBO J* **2019**, *38*, e101153, doi:10.15252/embj.2018101153.
552. Baran-Gale, J.; Fannin, E.E.; Kurtz, C.L.; Sethupathy, P. Beta cell 5'-shifted isomiRs are candidate regulatory hubs in type 2 diabetes. *PLoS One* **2013**, *8*, e73240, doi:10.1371/journal.pone.0073240.
553. Bofill-De Ros, X.; Yang, A.; Gu, S. IsomiRs: Expanding the miRNA repression toolbox beyond the seed. *Biochim Biophys Acta Gene Regul Mech* **2020**, *1863*, 194373, doi:10.1016/j.bbagrm.2019.03.005.
554. Gebert, L.F.R.; MacRae, I.J. Regulation of microRNA function in animals. *Nat Rev Mol Cell Biol* **2019**, *20*, 21-37, doi:10.1038/s41580-018-0045-7.

555. Llorens, F.; Banez-Coronel, M.; Pantano, L.; del Rio, J.A.; Ferrer, I.; Estivill, X.; Marti, E. A highly expressed miR-101 isomiR is a functional silencing small RNA. *BMC Genomics* **2013**, *14*, 104, doi:10.1186/1471-2164-14-104.
556. Mercey, O.; Popa, A.; Cavard, A.; Paquet, A.; Chevalier, B.; Pons, N.; Magnone, V.; Zangari, J.; Brest, P.; Zaragosi, L.E.; et al. Characterizing isomiR variants within the microRNA-34/449 family. *FEBS Lett* **2017**, *591*, 693-705, doi:10.1002/1873-3468.12595.
557. Burroughs, A.M.; Ando, Y.; de Hoon, M.J.; Tomaru, Y.; Suzuki, H.; Hayashizaki, Y.; Daub, C.O. Deep-sequencing of human Argonaute-associated small RNAs provides insight into miRNA sorting and reveals Argonaute association with RNA fragments of diverse origin. *RNA Biol* **2011**, *8*, 158-177, doi:10.4161/rna.8.1.14300.
558. Sanchez Herrero, J.F.; Pluvinet, R.; Luna de Haro, A.; Sumoy, L. Paired-end small RNA sequencing reveals a possible overestimation in the isomiR sequence repertoire previously reported from conventional single read data analysis. *BMC bioinformatics* **2021**, *22*, 215, doi:10.1186/s12859-021-04128-1.
559. Ye, J.; Xu, M.; Tian, X.; Cai, S.; Zeng, S. Research advances in the detection of miRNA. *J Pharm Anal* **2019**, *9*, 217-226, doi:10.1016/j.jpha.2019.05.004.
560. Schamberger, A.; Orban, T.I. 3' IsomiR species and DNA contamination influence reliable quantification of microRNAs by stem-loop quantitative PCR. *PLoS One* **2014**, *9*, e106315, doi:10.1371/journal.pone.0106315.
561. Magee, R.; Telonis, A.G.; Cherlin, T.; Rigoutsos, I.; Londin, E. Assessment of isomiR Discrimination Using Commercial qPCR Methods. *Noncoding RNA* **2017**, *3*, doi:10.3390/ncrna3020018.
562. Zhou, Y.; Huang, Q.; Gao, J.; Lu, J.; Shen, X.; Fan, C. A dumbbell probe-mediated rolling circle amplification strategy for highly sensitive microRNA detection. *Nucleic Acids Res* **2010**, *38*, e156, doi:10.1093/nar/gkq556.
563. Honda, S.; Kirino, Y. Dumbbell-PCR: a method to quantify specific small RNA variants with a single nucleotide resolution at terminal sequences. *Nucleic Acids Res* **2015**, *43*, e77, doi:10.1093/nar/gkv218.
564. Androvic, P.; Valihrach, L.; Elling, J.; Sjoback, R.; Kubista, M. Two-tailed RT-qPCR: a novel method for highly accurate miRNA quantification. *Nucleic Acids Res* **2017**, *45*, e144, doi:10.1093/nar/gkx588.
565. Podini, D.; Vallone, P.M. SNP genotyping using multiplex single base primer extension assays. *Methods Mol Biol* **2009**, *578*, 379-391, doi:10.1007/978-1-60327-411-1_23.
566. Zhang, Y.; Zang, Q.; Xu, B.; Zheng, W.; Ban, R.; Zhang, H.; Yang, Y.; Hao, Q.; Iqbal, F.; Li, A.; et al. IsomiR Bank: a research resource for tracking IsomiRs. *Bioinformatics* **2016**, *32*, 2069-2071, doi:10.1093/bioinformatics/btw070.
567. Bhattacharya, A.; Ziebarth, J.D.; Cui, Y. PolymiRTS Database 3.0: linking polymorphisms in microRNAs and their target sites with human diseases and biological pathways. *Nucleic Acids Res* **2014**, *42*, D86-91, doi:10.1093/nar/gkt1028.
568. Liu, C.J.; Fu, X.; Xia, M.; Zhang, Q.; Gu, Z.; Guo, A.Y. miRNASNP-v3: a comprehensive database for SNPs and disease-related variations in miRNAs and miRNA targets. *Nucleic Acids Res* **2021**, *49*, D1276-D1281, doi:10.1093/nar/gkaa783.
569. Bofill-De Ros, X.; Luke, B.; Guthridge, R.; Mudunuri, U.; Loss, M.; Gu, S. Tumor IsomiR Encyclopedia (TIE): a pancancer database of miRNA isoforms. *Bioinformatics* **2021**, doi:10.1093/bioinformatics/btab172.
570. Telonis, A.G.; Magee, R.; Loher, P.; Chervoneva, I.; Londin, E.; Rigoutsos, I. Knowledge about the presence or absence of miRNA isoforms (isomiRs) can successfully discriminate amongst 32 TCGA cancer types. *Nucleic Acids Res* **2017**, *45*, 2973-2985, doi:10.1093/nar/gkx082.

571. Wang, S.; Zheng, Z.; Chen, P.; Wu, M. Tumor classification and biomarker discovery based on the 5'isomiR expression level. *BMC Cancer* **2019**, *19*, 127, doi:10.1186/s12885-019-5340-y.
572. Lan, C.; Peng, H.; McGowan, E.M.; Hutvagner, G.; Li, J. An isomiR expression panel based novel breast cancer classification approach using improved mutual information. *BMC Med Genomics* **2018**, *11*, 118, doi:10.1186/s12920-018-0434-y.
573. Kozubek, J.; Ma, Z.; Fleming, E.; Duggan, T.; Wu, R.; Shin, D.G.; Dadras, S.S. In-depth characterization of microRNA transcriptome in melanoma. *PLoS One* **2013**, *8*, e72699, doi:10.1371/journal.pone.0072699.
574. Babapoor, S.; Fleming, E.; Wu, R.; Dadras, S.S. A novel miR-451a isomiR, associated with amelanotypic phenotype, acts as a tumor suppressor in melanoma by retarding cell migration and invasion. *PLoS One* **2014**, *9*, e107502, doi:10.1371/journal.pone.0107502.
575. Dika, E.; Riefolo, M.; Porcellini, E.; Broseghini, E.; Ribero, S.; Senetta, R.; Abate, S.O.; Scarfi, F.; Lambertini, M.; Veronesi, G.; et al. Defining the prognostic role of microRNAs in cutaneous melanoma. *J Invest Dermatol* **2020**, doi:10.1016/j.jid.2020.03.949.
576. Dika, E.; Broseghini, E.; Porcellini, E.; Lambertini, M.; Riefolo, M.; Durante, G.; Loher, P.; Roncarati, R.; Bassi, C.; Misciali, C.; et al. Unraveling the role of microRNA/isomiR network in multiple primary melanoma pathogenesis. *Cell Death Dis* **2021**, *12*, 473, doi:10.1038/s41419-021-03764-y.
577. FastQC. **2015**.
578. Martin, M. Cutadapt removes adapter sequences from high-throughput sequencing reads. *EMBnet.journal* **2011**, *17*, 10, doi:10.14806/ej.17.1.200.
579. Dobin, A.; Davis, C.A.; Schlesinger, F.; Drenkow, J.; Zaleski, C.; Jha, S.; Batut, P.; Chaisson, M.; Gingeras, T.R. STAR: ultrafast universal RNA-seq aligner. *Bioinformatics* **2013**, *29*, 15-21, doi:10.1093/bioinformatics/bts635.
580. Anders, S.; Pyl, P.T.; Huber, W. HTSeq--a Python framework to work with high-throughput sequencing data. *Bioinformatics* **2015**, *31*, 166-169, doi:10.1093/bioinformatics/btu638.
581. Love, M.I.; Huber, W.; Anders, S. Moderated estimation of fold change and dispersion for RNA-seq data with DESeq2. *Genome Biol* **2014**, *15*, 550, doi:10.1186/s13059-014-0550-8.
582. Loher, P.; Karathanasis, N.; Londin, E.; Bray, P.; Pliatsika, V.; Telonis, A.G.; Rigoutsos, I. IsoMiRmap-fast, deterministic, and exhaustive mining of isomiRs from short RNA-seq datasets. *Bioinformatics* **2021**, doi:10.1093/bioinformatics/btab016.
583. Loher, P.; Rigoutsos, I. Interactive exploration of RNA22 microRNA target predictions. *Bioinformatics* **2012**, *28*, 3322-3323, doi:10.1093/bioinformatics/bts615.
584. Ke, Y.; Zhao, W.; Xiong, J.; Cao, R. miR-149 Inhibits Non-Small-Cell Lung Cancer Cells EMT by Targeting FOXM1. *Biochem Res Int* **2013**, *2013*, 506731, doi:10.1155/2013/506731.
585. Gregory, P.A.; Bert, A.G.; Paterson, E.L.; Barry, S.C.; Tsykin, A.; Farshid, G.; Vadas, M.A.; Khew-Goodall, Y.; Goodall, G.J. The miR-200 family and miR-205 regulate epithelial to mesenchymal transition by targeting ZEB1 and SIP1. *Nat Cell Biol* **2008**, *10*, 593-601, doi:10.1038/ncb1722.
586. Park, S.M.; Gaur, A.B.; Lengyel, E.; Peter, M.E. The miR-200 family determines the epithelial phenotype of cancer cells by targeting the E-cadherin repressors ZEB1 and ZEB2. *Genes Dev* **2008**, *22*, 894-907, doi:10.1101/gad.1640608.
587. Londin, E.; Loher, P.; Telonis, A.G.; Quann, K.; Clark, P.; Jing, Y.; Hatzimichael, E.; Kirino, Y.; Honda, S.; Lally, M.; et al. Analysis of 13 cell types reveals evidence for the expression of numerous novel primate- and tissue-specific microRNAs. *Proc Natl Acad Sci U S A* **2015**, *112*, E1106-1115, doi:10.1073/pnas.1420955112.
588. Barnhill, R.L.; Mihm, M.C., Jr. The histopathology of cutaneous malignant melanoma. *Semin Diagn Pathol* **1993**, *10*, 47-75.
589. Carrera, C.; Gual, A.; Diaz, A.; Puig-Butille, J.A.; Nogues, S.; Vilalta, A.; Conill, C.; Rull, R.; Vilana, R.; Arguis, P.; et al. Prognostic role of the histological subtype of melanoma on

the hands and feet in Caucasians. *Melanoma Res* **2017**, *27*, 315-320, doi:10.1097/CMR.0000000000000340.
590. Egger, M.E.; Dunki-Jacobs, E.M.; Callender, G.G.; Quillo, A.R.; Scoggins, C.R.; Martin, R.C., 2nd; Stromberg, A.J.; McMasters, K.M. Outcomes and prognostic factors in nodular melanomas. *Surgery* **2012**, *152*, 652-659; discussion 659-660, doi:10.1016/j.surg.2012.07.006.
591. Egger, M.E.; Stepp, L.O.; Callender, G.G.; Quillo, A.R.; Martin, R.C., 2nd; Scoggins, C.R.; Stromberg, A.J.; McMasters, K.M. Outcomes and prognostic factors in superficial spreading melanoma. *Am J Surg* **2013**, *206*, 861-867; discussion 867-868, doi:10.1016/j.amjsurg.2013.09.003.
592. Ge, L.; Vilain, R.E.; Lo, S.; Aivazian, K.; Scolyer, R.A.; Thompson, J.F. Breslow Thickness Measurements of Melanomas Around American Joint Committee on Cancer Staging Cut-Off Points: Imprecision and Terminal Digit Bias Have Important Implications for Staging and Patient Management. *Ann Surg Oncol* **2016**, *23*, 2658-2663, doi:10.1245/s10434-016-5196-1.
593. Patrick, R.J.; Corey, S.; Glass, L.F. The use of sequential serial sectioning of thin melanomas in determining maximum Breslow depth. *J Am Acad Dermatol* **2007**, *57*, S127-128, doi:10.1016/j.jaad.2006.02.007.
594. Lattanzi, M.; Lee, Y.; Simpson, D.; Moran, U.; Darvishian, F.; Kim, R.H.; Hernando, E.; Polsky, D.; Hanniford, D.; Shapiro, R.; et al. Primary Melanoma Histologic Subtype: Impact on Survival and Response to Therapy. *J Natl Cancer Inst* **2019**, *111*, 180-188, doi:10.1093/jnci/djy086.
595. Fattore, L.; Costantini, S.; Malpicci, D.; Ruggiero, C.F.; Ascierto, P.A.; Croce, C.M.; Mancini, R.; Ciliberto, G. MicroRNAs in melanoma development and resistance to target therapy. *Oncotarget* **2017**, *8*, 22262-22278, doi:10.18632/oncotarget.14763.
596. Torres, R.; Lang, U.E.; Hejna, M.; Shelton, S.J.; Joseph, N.M.; Shain, A.H.; Yeh, I.; Wei, M.L.; Oldham, M.C.; Bastian, B.C.; et al. MicroRNA Ratios Distinguish Melanomas from Nevi. *J Invest Dermatol* **2020**, *140*, 164-173 e167, doi:10.1016/j.jid.2019.06.126.
597. Grignol, V.; Fairchild, E.T.; Zimmerer, J.M.; Lesinski, G.B.; Walker, M.J.; Magro, C.M.; Kacher, J.E.; Karpa, V.I.; Clark, J.; Nuovo, G.; et al. miR-21 and miR-155 are associated with mitotic activity and lesion depth of borderline melanocytic lesions. *Br J Cancer* **2011**, *105*, 1023-1029, doi:10.1038/bjc.2011.288.
598. Satzger, I.; Mattern, A.; Kuettler, U.; Weinspach, D.; Niebuhr, M.; Kapp, A.; Gutzmer, R. microRNA-21 is upregulated in malignant melanoma and influences apoptosis of melanocytic cells. *Exp Dermatol* **2012**, *21*, 509-514, doi:10.1111/j.1600-0625.2012.01510.x.
599. Forloni, M.; Dogra, S.K.; Dong, Y.; Conte, D., Jr.; Ou, J.; Zhu, L.J.; Deng, A.; Mahalingam, M.; Green, M.R.; Wajapeyee, N. miR-146a promotes the initiation and progression of melanoma by activating Notch signaling. *Elife* **2014**, *3*, e01460, doi:10.7554/eLife.01460.
600. Pu, W.; Shang, Y.; Shao, Q.; Yuan, X. miR-146a promotes cell migration and invasion in melanoma by directly targeting SMAD4. *Oncol Lett* **2018**, *15*, 7111-7117, doi:10.3892/ol.2018.8172.
601. Rebane, A.; Akdis, C.A. MicroRNAs: Essential players in the regulation of inflammation. *J Allergy Clin Immunol* **2013**, *132*, 15-26, doi:10.1016/j.jaci.2013.04.011.
602. Cook, M.G.; Spatz, A.; Brocker, E.B.; Ruiter, D.J. Identification of histological features associated with metastatic potential in thin (<1.0 mm) cutaneous melanoma with metastases. A study on behalf of the EORTC Melanoma Group. *J Pathol* **2002**, *197*, 188-193, doi:10.1002/path.1093.
603. Aung, P.P.; Nagarajan, P.; Prieto, V.G. Regression in primary cutaneous melanoma: etiopathogenesis and clinical significance. *Lab Invest* **2017**, doi:10.1038/labinvest.2017.8.
604. Soura, E.; Eliades, P.J.; Shannon, K.; Stratigos, A.J.; Tsao, H. Hereditary melanoma: Update on syndromes and management: Emerging melanoma cancer complexes and genetic

counseling. *J Am Acad Dermatol* **2016**, *74*, 411-420; quiz 421-412, doi:10.1016/j.jaad.2015.08.037.
605. Lynch, H.T.; Krush, A.J. Heredity and malignant melanoma: implications for early cancer detection. *Can Med Assoc J* **1968**, *99*, 17-21.
606. Liu, C.G.; Calin, G.A.; Meloon, B.; Gamliel, N.; Sevignani, C.; Ferracin, M.; Dumitru, C.D.; Shimizu, M.; Zupo, S.; Dono, M.; et al. An oligonucleotide microchip for genome-wide microRNA profiling in human and mouse tissues. *Proceedings of the National Academy of Sciences of the United States of America* **2004**, *101*, 9740-9744, doi:10.1073/pnas.0403293101.
607. Volinia, S.; Calin, G.A.; Liu, C.G.; Ambs, S.; Cimmino, A.; Petrocca, F.; Visone, R.; Iorio, M.; Roldo, C.; Ferracin, M.; et al. A microRNA expression signature of human solid tumors defines cancer gene targets. *Proc Natl Acad Sci U S A* **2006**, *103*, 2257-2261, doi:10.1073/pnas.0510565103.
608. Hwa, C.; Price, L.S.; Belitskaya-Levy, I.; Ma, M.W.; Shapiro, R.L.; Berman, R.S.; Kamino, H.; Darvishian, F.; Osman, I.; Stein, J.A. Single versus multiple primary melanomas: old questions and new answers. *Cancer* **2012**, *118*, 4184-4192, doi:10.1002/cncr.27407.
609. Utjes, D.; Lyth, J.; Lapins, J.; Eriksson, H. Reduced disease-specific survival following a diagnosis of multiple primary cutaneous malignant melanomas-a nationwide, population-based study. *Int J Cancer* **2017**, *141*, 2243-2252, doi:10.1002/ijc.30925.
610. Savoia, P.; Osella-Abate, S.; Deboli, T.; Marenco, F.; Stroppiana, E.; Novelli, M.; Fierro, M.T.; Bernengo, M.G. Clinical and prognostic reports from 270 patients with multiple primary melanomas: a 34-year single-institution study. *J Eur Acad Dermatol Venereol* **2012**, *26*, 882-888, doi:10.1111/j.1468-3083.2011.04181.x.
611. Grossman, D.; Farnham, J.M.; Hyngstrom, J.; Klapperich, M.E.; Secrest, A.M.; Empey, S.; Bowen, G.M.; Wada, D.; Andtbacka, R.H.I.; Grossmann, K.; et al. Similar survival of patients with multiple versus single primary melanomas based on Utah Surveillance, Epidemiology, and End Results data (1973-2011). *J Am Acad Dermatol* **2018**, *79*, 238-244, doi:10.1016/j.jaad.2018.02.055.
612. Guarino, M.; Rubino, B.; Ballabio, G. The role of epithelial-mesenchymal transition in cancer pathology. *Pathology* **2007**, *39*, 305-318, doi:10.1080/00313020701329914.
613. Caramel, J.; Papadogeorgakis, E.; Hill, L.; Browne, G.J.; Richard, G.; Wierinckx, A.; Saldanha, G.; Osborne, J.; Hutchinson, P.; Tse, G.; et al. A switch in the expression of embryonic EMT-inducers drives the development of malignant melanoma. *Cancer Cell* **2013**, *24*, 466-480, doi:10.1016/j.ccr.2013.08.018.
614. Tang, A.; Eller, M.S.; Hara, M.; Yaar, M.; Hirohashi, S.; Gilchrest, B.A. E-cadherin is the major mediator of human melanocyte adhesion to keratinocytes in vitro. *J Cell Sci* **1994**, *107 (Pt 4)*, 983-992.
615. Kreizenbeck, G.M.; Berger, A.J.; Subtil, A.; Rimm, D.L.; Gould Rothberg, B.E. Prognostic significance of cadherin-based adhesion molecules in cutaneous malignant melanoma. *Cancer Epidemiol Biomarkers Prev* **2008**, *17*, 949-958, doi:10.1158/1055-9965.EPI-07-2729.
616. Silye, R.; Karayiannakis, A.J.; Syrigos, K.N.; Poole, S.; van Noorden, S.; Batchelor, W.; Regele, H.; Sega, W.; Boesmueller, H.; Krausz, T.; et al. E-cadherin/catenin complex in benign and malignant melanocytic lesions. *J Pathol* **1998**, *186*, 350-355, doi:10.1002/(SICI)1096-9896(199812)186:4<350::AID-PATH181>3.0.CO;2-K.
617. Ivanova, N.B.; Dimos, J.T.; Schaniel, C.; Hackney, J.A.; Moore, K.A.; Lemischka, I.R. A stem cell molecular signature. *Science* **2002**, *298*, 601-604, doi:10.1126/science.1073823.
618. Ramalho-Santos, M.; Yoon, S.; Matsuzaki, Y.; Mulligan, R.C.; Melton, D.A. "Stemness": transcriptional profiling of embryonic and adult stem cells. *Science* **2002**, *298*, 597-600, doi:10.1126/science.1072530.

619. Krebsbach, P.H.; Villa-Diaz, L.G. The Role of Integrin alpha6 (CD49f) in Stem Cells: More than a Conserved Biomarker. *Stem Cells Dev* **2017**, *26*, 1090-1099, doi:10.1089/scd.2016.0319.
620. Rouault, J.P.; Falette, N.; Guehenneux, F.; Guillot, C.; Rimokh, R.; Wang, Q.; Berthet, C.; Moyret-Lalle, C.; Savatier, P.; Pain, B.; et al. Identification of BTG2, an antiproliferative p53-dependent component of the DNA damage cellular response pathway. *Nat Genet* **1996**, *14*, 482-486, doi:10.1038/ng1296-482.
621. Mao, B.; Zhang, Z.; Wang, G. BTG2: a rising star of tumor suppressors (review). *Int J Oncol* **2015**, *46*, 459-464, doi:10.3892/ijo.2014.2765.
622. Zhang, L.; Huang, H.; Wu, K.; Wang, M.; Wu, B. Impact of BTG2 expression on proliferation and invasion of gastric cancer cells in vitro. *Mol Biol Rep* **2010**, *37*, 2579-2586, doi:10.1007/s11033-009-9777-y.
623. Wei, S.; Hao, C.; Li, X.; Zhao, H.; Chen, J.; Zhou, Q. Effects of BTG2 on proliferation inhibition and anti-invasion in human lung cancer cells. *Tumour Biol* **2012**, *33*, 1223-1230, doi:10.1007/s13277-012-0370-y.
624. Wagener, N.; Bulkescher, J.; Macher-Goeppinger, S.; Karapanagiotou-Schenkel, I.; Hatiboglu, G.; Abdel-Rahim, M.; Abol-Enein, H.; Ghoneim, M.A.; Bastian, P.J.; Muller, S.C.; et al. Endogenous BTG2 expression stimulates migration of bladder cancer cells and correlates with poor clinical prognosis for bladder cancer patients. *Br J Cancer* **2013**, *108*, 973-982, doi:10.1038/bjc.2012.573.
625. Goto, Y.; Arigami, T.; Kitago, M.; Nguyen, S.L.; Narita, N.; Ferrone, S.; Morton, D.L.; Irie, R.F.; Hoon, D.S. Activation of Toll-like receptors 2, 3, and 4 on human melanoma cells induces inflammatory factors. *Mol Cancer Ther* **2008**, *7*, 3642-3653, doi:10.1158/1535-7163.MCT-08-0582.
626. Takazawa, Y.; Kiniwa, Y.; Ogawa, E.; Uchiyama, A.; Ashida, A.; Uhara, H.; Goto, Y.; Okuyama, R. Toll-like receptor 4 signaling promotes the migration of human melanoma cells. *Tohoku J Exp Med* **2014**, *234*, 57-65, doi:10.1620/tjem.234.57.
627. Wei, C.Y.; Wang, L.; Zhu, M.X.; Deng, X.Y.; Wang, D.H.; Zhang, S.M.; Ying, J.H.; Yuan, X.; Wang, Q.; Xuan, T.F.; et al. TRIM44 activates the AKT/mTOR signal pathway to induce melanoma progression by stabilizing TLR4. *J Exp Clin Cancer Res* **2019**, *38*, 137, doi:10.1186/s13046-019-1138-7.
628. Chawla, G.; Deosthale, P.; Childress, S.; Wu, Y.C.; Sokol, N.S. A let-7-to-miR-125 MicroRNA Switch Regulates Neuronal Integrity and Lifespan in Drosophila. *PLoS Genet* **2016**, *12*, e1006247, doi:10.1371/journal.pgen.1006247.
629. Le, M.T.; Xie, H.; Zhou, B.; Chia, P.H.; Rizk, P.; Um, M.; Udolph, G.; Yang, H.; Lim, B.; Lodish, H.F. MicroRNA-125b promotes neuronal differentiation in human cells by repressing multiple targets. *Mol Cell Biol* **2009**, *29*, 5290-5305, doi:10.1128/MCB.01694-08.
630. Mort, R.L.; Jackson, I.J.; Patton, E.E. The melanocyte lineage in development and disease. *Development* **2015**, *142*, 620-632, doi:10.1242/dev.106567.
631. Wang, W.; Chi, T.; Xue, Y.; Zhou, S.; Kuo, A.; Crabtree, G.R. Architectural DNA binding by a high-mobility-group/kinesin-like subunit in mammalian SWI/SNF-related complexes. *Proc Natl Acad Sci U S A* **1998**, *95*, 492-498, doi:10.1073/pnas.95.2.492.
632. Battaglioli, E.; Andres, M.E.; Rose, D.W.; Chenoweth, J.G.; Rosenfeld, M.G.; Anderson, M.E.; Mandel, G. REST repression of neuronal genes requires components of the hSWI.SNF complex. *J Biol Chem* **2002**, *277*, 41038-41045, doi:10.1074/jbc.M205691200.
633. Kazantseva, A.; Sepp, M.; Kazantseva, J.; Sadam, H.; Pruunsild, P.; Timmusk, T.; Neuman, T.; Palm, K. N-terminally truncated BAF57 isoforms contribute to the diversity of SWI/SNF complexes in neurons. *J Neurochem* **2009**, *109*, 807-818, doi:10.1111/j.1471-4159.2009.06005.x.
634. Wang, L.; Baiocchi, R.A.; Pal, S.; Mosialos, G.; Caligiuri, M.; Sif, S. The BRG1- and hBRM-associated factor BAF57 induces apoptosis by stimulating expression of the cylindromatosis

tumor suppressor gene. *Mol Cell Biol* **2005**, *25*, 7953-7965, doi:10.1128/MCB.25.18.7953-7965.2005.

635. Baker, K.M.; Wei, G.; Schaffner, A.E.; Ostrowski, M.C. Ets-2 and components of mammalian SWI/SNF form a repressor complex that negatively regulates the BRCA1 promoter. *J Biol Chem* **2003**, *278*, 17876-17884, doi:10.1074/jbc.M209480200.
636. Papadakis, A.I.; Sun, C.; Knijnenburg, T.A.; Xue, Y.; Grernrum, W.; Holzel, M.; Nijkamp, W.; Wessels, L.F.; Beijersbergen, R.L.; Bernards, R.; et al. SMARCE1 suppresses EGFR expression and controls responses to MET and ALK inhibitors in lung cancer. *Cell Res* **2015**, *25*, 445-458, doi:10.1038/cr.2015.16.
637. Sethuraman, A.; Brown, M.; Seagroves, T.N.; Wu, Z.H.; Pfeffer, L.M.; Fan, M. SMARCE1 regulates metastatic potential of breast cancer cells through the HIF1A/PTK2 pathway. *Breast Cancer Res* **2016**, *18*, 81, doi:10.1186/s13058-016-0738-9.
638. Kagami, S.; Kurita, T.; Kawagoe, T.; Toki, N.; Matsuura, Y.; Hachisuga, T.; Matsuyama, A.; Hashimoto, H.; Izumi, H.; Kohno, K. Prognostic significance of BAF57 expression in patients with endometrial carcinoma. *Histol Histopathol* **2012**, *27*, 593-599, doi:10.14670/HH-27.593.
639. Abdel-Rahman, M.H.; Sample, K.M.; Pilarski, R.; Walsh, T.; Grosel, T.; Kinnamon, D.; Boru, G.; Massengill, J.B.; Schoenfield, L.; Kelly, B.; et al. Whole Exome Sequencing Identifies Candidate Genes Associated with Hereditary Predisposition to Uveal Melanoma. *Ophthalmology* **2020**, *127*, 668-678, doi:10.1016/j.ophtha.2019.11.009.
640. Mastronikolis, S.; Adamopoulou, M.; Papouliakos, S.; Manoli, A.; Katsinis, S.; Makri, O.; Monastirioti, A.E.; Tsiambas, E.; Georgakopoulos, C. Mutational landscape in Uveal Melanoma. *J BUON* **2021**, *26*, 1194-1197.
641. Ho, H.; Aruri, J.; Kapadia, R.; Mehr, H.; White, M.A.; Ganesan, A.K. RhoJ regulates melanoma chemoresistance by suppressing pathways that sense DNA damage. *Cancer Res* **2012**, *72*, 5516-5528, doi:10.1158/0008-5472.CAN-12-0775.
642. Shi, Y.; Chichung Lie, D.; Taupin, P.; Nakashima, K.; Ray, J.; Yu, R.T.; Gage, F.H.; Evans, R.M. Expression and function of orphan nuclear receptor TLX in adult neural stem cells. *Nature* **2004**, *427*, 78-83, doi:10.1038/nature02211.
643. Sun, G.; Yu, R.T.; Evans, R.M.; Shi, Y. Orphan nuclear receptor TLX recruits histone deacetylases to repress transcription and regulate neural stem cell proliferation. *Proc Natl Acad Sci U S A* **2007**, *104*, 15282-15287, doi:10.1073/pnas.0704089104.
644. Cheng, L.; Arata, A.; Mizuguchi, R.; Qian, Y.; Karunaratne, A.; Gray, P.A.; Arata, S.; Shirasawa, S.; Bouchard, M.; Luo, P.; et al. Tlx3 and Tlx1 are post-mitotic selector genes determining glutamatergic over GABAergic cell fates. *Nat Neurosci* **2004**, *7*, 510-517, doi:10.1038/nn1221.
645. Li, S.; Sun, G.; Murai, K.; Ye, P.; Shi, Y. Characterization of TLX expression in neural stem cells and progenitor cells in adult brains. *PLoS One* **2012**, *7*, e43324, doi:10.1371/journal.pone.0043324.
646. Murai, K.; Qu, Q.; Sun, G.; Ye, P.; Li, W.; Asuelime, G.; Sun, E.; Tsai, G.E.; Shi, Y. Nuclear receptor TLX stimulates hippocampal neurogenesis and enhances learning and memory in a transgenic mouse model. *Proc Natl Acad Sci U S A* **2014**, *111*, 9115-9120, doi:10.1073/pnas.1406779111.
647. McLennan, P.L.; Taylor, D.A. Antagonism by ketanserin of 5-HT-induced vasoconstriction unmasks a 5-HT-induced vasodilation. *Eur J Pharmacol* **1984**, *104*, 313-318, doi:10.1016/0014-2999(84)90407-2.
648. Hatano, M.; Roberts, C.W.; Minden, M.; Crist, W.M.; Korsmeyer, S.J. Deregulation of a homeobox gene, HOX11, by the t(10;14) in T cell leukemia. *Science* **1991**, *253*, 79-82, doi:10.1126/science.1676542.
649. Kennedy, M.A.; Gonzalez-Sarmiento, R.; Kees, U.R.; Lampert, F.; Dear, N.; Boehm, T.; Rabbitts, T.H. HOX11, a homeobox-containing T-cell oncogene on human chromosome 10q24. *Proc Natl Acad Sci U S A* **1991**, *88*, 8900-8904, doi:10.1073/pnas.88.20.8900.

650. Nava, C.; Lamari, F.; Heron, D.; Mignot, C.; Rastetter, A.; Keren, B.; Cohen, D.; Faudet, A.; Bouteiller, D.; Gilleron, M.; et al. Analysis of the chromosome X exome in patients with autism spectrum disorders identified novel candidate genes, including TMLHE. *Transl Psychiatry* **2012**, *2*, e179, doi:10.1038/tp.2012.102.
651. Ferreira, G.C.; McKenna, M.C. L-Carnitine and Acetyl-L-carnitine Roles and Neuroprotection in Developing Brain. *Neurochem Res* **2017**, *42*, 1661-1675, doi:10.1007/s11064-017-2288-7.
652. Melone, M.A.B.; Valentino, A.; Margarucci, S.; Galderisi, U.; Giordano, A.; Peluso, G. The carnitine system and cancer metabolic plasticity. *Cell Death Dis* **2018**, *9*, 228, doi:10.1038/s41419-018-0313-7.
653. Eich, M.L.; Chandrashekar, D.S.; Rodriguez Pen, A.M.; Robinson, A.D.; Siddiqui, J.; Daignault-Newton, S.; Chakravarthi, B.; Kunju, L.P.; Netto, G.J.; Varambally, S. Characterization of glycine-N-acyltransferase like 1 (GLYATL1) in prostate cancer. *Prostate* **2019**, *79*, 1629-1639, doi:10.1002/pros.23887.
654. Barfeld, S.J.; East, P.; Zuber, V.; Mills, I.G. Meta-analysis of prostate cancer gene expression data identifies a novel discriminatory signature enriched for glycosylating enzymes. *BMC Med Genomics* **2014**, *7*, 513, doi:10.1186/s12920-014-0074-9.
655. Singh, A.B.; Sharma, A.; Dhawan, P. Claudin family of proteins and cancer: an overview. *J Oncol* **2010**, *2010*, 541957, doi:10.1155/2010/541957.
656. Cherradi, S.; Martineau, P.; Gongora, C.; Del Rio, M. Claudin gene expression profiles and clinical value in colorectal tumors classified according to their molecular subtype. *Cancer Manag Res* **2019**, *11*, 1337-1348, doi:10.2147/CMAR.S188192.
657. Paquet-Fifield, S.; Koh, S.L.; Cheng, L.; Beyit, L.M.; Shembrey, C.; Molck, C.; Behrenbruch, C.; Papin, M.; Gironella, M.; Guelfi, S.; et al. Tight Junction Protein Claudin-2 Promotes Self-Renewal of Human Colorectal Cancer Stem-like Cells. *Cancer Res* **2018**, *78*, 2925-2938, doi:10.1158/0008-5472.CAN-17-1869.
658. Kimbung, S.; Kovacs, A.; Bendahl, P.O.; Malmstrom, P.; Ferno, M.; Hatschek, T.; Hedenfalk, I. Claudin-2 is an independent negative prognostic factor in breast cancer and specifically predicts early liver recurrences. *Mol Oncol* **2014**, *8*, 119-128, doi:10.1016/j.molonc.2013.10.002.
659. Zhang, X.; Wang, H.; Li, Q.; Li, T. CLDN2 inhibits the metastasis of osteosarcoma cells via down-regulating the afadin/ERK signaling pathway. *Cancer Cell Int* **2018**, *18*, 160, doi:10.1186/s12935-018-0662-4.
660. Mao, L.; Liu, S.; Hu, L.; Jia, L.; Wang, H.; Guo, M.; Chen, C.; Liu, Y.; Xu, L. miR-30 Family: A Promising Regulator in Development and Disease. *Biomed Res Int* **2018**, *2018*, 9623412, doi:10.1155/2018/9623412.
661. Huang, G.L.; Sun, J.; Lu, Y.; Liu, Y.; Cao, H.; Zhang, H.; Calin, G.A. MiR-200 family and cancer: From a meta-analysis view. *Mol Aspects Med* **2019**, *70*, 57-71, doi:10.1016/j.mam.2019.09.005.
662. Elson-Schwab, I.; Lorentzen, A.; Marshall, C.J. MicroRNA-200 family members differentially regulate morphological plasticity and mode of melanoma cell invasion. *PLoS One* **2010**, *5*, doi:10.1371/journal.pone.0013176.
663. Lund, A.H. miR-10 in development and cancer. *Cell Death Differ* **2010**, *17*, 209-214, doi:10.1038/cdd.2009.58.
664. Gunning, P.W.; Hardeman, E.C. Fundamental differences. *Elife* **2018**, *7*, doi:10.7554/eLife.34477.
665. Telonis, A.G.; Rigoutsos, I. Race Disparities in the Contribution of miRNA Isoforms and tRNA-Derived Fragments to Triple-Negative Breast Cancer. *Cancer Res* **2018**, *78*, 1140-1154, doi:10.1158/0008-5472.CAN-17-1947.

666. Heydarzadeh, S.; Ranjbar, M.; Karimi, F.; Seif, F.; Alivand, M.R. Overview of host miRNA properties and their association with epigenetics, long non-coding RNAs, and Xeno-infectious factors. *Cell Biosci* **2021**, *11*, 43, doi:10.1186/s13578-021-00552-1.
667. Tian, Y.; Zeng, J.; Yang, Z. MicroRNA-27b inhibits the development of melanoma by targeting MYC. *Oncol Lett* **2021**, *21*, 370, doi:10.3892/ol.2021.12631.
668. Poell, J.B.; van Haastert, R.J.; de Gunst, T.; Schultz, I.J.; Gommans, W.M.; Verheul, M.; Cerisoli, F.; van Puijenbroek, A.; van Noort, P.I.; Prevost, G.P.; et al. Correction: A Functional Screen Identifies Specific MicroRNAs Capable of Inhibiting Human Melanoma Cell Viability. *PLoS One* **2013**, *8*, doi:10.1371/annotation/ebea4bd5-2b96-4842-b110-2f7c156e5060.
669. Hayward, N.K.; Wilmott, J.S.; Waddell, N.; Johansson, P.A.; Field, M.A.; Nones, K.; Patch, A.M.; Kakavand, H.; Alexandrov, L.B.; Burke, H.; et al. Whole-genome landscapes of major melanoma subtypes. *Nature* **2017**, *545*, 175-180, doi:10.1038/nature22071.
670. Lunavat, T.R.; Cheng, L.; Einarsdottir, B.O.; Olofsson Bagge, R.; Veppil Muralidharan, S.; Sharples, R.A.; Lasser, C.; Gho, Y.S.; Hill, A.F.; Nilsson, J.A.; et al. BRAF(V600) inhibition alters the microRNA cargo in the vesicular secretome of malignant melanoma cells. *Proc Natl Acad Sci U S A* **2017**, *114*, E5930-E5939, doi:10.1073/pnas.1705206114.
671. Denaro, M.; Ugolini, C.; Poma, A.M.; Borrelli, N.; Materazzi, G.; Piaggi, P.; Chiarugi, M.; Miccoli, P.; Vitti, P.; Basolo, F. Differences in miRNA expression profiles between wild-type and mutated NIFTPs. *Endocr Relat Cancer* **2017**, *24*, 543-553, doi:10.1530/ERC-17-0167.
672. Mueller, D.W.; Rehli, M.; Bosserhoff, A.K. miRNA expression profiling in melanocytes and melanoma cell lines reveals miRNAs associated with formation and progression of malignant melanoma. *J Invest Dermatol* **2009**, *129*, 1740-1751, doi:10.1038/jid.2008.452.
673. Nabipoorashrafi, S.A.; Shomali, N.; Sadat-Hatamnezhad, L.; Mahami-Oskouei, M.; Mahmoudi, J.; Sandoghchian Shotorbani, B.; Akbari, M.; Xu, H.; Sandoghchian Shotorbani, S. miR-143 acts as an inhibitor of migration and proliferation as well as an inducer of apoptosis in melanoma cancer cells in vitro. *IUBMB Life* **2020**, *72*, 2034-2044, doi:10.1002/iub.2345.
674. Su, B.B.; Zhou, S.W.; Gan, C.B.; Zhang, X.N. MiR-330-5p regulates tyrosinase and PDIA3 expression and suppresses cell proliferation and invasion in cutaneous malignant melanoma. *J Surg Res* **2016**, *203*, 434-440, doi:10.1016/j.jss.2016.03.021.
675. Zhang, W.; Mao, K.; Liu, S.; Xu, Y.; Ren, J. miR-942-5p promotes the proliferation and invasion of human melanoma cells by targeting DKK3. *J Recept Signal Transduct Res* **2021**, *41*, 180-187, doi:10.1080/10799893.2020.1804280.
676. Wang, J.; Fang, Y.; Liu, Y.F.; Wang, X.; Wang, X.L.; Wang, R.Y.; Meng, Z.D. MiR-154 inhibits cells proliferation and metastasis in melanoma by targeting AURKA and serves as a novel prognostic indicator. *Eur Rev Med Pharmacol Sci* **2019**, *23*, 4275-4284, doi:10.26355/eurrev_201905_17932.
677. Couts, K.L.; Anderson, E.M.; Gross, M.M.; Sullivan, K.; Ahn, N.G. Oncogenic B-Raf signaling in melanoma cells controls a network of microRNAs with combinatorial functions. *Oncogene* **2013**, *32*, 1959-1970, doi:10.1038/onc.2012.209.